THE UNIVERSITY
of EDINBURGH

University of Edinburgh
School of Engineering
Institute for Infrastructure & Environment (IIE)

Properties, Functionality, and Potential Applications of Novel Modified Iron Nanoparticles For The Treatment of 2,4,6-Trichlorophenol

A THESIS SUBMITTED TO THE FACULTY OF THE UNIVERSITY OF EDINBURGH IN PARTIAL FULFILLMENT OF THE REQUIREMENTS FOR THE DEGREE DOCTORATE OF PHILOSOPHY

By

Laura A. Underwood

Advisor
Dr Andrea Semião

Edinburgh, Scotland, UK
June 25th, 2018

"I think it would be well, and proper, and obedient, and pure, to grasp your one necessity and not let it go, to dangle from it limp wherever it takes you. Then even death, where you're going no matter how you live, cannot you part. Seize it and let it seize you up aloft even, till your eyes burn out and drop; let your musky flesh fall off in shreds, and let your very bones unhinge and scatter, loosened over fields, over fields and woods, lightly, thoughtless, from any height at all, from as high as eagles."

Living Like Weasels- Annie Dillard

Declaration

I hereby declare that this submission is my own work and that to the best of my knowledge and belief it contains no material previously published or written by another person. Nor does this thesis contain material which has been accepted for the award of any other degree or diploma at the University of Edinburgh or any other educational institution, except where due acknowledgement has been made in the text.

I, therefore, declare that the intellectual content of this thesis is the product of my own work, except where assistance from others in the thesis' project design and execution, as well as, style, presentation, and linguistic expression is acknowledged.

Laura Ann Underwood
June 24th, 2018

Thesis Supervisors/Advisors

Dr Andrea Semião, University of Edinburgh, Institute for Infrastructure and Environment, Edinburgh, Scotland.

Dr Mark Wiesner, Duke University, School of Civil and Environmental Engineering, Durham, U.S.A.

Thesis Examiners

Professor JiaQian Jiang, Glasgow Caledonian University, School of Engineering and Built Environment, Glasgow, Scotland.

Professor Alistair Borthwick, University of Edinburgh, Institute for Infrastructure and Environment, Edinburgh, Scotland.

Underwood, Laura Ann
Properties, Functionality, and Potential Applications of Novel Modified Iron Nanoparticles For The Treatment of 2,4,6-Trichlorophenol
PhD Thesis, University of Edinburgh
Institute for Infrastructure and Environment
June 2018

Lay Summary

The increased use of pesticides in agriculture has led to higher occurrences of water contamination. Some of these contaminants, such as chlorinated aromatics, pose a health concern to human and aquatic life. Current treatment technologies for removing or degrading these contaminants are inadequate often resulting in incomplete removal or the formation of breakdown products. The development of new materials to improve current water and waste treatment are necessary.

Small nano-sized particles of iron (zero-valent iron) may provide a solution. These materials are affordable, non-hazardous, and can degrade a wide variety of water contaminants. Zero-valent iron (ZVI) has historically been applied in groundwater treatment, but advanced modifications to the material could open up a wider array of water and waste treatment applications.

This research developed a new iron composite material for augmented contaminant treatment in water. The new material's properties, functionality, and potential applications were examined through this work and could result in improved treatment for water contaminants and broader use of ZVI.

Abstract

2,4,6-trichlorophenol (TCP) is a pervasive carcinogenic water contaminant found in a wide variety of water and waste systems and is a pertinent model compound of broader aromatic organics, specifically organo-halide pesticides. These compounds are persistent in the environment and show resilience to regular water and waste treatment protocols thus warranting the development and implementation of novel treatment materials for improved contaminant removal.

Zero-valent iron (ZVI) has demonstrated the ability to remove or degrade a wide variety of inorganic and organic water contaminants, including chlorophenols, and has been widely applied for in-*situ* groundwater remediation where contamination is often localised in a low-oxygen environment. ZVI's broader applications in water treatment have remained mainly limited due to corrosion, particle dispersion, and confinement issues in deployment. This work, therefore, explored the development, functionality, and potential application of new modified nZVI materials (nZVI-Osorb) and assessed their potential to improve iron's intrinsic functionality while also gauging the material's viability for TCP remediation in water and waste systems.

Materials produced in this thesis were prepared utilising three different embedment procedures (1-pot, multiple additions, oxygen-free). All embedment methods resulted in tightly bound composites featuring high surface areas (340.2-449.1 sq. m/g) with net iron composition ranging from 10% to 29.78% by mass. Electron imaging microscopy verified even dispersion of iron throughout the substrate. Composite materials did not exhibit a delayed rate of atmospheric corrosion over nZVI controls evincing an 18% $nZVI^0$ loss per day until reaching a stabilised concentration (7%) after 48 hrs. nZVI-Osorb composites did produce more favourable iron oxide species which remain conducive to electron transfer from core Fe^0 atom. After 50 days, a majority of nZVI in nZVI-Osorb had oxidised to maghemite (30%) and magnetite (26%) compared to control nZVI producing 19% and 12% respectively. Unreactive hematite accounted for 47% of the control and just 36% of the composite. While 1-pot embedment allowed the most substantial control over final iron composition, the oxygen-free method allowed the most reliable preservation of

initial $nZVI^0$ concentrations through restricted oxidation. Materials generated through oxygen-free embedment were utilised in the following water treatment trials with TCP.

Parameters related to sorption and degradation mechanisms of TCP by nZVI-Osorb were tested in aerobic conditions, e.g. surface and potable water. nZVI-Osorb materials demonstrated high extraction capacity for TCP from aqueous solutions (Qe=1286.4 ±13.5 mg TCP/g Osorb, Qe=1253±106.7 mg TCP/g nZVI-Osorb, pH 5.1, 120mg/L TCP) and followed pseudo second order kinetics. In the broader class of chlorophenols, sorptive affinity mirrored partitioning values with highly substituted chlorophenols displaying the highest sorption capacities. Degradation of TCP by nZVI-Osorb or nZVI controls was not observed due to corrosive hindrance and inadequate reductive capacity, suggesting that materials may not be suitable for highly aerated surface and potable water treatment systems.

Environmental conditions pertinent to sorption and degradation mechanisms were evaluated to improve understanding and robustness of functionality in low-oxygen applications, such as wastewater and anaerobic digesters, where nZVI-Osorb treatment is anticipated to be advantageous to TCP sorption and methane production. pH was found to influence sorption dramatically. Acidic solutions below 5 found sorption >90%. This capacity was reduced to <30% when pH was raised above TCP pK_a value (6.23) to 7 and above. Further trials found a positive effect on TCP sorption (+7.55%) linked to net pH reduction (5.1 to 3.3) with the addition of secondary acids (volatile fatty acids: acetic, propionic, butyric, 3x 100mg/L) commonly found in anaerobic digester systems. Salinity did not affect TCP sorption. The removal of dissolved and atmospheric oxygen increased total sorption (40ppm-+1.94%, 100ppm- +7.93%, 200ppm- +0.89%, 400mg/L- +14.59%) through reduced iron corrosion and the production of favorable iron oxides, but did not facilitate contaminant degradation.

Biodegradation mechanisms for TCP have broadly been established, and new research has supported the improved cometabolic degradation of recalcitrant contaminants like TCP and PCP in nZVI-dosed anaerobic digesters. Model anaerobic digester systems (3.9 g/L nZVI-Osorb, 25mg/L TCP, 240 mg/L acetic, 120mg/L propionic, 120mg/L butyric acid) containing bioreactor sludge (62.5%) were observed through standard water quality diagnostics (pH, ORP, COD, head pressure) for 14 days and

suggested that nZVI-Osorb did not inhibit cellular processes. Increased electron activity from iron corrosion and hydrogen gas production, increased overall pH and decreased total ORP in these AD systems. TCP degradation by-products (DCP, CP) were detected in dilute concentrations (<0.01 mg/L) with poor recovery by LC-MS/MS. Results suggest that nZVI-Osorb may be well-suited additive for AD systems.

This study contributes to knowledge of the properties, functionality, and treatment mechanisms of metal-sorbent composites with a model chlorinated aromatic water contaminant in aerobic and anaerobic environments. The work identifies favourable environmental and process conditions to apply these materials in larger scale applications, particularly, anaerobic digestion and provides support for the continued refinement and improvement of nZVI based remediation systems.

Acknowledgements

This work is made possible by the tremendous support of numerous people and institutions. I would like to express my sincerest gratitude to Dr Andrea Semião for her guidance, constructive feedback, and continual support to produce the best thesis possible. This work would not have been possible without her.

I would also like to thank my second supervisor Dr Vasileios Koutsos for his enthusiasm and offers of support. Massive thanks are due to my first supervisor Dr Blanca Antizar-Ladislao for the opportunity to pursue a PhD. Her kindness, leadership, and support in my early Edinburgh years were essential. Thank you to Dr Mark Wiesner for welcoming me into his research group at Duke. His academic support and guidance helped shape the direction of this project and challenged me to justify my work with clarity and depth. Much gratitude is due to Dr Sarantuyaa Zandaryaa of UNESCO-IHP for her mentorship and guidance during my internship. Lastly, thanks to Dr Paul Edmiston my undergraduate supervisor and mentor. His guidance laid the foundation for my professional career, and I will be forever grateful.

The University of Edinburgh, School of Engineering and Duke University, Department of Civil and Environmental Engineering is acknowledged for providing the needed facilities and resources required to carry out this degree. Funding provided by the University of Edinburgh Principal's Career Development Scholarship, Edinburgh Global Research Scholarship, and Charles M. Vest NAE Grand Challenges for Engineering International Scholarship was much appreciated.

Many thanks to ABSMaterials Inc for providing use of their nanosorbent, Osorb. Thanks are also due to Nano iron s.r.o for providing samples of nZVI utilised in this research.

Many people have assisted in the usage of various equipment utilised within this work. Thanks to Massimiliano Curcio and Dr Jason Love within the Chemistry department for training and space within their anaerobic chamber. Michael Vidmar, Dr Amar Nath, and Airat Khasanov of the University of North Carolina- Asheville are thanked for their assistance with the Mössbauer analysis. Thanks to Dr Thalia Chatzisymeon for usage of the

COD meter. I am grateful to the lab and facility technicians Domnhall McGowan, Louise Hogg, Caroline Delahoyde, Jim Hutchenson, Derek Jardine of Edinburgh and Michelle Plue, Dr Ellen Cooper, Dwina Martin of Duke for their advice and assistance.

Thank you to my colleagues, Sorcha Daly, Michael Ross, Konstantina Davididou, and Dr Miriam Cogan of Edinburgh for their kindness and discussions. Thank you to Dr Alexis Carpenter and Stephanie Laughton for their collaboration on some works related to Anaerobic Digesters (Chapter 7) and Dr Aaron Forbis-Stokes of Duke for his training and support with the GC-FID/ECD.

Lastly, I would like to thank my friends and family. I owe everything to my parents and my sister Erin. Your love has shaped my world. Future Dr Richard Fitzpatrick and Dr Lucy Freem you have been the best of friends, and I am genuinely grateful to have you in my life. Ruari Kerr, I love you so much. Thank you for letting me make a home with you.

Table of Contents

CHAPTER 1 : LITERATURE REVIEW 1

1.1 CHLOROPHENOLS 3
1.1.1 2,4,6 Trichlorophenol 5

1.2 REMEDIATION TECHNOLOGY FOR 2,4,6-TRICHLOROPHENOL 9
1.2.1 Biodegradation 9

1.2.2. Disinfection Techniques for the Degradation of Organic Contaminants 20

1.2.3 Filtration, Aeration, and Thermal Processes 25

1.2.4 Water Treatment Additives (Sorbents, Nanomaterials) 26

1.3 ZERO-VALENT IRON 33
1.3.1 ZVI Treatment Mechanism 35

1.3.2 Degradation of Chlorophenols by ZVI 36

1.3.3 Environmental Factors Influencing Treatment 38

1.3.4 nZVI for TCP Treatment in Water Systems 40

1.3.5 Modifications to ZVI to Enhance Treatment 45

1.4 SUMMARY 53
1.5 THESIS AIMS AND OBJECTIVES 55

CHAPTER 2 : MATERIALS & METHODS 59

2.1 INTRODUCTION 59
2.2 MATERIALS 60
2.3 SYNTHESIS 60
2.3.1 Multiple Addition Synthesis 61

2.3.2 1-Pot Synthesis 63

2.3.3 Oxygen-Free Synthesis 64

2.4 CHARACTERIZATION 65
2.4.1 Particle Size 65

2.4.2 Surface Area 66

2.4.3 Surface Morphology 66

2.4.4 Metal Distribution 67

2.4.5 Iron Oxidation 67

2.5 CONTAMINANT PHYSIOCHEMICAL PROPERTIES 68
2.5.1 Representative Chlorophenols 68

2.5.2 Representative VFAs 68

2.6 CHEMICAL AND BACKGROUND SOLUTIONS 69
2.6.1 Chlorophenols 69

2.6.2 Volatile Fatty Acids (VFAs) 69

2.7 UNCERTAINTY AND ERROR 70
2.8 REPLICATION AND CONTROLS 70
2.9 ANALYTICAL TECHNIQUES 71
2.9.1 Chlorophenols *71*
2.9.2 Volatile Fatty Acids (VFAs) *73*
2.9.3 General Analytical Methods *74*
2.10 EXPERIMENTAL PROTOCOLS 75
2.10.1 Methods for Chapter 4: Contaminant Adsorption and Degradation of 2,4,6-Trichlorophenol *75*
2.10.2 Methods for Chapter 5: The Effect of Water Characteristics on TCP Sorption and Degradation by nZVI-Osorb *77*
2.10.3 Methods for Chapter 6: Complexity of Treatment in Real Applications *79*
2.11 MATERIAL TRANSPORT AND STORAGE 82

CHAPTER 3 : SYNTHESIS & CHARACTERIZATION OF NZVI-OSORB 85

3.1 INTRODUCTION 85
3.2 NZVI EMBEDMENT TECHNIQUES 86
3.2.1 Multi-Addition Embedment Method *87*
3.2.2 1-Pot Embedment Method *90*
3.2.3 Oxygen-Free Embedment Method *91*
3.3 MATERIAL CHARACTERIZATION 92
3.3.1 Iron and Bi-metal Distribution *93*
3.3.2 Surface Properties *98*
3.3.3 Iron Oxidation *102*
3.3.4 The Rate of Oxidation (50 Day Trial) *105*
3.3.5 The Rate of Oxidation (48 hr. Trial) *108*
3.4 SUMMARY 110

CHAPTER 4 : ADSORPTION AND DEGRADATION OF 2,4,6 TRICHLOROPHENOL BY NZVI-OSORB 113

4.1 INTRODUCTION 113
4.2 SORPTION PROPERTIES OF TRICHLOROPHENOL BY NZVI-OSORB 118
4.2.1 Absorptive Capacity and Contacting Time *118*
4.2.2 Sorption and the Effect of Contaminant Partitioning of TCP By-Products (DCP, CP, Phenol) *127*
4.2.3 Affinity and Leeching of TCP in Kinetic Systems *130*
4.3 DEGRADATION OF TCP BY NZVI-OSORB 134
4.3.1 TCP Degradation by nZVI Reported in Literature *135*
4.3.2 Modifications to Improve TCP Degradation by nZVI-Osorb *138*
5.4 SUMMARY 140

CHAPTER 5 : EFFECT OF WATER CHARACTERISTICS ON TCP SORPTION AND DEGRADATION MECHANISMS BY NZVI-OSORB 143

5.1 INTRODUCTION 143
5.2 EFFECT OF SALINITY ON TCP SORPTION BY NZVI-OSORB 146
5.3 THE EFFECT OF ATMOSPHERIC AND DISSOLVED OXYGEN ON TREATMENT 151
5.4 EFFECT OF PH ON TCP SORPTION BY NZVI-OSORB 155
5.5 EFFECT OF SECONDARY ACIDS (VFAS) ON TCP TREATMENT 163
5.6 SUMMARY 170

CHAPTER 6 : EFFECT OF NZVI-OSORB ON MODEL ANAEROBIC DIGESTER DOSED WITH TCP 174

6.1 INTRODUCTION 174
6.2 TREATMENT OF 2,4,6 TRICHLOROPHENOL IN A MODEL ANAEROBIC DIGESTER 179
6.2.1 Anaerobic Bioreactor Setup 179
6.2.2 Quantitative Water Quality Parameters 182
6.3 SUMMARY 194

CHAPTER 7 : CONCLUSIONS 196

CHAPTER 8 : FURTHER RESEARCH 201

GLOSSARY 205

LIST OF SYMBOLS 209

LIST OF FIGURES 211

LIST OF TABLES 215

THESIS RELATED PUBLICATIONS 217

PRESENTATIONS 217

APPENDIX 1 219

PERIODIC IRON OXIDE FORMATION (50 DAY TRIAL) 219
LANGMUIR ISOTHERM MODIFIED FOR BETTER FIT 220
ACID RECOVERY FOR AEROBIC VS ANAEROBIC SORPTION TRIALS 221
PRELIMINARY MODEL ANAEROBIC DIGESTION TRIAL EXCLUDING CONTROLS H AND I 223

REFERENCES 227

Chapter 1 : Introduction & Literature Review

As of 2015, the global population was 7.3 billion people. According to the revised United Nations 'World Population Prospects' report, the population is expected to grow by 1.2 billion people by 2030 and then by further 1.2 billion people by 2050[1]. This expanding population is anticipated to put additional strains on earth's critical resources, notably water. Increased demand coupled with overuse of current supplies, inadequate sanitation, and underleveraged waste recycling have made current consumption practices unsustainable[2]. Furthermore, a significant increase in greenhouse gas emissions has resulted in global climate change whose effect on ocean acidification, rising sea level, and increased severity and frequency of weather events could further strain water management and resources.

Despite these mounting issues, progress is being made both in policy and in technology. Access to water and sanitation were officially recognised as a human right by 2010's 64/292 UN Resolution. A Resolution that also went on to acknowledge that these water rights were essential to the realisation of all other human rights[3]. The Paris Agreement, initiated on 4 November 2016, unified 144 ratified nations for the first time to meet global emission targets and reduce forecasted climate change impacts (Fig. 1.1) [4].

Figure 1.1 Ministers representing 170 countries gathered to attend the 2016 signing of the Paris Agreement at UN headquarters in New York City[5].

Global investment to correct these mismanagements must start now. Currently, 40% of the world's population (approx. 2.92 billion people) deal with some issue related to water security because of political, economic, or climatological reasons. Over half (62.5%) of these water issues are directly related to inadequate sanitation. Individuals most affected by water concerns are in the developing regions of Africa, Asia, and Latin America[5]. These are the same regions forecast to see the most substantial population growth in the coming decades.

In developed water-rich nations, domestic and industrial activities have led to an influx of generated wastewaters, and chemical usage has led to a rise in non-point-source water contamination. Common pollutants include; industrial chemicals, volatile organic compounds (VOCs), plasticisers, pesticides, dioxins, polycyclic aromatic hydrocarbons (PAHs), disinfection byproducts like trihalomethanes (THMs), various chlorinated organics, personal care products (PPCPs), perfluorinated chemicals, pharmaceuticals and various metabolites[6, 7]. Often these detected compounds, pose a health risk to humans, plants, and various other animal life (even in low µg/L concentrations) while perpetuating the potential for further potable water contamination[8]. Most influent waters detect these

contaminants in dilute concentrations (μg/L), yet such concentrations do not necessarily negate associated health risks. Their dilute appearance can complicate remediation strategies mandating additional or alternative treatments [9]. Given these concerns, removal and treatment of these compounds remain critical for a thriving planet.

These significant environmental problems are slowly being addressed. Nations across the globe are working to manage and mitigate water contamination issues through continual advancement of water treatment and remediation technologies[10]. New materials, such as nanomaterials, are being developed and tested for application and improved contaminant treatment [11, 12]. Waste recycling processes, like anaerobic digestion, have seen growing demand to bolster sustainable energy production and reduce total greenhouse gas emission [13].

As population growth continues to place a higher demand on existing water systems, it is imperative that the water quality of discharged effluent is ensured not only for sustained environmental preservation but potential reuse as well[14]. This is just the beginning of the work required. There is a long road ahead. This thesis seeks to take a step in the direction of improved water quality by developing new remediative materials and assessing their properties, functionality, and application for the treatment of a specific model contaminant examined in the following sections, 2,4,6-trichlorophenol.

1.1 Chlorophenols

One type of water contaminant that has proven to be particularly pervasive in water is chlorophenols. Chlorophenols have a wide range of uses (Table 1.1) and are generated in industry at a rate of approx. 100-kilotons per annum. They have been detected in surface waters, groundwater, wastewaters, drinking water distribution channels, and soils[15]. Typical contaminant range can vary from ppb to the ppm concentrations depending on the water source[16]. These compounds are toxic (carcinogenic) at ppb levels, persistent with limited biodegradation, and onerous to remove from the environment via traditional water processing and treatment [15].

Table 1.1 General properties for phenol and various chlorophenols of interest[19].

Contaminant	Structure	Use	K_{sp} (g/L)	$LogK_{ow}$	pK_a
Phenol		Broad industrial use	83	1.46	9.99
o-Chlorophenol		Solvent, disinfectant	28	2.39	8.56
2,4 Dichlorophenol		Chemical intermediate	4.5	3	7.89
2,4,6 Trichlorophenol		Biocide	0.9	3.7	6.23
Tetrachlorophenol		Biocide	1	4.45	5.14
Pentachlorophenol		Pesticide, disinfectant	0.018	5.15	4.70

Phenol, composed of a phenyl group (C_6H_5) with one hydroxyl group (OH^-) forms the base structure of all chlorophenols. Phenol is a petroleum-derived substance commercially produced at an excess of 10 billion kg/yr. Usage of phenol is mostly for industrial synthesis and is an essential precursor in the synthesis of plastics, notably bisphenol-A[17]. Chlorinated species of phenol (chlorophenols) are primarily utilised in agriculture as a biocide. Chlorophenols also serve as useful model compounds because their advanced derivatives include a wide array of problematic water contaminants including organohalide pesticides and insulators such as polychlorinated biphenyls (PCBs)[18].

Properties such as water solubility (K_{sp}), partitioning values ($LogK_{ow}$) and dissociation constants (pK_a) detailed in Table 1.1 help to predict how individual compounds will behave in a particular water system. For example, within the group of chlorophenols, water solubility (K_{sp}) decreases with increasing chlorine substitution. Less substituted phenols have lower partitioning values ($LogK_{ow}$) making them more likely to persist in water rather than partitioning to soils. Importantly all chlorophenols are weak acids and tend to dissociate (pK_a) in solution above a given pH. Highly substituted chlorophenols such as trichlorophenol (TCP) (pK_a= 6.23) are onerous to remove from most water because their pK_a values are below 7 dictating that the compound will be dissociated or charged in

most natural and neutral waters. Their charge can complicate remediation by standard adsorption mechanisms which typically have the highest affinity for uncharged nonpolar chemical species [14].

Physical properties, such as the order of halide substitution, can also dictate toxicity. The most chlorinated form of chlorophenol, pentachlorophenol (PCP), has the highest level of toxicity of the various chlorinated species. Yet, due to this toxicity, usage and synthesis of PCP have primarily been curbed. Of the 19 possible constituents of chlorophenol; 2-chlorophenol (2-CP), 2,4-dichlorophenol (2,4-DCP), and 2,4,6-trichlorophenol (2,4,6-TCP) are most often detected in drinking-water[19]. The latter, 2,4,6-TCP, is a common chemical by-product and species intermediate in water chlorination and combustion[20]. This compound still maintains broad industrial and commercial usage despite contamination and toxicity issues making it the chlorophenolic compound of highest interest [21]. The work of this thesis was hence mainly focused on 2,4,6-TCP.

1.1.1 2,4,6 Trichlorophenol

2,4,6-Trichlorophenol is a weak acid composed of an aromatic ring with a hydroxyl group and three chlorine atoms attached to the 2nd,4th, and 6th carbon (Fig. 1.2). This molecule is a solid at room temperature and is typified by a pale-yellow colour and strong phenolic odour [22, 23].

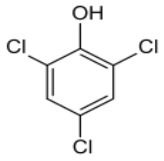

Figure 1.2 The chemical structure of 2,4,6 trichlorophenol.

As a compound, TCP is widely utilised for its antimicrobial properties as a fungicide, herbicide, insecticide, antiseptic, defoliant, glue & wood preservative, flame retardant, and chemical reagent [24]. Widespread usage as a biocide in land-based agriculture applications accounts for its typical non-point source water exposure [25]. TCP

can also enter water systems as a degradation by-product of more complex chlorinated hydrocarbons or from direct industrial waste discharges[26]. The contaminant can also be formed in the chlorination process in the final stages of water processing as a disinfection by-products (DBP) [27].

Production of TCP was first recorded in 1950 in the United States, and today three manufacturers located in China, India, and Europe produce TCP. Recent environmental releases of TCP were estimated to be 5,443 kg in the United States in 2005 with a majority injected directly into underground injection wells. The most recent available record from 2007 indicated that TCP environmental releases were substantially lower at 233 kg [28].

The calculation of total non-point source TCP discharges to water poses significant difficulty given the multitude of exposure pathways. It is clear however that TCP has been detected broadly in groundwater, wastewaters, soils, and the food chain (Table 1.2)[29]. The highest concentration of TCP appears in wastes and wastewaters where contamination levels are routinely higher.

Table 1.2 Detectable TCP concentration ranges found bioaccumulated in aquatic biota, excreted in human urine, and neat in various environmental systems[31].

Presence	**Location**	**Concentration Range** (µg/L)
Air[28]	United States	0.001
Groundwater[28]	United States	≤ 91.3
Surface Water[28]	Canada	≤ 30
Drinking Water[28]	United States, Canada, Finland	0.014 to 0.7
Wastewaters (Municipal Sewage)[30]	United States	0.05 to 22.6
Wastewaters (Municipal Sludge)[31]	United States	190 to $1.3x10^6$ *(µg, dry)*
Wastewaters (Industrial Effluent)[31]	United States	526 to 3,000
Soils (leachate)[31]	Canada	17
Anaerobic Digesters[32] *(variable by feedstock)*	India	Total Chlorine in Biogas 0 to 5,000 *(Inhibitory ≥ 500 to 1,000)*
Aquatic Biota (Goldfish)[28]	New Zealand	≤ 40.5
Urine of Adults[26] (Aged 18-68)	Germany	0.1 to 7.3

Removal and remediation of contaminated waters containing TCP are of consequence because of TCP's extreme toxicity to both humans and ecobiota eliciting acute toxicity, histopathological changes, mutagenicity, and cancer [24, 33]. TCP is listed as a 'probable human carcinogen' (Group B2) by the United States Environmental Protection Agency with specific links to lymphomas, liver cancer, and leukaemia in mice and rats[20]. The dominant exposure pathway for humans is largely occupationally associated via direct dermal exposure or inhalation [34]. However, exposure through potable water and the consumption of fish from a contaminated lake can exhibit symptoms similar to direct

occupation exposure with elevated incidences of Non-Hodgkin's lymphoma and soft-tissue cancers [35].

In Jarvela, Finland, a local timber mill in operation from 1940-1984 utilised fungicide 'KY-5', a compound composed of 2,3,4,6-tetrachlorophenol and 2,4,6-trichlorophenol. Mismanagement resulted in point-source TCP groundwater contamination between 56,000 and 190,000 μg/L. This groundwater was utilised as potable water for the town and monitoring of the utilised water in 1987 (three years after KY-5 discontinuation) detected TCP concentrations ranging from 70-140 μg/L in the treated waters. Villagers were also susceptible to additional TCP exposure from consumption of local fish in lakes contaminated from the plumes of groundwater contamination[35]. Usage of these contaminated water supplies was discontinued yet an updated study in 2013 found a continuing trend of elevated digestive tract infections, asthma, depression, and morbidity in residents[26].

TCP is regulated as a priority substance in processed waters under European Commission Council Directive 2008/105/EC with a maximum allowable concentration (MAC) of 0.4 μg/L[36]. In the United States, TCP is also regulated in processed waters by the US Environmental Protection Agency with a maximum allowable concentration level (MCL) of 0.5 μg/L in potable waters and 2 mg/L in wastewaters[37, 38]. The Agency for Toxic Substances and Disease Registry (ATSDR) of the U.S. Department of Health and Human Services established an oral Minimal Risk Level (MRL) at 0.003 mg/kg/day for TCP [39]. To limit exposure, the European Union set a target limit of 0.1 μg/L and a MAC of 0.5 μg/L for all organohalide pesticide residue on any food or feedstock[26].

Environmental fate of TCP varies dramatically by its location. It has a half-life of 26 days in air where it is photochemically reduced by hydroxyl radicals. It is expected that TCP will dissociate slightly in most aqueous environments. TCP has a longer half-life in surface waters with an average of 60 days in a river and 150 days in a lake. In these environments, TCP has a high potential for bioconcentration with residual molecules adsorbing to sediments/suspended solids or volatilizing to the atmosphere [28]. TCP is typically immobile in soils and presents reduced rates of biodegradability due to microtoxicity. TCP's half-life in soils is variable, ranging from 5 to 20 days in ideal environments that have a high level of biodegradation and photolysis, but in environments

where natural degradation factors are less amiable, the chemical may persist for years in soils[40].

It is understandable given TCP's high toxicity and broad detection in a variety of waters, wastes, and soils why many countries consider TCP to be a 'priority pollutant'. Developing and refining treatment technologies to remediate TCP is of apical importance [20].

1.2 Remediation Technology for 2,4,6-Trichlorophenol

Developing and improving remediation technologies in environmental systems is a complex task. Most water and waste treatment technologies are explicitly tailored to address their unique composition, often preventing universally applied solutions from dealing with specific contamination issues. This diversity in treatment often produces diversity in results. A concise overview of available treatment applications for TCP would allow determination of where these industries are succeeding and where new technologies might best be applied to refine existing treatment. For clarity, treatment strategies are discussed in order of increasing complexity starting first by examining natural biodegradation processes in a variety of waters, followed by a review of standard engineered treatment processes (flocculation/sedimentation, filtration, disinfection), and ending with additives (sorbents, nanomaterials) applied in tertiary treatments or as an amendment to prior treatment steps.

1.2.1 Biodegradation

Given the broad appearance and diversity of biological organisms in water systems and their importance in aiding TCP treatment, the following sections discussing biodegradation were grouped by source and water type starting with aerobic surface waters, then anaerobic groundwater systems, waste and sludge systems in water treatment, and then finally sludges and agricultural feedstock in anaerobic digesters. This in-depth examination of biodegradation will show that environmental context is highly important and that while bioremediation may provide sufficient treatment in some areas (e.g. surface

water), in other areas it does not, thus warranting secondary remediative and treatment processes.

Fate & Transport in Surface Waters, Aerobic Biodegradation

In surface waters, contamination routinely enters from non-point source factors such as industrial and agricultural runoff. This exposure pathway is typical of TCP contamination. High water volume coupled with the dilute contaminant concentration displayed by most contaminated surface waters complicate traditional remediation strategies because these systems were designed to address point-source groundwater contamination and wastewaters where contamination is usually localised and present in higher concentrations[41]. Given these attributes, contaminated surface waters are often managed not through remediation, which would require extremely high operational costs, but through limiting human exposure.

Efforts are made to prevent the consumption of aquatic resources such as fish or shrimp. Approaches to limit additional contamination from surrounding waste streams are commonly examined and implemented [42]. A deftly managed water system will also work to develop site-specific water quality criteria (WQC) to ensure the correct level of protection is applied [43].

Recent studies have focused on trichlorophenol contaminated surface waters to improve understanding of the fate and transport of these contaminants in open water systems as well as toxicological effects on aquatic biota. Studies have been conducted in the Netherlands [44], Finland [45], Canada [46], Sweden [47], United Kingdom [48] and China [49] with extensive work focused on Taihu or 'Tai Lake' in Jiangsu province, China [49-51]. In general, these various studies [20, 26, 45, 52, 53] have found that:

- TCP bioaccumulates in aquatic biota with varying levels of toxicity
- Partitioning into soils mainly follows K_{OC} predictions with deposition varying by pH and soil composition
- Some biodegradation is observed over time

In general, TCP is mostly resistant to aerobic degradation due to inherent micro-toxicity and compound stability. Detailed studies of Lake Tai, however, found some biodegradation by select organisms residing within the lake ecosystem. Bacteria, fungi, cyanobacteria *Chlorella vulgaris* and algae species *Anabaena flos-aquae* could degrade TCP through o-methylation to 2,4,6-trichloroanisole (TCA). While TCA is considered non-toxic and greatly preferable to TCP in water systems, TCA remains a problematic chemical intermediary because of its inherent taste and odour properties. Its presence in water produces a musky odour with a perception threshold as low as 4 ng/L [49]. TCA becomes an increased issue when surface waters containing the compound are utilised as source reservoirs for municipal drinking water where their odour and taste can be perceived by consumers (Fig. 1.3).

Figure 1.3 Lake Tai in Jiangsu province near Shanghai in China has been a useful case study in studying the effects of TCP contaminated surface waters. Surface waters have been found to contain 152.2 ng/L 2,4,6-TCA, a metabolite of TCP and familiar taste and odour compound[54].

Given the hefty cost associated with remediating surface waters and reservoirs, a secondary approach utilizing biodegradation and the adoption of active regulatory and discharge policies to prevent or limit the introduction of these toxic contaminants into the waterways should also be considered. Smart policy governing the control and use of these

materials can reduce cost down the line by preserving pristine water sources for potable consumption, limiting adverse health effects on flora and fauna, and reducing treatment costs where pristine water resources are scarce [55].

Anaerobic Biodegradation in Groundwater Bioattenuation

Organic contaminants in groundwater often result as an effect of industrial negligence and inadequate disposal of waste products. Modern legislation has sought to curtail this damaging contamination, yet in places where oversight is limited, point-source contamination still poses a threat. Sites, where historical contamination creates an issue to redevelopment or endangers a utilised groundwater resource, are also locations where remediation technology can be applied to neutralise, contain, or remediate groundwater contamination [56].

Every contaminated groundwater site is unique, and most remediation strategies are tailored to specific sites. In groundwater contamination, organics often form a pool in the water table known as a dense non-aqueous phase liquid (DNAPL) site. Routinely, groundwater remediation strategies will also consider contaminated soils which can reintroduce contaminants to the water table with various rain events [57].

Complex contaminant distribution and diverse subsurface geology make remediating these sites particularly challenging. Because of these complications, water remediation strategies are often costly endeavours involving ample material, infrastructure, and personnel costs. Natural bioattenuation for groundwater and soil sites is one of the most affordable treatment strategies to implement [58]. The process uses a combination of dispersion, sorption, volatilisation, chemical transformation, and biodegradation to degrade contaminants over time, but requires sites to have appropriate geochemistry and contamination profiles to be effective [56].

For a site to be suitable for bioremediation, the contaminant plume must no longer be mobile and must be held in a quasi-steady-state. Suitable contaminants typically are only short-chain hydrocarbons (e.g. BTEX) and chlorinated solvents which are readily degraded by anaerobic soil bacteria [59]. Successful treatment will depend on a multitude of environmental factors such as temperature, pH, macro- and micronutrient concentrations,

electron acceptor concentration and type, quantity, and metabolic capacity of the microorganisms [56].

Biodegradation occurs through typical oxidation and reduction reactions (redox) in which the contaminant is the electron donor and oxygen or nitrate is the electron acceptor. Additional electron acceptors such as iron oxides, sulphate, or carbon dioxide can be added to the soil if degradation becomes rate limited [56].

Studies have demonstrated success with bioattenuation of trichlorophenol in modelled soils and groundwater [40, 60]. One study co-immobilized microbial cells from activated sludge in polyvinyl acetate (PVA) to create a biological permeable barrier in a column reactor dosed with 300-600 mg/L loads of 2,4,6-TCP. In some cases, they found a removal efficiency of 99.9% with no formation of by-products[40]. Further studies would be required to examine whether this approach could be applied in other applications such as wastewater where total contaminant loads are higher in concentration.

The lack of by-products is uncharacteristic of broader trends in the field [61-64]. Incomplete mineralisation of TCP is often expected as mono- and di-chlorophenols have low degradation rates by anaerobic bacteria and are likely to persist in the environment[64, 65]. Biodegradation of chlorophenols, in general, is complicated by the group's inherent toxicity to microorganisms. This toxicity produces inhibitory effects which are elevated with increasing substitution of the phenol. This fact is demonstrated by pentachlorophenol which often presents little to no biodegradation in groundwater [64-66].

This inhibitory effect of chlorophenols coupled with incomplete biomineralisation have consequences for overall microbial health. Typically, metabolism of TCP produces intermediaries such as electrophilic metabolites like catechols, chlorocatechols, guaiacol, chloroguaiacol, and syringol that can bind or damage gene production or DNA in the cells [26].

Differences between degradation observed in the field compared to results obtained in bench studies, like the Razavi study from 2000 [40], are most likely due to the uncharacteristically high concentrations of TCP and microorganism loading as well as the fact that the microbes in the study were acclimatised to the contaminant over 24hrs to prevent cell death. The inclusion of a substrate (PVA) ensured high permeability which is not always assured in natural sites. Additional complexities of geological composition,

water flow, rain events, and heterogeneity in contaminant profile can also affect degradation results [40]. However, studies like Razavi's are a step in the right direction, and the development of additives that can aid biodegradation while remaining non-toxic to microbial organism has the potential to improve in-situ remediation despite inherent complexities within the process.

A few studies over recent years have taken a different approach to enhance bioattenuation treatment through the inclusion of specific species of plants like *Arabidopsis*[67] or fungus species like *Clitocybe maxima*[68] to propagate phytoremediation (Fig. 1.4). These two studies found uptake, bioaccumulation, and biodegradation of TCP within the organism's cells. An extensive review of bio- and phytoremediation species to degrade PCP was published in 2014 and hints at the promising potential for this field [69].

Figure 1.4 (Left) Arabidopsis thaliana known commonly as Mouse-Ear Cress and (Right) the mushroom species Clitocybe maxima[54].

Overall bioattenuation is an encouraging method for TCP treatment in groundwater. However, this treatment method, like others, faces challenges due to inhibition from natural biotoxicity and the multitude of environmental factors (geological composition and morphology) that complicate treatment models and effectiveness[14, 70, 71]. Research is underway to improve bioattenuation and phytoremediation treatment efficacy to isolate contaminant plumes more efficiently. If successful, such work could potentially broaden the applications usage in field sites and would reduce the need for costly secondary remediation methods [70].

Examinations of surface and groundwater have shown that while TCP does present a biotoxic effect on microbial life, the dilute contaminant concentrations coupled with an ample treatment window (months to years) have typically permitted adequate treatment of TCP contaminated waters. However, when contamination loads are increased, and treatment is required instantaneously, such as in water and wastewater treatment, bioremediative methods alone will not be sufficient and instead will often produce toxic intermediate compounds and by-products.

First, let us examine the standard treatment process. The first process in any water treatment system is phase separation. These procedures, known as sedimentation and flocculation, separate out suspended solids and particulate matter from the water held in treatment tanks[9]. Coagulants are added to destabilise suspensions in the flocculation process. These coagulants are typically metallic salts like aluminium sulphate or ferric sulphate[2]. In some cases powdered activated carbon (PAC) is added to assist coagulation in the flocculation process[41].

However, these materials do not offer a perfect solution. Some metallic coagulant have been found to contain µg levels of organic contamination[72] and these coagulants do not, in general, fully address contamination issues the waters[73]. Some newer studies have indicated the potential for more active coagulants, such as ferrate (VI), to act as an oxidant, disinfectant, and a coagulant in wastewater[74, 75]. A UK pilot trial utilizing ferrate was successful at reducing suspended solids, phosphate, COD, and BOD in low doses and improvements to the coagulants' stability and reduction in cost could further broaden its usage[76].

Once coagulated, solids then form a sludge blanket at the bottom of the holding tank that can be syphoned or drained off where needed. These sludge blankets are biologically active and are sometimes utilised to facilitate biodegradation (Fig. 1.5)[13].

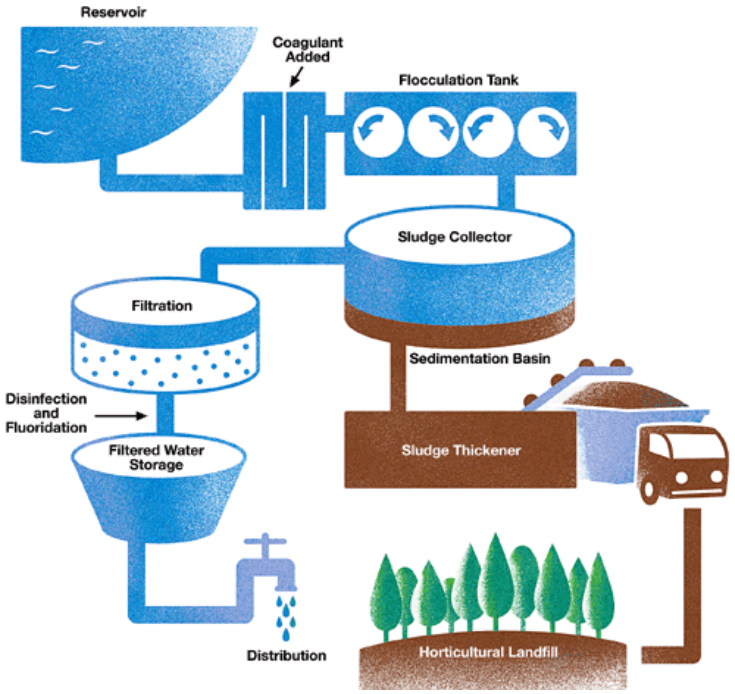

Figure 1.5 A simplified diagram of the standard water treatment process [77].

Fate and transport mechanisms of TCP in these wastewaters will vary depending on their water compositions. As detailed in Table 2.1 phenol and chlorophenols are soluble in water with low molecular weights and will not precipitate out of solution because of the addition of a metallic salt [78]. However, chlorophenols with higher degrees of substitution do have higher partitioning values and may in some cases be suitable for partial removal by sorption when PAC is present [79]. It is expected that some TCP will accumulate in the activated sludge blankets, but complete removal is not assured given the contaminants' detection in later stages of the water treatment process [49, 80].

Biodegradation methods have been studied for TCP mineralisation in anaerobic sludge relevant to both wastewater treatment and anaerobic digesters utilised in biogas production[81]. As with bioattenuation, anaerobic microorganisms in sludge reactors degrade highly chlorinated phenols through reductive dehalogenation [82].

Up-flow anaerobic sludge blanket (UASB) reactors utilised in wastewater treatment processes reclaim biogas through filtering untreated water through a sludge blanket and capturing mobilised gases in the up-flow system (Fig. 1.6) [83].

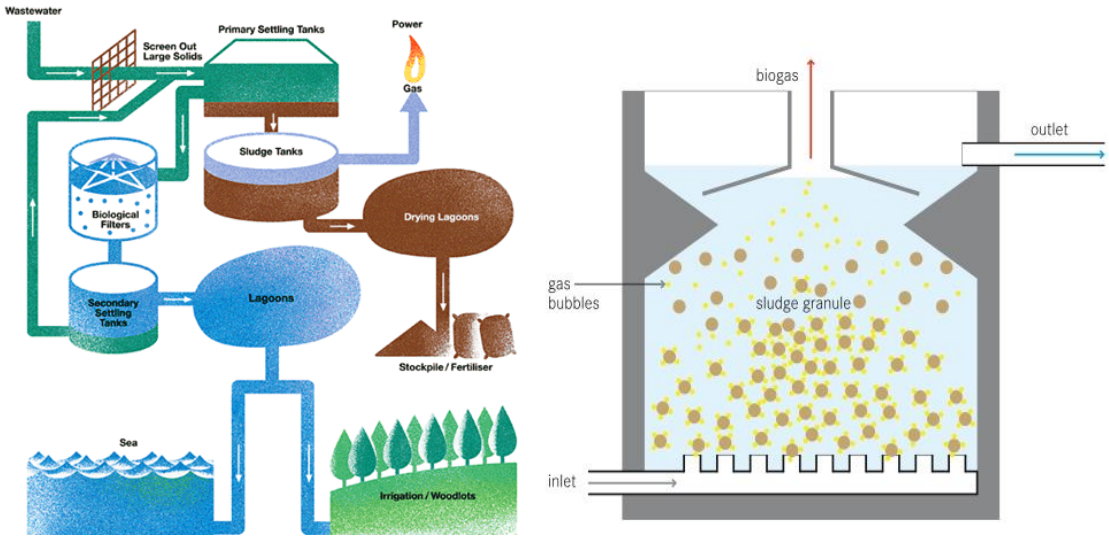

Figure 1.6 Left: A simplified model of wastewater treatment utilising a UASB system for biogas production[77]. Right: A simplified model of a UASB reactor[54].

In some laboratory trials, sludge blankets were impregnated with a secondary bacterium to aid degradation. In one model UASB with immobilised bacteria in an up-flow reactor containing 4.94-54.89 mg/L TCP per day was able to degrade 2,4,6 TCP to 4-CP. As expected, TCP concentrations above 24.88 mg/L displayed rate retardation from microbial inhibition. Anaerobic bacteria were co-immobilized with aerobic bacteria in air-limited conditions to achieve full mineralisation (1.97-99.91 mg/L TCP per day) [81].

While laboratory studies do indicate positive results for the biodegradation of wastewaters, the production of intermediate chlorophenols and other by-products still poses a significant concern[21, 84]. One solution could be the addition of aerobic bacteria applied in a polishing treatment which could allow for the final degradation of dichlorophenol and chlorophenol through aerobic catabolism and oxidation of the aromatic ring[60]. Alternatively, the development or addition of secondary elements such as reactive metals which could aid natural biodegradation (without enabling secondary toxicity) could be of benefit in this regard [85]. Without these additional treatments, less-chlorinated by-products are expected to persist within the system [81].

Biodegradation in Anaerobic Digesters

Wastewater biodegradation has significant overlap with processes related to anaerobic digesters utilised for biogas production and sludge detoxification in wastewater treatment and biogas production in stand-alone agricultural waste-focused reactors. The latter utilise various non-woody organic feedstocks and process waste streams from a variety of sources (agricultural, petroleum refining, tanning industries, industrial operations such as molasses fermentation)[86]. These wastes are then digested by anaerobic bacteria to produce a mixture of biogases containing methane (50-70%) and carbon dioxide. The digested feedstock can be reapplied as a soil conditioner to reduce the need for additional synthetic fertilisers, and the biogas can be utilised to produce heat, road fuel, or as fuel inputs into Combined Heat and Power (CHP) facilities[87] (Fig. 1.7).

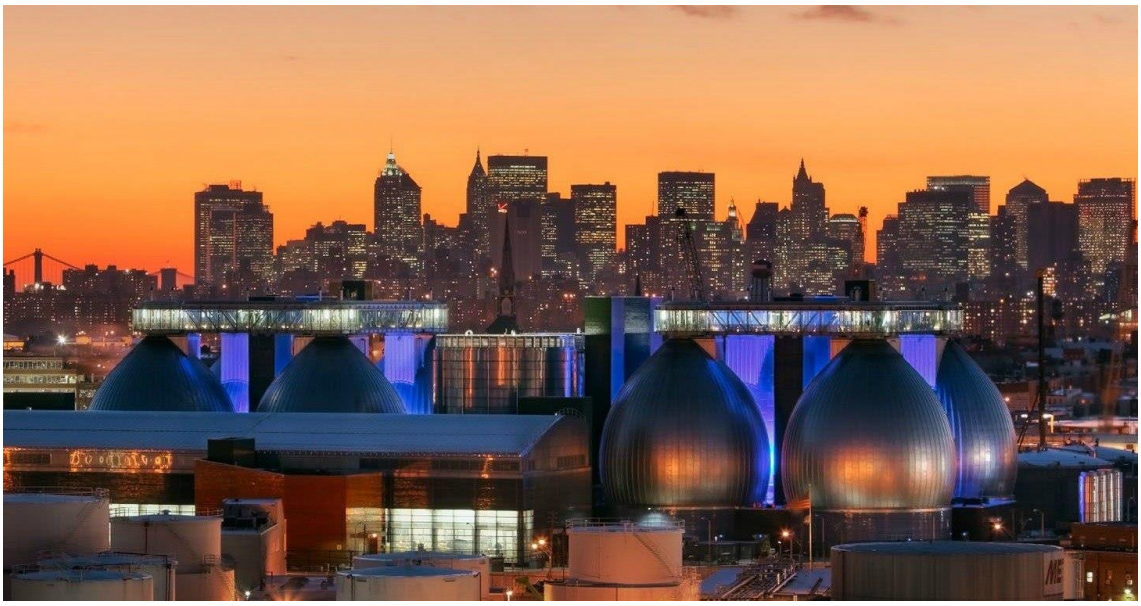

Photograph © Jeff Goldberg/Esto for Ennead Architects

Figure 1.7 A photo of anaerobic digesters within the Newtown Creek Wastewater Treatment Plant in Brooklyn, New York [88].

Contaminants are often introduced into these agricultural anaerobic digestion reactors from the intake feeds[89]. Chlorophenols are a significant component of these

contaminants because of their pervasive use in agriculture. Additionally, the higher presence of chlorophenols in a wide variety of water sources further contributes to their appearance and detection in downstream systems such as municipal wastewaters in concentrations ranging from 0.05 to 22.5 µg/L (ref: Table 1.2) [90].

Unlike TCP contamination in groundwater, surface water, and wastewater where remediation serves primarily to protect environmental flora and fauna; TCP treatment in anaerobic digesters serves a critical secondary function related to the system's overall process. Studies have shown that chlorophenols are inhibitory to methanogenic processes governing biogas production in anaerobic digester systems and in some cases high levels of chlorophenol contamination can fully compromise the entire functionality of the system[91]. This finding applies to other inhibitory contaminants also commonly found in intake feeds thus making contaminant management in anaerobic digesters a critical feature to their operation and hence an area of high scientific interest [92].

In anaerobic reactors, TCP is sorbed through the cell membrane of microorganisms where they disrupt the proton gradient and decrease overall cellular energy transduction between catabolic and anabolic reactions. As a direct result of this inhibition cell growth decreases[93]. The toxicities of independent chlorophenols depend on the position and number of chlorine ions present on the phenol [94]. Pentachlorophenol, the most toxic form of chlorophenol, has been found to inhibit both acidogens and methanogens at concentrations as low as 0.5-10 mg/L [93].

Microorganisms biodegrade chlorophenols through dehalogenation; yet often degradation is incomplete leading to toxic intermediaries such as trichlorophenol. The substitution of the chlorine atoms also affects the level of toxicity with meta > para >> ortho (decreasing order of toxicity). It was reported that 2,4,5 TCP > 2,3,5-TCP > 2,4,6 TCP > 2,3,6 TCP with 2,4,5 TCP being the most toxic configuration [14].

While this review has shown that biodegradation is possible within these anaerobic waste and wastewater systems, it does not provide a complete solution to the contamination issue. The detection of TCP in the final stage of the water treatment process and the production of TCP by-products in biodegradation continues to be problematic. The inhibitory effect of TCP on anaerobic digesters production of biogas is even more concerning. The development of new materials that could completely degrade TCP

without posing biological risk could be hugely advantageous to remote-treatments applied to surface waters, activated sludges in wastewater, and anaerobic bacteria in biogas digesters.

While biodegradation is a useful green method for contaminant degradation, it is exclusively utilised in the treatment of waters or wastes not intended for further human consumption and utilised in municipal wastewater treatment processes in tandem with more substantial systematic infrastructure and treatment. A further examination of how TCP is affected in standard water treatment processes could help elucidate which current treatment methods are best suited to TCP, where there is room for improvement, and where newer solutions could be implemented to enhance treatment.

1.2.2. Disinfection Techniques for the Degradation of Organic Contaminants

Disinfection is an essential part of drinking and wastewater treatment. Chlorination was the foundational method of treatment, but the modernisation of water treatment has seen the development of new disinfection methods such as irradiation by UV and advanced oxidation techniques. These methods are primarily utilised to treat biological components in the water yet these energy intensive processes may also affect organic pollutants within the water and therefore should be examined [9].

Advanced Degradation through Oxidation

Chemical and biological oxidation strategies have been successfully applied for TCP treatment in drinking and wastewaters producing a significant reduction in contaminant concentration[14]. Conversely, alternative chemical oxidation strategies applied in groundwater applications have shown little success in remediating these contaminants [95]. This discrepancy in results makes evaluating the process for both waters of interest.

In groundwater, oxidation strategies utilising potassium permanganate have been

implemented in the past for complex contamination sites including phenols but are discouraged for the treatment of organic contamination given the likelihood of by-product formation[96]. Other chemical oxidatives such as hydrogen-, calcium-, or magnesium peroxide, have also demonstrated potential to degrade phenols yet perform best under highly acidic conditions (2.5 to 3.5). Specific alkaline geology (e.g. limestone) or mildly basic soils will drastically limit the effectiveness of oxidisers [97]. In general, most oxidative remediation strategies have demonstrated little to no effect at degrading more complex chlorinated aromatics such as pesticides, polychlorinated biphenyls (PCBs), or polyaromatic hydrocarbons (PAHs) [95, 97].

Use of these oxidisers with TCP may even increase the compound's toxicity to microorganisms. Often these oxidative remediation strategies result in vast pH changes (usually a significant pH reduction) within the exposed groundwater. pH shifts are particularly problematic when working with chlorophenols[97]. Chlorophenols' toxicity is highest in the compound's non-dissociative form. Un-ionized chlorophenol molecules are more soluble in lipids allowing for more natural diffusion across cell membranes [98]. Therefore, chlorophenols present in low pH solutions below their pK_a (Table 1.1) will have an excess of protons (H^+), higher concentrations of non-dissociated phenol, and display the higher levels of toxicity to living organisms[14]. Additionally, changes in pH which will result in subsequent changes to overall solubility thus altering partitioning coefficients and further complicating fate and transport models for chlorophenols in groundwater [22].

In traditional wastewater treatment, water parameters show lower levels of variability and are easier to contain and control then subsurface in-*situ* treatment making oxidation a more suitable solution for TCP treatment in water and wastewater. A study of several wastewater plants utilising oxidative techniques found a reduction of total phenolic concentrations by 88.95 to 99.97%, a significant improvement over other treatment methods discussed in this review[30].

In this study of 5 municipal wastewater treatment plants, two plants were found to contain 2,4,6-TCP concentrations above US EPA discharge limits (1.4µg/L for water and organism consumption, 2.4 µg/L for organism consumption). A total of seventeen distinctive phenols were observed in influent waters, and five phenols (2,4,6-TCP, phenol, 2-CP, 2,5-DCP, 2,4-dichloro-3-ethyl-6-nitrophenol) were detected in the effluents.

Concentrations of chlorophenols in this water were all relatively low ranging from 0.05 to 22.6 µg/L. Conclusions about each treatment process from the study are detailed in Table 1.3 [30].

Table 1.3 A wastewater treatment study observing the effect of various processes to treated chlorophenols[30].

Treatment	Phenol Removal Eff. (%)	Suitable for Phen. & CP Treatment	Pros	Cons
anaerobic/anoxic/oxic (A^2/O)	100	Yes	Removed all CPs Can remove N_2 & P Other studies find ~98% phenol removal	Has the potential for by-product formation
Continuous microfiltration (CMF)	~40	No		No CP or phenol treatment
Ozone oxidation and Chlorination (O_3 +Cl_2)	5	No		Poor treatment Cl^- can form CPs
Anoxic/Oxic (A/O)	100	Yes	Removed five difs. phenols **Best treatment**	Created phenol as a by-product
Conventional Activated Sludge Treatment	~85	No		Produced phenol and 2,4,6-TCP byproducts **Worst treatment**
Hydrolysis acidification & biological filter	98	Yes	Better removal efficacy than activated sludge	Produced most by-products
Hydrolysis acidification & membrane bioreactor (MBR)	100	Yes	Slightly better than biological filter	Produced CPs MBR-difficulty removing low molecular weight particularly CPs
Chlorination (Cl_2)	0	No		Can produce CPs from phenol

The best treatment method was found to be A/O or A^2/O. The worst treatment method was conventional activated sludge which produced regulated phenol and 2,4,6-TCP by-products that were not present in the influent. Continuous microfiltration (CMF) system are not expected to retain dissolved species or particulates over >0.2 μm. However, in this study, higher chlorophenolic concentrations were detected in the effluent. Higher chlorophenol concentrations were attributed to partial adsorption and subsequent contaminant accumulation within the membrane over time. These results signal that both activated sludge and CMF treatment processes are inappropriate methods for treating chlorophenols in wastewaters[30].

Utilizing different treatment methods in tandem could help localise the by-product formation issues. The authors concluded that best treatment option for these phenol-contaminated wastewaters would be a combination of continuous microfiltration (CMF), anaerobic/anoxic/oxic (A^2/O), ozone oxidation (O_3), and chlorination [30]. Despite this effectiveness, there is indeed room for improvement. Most treatment options present some form of limitation such as reduced capacity, the generation of by-products, incomplete mineralisation, or high operating costs [99]. The development of new materials that could enhance oxidation treatments without dramatically raising costs would be in high demand.

Degradation of TCP by UV Irradiation

Often if wastewater or drinking water facilities are not using oxidation or chlorination for primary disinfection, they will most likely be utilising ultraviolet (UV) irradiation. UV disinfection offers a chemical-free alternative for water disinfection. While this method is extremely effective at treating microorganisms, particularly ones that are known to be chlorine resistant such as Giardia and Cryptosporidium, the process is ineffective against most inorganic (salt, heavy metals, etc.) and organic contaminants (pharmaceuticals, long chain carbons like petroleum)[100]. This is also the case for TCP which is not entirely degraded via standard UV processes [101].

Researchers have sought to improve TCP treatment with UV by adding further treatment steps including the use of peroxymonosulfate to aid degradation and activated

carbon to adsorb the degradation by-products [102]. Others looked at utilising photocatalysts like titanium dioxide (TiO_2) [101, 103, 104] or following UV treatment with a biological-based degradation [105]. While these modifications have enhanced UVs treatment range, these modifications often produced degradation by-products which are problematic[102]. By-products of regulated contaminants will typically need to be reprocessed for removal and existing treatment structures modified with speciality or tertiary treatment to ensure suitable discharge levels are met.

1.2.3 Filtration, Aeration, and Thermal Processes

Filtration

In filtration processes, waters are usually subjected to a series of filtrations to remove any remaining microscopic particulates. Filtration typically increases the effectiveness of disinfection in final stage chlorination which immediately precedes water distribution to the consumer.

In this process, water is filtered through a bed or series of beds composed of sand, fine sand, and a final layer of anthracite coal[9]. While effective at particulate removal, standard filtration processes are not suitable for trichlorophenol removal whose molecules are too small for this type of size exclusion[106]. Some partial adsorption of TCP may occur on sand [107] and carbon surfaces [108], but affinity is often weak with sorptive interactions counteracted by flow forces [109].

New studies have developed and evaluated novel membrane filtration systems such as nanofiltration and ultra-filtration systems for improved contaminant and particulate exclusion and treatment [110]. One group was able to successfully remove TCP from solution utilizing a powdered activated carbon (PAC) dosed feed tank (20% with 13µm PAC, 30% with 5µm PAC with initial 400 µg/L TCP) prior to secondary treatment of waters with a hollow-fibre ultrafiltration (UF) membrane[111]. Another group utilising colloid enhanced ultrafiltration was able to remove 90% of loaded TCP 4.93mg/L (25mM) [112].

While this field shows great promise at expanding the treatment range of contamination using filtration principles these systems are still costly, not universally applied in standard water treatment practices, and face significant issues with biological fouling [113-115].

Volatilization through Aeration and Thermal Sparging

When problematic molecules are not removed through filtration, other phase separation processes can be considered. Small molecule organic water contaminants typically have low boiling points and in many cases, will readily volatilize into the atmosphere[116]. These properties are exploited in groundwater with the use of thermal applications (i.e. steam flooding) and in groundwater and drinking water with the use of aeration [56]. Unfortunately, neither of these applications is well suited for the treatment of TCP [117].

Thermal applications such as steam flooding produce the risk of chemical by-products as well as incuring high energy and labour costs [97]. In municipal water treatment, aeration is useful in the removal of dissolved gases such as carbon dioxide, methane, and hydrogen sulphide but not appropriate for phenol or chlorinated phenols. Similarly in groundwater treatment air sparging has successfully been used to remove lighter chlorinated organics such as trichloroethylene which can readily be mineralised yet is also considered inappropriate for aromatics which do not quickly degrade and are less volatile [95]. Air sparging is particularly ineffective in groundwater applications if the contaminant plume is particularly mobile or soils present low-permeability. Utilizing these methods for TCP could potentially worsen contamination by increasing the volume of contamination either by soil or air [97].

1.2.4 Water Treatment Additives (Sorbents, Nanomaterials)

This review has demonstrated that TCP is a problematic contaminant and current treatment and remediation practices are inadequate at completely removing the

contaminant and often produce by-products in degradation. New materials may provide a solution to the issue of incomplete mineralisation and limited contaminant removal if they can be easily integrated into existing treatment infrastructure and demonstrate effectiveness at removing problematic species. There remains an extensive body of research on sorbents, and more recently nanomaterials, testing innovative bench-scale approaches to water contamination issues [118].

So far the implementation of these new techniques has remained limited to specific applications because of cost, issues in scale-up, or reproducibility[2]. A more in-depth exploration of sorbent and nanomaterial additives and their ability to treat chlorophenol in waters has the potential to aid the development of new treatment technologies that can either replace or modify existing treatment structures in all water and waste environments.

Sorbents

When contaminants persist through to the final stages of treatment often tertiary options are considered. Typical examples of this tertiary treatment include nanofiltration or reverse osmosis which utilises adsorption or ion exchange processes[119]. Ion exchange is utilised for the removal of ionic contaminants such as arsenic, fluoride, nitrates and is not appropriate for the removal of trichlorophenol[120]. Adsorbents, conversely, are suitable for organic contaminants and offer the most effective method for targeted removal of contaminants [121].

The most promising method of treatment of chlorophenols and their byproducts in water treatment is through physiochemical adsorption. In this process, high-affinity matrices are utilised for the concentration of dilute contaminants in a heterogeneous media[122]. This process, unlike oxidation or irradiation, produces the likelihood of removal without producing additional byproducts[30]. Sorption is also advantageous over other separation processes (extraction, distillation, filtration, or precipitation) because the sorbates are concentrated and contained in a solid phase bed which can be either regenerated or easily discarded [123]. In general, sorbents incur significantly lower overhead costs compared to expensive membrane treatments like nanofiltration or reverse osmosis.

Materials such as activated carbon, zeolites, and modified cationic clays have been well tested in the field [124, 125].

Sorption mechanisms for organics onto organic sorbents such as activated carbon, rely on a large negatively charged surface of small pores to facilitate physisorption of the contaminant. Similar sorption mechanisms are displayed in inorganic sorbents like silica, which while uncharged, still facilitate physisorption through a porous matrix. Importantly, adsorbate size and functional groups strongly influence adsorption affinity. In the case of these adsorbents, adsorption is favourable to nonpolar, low-solubility contaminants that have low affinity for water and will readily adhere. These properties explain why higher sorption is typically found for more substituted molecules with higher hydrophobicity for most sorbents[22]. For example, pentane, a small nonpolar molecule, has shown adsorption upwards of 225 mg/g with 30 minutes of contact by GAC[126] compared to 109.9 mg/g of 4-chlorophenol adsorbed by a similar GAC sorbent[127]. Chlorophenols, in general, are particularly tricky to treat with sorption alone because of their partial solubility in water and moderate polarity.

However, sorbent and sorbate properties are not the end of the story. Environmental conditions such as pH, temperature, salinity, the mixture of the compounds, and grain size of the sorbent can further influence sorption mechanisms and can complicate the treatment process[127]. These factors are particularly important in consideration of TCP. As a weak acid, alterations in pH can change the protonation of the chlorophenol species (especially if these pH changes occur around the compound's pK_a) [22]. In sorbents that have a significant negatively charged surface, like activated carbon, the deprotonation of a sorbate can result in charge exclusion that decreases overall sorption [128]. Adjustments in temperature can change the sorption equilibrium and sorption kinetics of a system as well as the desorption rates[129]. Salinity can likewise alter sorption equilibrium through changing the contaminant's partitioning in solution among other charge exclusion and 'salting out' effects [130]. Sorptive affinity for the individual compound is always unique, and the addition of various potential sorbates can lead to competitive exclusion [66]. Finally, the grain size of the sorbent can influence the overall available surface area which in turn would affect sorption rates[25]. All of these environmental factors are of interest and should be considered in the development of any new sorbent for water remediation applications.

Adsorption capacities of chlorophenols utilising a variety of common sorbents were recorded in Table 1.4 [22].

Table 1.4 Sorption capacities (mg/g) for a variety of sorbents for various chlorophenols [127].

Sorbent	2-CP	4-CP	DCP	TCP
Bituminous Shale	3.1		4.2	
Chitosan			0.14	
Hollow Fibers	26.1	25		35.4
Amino-Modified Mesoporous Silica	275.4			338.8
Granular Activated Carbon		109.9		
Activated Carbon from Milk Vetch		87		
Activated Carbon from Coconut Vetch			19	
Carbon Coated Monoliths		93.7	117.5	
Magnetic Reduced Graphene Oxide	63.8	75	102.3	169.6
Pristine Graphene	88.1	114.2	155.3	175.8

Carbons and graphene adsorption capacities for a variety of chlorophenols range from as low as 19 mg/g for DCP with activated carbon produced from coconut vetch to as high as 175.8 mg/g for TCP using pristine graphene. This capacity while significant is modest when compared to adsorption rates achieved by amino-functionalized mesoporous silica which had adsorption capacities of 275.4 mg/g for 2-CP and 338.8 mg/g for TCP [127]. High sorption capacities of the silica are linked to high porosity and surface areas along with favourable amino-TCP interactions in solution and would suggest that silica-based sorbents are a more appropriate choice for chlorophenol removal than carbon-based sorbents like GAC when judged solely on removal capacity.

Yet, most potable water treatment facilities utilise GAC for final water polishing and volatile organic contaminant (VOC) removal over sorbent alternatives. This sorbent is reasonably priced, readily available, useful for a wide range of contaminants, well studied,

and has established infrastructure for smooth implementation. The adsorbent is particularly suitable for removing oils and nonpolar solvents [131].

However, this material is not without flaws. GAC is typically utilised in a stationary bed in-line with a fluid stream. Adsorption can rapidly diminish as active sites become filled by sorbate. The bed must undergo periodic regeneration to regain functionality, before ultimately becoming permanently exhausted. Natural organic matter (NOM) can block GAC active sites required to sorb organic contaminants shortening reactor lifespan to 90-120 days[132]. Other organic compounds such as trihalomethane (THM) or haloacetic acids (HAAs) in drinking water processes can reduce lifespan to <30 days[133]. Incomplete sorption of chlorophenols would require longer dwell times in GAC reactors and may require additional treatments.

These issues would suggest that there is a need for new materials that can effectively treat contaminants that prove challenging to remediate by standard practices. Silica-based sorbents have been shown to outperform carbon-based sorbent in terms of organic sorption capacity and therefore have a high potential to increase adsorption rates for chlorophenols in water treatment[133-136]. While silica-based sorbents are significantly more costly than GAC, their material costs are on par with other engineered nanomaterials such as graphene, and could likely become more price competitive with increased usage[137]. Furthermore, silica's chemistry lends itself to relatively easy functionalization (such as the amino-functionalized silica detailed in Table 1.4). This creates the potential for molecular imprinting and selective adsorption a feature that could prove particularly useful in water treatment and remediation [124, 138].

Furthermore, the development of novel materials that could adsorb problematic compounds with high capacity and selectivity would be in high demand. These systems coupled with a reactive element to degrade target contaminants could prove particularly useful in these water systems. This model creates the potential for a catalytic system that can concentrate sorbates at reactive sites where they can be degraded efficiently. Such a system creates the potential for a more efficient treatment model in water systems. The sorptive element in this system could be a silica-based material. The reactive element in the proposed system could, for example, be a non-toxic metal catalyst, like iron.

Nanomaterials

The most prominent leap forward in contemporary material science has been the broad implementation of nanomaterials. Their small size produces high reactivity and unique functionality that has been broadly applied in electronics, medicine, and even water treatment processes [10].

High surface areas and high throughput values make them advantageous in membrane technologies with the development of nanofiltration, nano-bioreactors, and aids in turbidity removal[2]. Reactive nanoelements have been applied to improve both chemical and UV disinfection processes [139, 140]. Nanomaterials have also been applied in water sensors to enable better water resource management and contaminant detection and monitoring [12]. Some types of nanomaterials and their potential applications in water treatment are detailed in Table 1.5.

Table 1.5 A overview of available nanomaterials and their potential applications in water treatment [2, 141].

Class of Nanomaterials	Nanomaterial	Target Contaminants
Nanostructured Membranes	Carbon Nanotubes (CNTs)	Bacteria & Viruses
Nano-Reactive Membranes	Alumina Silica Pt/Fe Bimetals Alumina/ Au	Dyes Metals TCE N_2 & Phenols
Polymer-Supported Membranes	Polymer TiO_2 Polymer Al, Si, C	PAHs THMs, PAH, Pesticides
Zeolites	Toluene, NO_2, C, ACF CeO_2, CNT	BTEX Metals
Carbon Nanotubes	CNT/Polymers CNT/Fe CNT Multiple CNTs	Nitrophenols, Benzene, Toluene Metals THMs Herbicides, Metals, THMs
Self-Assembled Monolayered Mesoporous Support	SAMMAS	Inorganic Ions, Heavy Metals, Actinides
Biopolymers	Chitosan	Dyes, Metals
Single Enzyme Nanoparticles	SEN	Enzyme Stabilization for Biodegradation
Bimetallic Nano Iron Particles	Pd-ZVI	Heavy Metals, Halogenated Organics, PCBs, Chlorophenols, Nutrients, Radioelements, Microorganisms
Nanoscale Semiconductor Photocatalysts	Crystal TiO_2 N-TiO_2 Fe(III)TiO_2 TiO_2 Nanotubes	Metals Azo Dyes Aromatics Toluene

Nanomaterials have been applied for the treatment of TCP and chlorophenols with varying degrees of success. Nanosorbents, such as a synthetic zeolite or halloysite nanotubes, have demonstrated adsorption of trichlorophenol in varying capacities from water[142, 143]. One group has even gone so far as to molecularly imprint a polymer for selective adsorption of TCP [144]. However, these materials cannot degrade the contaminant and will become saturated after a period of use [143].

A group utilising Fe_3O_4/g-C_3N_4 nanocomposites was able to degrade TCP to hydroxyl radicals utilising advanced photodegradation methods, but their material presented limited reusability [145]. Another group utilising nano- $SrTiO_3$ also for photodegradation of TCP observed similar issues[146]. Titanium dioxide (TiO_2), a conventional photocatalyst, has been used on several occasions to degrade chlorophenols[103] and phenols [101, 104, 147] however complete mineralisation was not always assured often resulting by-product formation.

While these sophisticated nanomaterials have demonstrated promise both in sorption and degradation of TCP their broader application in water treatment is restricted mostly due to cost, scaling issues, instability, and limited reusability[11]. One nanomaterial that breaks this trend is nano-scale zero valent iron (nZVI). nZVI has remained relatively affordable, is non-toxic to humans, presents high reactivity with a broad range of treatable contaminants including extensive usage in large-scale groundwater applications for the degradation of chlorinated organics [148, 149].

These factors have made nZVI one of the most studied nanomaterials for water treatment [150]. Given this significance, it is necessary to take a more in-depth study of nZVI to understand the materials properties, mechanisms of treatment, environmental factors influencing treatment, results from experimental trials and further methods for modifying and improving treatment.

1.3 Zero-Valent Iron

The base molecule, Iron (Fe), is element number 26 existing the first row of transition metals in the periodic table. The most abundant element on Earth, iron

composes roughly 5% of the planet's surface. Iron is also a reactive metal possessing a wide range of oxidation states from -2 to +6 with Fe (II) (ferrous) and Fe (III) (ferric) being the most common. As such, iron is typically found in nature as iron oxides (commonly Fe_3O_4 or Fe_2O_3) [151]. Iron becomes zero-valent iron (ZVI) when iron oxides or iron halides have been reduced to metallic iron and contains no charge (Fe^0) due to a filled outer electron valence shell. This process occurs readily creating a metallic iron that is highly reactive with a substantial reduction potential (E^0=-0.44V)[151] and has produced a significant demonstrated efficiency for the rapid degradation or removal of a wide variety of contaminants (Table 1.6).

Table 1.6 A list of the types of contaminants that can be removed or treated by ZVI [150].

Type of Contaminants treated by ZVI	**Examples**
Antibiotics (β-Lactim / Nitroimidazole)	Penicillin Derivatives, Megazol
Azo dyes	Dinitroaniline Orange
Organophosphates	Malathion, Chloropyrifos
Nitroamines	RDX
Nitroaromatics	Trinitrotoluene
Inorganic Ions	Nitrate, Perchlorate
Alkaline Earth Metals	Barium, Beryllium
Transition Metals	Chromium, Cobalt, Copper, Lead, Nickel, Silver
Post-Transition Metals	Zinc, Cadmium
Metalloids	Arsenic, Selenium
Actinides	Uranium, Plutonium
Chlorophenols	p-chlorophenol
Chlorinated Solvents	Chloromethanes, Chlorobenzene, Chloroethylenes
Chlorinated Pesticides	Lindane, DDT, Atrazine
Polybrominated Diphenyl Ethers	Decabrominated diphenyl ether
Polychlorinated Biphenyls	PCBs

1.3.1 ZVI Treatment Mechanism

These treatment pathways for these contaminants can include sorption, complexation, (co)precipitation, and surface-mediated reduction. Precipitation and adsorption mechanisms are considered reversible while co-precipitation and reductive mechanisms are irreversible [150].

ZVI can not degrade inorganic contaminants (metals, metalloids, ions). With these inorganic compounds, ZVI is often utilised to form insoluble metals and ion complexes that precipitate and immobilise the contaminant in the water source. This process occurs by direct electron transfer from the iron to the contaminant [152].

In most cases, a reduction and degradation mechanism can occur if the contaminant is organic. In the presence of dissolved oxygen, this reduction mechanism is referred to as Fenton's reactions (H_2O_2 & Fe^{2+}). Fenton's reactions can proceed with iron in its zero-valent state as ZVI (Fe^0) or in its oxide formations as maghemite (Fe_2O_3) [153] or magnetite (Fe_3O_4) [154].

The reduction involves a two-electron transfer with ZVI and dissolved oxygen (O_2) in water to produce hydrogen peroxide (H_2O_2) **(1.1)**. ZVI can undergo further reduction by an additional 2-electron transfer from remaining Fe^0 **(1.2)** or react with Fe^{2+} in Fenton's reaction to produce hydroxyl radicals **(1.3).** These free radicals have strong reduction potential and are active in the breakdown of organic contaminants [155].

$$Fe^0 + O_2 + 2H^+ \rightarrow Fe^{2+} + H_2O_2 \quad \textbf{(1.1)}$$

$$Fe^0 + H_2O_2 + 2H^+ \rightarrow Fe^{2+} + 2H_2O \quad \textbf{(1.2)}$$

$$Fe^{2+} + 2H_2O_2 \rightarrow Fe^{3+} + \cdot OH + OH^- \quad \textbf{(1.3)}$$

Iron's reductive properties are particularly useful when it comes to halogenated organics, in particular, chlorinated aliphatic (R-Cl). ZVI has been harnessed for *in-situ* groundwater treatment for the reduction of compounds such as chloromethanes and chloroethanes [151, 156] since the early 1990s [155].

The treatment mechanism for these chlorinated compounds involves the corrosion of iron and the concurrent reduction of a chlorinated species as seen by the generalised reaction **(1.4).** In aqueous environments, iron oxidation leads to an increase in pH and the formation of an iron hydroxide precipitate **(1.5)** [152].

$$RCl + H^+ + Fe^0 \rightarrow RH + Fe^{2+} + Cl^- \quad \textbf{(1.4)}$$

$$Fe^0 + 2H_2O \rightarrow Fe^{2+} + H_2 + 2OH^- \quad \textbf{(1.5)}$$

This foundational underpinning of ZVI's treatment mechanism for organic contaminants provides a framework for comprehending iron degradation mechanisms specific to chlorinated aromatics like chlorophenols.

1.3.2 Degradation of Chlorophenols by ZVI

In the specific case of chlorophenols, treatment mechanisms are similar but have a few distinct differences. Unlike reactions in open chain structures (such as chloroethane), halides spatial orientation is typically restricted sterically by the cyclic structure of the aromatic ring and even further by phenol's hydroxyl group [157]. This aromatic steric hindrance will promote the reduction of the chlorines located in an anti-orientation[158]. Therefore, Cl^- ions in the *ortho*-position are always cleaved first followed by *meta*- and *para*- positioned atoms [159]. Cleavage of the chlorine by ZVI is considered a stepwise process following an electron-transfer catalysed aromatic $S_{RN}1$ substitution[160] **(1.6).**

Halide cleavage: $C_6H_5OHCl_3 + H^+ + Fe^o \longrightarrow C_6H_5OHCl_2 + Fe^{2+} + Cl^-$ **(1.6)**

One-electron reduction: $C_6H_5OH \longrightarrow C_6H_5O\cdot + e^- + H^+$ **(1.7)**

Complete mineralization: $C_6H_5OH + 14\ H_2O_2 \longrightarrow 6\ CO_2 + 17\ H_2O$ **(1.8)**

Further reduction of phenol results from Fenton's reactions detailed above aided by partial sorption and precipitation mechanisms **(1.7, 1.8)**[161]. Both degradation processes can occur concurrently. π-π stacking interactions stabilise aromatic structures and

therefore will require significant energy inputs (excess of -3,070 kJ/mol) for ring cleavage [157, 162]. Aromatic carbon-chlorine cleavage requires less dissociation energy (-407 kJ/mol) and will more readily occur in solution with ZVI [163, 164].

Various studies have found that more chlorinated phenols, such as PCP, show lower rates of degradation. The energetic electron donating hydroxyl (-OH) group and the strong electron withdrawing groups (Cl^-) substituted on the aromatic ring influence the acid-base behaviour of the phenol and its overall reduction by radical intermediates implicit in both halide cleavage and aromatic cleavage. This change is observed quantitatively by the standard reductive potential for the various compounds (E_{red}^0) (Table 1.7) [14, 165].

Table 1.7 A list of pK_a and standard reductive potential (pH=12) for various chlorophenol [165]. The standard reductive potential is a value that demonstrates the compounds propensity to be reduced under standard conditions.

Contaminant	**Structure**	**pK_a**	**E_{red}^0 (pH 12)**
Phenol		9.98	0.86
o-chlorophenol		8.56	0.93
2,4 Dichlorophenol		7.89	0.88
2,4,6 Trichlorophenol		6.23	0.90
Tetrachlorophenol		5.14	0.99
Pentachlorophenol		4.70	0.99

In general, the more substituted the phenol, the more reductive potential will be required for a 1-electron transfer reduction. Reduction potential is unusually high for o-chlorophenol because the single chlorine group is located next to the hydroxyl group creating a robust steric hindrance. The further the chlorine is located from the hydroxide

group the lower the steric hindrance and lower the required reductive potential (3CP E_{red}^0=0.88; 4CP E_{red}^0=0.85)[165].

The full mineralisation of phenol to carbon dioxide and water in equation **(1.8)** utilizing ZVI is possible under amiable conditions; however, in the degradation process of TCP, it is expected that some intermediate will form. For TCP these intermediates will include less chlorinated phenols (DCP, CP) and phenol [155]. Intermediate species will be produced either in the interim of the reaction or because of incomplete mineralisation from a lack of available hydroxide radicals produced from Fe^0 electron transfer. Fe^0 loses this reactivity mostly when the atomic surface becomes fully oxidised and forms various iron hydroxides [132]. The formation of an iron hydroxide precipitate along with other insoluble mineral species deposited on the metal surface will decrease iron's reactivity over time[166].

1.3.3 Environmental Factors Influencing Treatment

Physical properties and environmental factors such as particle size, pH, and the availability of oxygen will all strongly influence iron behaviour in treatment. As with most nanomaterials, the small particle size of nano-sized zero-valent iron (nZVI) produces a high surface area to volume ratio manifesting in increased reactivity [152]. Iron as a ferromagnetic element will readily self-agglomerate in solution. This agglomeration limits total surface area and overall reduction capacity. Maintaining high exposed surface area by decreasing particle size and ensuring even particle distribution is essential for maintaining optimal reaction rates.

The acidity or alkalinity of a solution will also strongly affect ZVI not only in influencing the formation of its oxide species but in its reduction rates with target species as well. In general, a low pH produces a reducing environment that is favourable to dechlorination[167]. Acid conditions tend to favour the formation of Fe^{3+} ions which are more conducive to Fenton's reactions and can accelerate the reduction of a target species. Conversely, in alkaline environment iron oxides tends to form as ferrous hydroxide ($Fe(OH)_2$) which is less favourable to Fenton's reactions [168]. Protonation dynamics of an

acidic sorbate, like TCP, which will be negatively charged above its pK_a are expected to influence degradation mechanisms by increasing overall electronegativity and should be experimentally evaluated.

Lastly, nZVI is considered unstable in aqueous solutions and will readily form a surface shell of iron-oxides. This process, when referring specifically to formed iron-hydroxides, is colloquially referred to as corrosion. It is widely held that corrosion is the most substantial issue limiting ZVI broad application in water remediation & treatment [169].

Corrosion occurs when the reductant, metallic iron, becomes oxidised. This process occurs readily for iron given the metal's strong thermodynamic drive to return to a low-energy state [150]. Corrosion can occur in both anaerobic conditions **(1.9)** by water and aerobic conditions **(1.10)** by dissolved oxygen in the water. Corrosion by dissolved oxygen is more thermodynamically favoured leading to faster corrosion rates. Corrosion of iron remains one of the main limitation of ZVI when applied in water treatment by reducing the materials overall reactive lifespan [170].

Anaerobic	$Fe^0 + 2H_2O \rightarrow Fe^{2+} + H_2 + 2OH^-$	(E^0 =+1.67)	**(1.9)**
Aerobic	$2Fe^0 + O_2 + 2H_2O \rightarrow 2Fe^{2+} + 4OH^-$	(E^0 = -0.39)	**(1.10)**

The Fe^{2+} resulting from this corrosion can undergo further oxidation to become Fe^{3+} **(1.11, 1.12).** This process is usually accompanied by an increase in pH from the formation of additional hydroxyl ions and consumption of hydrogen's protons [150].

$2Fe^{2+} + 2H^+ + 1/2O_2 \rightarrow 2Fe^{3+} + H_2O$	(E^0 =+0.46)	**(1.11)**
$2Fe^{2+} + 2H_2O \rightarrow 2Fe^{3+} + H_2 + 2OH^-$	(E^0 = -1.60)	**(1.12)**

This corrosion process is irreversible in solution and reduces the further electron transfer needed to reduce target contaminants. The addition of a strong reductant like sodium borohydride can scrub surface oxides to expose deeper layers of reactive Fe^0 but is costly and inappropriate for most water treatment processes[152]. Modifications to iron that could reduce undesired corrosion and preserve reactivity would be highly sought in the marketplace and should be developed.

Now that a clear understanding of fundamental properties of ZVI, its treatment mechanism, and conditions influencing its treatment has been discussed, attention can turn to laboratory results of nZVI applied for TCP treatment in a variety of waters.

1.3.4 nZVI for TCP Treatment in Water Systems

nZVI has widely been applied in groundwater remediation since 1995. In the intervening decades over 200 contaminated groundwater sites have utilised nZVI deployed in permeable reactive barriers (PRBs) for remediation. These nZVI PBRs were designated as a 'standard remediation technology' in 2002 by the US EPA[155]. 90% of papers published in the last decade focused on nZVI or ZVI applied for groundwater contaminant remediation making groundwater a starting point in this review section [155].

Groundwater

Unsurprisingly, nZVI is also one of the most promising materials for treating chlorophenols in water when deployed in a PRBs for groundwater remediation[24, 41, 90, 107]. PRBs can be composed of a variety of remediative materials with various internal deployment mechanisms but are most commonly composed of nanoscale zero-valent iron (nZVI). nZVI is particularly suitable for in-situ treatment because of its effectual contaminant remediation, suitable mobility in porous media, sufficient reactive longevity, and low toxicity [171].

In bench research, one group was able to mineralise 90% of phenol by nZVI in 24 hours when aided by ultrasonic radiation which increased contaminant/metal contact[172]. This rapid rate of treatment is significant given that reaction pathways of chlorophenols and phenols are notoriously slow[29] with dechlorination rates increasing with additional levels of chlorination[173]. Another study was able to reduce 2,4-dichlorophenol in a model permeable reactive barrier (PRB) also within the first 24 hours with ZVI supported on the granular sand. In this study, reactivity was preserved for ten days before the loss of reactivity from corrosion [161].

To improve degradation and reduce inhibition of troublesome compounds like PCP new work has focused on co-metabolism mechanisms utilising both bacteria and zero-valent iron. In one study a colony dosed with PCP and 1g/L ZVI was able to increase electron transport system activity (ETS) (a method utilised to measure the respiratory activity of microorganisms) to a maximum leading to improved rates of reductive bio - dechlorination and better degradation of PCP [21].

The main issue with nZVI deployed in PBRs centres on the limited longevity of the reactive iron. Treatment of contaminants by iron requires the oxidation of the iron core, and undesired corrosion can occur through contact with subterranean water [174]. Once oxidised reductive potential is lost, new injections of ZVI will be required periodically to continue the groundwater treatment process. A secondary concern with ZVI is limited subsurface mobility and transport given ZVI affinity to self-agglomerate [175].

To address concerns of agglomeration, ZVI is typically injected as a slurry with a mild surfactant such as sodium dodecyl sulphate (SDS). This process has allowed for excellent dispersion in soils and some reduction in self-agglomeration[176]. However, SDS is not bound to the iron and therefore only assists initial dispersion and cannot aid sorption or degradation once ZVI is dispersed.

Various other studies have been undertaken to increase ZVI reactivity and longevity in-situ with mixed results. Some have attempted to limit corrosion through the addition of a surface coating, but this can also have the dual effect of reducing reactivity towards degradation[177]. Other work has looked at adding a second metal to increase reactivity but could prove cost prohibitive on a large scale. Current work is still underway to address corrosion issues inherent to ZVI and more broadly reactive metals [174].

Future developments and improved nZVI materials which could maintain high reactivity for extended periods of time and would allow for easy dispersion in soils would help improve its application in groundwater remediation[155]. Additionally, advancements in manufacturing that could further reduce the price per kilogram of ZVI would help support its use in groundwater remediation over cheaper oxidative processes [150].

Potable Water

Over the past several decades research has slowly expanded to study the use of nZVI in other areas of the water treatment process including potable water and wastewater treatment[178, 179]. The most common application for ZVI to potable water is for remote treatment of arsenic in well water. In this case, ZVI is not utilised as reductant but as a coagulant to precipitate out arsenic from solution [180-182]. High concentrations of dissolved oxygen as well as atmospheric exposure exacerbate iron corrosion rates and drastically hinder iron's reactivity. Reduced reactivity and significant corrosion would have high associated costs requiring continual iron replacement and thus dramatically limit nZVI applicability for contaminant treatment in potable water [9, 183].

These concerns are also illustrated in bench scale research on the topic of ZVI degradation of chlorophenols in aerobic conditions. Overall results remained mixed. Some studies found decent dechlorination of TCP (25-45% in 30 mins; 40-60% in 60mins, 60-80% in 90mins. 80-95% in 120mins., 100% after 150mins.) [184]. Others found no dechlorination of trichlorophenol[29] or pentachlorophenol[29, 185] by ZVI. The variability of chlorophenol degradation within the literature is most likely attributed to variations in the experimental setup and is a topic that is evaluated experimentally through a variety of environmental conditions and parameters tested in this research to provide greater clarity and mechanistic understanding.

In general, studies found more consistent results and high percentages of TCP reduction when the iron was modified with a secondary metal (Pd or Ni) to catalyse the reaction and improve aerobic degradation. One study, in particular, found 81% and 93% removal percentages of pentachlorophenol by ZVI when complexed with Pd[186]. Another group utilised ZVI/Pd and ZVI/Ni composites and found dechlorination of 2,4,6-TCP in PRBs at faster rates, and in higher percentages of dechlorination than ZVI applied alone. Pd/ZVI systems were able to dechlorinate completely TCP within five days compared to the ZVI reactor which was able to reduce the TCP concentration by 69.96% within the 30 minutes but then saw no further degradation[29].

In bimetal complexes with ZVI, the iron acts as an electron donor and the secondary metal become the primary catalyst often increasing reaction rates [187]. Each

secondary metal will have its own unique catalysation potential following the trend listed in **(1.13)**.

Pd>>Fe-Ni > Fe-Pt ~Fe-Cu ~Fe **(1.13)**

Despite this hierarchy, comparable results to the Tso and Shih study were found by a group utilising nanoscale ZVI/Ni particles to degrade PCP [188]. Another group utilising similar ZVI/Ni materials was able to entirely reduce PCP in 7 days under ambient aerobic conditions[187]. In general, faster dechlorination rates for PCP were observed when a secondary metal was present[188].

Low reactivity of uncomplexed ZVI is most likely due to slow reaction times standard for PCP (first-order at 3.9 $x10^{-3}$/h ±0.7)[189]. It is also known that pH can significantly affect reduction rates with low pH producing a reducing environment favourable to dechlorination [168].

Another study found dechlorination of 2-chlorophenol at a pH of 4 with ZVI as the lone metal. Increased treatment rates were observed when radiation was applied [168]. Supporting these findings one group was able to reduce para-chlorophenol by 93.89% in 5 mins. utilising nZVI at a pH 4 [190]. Several studies indicated that agglomeration and or advanced oxidation of the surface of the metal could have hindered treatment of the chlorophenols [186, 190-192].

Wastewater

Treatment by nZVI in wastewaters faces similar complications as potable water treatment, but contamination concentrations are typically higher in these waters. Often additional complex discharges from domestic and industrial effluents as well as sewage and atmospheric deposition compound the issue of contamination and permit nZVI to have broader applicability [124]. A variety of laboratory studies have utilised ZVI to amend various wastewater treatment processes for the treatment of chlorophenols[21, 94, 190], in addition to other contaminants more generally [83, 182, 193, 194], suggesting that use of ZVI in wastewater

treatment might have the relevant potential for further development.

One particularly promising study in 2015 demonstrated that amino-functionalized particles of silica coated nZVI particles were able to enhance the degradation of chlorinated organic contaminants in anaerobic microbial systems such as anaerobic granular sludge treatment. Utilizing this material, Guan found a 94.6% reduction of total 2,4,6-TCP in the system with the added benefit of decreased toxicity to the anaerobic microorganisms. Guan believed that the decreased toxicity of the overall systems accounted for the overall boost in methane production and increased electron transport activity in the system. Unfunctionalized ZVI and unfunctionalized uncoated nZVI particles were less effective in TCP removal indicating respectively ~39% and ~10% reduction compared to ~50% with nZVI-SiO_2 [179].

While some treatment methods differ in effectiveness for chlorophenol treatment, by-product formation remained a common trend. ZVI has demonstrated potential to degrade and mineralise some chlorophenols completely[174, 195]. ZVI utilised in tandem with anaerobic processes such as A/O, or A^2/O could help reduce potential byproduct formation in wastewater treatment and better control treatment[78]. Anaerobic and Anoxic conditions in these treatments could help preserve iron reactivity and limit metal corrosion[85]. ZVIs overall low cost, nontoxicity, and effectiveness against a wide range of contaminants could be equally beneficial[155]. Coupling these effects with a sorbent, such as silica as discussed in the previous section, could further boost the treatment and remediation potential [138].

Anaerobic Digesters

A field outside the strict realm of water treatment and water remediation that has significant overlap with the anaerobic wastewater treatment processes and mechanisms discussed comprises Anaerobic Digesters (AD). Anaerobic digesters (AD) rely on a variety of sludge and feedstocks to fuel biogas-producing microbes turning waste into energy [32]. These microbes have proven particularly sensitive to incoming contaminants present in the incoming feedstocks[93]. Chlorophenols are of particular concern, and new studies have

indicated that the addition of ZVI to the reactors can increase biogas yields of methane [196-198].

The low oxygen environment found in these reactors may help reduce corrosion rates of the iron while concurrently allowing for chlorophenol degradation and enhanced methane production[198]. All these factors make AD particularly well suited for trials with advanced ZVI materials and emphasise the need for the study of iron interactions with chlorophenol contaminants in anaerobic environments and anaerobic environments that model anaerobic digesters.

Field Trials

While various laboratory studies have demonstrated successful halide stripping and degradation of halogenated aromatics utilising nZVI, it is not widely applied outside of in-*situ* groundwater remediation. This may be due in part to the difficulty in analysis (given TCPs low solubility and concentrations in water), the complexity of the contamination in a given water system [199], the availability of other degradation pathways such as bioremediation for phenols[67, 68, 200], cost of treatment, or availability to other uncontaminated source waters to municipalities [155].

Improvements to nZVI that could ensure longer lifespans, higher reactivity, and lower corrosion propensity, could encourage water providers and utilities to trial larger scale projects with nZVI. Modifications to base nZVI materials are likely required to achieve these objectives.

1.3.5 Modifications to ZVI to Enhance Treatment

Zero-valent iron is prized for its high reactivity and ability to degrade a wide variety of chemical contaminants; however these attributes are often hindered by nZVI's susceptibility to atmospheric oxidation and self-agglomeration [171]. Many studies have been

conducted to modify nZVI to limit these negative features and increase stability and mobility.

Sometimes these modifications include the addition of secondary compounds such as oil [201], polyacrylic acid [202], carboxymethyl cellulose [203, 204], starch[205] or humic matter[206] to encapsulate the nZVI [207, 208]. These surface coatings have been found to reduce corrosion and increase subsurface dispersion, but often the modifications are associated with a decreased rate of reactivity towards target compounds[155]. This observed phenomenon may be due to the decreased surface availability of nZVI in treatment[209].

One study that illustrated this interaction, utilised nZVI coated with calcium hydroxide to enhance subsurface mobility in the treatment of chromium-contaminated groundwater[207]. While particle mobility increased in soils, there was a notable decrease in the reactivity of nZVI. Bare nZVI reduced a Cr(VI) solution by 90% within 30 mins. Conversely, nZVI that had the calcium hydroxide surface coating took six times longer to remove 85% of Cr(VI). When the added coating was washed off the nZVI treatment rates matched those of bare nZVI[207].

While surface coatings can prove to be problematic in nZVI treatment if they hinder nZVI interaction with contaminants, there is still potential for other materials, particularly advanced substrates, to optimise nZVI's functionality by improving iron dispersion and enhancing particle stability. Secondary support such as silica [137, 138, 210-213], activated carbon[214], resin[215], chitosan[216], bentonite [177, 217, 218], pillared clays [176, 219, 220], and polystyrene resins [221] to name a few, have all been trialled. Most commonly, metal nanoparticles like iron have been incorporated in activated carbon[222] supports, but a variety of other novel nanoscale supports have been researched including nanofibers[223], detrimers[224, 225], fullerenes, and carbon nanotubes[226].

Embedding metal and bimetal nanoparticles into a support structure such as organic or inorganic adsorbents or cellulosic material has many advantages[170];

- The potential to decrease particle loss in field application.
- Prevention of self-agglomeration that would result in loss of active sites (nZVI aggregates at diameters above 15nm by ferromagnetism).
- Increased matrix permeability and convective flow within the system.

- A conducive environment for reactivity and free cation flow (H^+) which can perpetuate favourable acidic conditions that hinder the formation of metal oxides and other metal precipitates.
- Direct adsorption of contaminants which could concentrate contaminants at the active sites of the embedded metal for enhanced degradation.
- Potential for better emplacement and effortless regeneration of the oxidised iron particles.

While these metal/granulated activated carbon (GAC) composites are the most common and have demonstrated success at dechlorination of various halogenated organic hydrocarbons the technology remains less than ideal. Whereas GAC can adsorb a variety of organic pollutants, the composite does not prevent the formation or release of breakdown products, does not protect or prevent the early formations of metal hydroxides, and cannot prevent leaching of the embedded nanoparticles[226]. As discussed, there remains a wide body of novel nanomaterial composite alternatives to GAC, but the applicability and commercial viability of these supports are hindered in part due to cost, difficulty in synthesis, and lack of structural integrity to withstand water flow forces[141]. Furthermore, the treatment mechanisms and the interplay between sorption and degradation in these composites remain somewhat unclear. Further studies assessing the treatment mechanism are needed to enhance understanding and provide direction in remedying these drawbacks for future applications.

Other studies which looked distinctly at embedding nZVI into silica have found that the metal can be bound tightly and in some cases iron corrosion could be reduced[137, 138, 184, 208, 210-213, 227]. One study of note looked at embedding nZVI into hydrophilic silica beads and found that this embedment led to an increased shelf life of the nZVI. nZVI stored under atmospheric conditions for one week presented identical XRD spectra to freshly prepared nZVI. The result suggests that surface corrosion was limited in these samples through the addition of a silica substrate[184]. However, in the larger field, there remains great diversity on the effect of silica on iron corrosion. In some cases, iron corrosion is reduced at the expense of iron reactivity, in others the silica network enables continued reactivity but does not restrict corrosion[137, 138, 184, 208, 210-213, 227]. The discrepancies in results

are attributed to variations in the many types of silica utilized and whether the material acts more as a surface coating or a substrate in the composite.

Silica-nZVI composite materials more broadly, have also been found to degrade successfully a variety of water pollutants such as p-nitrophenol[137], nitrobenzene[211], decabromodiphenyl[212], and trichloroethylene[228]. In the study discussed, the silica substrate acted as a surface coating and did not appear to prohibit iron's reactivity towards contaminant degradation allowing for the full dechlorination of 100mg/L samples of 2,4,6-trichlorophenol, dichlorophenol, and 4-chlorophenol respectively after four hours of recirculation within their nZVI-silica packed bed[184]. The closed system in the reaction vessels could have additionally reduced oxygen exposure prolonging nZVI use in degradation and contributed to the successful results observed. The silica utilised in this trial was hydrophilic, and while it is useful as a substrate, the material would not be appropriate for any type of nonpolar organic sorption.

As previously discussed, sorption of organic contaminants from aqueous streams is highly desirable in the treatment of dilute water pollutants. Silica sorbents, in general, have traditionally displayed higher sorption capacities than carbon-based materials (Table 2.4)[15]. Modifications to silica composites that could promote enhanced sorption of organic contaminants both in terms of capacity and range without compromising iron's reactivity could mirror treatment mechanisms at play in carbon-iron composites and could be greatly advantageous in use. One silica-based nanosorbent that is particularly promising is a newly manufactured material called Osorb (Fig. 1.8).

Figure 1.8 Osorb nanomaterial utilised in the synthesis of the novel nanomaterials generated in the present. The materials are composed of semi-opaque granular particles.

More generally, Osorb shares the attributes of other market sorbents such as activated carbon and molecular sieves with regard to (1) possessing a large surface area, (2) general hydrophobicity, and (3) provides enhanced dispersion of embedded materials [141, 183]. Despite these advantages, Osorb is currently not as widely available or utilised as GAC making cost and scale issues in implementation [229].

Unlike most adsorbents such as activated carbon or molecular sieves, which use a highly porous network for the physioadsorption of compounds from water[230], Osorb is a silica-based sorbent that functions on principles of both adsorption and absorption. By this process, dilute concentrations of sorbate adhere to surface structures of the sorbent. Adsorbed analytes then trigger a structural change in the morphology of the sorbent releasing stored energy held in the tensile forces of the collapsed silica matrix created in synthesis. This mechanism, while rare in materials and unique to sol-gel derived silicas[231-233], is referred to as swelling (Fig. 1.9).

Figure 1.9 A series of photographs showing the swelling of Osorb at 0, 5, and 10 seconds from the dropwise addition of acetone onto the matrix in real time[134].

During swelling, compounds of affinity are absorbed into the internal structures of the nanomaterial e.g. absorption (Fig. 1.10). Swelling occurs instantaneously upon contact with organics of affinity but importantly remains hydrophobic and does not swell in water. This functional behaviour creates unique properties that allow for the uptake of nonpolar organic contaminants from aqueous streams[134] and gas phases[135] with higher capacities then sorbents which solely utilise adsorptive mechanisms within fixed structures like GAC[245].

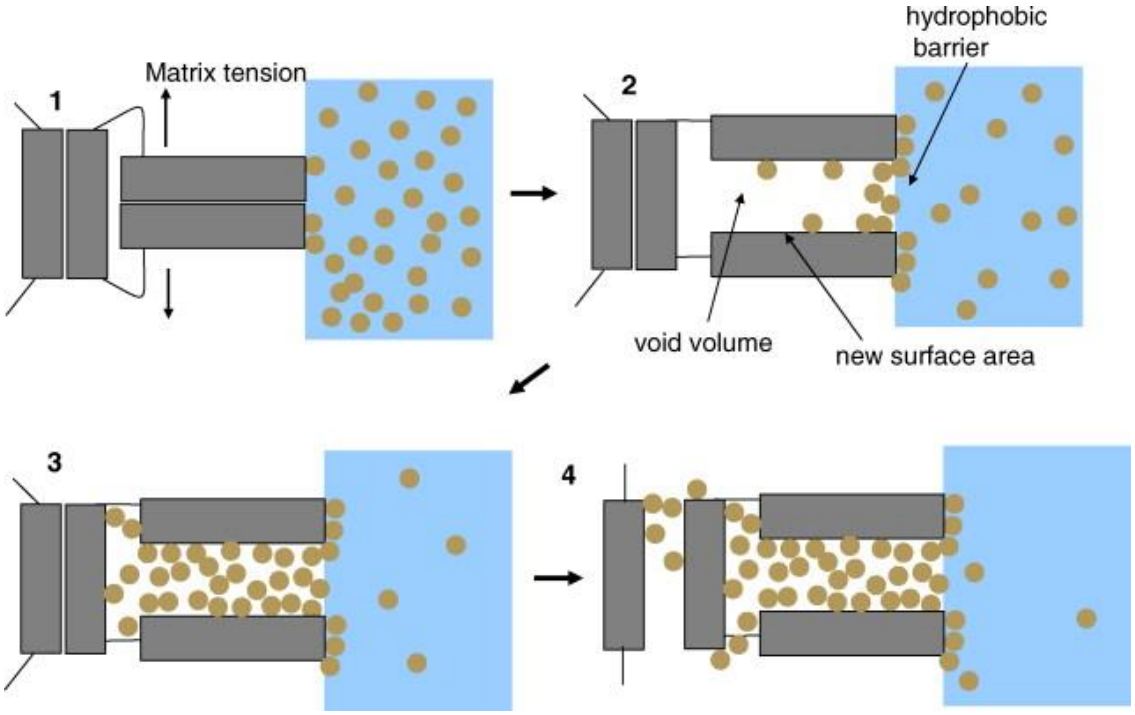

Figure 1.10 A sorption model demonstrating the uptake of an organic compound from an aqueous solution by Osorb. (1) Organics in the water adsorb onto the surface of Osorb. (2) Initial sorption triggers the release of the tensioned silica matrix resulting in swelling, i.e. the expansion of the of the sorbent matrix, thus exposing new surface area and permitting the absorption of organics from solution. (3) Pores become filled with sorbate facilitating further transport of organics deeper into the silica matrix. (4) Additional swelling increases both void volume and available surface area allowing further sorptive processes to proceed[134].

Sorption of organic compounds by this nanosorbent are typically classified as nonspecific and reversible with ambient or heat applied evaporation[135]. Sorption affinities are comparable and in some cases improved over affinities observed with adsorption onto granular activated carbon for organic compounds dispersed in water[134]. As with activated carbon, Osorb's absorption capacity and affinity are higher for non-polar species than polar species. However, Osorb has demonstrated a broader range of sorption capacity than comparable sorbents like activated carbon or molecular sieves, thus enhancing its marketability (Table 1.8).

Table 1.8 Masses of various contaminants sorbed by three different sorbents (Osorb, Activated Carbon, and Molecular Sieves) in a stationary dry bed mass (μg/mg). The elution constant C is measured at bed exit when the concentration entering the bed was at 10% and 90% wherein C_0: C/C_0=0.1 and C/C_0= 0.9 [134].

Dissolved Contaminant	Log $K_{O/W}$	Osorb		Activated Carbon		Molecular Sieves	
		C/C_0= 0.1	C/C_0= 0.9	C/C_0= 0.1	C/C_0= 0.9	C/C_0= 0.1	C/C_0= 0.9
Methyl t-butyl ether (MTBE)	0.94-1.6	5	720	No Sorption		No Sorption	
Trichloroethylene (TCE)	2.40	300	920	930	1500	20	135
Toluene	2.69	350	870	440	480	65	66
Perchloroethylene (PCE)	3.40	660	1080	620	780	170	204
Naphthalene	3.29	149	365*	160	185	**	

* Mass bound/bed mass at C/C0=0.8 (50,000 bed volumes)
**Not Performed

Table 1.8 indicates that Osorb has a broader sorption capacity than comparable sorbents which could not adsorb high solubility compounds like MTBE and showed poor sorption of low solubility compounds like naphthalene, perchloroethylene, and benzene. The sorption capacity of Osorb at 10% elution was on par with activated carbon, and significantly improved over molecular sieves. At 90% elution, Osorb's higher sorptive capacities for organics over AC and molecular sieves become more apparent. Osorb's higher capacity is linked to its unique contaminant uptake mechanism discussed in the previous figure (Fig. 1.10). Both the high capacity and sorptive range of Osorb, support the case for further evaluation and study despite the cost and reduced availablity[134].

In this research, Osorb was selected for use over GAC because initial studies had indicated good sorption of a wide range of organic compounds from water [134, 135]. Sorption studies on chlorophenols utilizing Osorb have not yet been examined, but the broader trend of published results would suggest that partial sorption of these contaminants should be observed in experimental trials. Silica, in general, lends itself to easy chemical modification allowing for the future possibility to imprint the sorbent for selective absorption if initial experimental trials prove promising[234].

Previous studies have indicated that nZVI and nZVI-bimetal could be embedded into the nanosorbent matrix with relative ease and stability[228, 235]. However, these trials did not examine multiple methods of embedment or relate embedment techniques to quantitative results such as particle leeching or efficacy in treatment. Metals once embedded in these foundational trials appeared to retain reactivity suggesting the possibility of delayed oxidation of the iron[236]. However, once again these studies did not directly measure iron corrosion or relate corrosion principles to material reactivity leaving large gaps in the mechanistic understanding of the material in application.

The novel nature of this material means that research is only just developing and this therefore gives a large window of opportunity to explore potential and new applications of use. Previous work has indicated that Osorb is chemically inert and therefore should not have detrimental effects on biological organisms[235] thus encouraging the use of this material in new applications such as in bioactive sludges in wastewaters and anaerobic digesters.

Novel nanomaterials generated by this research utilising Osorb and then embedded with various metals are not expected to have higher removal capabilities than values demonstrated in the primary literature[134]. Sorption still governs the primary method of interaction with these contaminants, and the incorporated metals should not drastically aid or hinder sorptive properties [228, 235].

To improve the overall reactivity of these metal-substrate systems and increase contaminant treatment rates and range, several studies have incorporated secondary metals with high reductive potential. Through embedding a secondary metal, the reactivity of the breakdown can be significantly increased with further potential to prevent toxic byproduct formation [237].

In the treatment of chlorinated organics with nZVI, the initial reaction mechanisms are dichloro elimination (-2Cl) and dehydrohalogenation (-HCl). Increased reactivity with the addition of a second metal is assumed because iron acts as an electron donor (reductant) in the reaction and the secondary metal remains protected and functions as a catalyst. By-product formation can be reduced in these situations by driving nZVI contaminant reduction toward hydrogen reduction rather than by direct electron transfer. The product ratios of formed by-products will depend on the type of bimetal chosen and

the availability of hydrogen in solution[237]. Suitable bi-metals for contaminant dehalogenation range in catalytic activity. The most reactive bi-metal utilised was Pd **(1.13)** [238].

Pd has been used in a variety of tests[16,239], given the high metal reactivity. In one study, the dehalogenation rates of trichloroethylene were increased by 30 fold with the incorporation of Pd on nZVI [23, 240]. The most successful tests in the dechlorination of chlorophenols utilised Pd amended nZVI particles [29, 195, 241, 242].

Despite this reactivity, Pd's applicability is hindered by prohibitive costs of use. New trials have demonstrated efficacy with cheaper and more affordable nanometals such as zero valent aluminium [243], tin [170], copper [238], and nickel [132, 141]. A few studies have indicated that chlorophenols can be reduced by nZVI particles alone decreasing the financial burden and complexity in synthesis further [21, 168, 217].

While bi-metals aid dechlorination these advantages are often hindered by the rapid formation of metal oxides and hydroxide films, the blockage of active sites, and the loss of loosely bound secondary metals [175]. Studies have been undertaken to embed nZVI and various other bimetal nanoparticles into support structures, like the carbon or silica-based ones discussed previously, to combat these issues [138].

The evaluation of modifications to nZVI particles expressed in literature, has demonstrated the potential for nZVI-Osorb composite materials to remedy the inherent limitations of nZVI particles, and suggests that these composites could supersede the performance of materials cited in literature for the treatment of chlorophenols in water.

1.4 Summary

The industrialisation of manufacturing and agriculture has led to a significant increase in point-source and non-point source water contaminants. 2,4,6-trichlorophenols is a harmful water pollutant, that is of particular interest given its wide range of uses and its broad detection in soils and surface-, ground-, drinking-, and wastewaters[26]. Contaminant concentrations in these sites can vary dramatically from ppb to ppm depending on the source[16]. Given their inherent toxicity to aquatic flora and fauna and

their potential threat to humans in dilute ppb concentrations it is essential that these compounds be removed from water[20, 26].

Currently, there is no universal treatment applied to remediate chlorophenols in water and typical treatment relies on the long-standing treatment options common to each water. The level of treatment for chlorophenols varies widely across the field with most degradation-driven treatments resulting in toxic by-product and incomplete removal. There is room to improve current treatment practices for TCP in water and waste systems.

One material that has shown strong potential for the degradation of a wide variety of organic contaminants including trichlorophenol is zero valent iron (ZVI)[107, 186, 244-246]. While ZVI is an incredibly safe, affordable, and effective reductant, the metal has several inherent limitations, e.g. corrosion, reactivity, and dispersion[174, 176, 190]. ZVI is unstable in water and will readily corrode in the presence of oxygen[247, 248]. Oxide formation reduces the reactivity of the metal and can dramatically decrease its longevity in application[249]. Furthermore, ZVI is ferromagnetic and will readily self-agglomerate in solution. This agglomeration reduces the availability of active sites which can further decrease reactivity and complicates dispersion and deployment designs[155, 209].

These limitations have dramatically reduced ZVI's use outside of groundwater remediation applications where more complex infrastructure is available and dissolved oxygen content is typically higher[138, 191, 250]. Modifications to ZVI that could address these fundamental issues and improve ZVI stability and dispersion could allow enhanced treatment both in terms of reactivity and longevity, as well as open pathways to broader applicability in water and waste treatments where issues of contaminant degradation and treatment persist[249]. nZVI could be particularly useful in anaerobic systems in wastewater and anaerobic digestion as a microbial aid which can assist biodegradation of organic contaminants such as TCP and boost biogas production.

To date, a variety of contemporary research has sought to modify nZVI to remedy these intrinsic functional limitations. Most of these modifications include the addition of a substrate (stability / dispersion / reactivity)[107, 213, 251, 252], a surface coating (corrosion / dispersion)[177, 202, 208], a secondary reactive metal (reactivity)[166, 241, 253], or modification to adjust and control particle size (dispersion / reactivity)[192, 219] . While some attempts are more successful than others, the resulting materials usually suffer from low stability, high

cost, and exacerbated corrosion[152, 254]. The development of a new ZVI based material that could improve treatment, restrict self-agglomeration, and delay corrosion is still in high demand and could expand the current application of the material in water treatment[16, 255, 256].

Advanced materials such as sorbents and nanomaterials may provide a solution to improving treatment systems either in tertiary treatment or as amendments to current processes. Silica-based sorbents have demonstrated a high capacity for TCP and provide an exciting opportunity for extraction-based treatment. These sorbents could also be coupled with reactive elements, such as reactive nanomaterials, to concentrate and then degrade problematic water pollutants. A new nZVI-sorbent composite that could have increased effectiveness for chlorophenol remediation and treatment in aerobic and anaerobic water and waste applications should be developed and studied with a robust evaluation of the material's properties, functionality, and potential application.

1.5 Thesis Aims and Objectives

The primary objective of this work is to prepare ZVI-based composite materials with the potential to improve ZVI dispersion and reactivity and then assess the material's performance in terms of properties, functionality, and application for a specific model contaminant 2,4,6-trichlorophenol. A deep understanding of these features could contribute to the development of better treatment materials and protocols for chlorophenols where ZVI is already in use, i.e. groundwater remediation, and possibly expand iron's usage to new treatment applications, e.g. wastewater treatment, anaerobic digestion.

To prepare and assess the materials developed in this work, the primary aim of this thesis was divided into three concrete objectives.

1. **Development**: preparation of nZVI composite materials through embedding iron into a novel nanosorbent, Osorb, for enhancing stability and iron dispersion by physically restricting iron agglomeration, and improve reactivity by increasing iron

particle availability and the further sorption and concentration of contaminants from aqueous solutions near iron reactive sites within the matrix of the material. Then once synthesised, establish an understanding of the material's intrinsic properties through advanced characterisation techniques and oxidation studies.

- Assess three different embedment techniques for metal composition and dispersion with advanced microscopy techniques (SEM-EDS, TEM).
- Quantify physical properties relevant to transport and reactivity (particle size, morphology, surface area) utilising particle sizers, SEM imaging, and BET analysis.
- Quantify the oxidation state of iron in the composite materials and determine the rate of oxidation by atmospheric oxygen through Mössbauer analysis to establish maximum rates of degradation.

2. **Functionality:** evaluation of the nanocomposite's performance in sorption and degradation of a model contaminant (2,4,6-trichlorophenol) in aerobic and certain anaerobic conditions relevant to the surface, drinking, and wastewaters.
    - Determine optimal contact time, sorption capacity, and treatment mechanism critical for an application utilising a free deployment system and GC-FID for TCP quantification.
    - Determine how various environmental factors such as pH, salinity, atmospheric composition, and secondary compounds like VFAs influence sorption and degradation mechanisms.

3. **Application:** apply knowledge of nZVI-Osorb's properties and functionality to interpret effects of nZVI-Osorb deployment in a simplified model application (anaerobic digestion) dosed with TCP.
    - Prepare and evaluate a series of mini-bioreactors modelling anaerobic digesters with a 25 mg/L TCP and 3.9g/L nZVI-Osorb for causal effect and degradation utilising water quality measurements (COD, ORP, pH, head pressure) and TCP concentration utilising LC/MS.

- Determine suitability of the material for anaerobic digester application

The body of this dissertation contains eight chapters. The literature review detailed TCPs treatment in water systems with a focus on nZVI-based treatments. This review established the current gaps in knowledge within the field demonstrating the focused need for improved treatment practices for TCP and areas where advanced iron-based materials could be applicable. Chapter 2 details the materials and methodology utilised in this thesis to conduct and analyse results. It includes methods of synthesis, equipment specifications, and detailed descriptions of prepared solutions and analytical techniques.

The following four experimental chapters are organised first to establish information relating the prepared materials properties (Objective 1), followed by an establishment of the functionality of the material in the treatment of a model contaminant (Objective 2), and lastly, assess features of the materials use in application (Objective 3).

In Chapter 3, material characterisation techniques (SEM-EDS, TEM, BET, and Particle Sizers) were utilised to quantify physical properties of the material. Mössbauer analysis was utilised to determine Fe^0 composition and rates of iron corrosion. These results allowed for the identification of the best embedment procedure (1-Pot), knowledge of the material's reactivity over time (highest reactivity in first 48hrs of aerobic exposure), and determination of the best materials to use in all following experiments (oxygen-free).

Chapter 4 utilised GC-FID analysis to quantify TCP concentration before and after treatment with nZVI-Osorb in aerobic condition. Such experiments allowed for the determination of optimal contact time, sorption capacity, and proposed mechanism of treatment. These critical results were carried forward into the experimental design of Chapter 5 which explored environmental factors that could alter standard TCP sorption and degradation properties such as pH, salinity, atmospheric composition, and secondary organics in solution.

Chapter 6 examines the role of nZVI-Osorb on TCP in a model anaerobic digester over 14 days. Water quality measurements (COD, ORP, pH, head pressure) and TCP concentration by advanced LC/MS was recorded. The formulation of these model reactors was carried out in collaboration with colleagues examining the role of nZVI on biogas production in anaerobic digesters[198]. The experimental results of this chapter are utilised

to establish the suitability and potential of nZVI-Osorb for chlorophenol remediation in anaerobic digestion.

Chapter 7 details the conclusions produced from this work and the concluding chapter, 8, contains a detailed discussion of future work and further research to be pursued.

Chapter 2 : Materials & Methods

2.1 Introduction

The work detailed in this thesis centres around the development of new materials for the treatment of a model water contaminant with a detailed examination of the material's properties, functionality, and application. To achieve this goal three types of synthesis procedures and a variety analytical equipment for characterisation and experimental quantification were utilised. This methodology chapter details all synthesis, instrumentation, and testing protocol utilised to achieve this thesis' scientific goal.

This chapter first details the materials utilised for this research and their respective suppliers. This section is followed by a description of the three synthesis procedures (multiple-addition, 1-pot, and oxygen-free) conducted and where the resulting materials were utilised in experimentation. A detailed account of instrumentation utilised for the characterisation of the produced materials was then discussed. Characterization techniques included examinations of particle size, surface area, surface morphology, metal distribution, and iron oxidation.

After the full examination of the synthesis procedures and characterisation studies of the produced materials was detailed, the focus was turned to experiments and equipment utilised to quantify contaminant concentration in water before and after treatment with the developed materials. Features relevant to the model contaminant including, physiochemical properties of target analytes (chlorophenols and VFAs), the creation of chemical and background solutions, and replication and control procedures utilised to ensure valid results are detailed. Analytical techniques utilised to quantify contaminant concentration are discussed in detail. Details include extraction techniques for chlorophenols from water, methods of acid digestion to recover sorbed chlorophenol, and chromatography instrumentation and methods utilised to quantify contaminant concentration are discussed. Analytical techniques and equipment utilised to quantify VFA concentrations and other chemical properties (pH, COD, ORP) are also detailed.

The chapter concludes with a detailed list of experimental protocols utilised in chapters 4-6. These protocols are organised by chapter in which the work is discussed.

Chapter 4 and 5 are focused on the examination of the developed materials' properties and functionality in the treatment of chlorophenols within different environmental conditions. Chapter 6 is primarily focused on evaluating the materials performance in a model anaerobic digestion application. Lastly, details relevant to material transport and storage are discussed.

2.2 Materials

ABSMaterials (Wooster, OH, USA) provided the nanosorbent Osorb. Bulk zero valent iron, Nanofer 25, was provided by Nano Iron S.R.O (Rajhrad, Czech Republic). Activated carbon (acid washed, 12-20 mesh granular) was obtained from Sigma Aldrich. Metals (iron (II) sulphate, sodium borohydride, nickel (II) chloride, copper (II) sulphate), solvents (dichloromethane, acetonitrile), and chemical contaminants (trichlorophenol (2,4,6), dichlorophenol (2,4), phenol) were obtained from Sigma-Aldrich. Additional solvents (acetone, hexane, ethanol, diethyl ether), acids (acetic acid, propionic acid, butyric acid, 1M hydrochloric acid), bases (sodium hydroxide), and salts (lithium chloride) were obtained from Fischer Scientific UK. Type 1 water was prepared using ADEPT pure water. All solvents were HPLC-UV grade and utilised without further purification.

2.3 Synthesis

Three different methods (multiple addition, 1-pot, and oxygen-free) were utilised to synthesise the nZVI-Osorb, Cu-nZVI-Osorb, and Ni-nZVI-Osorb material created for this dissertation. Materials created using all three methods were utilised in the experiments detailed in Chapter 3. Only materials created through the oxygen-free method were utilised in Chapter 4-6.

The three synthesis methods utilised vary slightly from each other. Modifications were conducted to shorten the duration of synthesis and to prevent unwanted oxidation of the reduced zero-valent iron. The multiple-addition synthesis was the first synthesis

method utilised to physically embed nZVI and bi-metals (Ni; Cu) into the nanosorbent matrix. In this method, reduced iron suspended in a minimum of ethanol was added in aliquots to the nanosorbent.

The 1-pot synthesis method was also utilised to physically embed nZVI and bi-metals (Ni; Cu) into the nanosorbent matrix. However, in 1-pot synthesis, the desired quantity of iron is reduced from $FeSO_4$ in a solution containing the suspended nanosorbent. The resulting product was then rinsed and dried in a rotary evaporator.

Lastly, oxygen-free synthesis utilises commercially acquired nZVI that was mixed with dried nanosorbent (similar to multiple-addition) in an anaerobic chamber. This method was utilised to produce only nZVI embedded nanomaterials. Bimetals compositions were not synthesised by this method. A detailed synthesis of composite materials made by each method is discussed below including preparation, embedment, oxidation and drying, and stability examinations and procedures.

Mass calculations to determine percent bimetal in the composites by each of these synthesis methods were undertaken by measuring the net mass gain (g) after embedment and processing and the result was converted to moles (g x g/mol) utilising molar mass for direct comparison with moles of the sorbent for percent compositions detailed in Table 3.1 and 3.2.

2.3.1 Multiple Addition Synthesis

Preparation of the nZVI and nZVI-bimetals (Cu, Ni)

Ni-nZVI nanoparticles[257] and Cu-nZVI nanoparticles[238] were prepared in order to utilise a modified water-based approach. 25g $FeSO_4$-$7H_2O$ and 5g $CuSO_4$ solution were dissolved in 500mL ultrapure water and purged with nitrogen for 30 mins. A $NaBH_4$ solution was prepared by dissolving 10.0g $NaBH_4$ in 500mL ultrapure water, and the solution was added drop-wise to reduce the Fe-Cu metals. Black particles formed and were mixed in solution under vacuum until H_2 gas ceased to evolve after 20 min. Particles were isolated by vacuum filtration using a PES 0.22µm 47mm Millipore Hirsch filter and washed

with 2x 200mL ultrapure water then 1x 50mL ethanol to remove excess borohydride. Nanoparticles were then stored under ethanol for use. An identical protocol was utilised for nZVI-Ni nanoparticles (10g NiCl) and nZVI nanoparticles (25g $FeSO_4$). Total processing time was 48 hours for 1 addition cycle of nZVI. Multiple addition cycles were required to achieve the iron loadings reported in Ch. 3 which were determined through the mass calculation discussed in the previous section.

Embedment into Osorb nanosorbent

nZVI nanoparticles, nZVI-Cu or nZVI-Ni bimetal nanoparticles were embedded into the Osorb carrier through physical embedment. Synthesized nanoparticles were sonicated in ethanol for 30 min immediately before addition to the absorbent. A fixed volume of absorbent was placed in a 10mL test tube agitated by an IKA Vortex Genius 2. Bimetals suspended in minimal ethanol were added dropwise to the absorbent. The optically transparent absorbent swelled in the presence of an ethanol solvent and became black indicating the uptake of metals.

Oxidation and Drying

The resulting material was rinsed with DI water, dried in a rotary evaporator, and then baked overnight at 80C. The resulting materials were black and indicated no sign of oxidation.

Stability

Qualitative observations about the resulting colour of the resulting nanomaterials were observed. Synthesized sorbents were rinsed with acetone solvent for two days utilising a Soxhlet extractor apparatus. Observations about the rinsate were recorded and tested for leached iron by IC. The nanomaterials were dried in an oven (100C, 8hrs) before use in experimental testing.

2.3.2 1-Pot Synthesis

Preparation of the nZVI and nZVI-bimetals (Cu, Ni)

Ni-nZVI nanoparticles[257] and Cu-nZVI nanoparticles[238] were prepared to utilise a modified water-based approach. 50g $FeSO_4$-7H2O and 10g $CuSO_4$ solution were dissolved in 500mL ultrapure water and purged with Nitrogen for 30 mins. A $NaBH_4$ solution was prepared by dissolving 10.0g $NaBH_4$ in 500mL ultrapure water, and the solution was added drop-wise to reduce the Fe-Cu metals. Black particles formed and were mixed in solution under vacuum until H_2 gas ceased to evolve after 20 min. An identical protocol was utilised for nZVI-Ni nanoparticles (20g NiCl) and nZVI nanoparticles (50g $FeSO_4$). Particles were isolated by vacuum filtration using a PES 0.22µm 47mm Millipore Hirsch. The net weight of each of the resulting nanomaterials was recorded and then immediately transferred for embedment into the nanosorbent. Total embedment time was 2 hours.

Embedment into Osorb nanosorbent

A new solution was prepared (500mL DI water, 2.5g $NaBH_4$) and various amounts of Osorb were added to the reducing solution so that the resulting composite material would be composed of 10% nZVI metal or 10% nZVI-bimetal. This mixture of Osorb and nZVI was stirred at moderate speed for 60 minutes, and the composite nanomaterials were again filtered through vacuum filtration. Isolated particles were washed with 3x 200mL ultrapure water then 1x 50mL ethanol to remove excess borohydride. Nanoparticles were then stored under ethanol for use.

Oxidation and Drying

The resulting material was rinsed with DI water, dried in a rotary evaporator, and then baked overnight at 80C. The resulting materials were black and indicated no sign of oxidation.

Stability

Qualitative observations about the colour of the resulting nanomaterials were observed. Synthesized sorbents were rinsed with acetone solvent for two days utilising a Soxhlet extractor apparatus. Observations about the rinsate were recorded and tested for leached iron by IC. The nanomaterials were dried in an oven (100C, 8hrs) before use in experimental testing.

2.3.3 Oxygen-Free Synthesis

Preparation of the nZVI

Nanofer25 (zero valent iron) was received directly from the manufacturer Nano Iron S.R.O. and utilised without further purification for embedment into the nanosorbent Osorb.

Embedment into Osorb nanosorbent

Nanofer25 once received, and Osorb were transferred into a Vacuum Atmospheric Glove Box under an atmosphere of dried deoxygenated dinitrogen (O_2 <0.1 mg/L). 13.488g of Osorb were mixed in the chamber with 18.0g of Nanofer25 iron slurry until the iron fully covered Osorb.

Oxidation and Drying

The mixed slurry was left to dry in a vial in the chamber for 48 hrs. The resultant slurry was rinsed 3 x 10mL aprotic solvent diethyl ether. The mixture was left open in the chamber for an additional 48hrs to dry. The dried weight of the resulting material was

recorded, and iron composition (29.78%) was calculated. The vial was sealed with a screw top PPE lid and left in the anaerobic chamber for the duration of its usage.

Stability

Aliquots of the resulting nanomaterials were removed periodically in sealed vials before immediate use in various experimentation in chapter 5-7. For experimentation in chapter 6 aliquots removed from the anaerobic chamber were transferred to a sealed nitrogen purged Glas-Col glove bag containing a minimum of oxygen (<5%) where experiments were conducted. Oxygen levels in the bag were monitored every few hours with a BW Gas Alert O_2 Extreme. For experiments in chapter 7 sealed vials of nanomaterial were transferred into a Coy Labs Type A anaerobic chamber as detailed in the bioreactor setup.

2.4 Characterization

Materials generated by the three synthesis methods discussed were then characterised utilising a variety of analytical instrumentation. Particle size, surface area, surface morphology, metal distribution, and iron oxidation were examined to determine the physical properties of the developed materials.

2.4.1 Particle Size

Particle size was determined using an Occhio Flowcell FC200S +HR operated by Callisto software. This instrument utilised an 'optical morphogranulometer' and an advanced image analysis program to calculate particle size of suspended particles passing the front of the detector in a flow cell.

Solutions were prepared by mixing 500mg of the desired nanomaterial in 10mL DI water. A few drops of SDS surfactant were added to the mixture to enhance suspension.

Particles counted were between 4,000-5,000 particles for each sample. This instrument was the property of Duke University.

2.4.2 Surface Area

A Beckman Coulter SA3100 determined the total surface area of the nanomaterials. The instrument utilised the applied standard ISO 9277 : 2010 [258] to calculate the external and internal surface areas of the dispersed porous solid by measuring adsorption and desorption of an inert gas (He). Brunauer-Emmett-Teller (BET) theory [259] was applied in this standard method.

All samples were baked at 60C overnight before testing and degassed in the instrument's degassing ports for 2 hours at 80 C before analysis. Nanoparticles were measured without additional milling. Sample weight (mg), surface area (sq. m/g), monolayer volume (cc/g), total surface area (sq. m), and correlation coefficient were recorded. This instrument was the property of Duke University.

2.4.3 Surface Morphology

Scanning Electron Microscopy (SEM) and Transmission Electron Microscopy (TEM) imaged and analysed the surface morphology of the synthesised nanomaterials. An FEI XL30 SEM-FEG (resolution 2nm) and an FEI Tecnai G2 Twin (resolution 0.3nm) captured high-resolution images of the material's surface.

SEM samples were mounted on carbon tape and sputter-coated with a Kurt Lesker PVD 75. TEM samples were prepared for imaging by the lead operating technician. Both instruments were the property of Duke University's Shared Materials Instrumentation Facility (SMiF) and utilised with permission.

2.4.4 Metal Distribution

Further imaging and elemental mapping of the produced nanomaterials were conducted on an FEI XL30 Environmental Scanning Electron Microscope (ESEM) fitted with a Bruker Quantax Energy Dispersive X-Ray Spectrometer (EDS) utilising a Bruker XFlash 4010 detector. The instrument is fitted with a motorised Microtest 200N Tensile Stage, and Peltier cooled detector. The ESEM has a resolution of 100nm, and the EDS has a 10mm^2 active area, stability from <1 to >100,000 cps, and element detection range from boron to americium. This instrument was the property of Duke University's Shared Materials Instrumentation Facility (SMiF) and utilised with permission.

2.4.5 Iron Oxidation

Two different approaches were utilised to determine the oxidative state of the iron embedded within the nanomaterials. These approaches include the utilisation of X-Ray Photoelectron Spectrometer (XPS) and a Mössbauer Spectrometer.

The XPS utilised was a Kratos Analytical Axis Ultra. The depth of x-ray penetration was approx. 5nm from the surface with a scan region of 300 x 700 μm. XPS spectra of Osorb were utilised as a control to determine background peaks. Peaks were observed from 975 to 100 mm with peaks corresponding to metal oxides occurring between 528 - 531 mm and iron oxides occurring around 706-713 mm in the spectra. While iron oxides were detected, there was too much peak overlap to determine exact iron species present. This instrument was the property of Duke University's Shared Materials Instrumentation Facility (SMiF) and utilised with permission.

Mössbauer Spectrometer tests were conducted at 32C and utilised a constant acceleration spectrometer with a ^{57}Co source in a rhodium matrix. The spectrometer was calibrated with an α-Fe sample with spectral fit using either a single doublet or two doublets [260]. The runtime for each sample was 24hrs. Samples were transported for testing in vials sealed in an anaerobic chamber and run as soon as possible on the instrument. The instrument was the property of the University of North Carolina- Asheville's Mössbauer

Effect Data Center, and the operating technician conducted the spectral analysis on the instrument.

2.5 Contaminant Physiochemical Properties

2.5.1 Representative Chlorophenols

The focal point of this study is 2,4,6-trichlorophenol (TCP). TCP is 1 of 19 possible chlorinated constituents of the base molecule, phenol. In this study 2,4,6-trichlorophenol and its less chlorinated breakdown products, 2,4-dichlorophenol, o-chlorophenol, and the unchlorinated phenol are utilised and measured. The molecular structure and general properties of these compounds were listed in Table 1.1 in the prior chapter.

2.5.2 Representative VFAs

Three Volatile Fatty Acids (VFAs) are utilised in this research. These compounds were applied in experimentation detailed in Ch. 6 of this thesis. The acids are acetic acid, propionic acid, and butyric acid. The molecular structure and general properties of these compounds are listed in Table 2.1.

Table 2.1 General properties of the utilised volatile fatty acids[261].

Acid	**Structure**	**M.W. (g/mol)**	**LogK_{ow} (P)**	**pK_a (25C)**
Acetic		60.1	-0.32	4.76
Propionic		74.1	0.33	4.88
Butyric		88.1	0.79	4.82

2.6 Chemical and Background Solutions

2.6.1 Chlorophenols

Individual 20,000 mg/L stock solutions of 2,4,6 trichlorophenol, 2,4 dichlorophenol, chlorophenol, and phenol were prepared in ethanol and used via dilution for the creation of all calibration and test solutions. Calibration, limit of detection, and control samples were all prepared in water and extracted with hexane for analysis in identical extraction procedures utilised to test all other samples. 6-point calibrations of each chlorophenol (100, 75, 50, 25, 12.5, 6.25 mg/L) were run on GC-FID before each set of individual experiments were undertaken. Experiments utilizing TCP concentrations above 100 mg/L utilised a 6-point calibration curve at a higher range (1,000, 500, 300, 100, 10, 1 mg/L).

Limits of detection for the gas chromatographs (GC-FID and GC/MS) were established by measuring samples of decreasing concentration (50,000, 1,000, 500, 250, 100, 50, 10, 5, 2.5, 1 µg/L) (Table 2.2).

Table 2.2 The determined limit of detection for various chlorophenols and phenol on GC-FID and GCMS.

Instrument	TCP	DCP	CP	Phenol
GC-FID	1ppm	1ppm	1ppm	25ppm
GCMS	500ppb	250ppb	100ppb	500ppb

2.6.2 Volatile Fatty Acids (VFAs)

500 mg/L and 20,000mg/L individual stock solutions of each testing VFA were prepared in water and utilised for the creation of all calibration curves and testing solutions containing these acids. 7-point calibration curves (500, 350, 250, 100, 50, 25, 6 mg/L) of

each VFA and samples containing an equal mix of all three organic acids were run on the IC before each bioreactor sample set utilised in chapter 5.

The limit of detection for the ion chromatograph (IC) was established by measuring samples of decreasing concentration (500, 250, 100, 50, 10, 5, 2.5, 1 µg/L). The limit of detection was determined to be 250 µg/L for each acid.

2.7 Uncertainty and Error

A level of error is expected in all scientific measurements. Standard human error (±0.1) in sample extraction processes are expected in analysis with volume of solvent controlled by automatic pipettes (±0.01). Error in quantitative measurements of anaerobic biodigester systems (±0.001) and in concentration of analytes measured by solution by GC (±0.001) and IC (±0.1) were expected and controlled through sample replication to determine mean standard deviations and the use of control solutions. There is a level of uncertainty in all scientific works and experimental conclusions should not be considered settled science but a means to develop concepts further based on foundational principals.

2.8 Replication and Controls

All test samples were conducted in triplicate unless explicitly stated. Each of the samples run on GC-FID were also run in triplicate. Controls, such as the untreated contaminated solutions for each experiment, were utilised to confirm results. In some cases, such as in solutions that contained VFA, secondary controls were also utilised containing the base solution and the nanomaterial without chlorophenol to monitor interactions. Samples were prepared fresh in each trial, and each experiment was always conducted and analysed as a full set of data.

2.9 Analytical Techniques

2.9.1 Chlorophenols

All chlorophenols and phenol concentrations considered in chapter five and six were measured using Gas Chromatography (GC) with a Flame Ionization Detector (FID). In some cases, additional analysis by Gas Chromatography-Mass Spectroscopy (GC-MS) was utilised for additional confirmation of species of chlorophenols present in solution. All concentrations of chlorophenols in Ch. 6 were measured using Liquid Chromatography-Mass Spectroscopy (LC-MS).

Extraction

Solutions of TCP and the iron nanomaterial were mixed in the test vials by 30 seconds of contact with a vortex and then 24hrs of mixing on a rotary shaker with the vials situated on their side. After the desired contact time, samples were removed and left to settle on a countertop for a minimum of 30 mins.

7mL of the supernate was removed via Pasteur pipette to a new vial. 2mL of hexane was added to the solution and samples were mixed again via 30 seconds on the vortexer and then by 3 hours on a rotary shaker again orientated on their sides.

Extracted samples were left to settle on the countertop for a minimum of 15 minutes, and then a top layer of hexane was removed via pipette to corresponding GC vials where they were then analysed via GC-FID or GC-MS. Control samples containing no nanomaterial were processed identically for analysis. Separate studies containing the test solution without chlorophenol but with the nanosorbent were also analyzed to validate results.

Acid Digestion

In designated experiments, the nanomaterial underwent further processing after contact with the TCP solution. The remaining TCP solution surrounding the settled nanomaterial was removed via pipette and then discarded. The remaining nanomaterial was then mixed with 7 mL of ethyl acetate and 2 mL 1M HCl for 24 hrs on a rotary shaker. The mixture was left to settle, and a sample of the top layer of ethyl acetate was removed for GC-FID analysis.

After treatment, waste solutions were discarded into their appropriate receptacle and vials were washed and air-dried for additional usage.

GC Analysis

A ChromQuest Trace 2000 GC from Thermoquest CE instruments, enabled with a stacked flame ionisation detector (FID) and electron capture detector (ECD), was utilised (Fig. 2.1). The spectrum analysis was conducted on ChromQuest. The column was a Perkin-Elmer Elite 5MS (30m x 0.25mm x 0.25µm). The inlet temperature was 250˚C with a split flow 50 mL/min. The injection volume was 0.5µL. The temperature program was 50˚C held for 5 mins then increased to 200˚C at a rate of 6˚C/min and held for 5 mins.

Figure 2.1 The ChromQuest Trace 2000 utilised for experimentation.

A Thermo Scientific Trace 1300 GC with an ISQ LT Single Quadrupole MS was utilised for analysis. The column was a Thermo Scientific TG-SQC (15 m x 0.25 mm x 0.25 µm). The injection port was at 250˚C. The injection volume was 1 µL. The oven program was 60˚C held for 10 mins, raised to 220˚C at a rate of 4˚C/min, held for 10 mins, and then raised to 260˚C at 1C/min. The mass range was 35-425 at 70ev.

Chlorophenol analysis in chapter 6 utilised a Thermo Accela Ultra-High-Pressure Liquid system (LC) with Thermo Vantage Triple Quadrupole Mass Spectrometer (MS) utilising atmospheric pressure chemical ionisation. Injection volume was 10 µL. The column was a Thermo Hypsersil Gold (100 mm x 2.1 mm, 1.2 µL). Internal standards for each chlorophenol, as well as three blanks, were utilised in each sample set. GC-FID/ECD instrumentation was utilised at both the University of Edinburgh and Duke University. LC/MS instrumentation and analysis was conducted and utilised at Duke University.

2.9.2 Volatile Fatty Acids (VFAs)

All concentrations of VFA in chapter 6 were monitored by 883 Basic IC Plus Metrohm Ion Chromatography (IC) using an 863-compact autosampler (Fig 2.2). Magic IC Net 3.1 software analysed spectrum. The column was a Metrosep Organic Acids 250/7.8 column with a Metrosep Organic Acids guard column. Data acquisition was 25.6 mins. The flow rate was 0.5mL/min with 3-min startup time. MSM intervals were 10mins with conductivity at 2.3%/˚C. Eluent (0.054 mL sulfuric acid and 300 mL acetone, diluted to 2L with DI water) and regenerative (0.5g LiCl diluted to 1L with DI water) solutions were prepared before testing, and the column was primed and then flushed for 2 hours.

Figure 2.2 The 883 Basic IC Plus Metrohm Ion Chromatography (IC) and 863-compact autosampler utilised for VFA analysis.

In experiments containing VFAs, the standard volume of tests was increased to 20 mL, and the standard treatment volume of nZVI-Osorb was also doubled to 50 mg. Mixing the solutions was identical to TCP only methods, and after the treatment period, 10mL of the treated TCP solution was transferred to a new vial and then transferred to an IC vial for analysis. These vials were covered via parafilm on the IC carousel while in the queue for analysis. The remaining 10mL of the solution was processed for TCP concentration by the method stated above. Waste solutions were discarded, and vials were washed and air-dried for additional usage.

2.9.3 General Analytical Methods

A Hanna Instruments HI 9025 was utilised to measure pH and Oxidative Reductive Potential (ORP) using an Elite ORP 31C Electrode. Probes were calibrated and stored in standard solutions between usages. Chemical oxygen demand (COD) was measured utilising a YSI Instruments 910 COD Colorimeter by PL454 vials acquired from Palintest with a COD range of 50-2,000 mg/L. Samples were prepared by adding 200 µL aqueous samples per vial with a 2-hour incubation period at 150C. Samples were left to cool to room temperature and then measured at mid-range after calibration with a blank of DI water.

2.10 Experimental Protocols

To establish a firm understanding of the produced material's properties, functionality, and potential role in a model application an extensive series of experiments was conducted (each with a unique set-up tailored to a specific testing parameter). Material and method details for Chapter 3 were discussed in the body of this chapter before this section. Methods for chapter 4 through 6 are detailed below and organised by the experimental chapter in which they occur. Experiments in Chapter 4 focused on establishing material functionality in terms of sorption and degradation of the model contaminant TCP. Chapter 5 utilized these findings to examine the effect of environmental conditions on sorption & degradation mechanisms. Chapter 6 concluded the experimental chapters and applied results for the previous chapters to interpret nZVI-Osorb effect in a model anaerobic digestion system doped with TCP.

2.10.1 Methods for Chapter 4: Contaminant Adsorption and Degradation of 2,4,6-Trichlorophenol

Desired tests solutions were prepared from stock solutions (20,000 mg/L and 1,000 mg/L). The standard concentration of TCP in tests was 100 mg/L. While this value is significantly above typical environmental concentrations discussed in the literature review, 100 mg/L was the optimal concentration to adequately assess and evaluate the nanocomposite's TCP removal capabilities before and after treatment and fit the contamination detection range best suited to the analytical equipment utilised in this research. The standard treatment mass of nZVI-Osorb was 25 mg. The standard volume of tests was 10mL with each sample conducted in triplicate. DI water used for the tests solutions was autoclaved utilising Tuttnauer 5075 EL autoclave for 1hr at 250°C to degas dissolved oxygen unless stated otherwise.

Contact Time

Optimal contact time between the nanomaterial and contaminant was tested through varying the exposure time from 5 mins to 2 days. Contact time began when the nanomaterial first entered the 100 mg/L solution and ended once 7mL of the test solution was pipetted to a new vial after particle settling.

nZVI-Osorb Capacity

Treatment capacity for nZVI-Osorb to reduce TCP was measured through the addition of 50, 25, 10, and 5 mg of material mixed in a 100 mg/L solution of TCP. This same method was applied to activated carbon. Reduction in TCP concentration was calculated from GC-FID results.

Osorb Capacity

Osorb sorption capacity was tested through the application of 25 mg in 100 mg/L solutions of various chlorophenols. Similarly, various amounts of Osorb were applied to 500 mg/L solutions of TCP and the percent reduction in contaminant calculated. Higher TCP starting concentrations were required to assess capacity as saturation limits are not reached at 100 mg/L concentrations.

9-Day Trial

In the 9-day trial, to monitor desorption and leaching, 3x Osorb, nZVI-Osorb, nZVI, and control were mixed with 100 mg/L TCP. The concentration of TCP in the water was monitored periodically over the course of 9 days. Samples were also analysed periodically for the presence of any breakdown products by GC-FID and GCMS. The final test materials were acid digested for chlorophenol recovery after treatment.

24-Hour pH Trial

A 24-hour study observing pH changes within the tests 100 mg/L TCP test water with 25mg nZVI-Osorb was conducted. Initial pH in pH-adjusted samples was completed through the manual addition of 1M HCl or 1M NaOH. pH was recorded every minute at the beginning of the experiments and then periodically after 2 hours.

Leaching

150 mg of nZVI-Osorb were mixed in a 60 mL, 100 mg/L solution of TCP for 24 hrs. The solution was left to settle, and the liquid was removed via pipette. An aliquot (7 mL) was removed from the water and extracted for analysis by GC-FID. The remaining nZVI-Osorb was covered in fresh water and rinsed with 4x 60 mL water for 30 mins. TCP concentration was determined for each wash. 60 mL of DI water was added to the remaining nanomaterial and stirred at a moderate speed for 7 days. Samples were extracted at days 1, 2, 5, and 7 for GC-FID analysis.

2.10.2 Methods for Chapter 5: The Effect of Water Characteristics on TCP Sorption and Degradation by nZVI-Osorb

Desired test solutions were prepared from stock solutions. The standard concentration of TCP in tests was 100 mg/L. The standard treatment volume of nZVI-Osorb was 25 mg. The standard volume of tests was 10mL with each sample conducted in triplicate. DI water used for the test solutions was autoclaved for 1hr to degas dissolved oxygen unless stated otherwise. VFA and anaerobic versus aerobic trials were conducted in anaerobic conditions. Salinity and pH trials were conducted under aerobic conditions.

Salinity

Salinity's effect on adsorption of TCP was tested at five concentrations (0, 1, 3, 6, and 20 %). Dilutions were prepared from a saturated saline stock containing an excess of NaCl to 1L DI water at room temperature. The stock saline solution was vigorously shaken before addition to various test solutions. Test samples were extracted with hexane without further purification or desalination.

Anaerobic versus Aerobic Treatment of TCP

A side-by-side comparison of anaerobic vs aerobic treatment utilising 5 masses (50, 25, 10, 5, 0 mg) of both nZVI-Osorb and Osorb was undertaken. Samples under anaerobic conditions were mixed in an anaerobic nitrogen glove bag. Pre-weighed masses and solutions were prepared and transferred into the bag. The bag was purged several times with nitrogen and sealed. Solutions were not mixed until oxygen within the bag was below 1% and relatively stable. Anaerobic samples remained in the bag for the course of the experiment until they were removed for extraction and analysis. Nitrogen in the glove bag was periodically topped up throughout the experiment to maintain anaerobic conditions. Start time for aerobic and anaerobic samples was kept consistent. The recovered nanomaterials were acid digested for TCP recovery.

Variable pH

A 100 mg/L TCP solution was adjusted to four pHs (3, 5, 7, 9) by manually adding 1M HCl or 1M NaOH dropwise to the solution. The starting solution was deemed at equilibrium when the pH held stable for two mins at one reading.

VFA Interactions and Effect on TCP Treatment by nZVI-Osorb

Various tests were conducted to examine the effect of individual interactions between the sorbent and VFAs and the VFAs and TCP. Both TCP and organic acid (OA) concentrations were monitored for all tests.

Two studies were conducted to determine the effect organic acids pose on the treatment of TCP by nZVI-Osorb. In one test 100mg/L solutions of TCP and various concentrations (100, 50, 25, 10, 0 mg/L) of each of the organic acid (acetic, propionic, butyric) were mixed with 25mg nZVI-Osorb. Conversely, various amounts of nZVI-Osorb (100, 50, 25, 10, 0 mg) were applied to 100mg/L TCP waters also containing 100 mg/L of a selected acid to measure treatment capability.

The effects of a mixture of three acids all at 100mg/L on TCP treatability were studied. nZVI-Osorb at various masses (100, 50, 25, 10, 0 mg) were mixed with and without the presence of the organic acid mix. This OA mix was also used to determine the effect on TCP treatability at four starting pHs (3, 5, 7, 9).

2.10.3 Methods for Chapter 6: Complexity of Treatment in Real Applications

Mini Bioreactors for Baseline Values (No Sludge)

All control experiments in this chapter not utilising biological matter were conducted in anaerobic conditions within a nitrogen glove bag. For each experiment, pre-weighed masses and solutions were prepared in aerobic conditions in the fume hood and then transferred into the bag. The bag was purged several times with nitrogen and sealed. Solutions were not mixed until oxygen within the bag was below 1 % and relatively stable. Anaerobic samples remained in the bag for the course of the experiment until they were removed for extraction and analysis. Nitrogen in the glove bag was periodically topped up throughout the experiment.

Bioreactor solutions were prepared in 1L screw-top bottleneck glass vials. DI water used for the tests solutions was autoclaved for 1hr to degas dissolved oxygen. Aliquots from stock solutions of the organic acids and TCP were added to create the desired solutions with a total reactor volume of 500 mL (Table 2.3). Three types of reactors were created (nZVI-Osorb, nZVI, or Control) and each was prepared in triplicate. pH of the reactors was adjusted to 7 before the final addition of the nanomaterial.

Table 2.3 Concentrations of primary components in the anaerobic bioreactors.

Component	Concentration
nZVI-Osorb or nZVI	3.9 g/L
2,4,6-Trichlorphenol	25 mg/L
Acetic Acid	240 mg/L
Propionic Acid	120 mg/L
Butyric Acid	120 mg/L

10mL aliquots of each reactor were sampled at days (0, 1, 2, 3, 4, 7, 9, 11, 14). These samples were removed from the anaerobic chamber and utilised to measure pH, ORP, COD, TCP concentration, and VFA concentration.

Mini Bioreactors (Containing Sludge)

Bioreactors which were not controls and contained biomass include aliquots of a buffer solution, stock reagent solutions, and reference solutions to sustain microbial life within the reactors.

The buffer solution was prepared by adding 23.83 g of HEPES into 2 L of DI water. This solution was autoclaved to sterilise and then adjusted to a pH of 7. The feed solutions were composed of three individual solutions. A VFA solution containing 4 g acetic acid, 2 g propionic acid, and 2 g of butyric acid dissolved into 20 mL of DI water. The nutrient solution containing 0.955 g NH_4Cl and 0.22 g KH_2PO_4 dissolved in 5 mL DI water. The iron solution contained 0.2381 g $FeCl_3$-$6H_2O$ dissolved in 2 mL DI water. Aliquots of these solutions were then added to create a broader feed solution.

The feed solution was prepared by adding 0.3296mL of nutrient solution, 0.04mL of the iron chloride solution, 0.28 mL of a micronutrient solution, 0.016g of dried active

yeast, 0.336 g $NaCO_3$, 0.6528 g acetate, 2.4 g TCP, and VFA solution to 400 mL DI water. The final feed solution was adjusted to 6.5 pH.

Each bioreactor was prepared in a 1L crimp top bottle with pierceable rubber septum closure. Bottles were autoclaved before use. Each reactor contained 125mL of locally obtained biomass utilised in a commercial anaerobic digester, 12.5mL of a feed solution, and 62.5 mL of a buffer solution containing the suspended nanomaterials. Solutions were prepared so that all reactors including controls contained the same total volume (200 mL). Base contents of the reactors are detailed in Table 2.4.

Table 2.4 Total composition of each reactor & the concentration of components of interest.

Bioreactor Contents	**Volume**
Biomass	125 mL
Feed	12.5 mL
HEPES Buffer	62.5 mL

Component	**Concentration**
nZVI-Osorb or nZVI Control	3.9 g/L
2,4,6-Trichlorphenol	25 mg/L
Acetic Acid	240 mg/L
Propionic Acid	120 mg/L
Butyric Acid	120 mg/L

All biologically active reactors were prepared in an anaerobic chamber (Fig. 2.3), and, once the top closure was sealed, the vials were transferred to the rotary incubator where samples were held at 30 C and shaken at low speeds between sampling periods. This experiment was repeated twice with the first trial data detailed in Appendix 1.

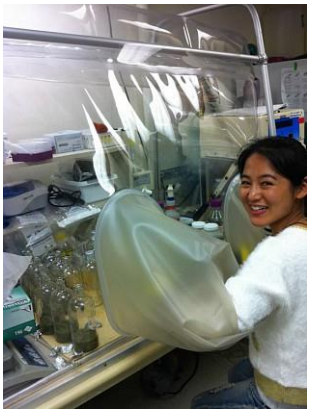

Figure 2.3 A photograph showing the preparation of bioreactor samples in the anaerobic chamber.

5 mL samples were collected at days 1, 5, 10, and 14 from the reactors in an anaerobic chamber. These samples were utilised to monitor pH, ORP, COD, and TCP concentration. Head pressure was measured before sampling via a pressure gauge attached to a needle that was inserted directly into the rubber top septum. Remaining biogas was purged via a needle attached to a tube submerged in deoxygenated water before transfer to the anaerobic chamber for sampling.

2 mL of the sample from each vial for each sampling period was stored in a glass vial and frozen until the LC-MS was available for TCP analysis. Method development and LC-MS analysis were carried out by Eileen Cooper of the Duke University Analytical Core.

2.11 Material Transport and Storage

Materials synthesised utilising the 1-pot of multiple addition synthesis methods were stored in glass vials on a bench under normal atmospheric conditions. Materials that were later synthesised utilising the oxygen-free method were stored in anaerobic chambers where oxygen and oxygen exposure was at a minimum. If samples of this material were required for testing an aliquot would be transferred into a screw top glass vial, sealed with parafilm within the chamber, and then transferred out through a purgable door attached to the chamber. Samples were then immediately used in experiments such as in Chapter 5

or were transferred to a nitrogen purged glove bag for additional anaerobic use. Every effort was made to limit undesired oxygen exposure and oxidation of the nanomaterials.

Chapter 3 : Synthesis & Characterization of nZVI-Osorb

3.1 Introduction

In the development of any new material, several essential features need to be considered. One important factor is an understanding of synthesis and embedment procedures required to produce the material, how variations in embedment alter the final material and the material's overall reproducibility [121]. Clarity in these areas can encourage further scientific work within the field and guide those wishing to replicate studies.

A second factor is a keen understanding of the material's physical properties such as particle size, stability, and morphology. In sorbents, these features can influence essential application parameters such as sorptive capacity and provide useful information when designing deployment apparatus[126]. Features related to reactivity (rates of corrosion, metal composition, and metal distribution) are equally important in predicting and understanding contaminant treatment rates and efficiency[178]. Overall a strong characterisation profile contributes vital information that aids the interpretation of experimental and field data, and should not be overlooked in environmental engineering research.

As evidenced by the literature review, there is a need for improved contaminant treatment in water systems. Contaminants such as TCP are particularly problematic as they are highly toxic, persistent, and often produce by-products during treatment[251]. nZVI is a promising material to improve existing treatments, particularly for TCP, but its applicability suffers from certain inherent limitations[29]. There is a need for the development of highly reactive metal nanoparticles that can entirely strip halogenated organics in a support structure and protect against early oxidation, agglomeration, leaching, and by-product formation, all the while remaining non-toxic to microorganisms[175]. While many materials have been developed to address these issues, rarely do they accomplish all these factors simultaneously.

Improved support structures, like organically silicas, remain under-utilised and their high sorptive capacities have the potential to increase treatment through

concentrating contaminants at metal reactive sites and reducing by-product release necessitating further development and study[235]. Successful embedment of metals into silicas have been observed with composites achieving even metallic dispersion[138, 179]. Yet, as with other novel composites, these composites often demonstrate a propensity to leach and further work is required to improve metal retention in the matrix[208, 213]. Issues pertaining to corrosion remain complex given the high instability of nZVI in solution and the loss of reactivity often observed when iron particles are coated to reduce oxygen exposure[178, 247]. While advanced silica-based materials have yet to offer a perfect solution to metallic corrosion, their study is warranted given the diversity of silica-based materials and their wide range of physical properties and characteristics[262]. Such developments in metallic dispersion, retention, longevity, and treatment within composites would expand the effectiveness and contaminant range of nZVI when applied in in-*situ* groundwater treatment, as well as offering some unique opportunities to investigate its use in other more novel scenarios such as anaerobic digestion or wastewater treatment.

This chapter will focus on the three methods of physical embedment of nZVI within this novel nanosorbent and evaluate the three methods regarding practicality and quality of materials produced. Materials that retained embedded iron after final processing and rinsing, displayed even distributions of iron and bi-metals, and indicated some degree of reduced corrosion, were deemed successful. The most successful materials detailed in this chapter were then utilised in following chapters for their abilities to remediate a model contaminant in both simple and complex water environments.

3.2 nZVI Embedment Techniques

nZVI was prepared through the reduction of iron salts and obtained commercially from a European supplier. Osorb was an organically modified silica nanosorbent prepared through propriety sol-gel processes and obtained from a commercial supplier in the United States of America.

Three distinct methods were utilised in the production of the nZVI-Osorb hybrid nanomaterials. These methods are referred to as (1) multi-addition, (2) 1-pot, and (3)

oxygen-free. Multi-addition was a method adapted from primary literature and combined separately with synthesized nZVI and Osorb sorbent[235]. While this embedment technique was successful at securing iron particles, it proved difficult to control total concentration of iron embedded and metallic corrosion. Furthermore, extensive synthesis time and labor made this embedment method impractical for scaled-up synthesis operations. Therefore, the 1-pot method was experimentally developed to address these issues and reduce embedment time through the combination of reduction and embedment steps in processing. Iron corrosion remained a likely issue so the final method, oxygen-free, was developed to reduce iron corrosion and followed muti-addition embedment but within the confines of an anaerobic chamber (ref. Ch.2.3).

In all methods, nZVI was physically embedded into the internal structures of the nanosorbent matrix by exploiting the swelling properties of the material. In this process, the addition of nZVI in a solvent swelled the sorbent allowing iron particles to become distributed throughout the silica matrix. After addition, the composite was dried thus re-tensioning the matrix and locking embedded iron particles in place.

Materials made utilising the multi-addition, or 1-pot synthesis were rinsed to remove excess and loosely bound surface iron. This process was repeated until the filtrate was clear. A final post rinse wash for each material was analysed by IC and no residual concentration of iron was found (ref. Ch.2.3). These results indicated that all loosely bound iron was removed and no further leeching of iron from the nanosorbent matrix should occur. Oxygen-free materials were not rinsed to keep oxygen exposure to a minimum before use.

3.2.1 Multi-Addition Embedment Method

In multi-addition synthesis, nZVI was synthesised separately and then added dropwise to the sorbent. The sorbent was rapidly shaken in the metal addition process to increase iron dispersion. This embedment process was repeated more than 10 times, with the material thoroughly dried in a rotary evaporator between each iron addition. This technique for synthesis was time consuming (both in procedure and processing time)

making it impractical for scale-up and challenging to prevent atmospheric oxidation of the iron, as observed in Figure 3.1.

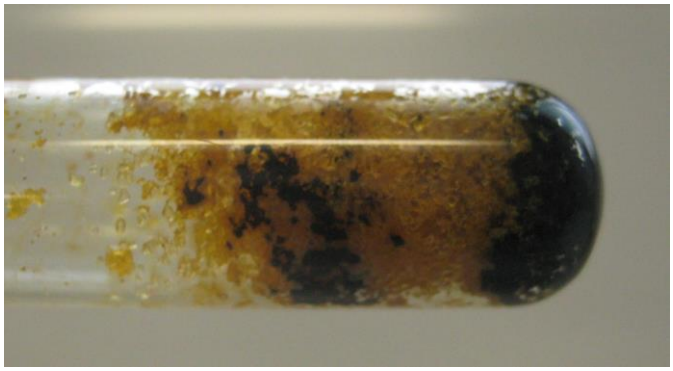

Figure 3.1 Iron improperly embedded into Osorb with black indicating zero valent iron and the burnt orange indicating the formation of iron oxide.

After a series of unsuccessful trials like the one in Fig. 3.1 that showed significant iron corrosion, three types of nanomaterials were successfully synthesised using the multi-addition method by increasing the drying time of the material in a rotary evaporator after every addition. These materials consisted mostly of a nanosorbent doped with nZVI. In two variations of the material, a percentage of a second metal (25% nickel or 20% copper) were added to the iron to form a bimetal complex (Table 3.1).

Table 3.1 The three resulting materials produced by multi-addition synthesis.

Sample	Bimetal	Bimetal:nZVI	% Metal	Final Mass (g)
1	x	x	4.2%	3.1
2	Ni	1:4	10.8%	3.2
3	Cu	1:5	9.9%	3.0

Mass ratios of bi-metal: nZVI were controlled by reagent inputs in synthesis. Percentages of metal (nZVI or bimetal complex) in each sample were determined by mass calculations of the final product after processing. A 10% nZVI: Osorb ratio was desired for the final materials. It was hoped that a 10% iron composition would allow for sufficient reactivity per gram of total material while still allowing enough sorbent to support thoroughly the individual iron particles. The predetermined ratio of nZVI: Osorb was based

on previous work utilising nZVI-Osorb to dechlorinated trichloroethylene in groundwater[235]. However, this 10% metal target proved difficult to control by the multi-addition method. Sample 1 had a low iron composition of 4.2%. Samples 2 and 3 had a higher bimetal concentration in the sorbent at 10.8 and 9.9%. This variation in metallic concentration could be accounted for by uneven mixing of the iron and the sorbent during embedment.

The materials produced via this embedment were coloured deep brown (Figure 3.2). The brown colour of the final materials suggested that some oxidation of the material during synthesis may have occurred. Materials were left open to the atmosphere after processing, and no apparent colour change was observed thereafter. This suggested that iron embedded in the materials, post-drying, did not undergo further significant oxidation as observed in the prior trials (Fig. 3.1).

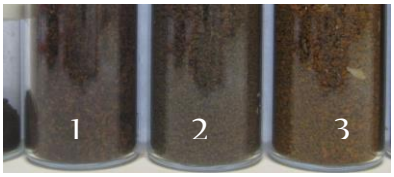

Figure 3.2 An image of the three types of material produced utilising muti-addition synthesis. (1) 3.1 g nZVI-Osorb, (2) 3.2 g Ni-nZVI-Osorb, (3) 3.0 g Cu-nZVI-Osorb. The dark colour indicated that embedment was successful and prior issues with iron oxidation did not occur at comparable severity.

While the multi-addition method proved successful at generating materials that retained iron after rinsing and qualitatively appeared to reduce the rate of oxidation (e.g. retained a dark colour) compared to control nZVI materials; the method had two significant drawbacks. The embedment process from start to finish required a significant amount of time (>48 hrs) in which it was difficult to limit atmospheric exposure and reduce iron corrosion during the processing of the materials. Secondly, the technique applied for embedment resulted in reduced control over final iron concentrations. To reduce these negative features, a second method (1-Pot) for metal embedment was developed.

3.2.2 1-Pot Embedment Method

The 1-pot embedment technique utilised the same method as the multi-addition technique to synthesise nZVI, copper, and nickel nanometals, but instead of adding the metals to the vortexed sorbent in a dropwise fashion, the sorbent was added directly to the bulk batch of nano-sized iron (in the same solution in which nZVI was produced from metal salts). The resulting materials were mixed by hand in the reaction vessel and then immediately dried on a rotary evaporator. This method was developed from first principles in the expectation that the reductive solution would not alter the nanosorbents' physical properties[134] and successfully reduced the embedment procedure time from several hours to less than 60 minutes (Table 3.2).

Table 3.2 Three resulting materials produced by 1-pot synthesis.

Sample	Bimetal	Bimetal:nZVI	% Metal	Final Mass (g)
1	x	x	10.0%	75.85
2	Ni	1:4	10.1%	39.76
3	Cu	1:5	10.3%	47.86

Materials from the 1-pot synthesis were produced in larger volumes than the multi-addition method and, like the previous method, included variants with nickel and copper bimetals (synthesised in equal ratios). The overall % iron by mass in each sample was closer to the desired 10% with variation within 1/10 of a percent.

The final materials produced by this 1-pot embedment were also darker in colour than materials using the multi-addition method (Figure 3.3). This darker colour could indicate a lesser degree of oxidation of iron within the material and was a factor that was quantified in studies detailed later in this chapter (Section 3.3).

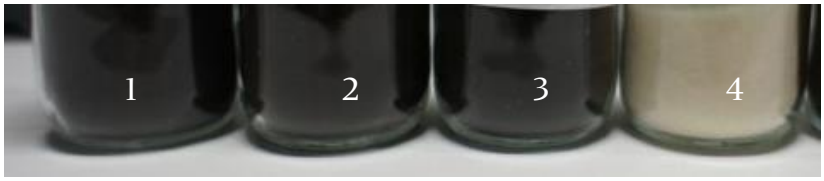

Figure 3.3 The resulting nanomaterials from 1-pot synthesis (1) 75.85g nZVI-Osorb (2) 47.86 g nZVI-Ni-Osorb, (3) 39.76 nZVI-Cu-Osorb, (4) 31.355g Osorb. The dark colour indicated that embedment was successful and prior issues with iron oxidation observed in Figure 3.1 did not occur.

Preemptive oxidations of iron to some extent before embedment by both the Multi-Addition and 1-Pot method were highly probable given the aerobic processing conditions of these embedments and nZVI's high instability in the presence of oxygen. A final method of iron embedment, Oxygen-Free embedment, was developed to reduce anticipated corrosion and maintain high nZVI concentrations.

3.2.3 Oxygen-Free Embedment Method

In the Oxygen-Free embedment method, commercial nano-sized zero valent iron (Nanofer 25) was obtained directly from a supplier and embedded into Osorb using the multi-addition approach within an anaerobic chamber. While 1-pot was a more suitable embedment procedure, metal reduction could not be carried out due to expected hydrogen evolution and experimental limitations restricting protic reagents within the shared anaerobic chamber. For these reasons, bimetal variations were not synthesised using this anaerobic method. Produced materials were left to dry within the chamber via evaporative processes at ambient temperature.

Materials produced through Oxygen-Free embedment were determined to contain 29.78% nZVI by mass. These materials were not rinsed, and so it was likely that higher iron compositions were due to residual unbound iron within the samples. Additionally, the slower drying process (anaerobic evaporative processes vs. a rotary vacuum dryer) may

have allowed for better emplacement of iron within the silica matrix. The materials did not present any qualitative indications of corrosion (Fig. 3.4).

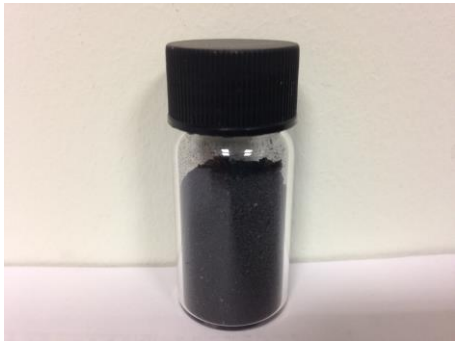

Figure 3.4 19.21g of nZVI-Osorb produced in an oxygen-free environment.

While the 1-pot method had significant advantages over the multi-addition method regarding the practicality of method execution and qualitative aesthetic of the final materials; further characterisation would be required to determine how iron is distributed within the sorbent matrix and how the various embedment methods affected the extent of iron oxidation within the materials. Additional characteristics such as particle size, morphology, surface area, and the dispersion of iron within the material are essential considerations in deployment and should be studied.

3.3 Material Characterization

An ideal iron nanocomposite would increase nZVI longevity by limiting oxidation of the iron without compromising particle reactivity and would retain high iron surface area through limiting particle agglomeration [179]. Both increased longevity and a reduction of the self-agglomeration could result in enhanced reactivity leading to better contaminant treatment with reduced by-product formation and may help composite materials maintain a competitive edge over bulk nZVI in remediative applications despite potentially higher material costs [175].

A variety of physical characterisation and experiments were undertaken to assess iron embedment and the potential to limit undesirable corrosion in the various nanocomposites. Materials' physical characteristics such as particle size, morphology, surface area, and chemical composition, were also evaluated to serve as a useful reference for material deployment in future applications, and contribute to the more significant body of knowledge in related fields.

3.3.1 Iron and Bi-metal Distribution

Even metallic distribution within the nZVI-Osorb composites was desired because the improved dispersion of iron particles typically increases the likelihood that contaminants absorbed into the sorbent will have higher rates of interaction with sequestered metal particles thus increasing overall treatment and degradation rates[175]. SEM-EDS and TEM microscopy techniques were utilised to examine further the particle dispersion of iron embedded in the nanosorbent. Utilizing Transmission Electron Microscopy (TEM), it was possible to observe iron distribution at a series of increasing magnifications (Figure 3.5).

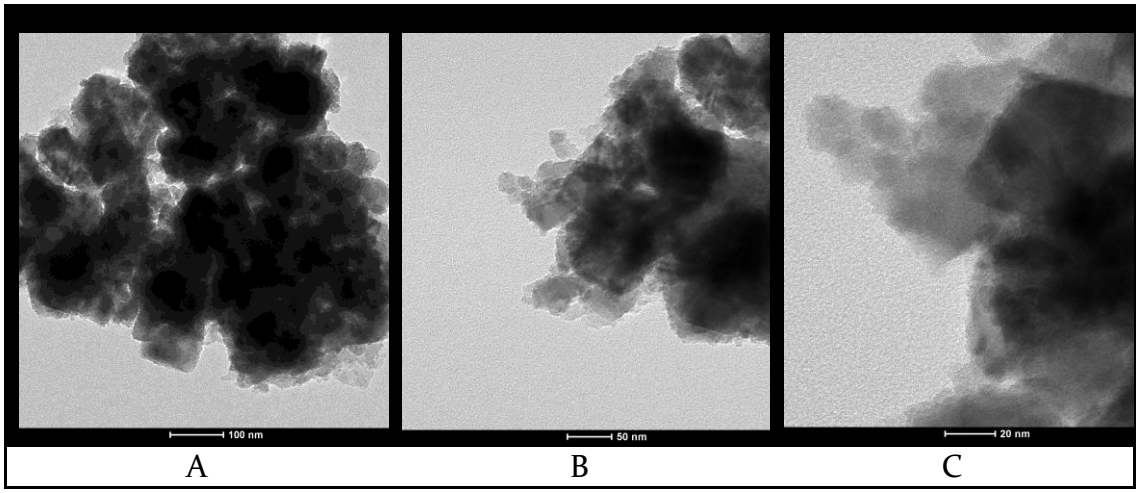

Figure 3.5 TEM images of a 1-pot nZVI-Osorb at increasing levels of magnification.

Iron is electronically dense and will appear significantly darker in imaging than less dense materials such as the sorbent, Osorb. TEM results would suggest that iron was evenly dispersed throughout the composite including within the materials' internal structures. To verify these conclusions and metal distribution, Scanning Electron Microscopy (SEM) enabled with Energy-Dispersive X-ray Spectroscopy (EDS) was utilised. This technique allowed mapping of specific elements, coupled with the imaging abilities of SEM. Figure 3.6 shows the dispersion of iron on the surface of materials embedded by two different methods of iron addition.

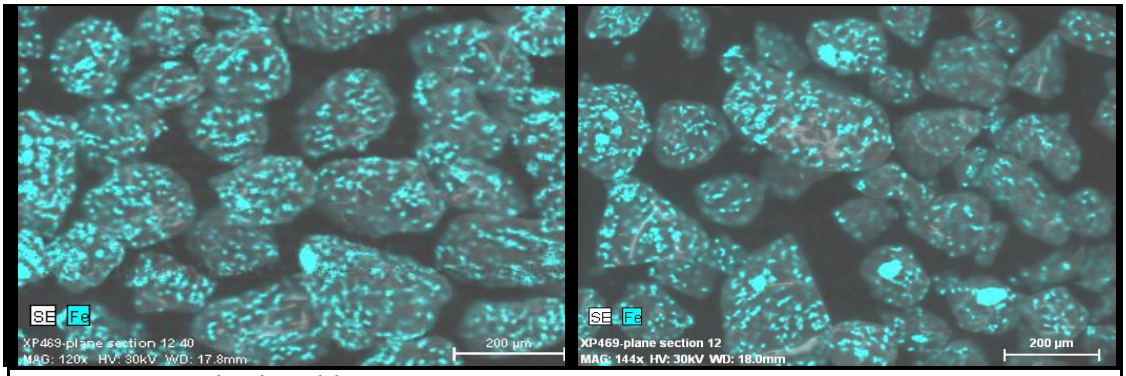

Multiple Addition | 1-Pot

Figure 3.6 Side-by-side comparison of iron distribution between materials synthesised by two different synthesis techniques (Multiple Addition vs 1-Pot) in nZVI-Osorb materials.

In both methods, iron appeared to be evenly distributed throughout the material with a few areas of high iron density 'hot spots'. These images would suggest that the embedment method was successful at preventing iron from self-agglomerating within the material and near its surface. There was no clear difference in metal distribution between iron embedded through multi-addition or 1-pot regarding distribution.

In Fig. 3.6, the material's surface appears smooth but as observed at closer magnifications (such as Fig. 4.8c), and in figures where charging of the surface with x-rays occurred such as in Fig. 3.7, the roughness of the particles surface becomes apparent.

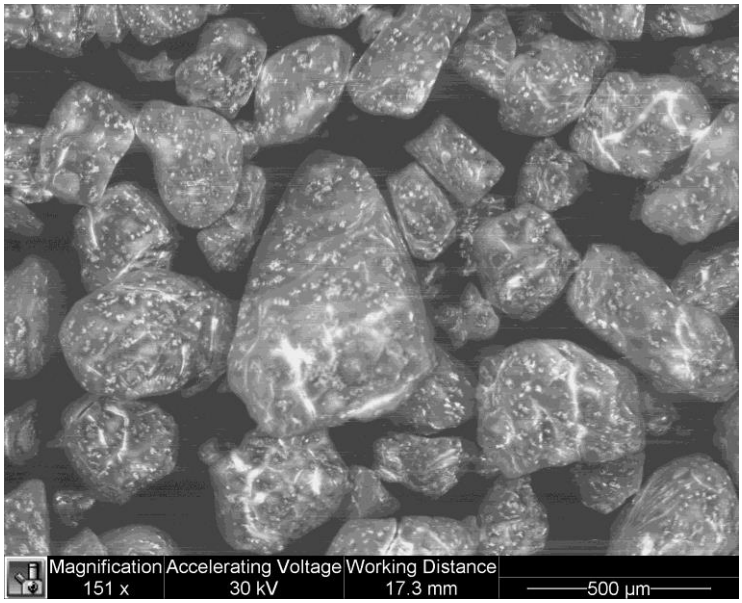

Figure 3.7 An image of nZVI-Osorb synthesised by Multiple Addition by SEM-EDS. Various rough patches on the surface of the material appear brighter from charging effects highlighting the roughness of the surface of the material.

Elemental analysis of the samples also supported the successful embedment of iron within the samples, with iron comprising roughly 1% of the total elemental makeup of the detected sample (Table 3.3). Slight variations, such as observed with iron (1.03-1.24%), were to be expected because values are only representative of the detection window of the material on the microscopic slide and not the total composition of the material by mass (e.g. Tables 3.4 and 3.5) which provide a more holistic assessment of total iron composition.

Table 3.3 A representation of the elemental composition of the various nanomaterials resulting from Scanning Electron Microscopy enabled with Energy Dispersive X-Ray Spectroscopy (EDS). In this spectroscopy, a high-energy incident beam excites outer electrons causing numerous X-rays of various energies to be emitted. These X-rays are matched to the unique peaks of the electromagnetic emission spectrum allowing for elemental determination. Analyzing the breadth of the total emitted X-rays the software determined the percent composition of each element detected in every sample within its detection window[263].

Sample	% C	% O	% Si	% Fe	% Cu	% Ni
1-Pot nZVI	68.24	24.81	5.81	1.14	0.00	0.00
1-Pot Cu	67.02	25.18	6.54	1.24	0.02	0.00
MA- nZVI	68.58	24.35	5.89	1.17	0.00	0.00
MA-Cu-nZVI	70.30	23.33	4.12	1.04	0.14	0.00
MA-Ni-nZVI	70.86	22.69	5.43	1.03	0.00	0.00

While elemental analysis of the samples supported the successful embedment of iron, this was not the case with bi-metal addition. Nickel was not detected in any of the nickel bi-metal samples. The multi-addition embedment method was much more successful at embedding copper at 0.14% than 1-pot embedment which only detected 0.02% copper despite similar ratios of the element added in each synthesis method.

Imaging results also confirmed lower concentrations of copper than desired in the final materials (>>1:5 Cu:nZVI). This comparison was particularly visible in images B and C where iron and copper are both mapped on the images of the composite material (Fig. 3.8).

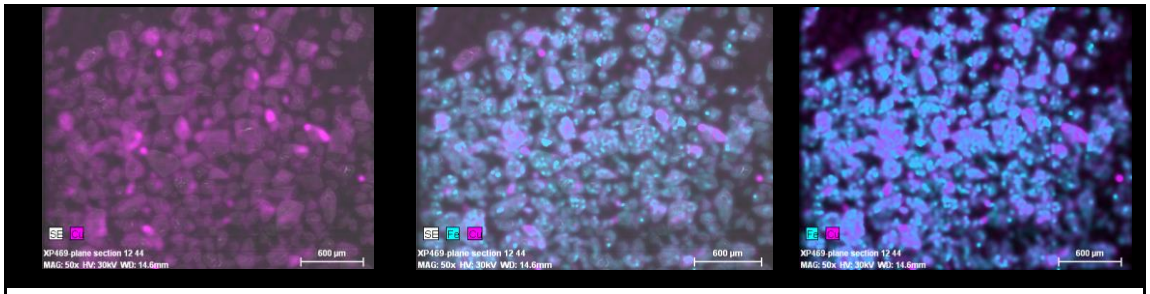

Figure 3.8 Indication of copper bimetal (A) and copper/iron distribution (B, C) from multi-addition synthesis.

It was possible that after copper was reduced and mixed with the iron in synthesis, the mixture was not complete, and some copper particles were not suspended in the metallic slurry with iron. Copper and the nickel nanoparticles, similarly to iron, self-adhered and could have done so either to themselves or the side of the reaction vessel[226]. If the particles did self-adhere, this would result in decreased concentrations in the bulk iron pre-embedment and later after processing in the final material.

However, the copper that was embedded, shown in image A, was found to be satisfactorily distributed throughout the material despite not being as well distributed as the iron in the composites (B, C). Copper nanoparticles did appear to have slight aggregation, with individual markers or 'hot spots' for copper appearing bulkier than the particle sizes of iron.

To address this issue in future work, modifications in synthesis to include the addition of environmentally friendly surfactants, such as sodium dodecyl sulphate (SDS), after reduction of the nickel and copper particles should be examined. The surfactant could help increase dispersion through increased particle mobility upon iron addition and prevent self-adherence counteracting this mild copper and observed nickel aggregation thus improving embedment yields of secondary metals.

Overall, imaging results would suggest that embedding nZVI into Osorb is an advantageous way to prevent iron from self-agglomerating and to preserving the full surface area of individual iron particles. Use of composite substrates is advantageous over the sole usage of surfactants and emulsifiers to prevent agglomeration and increase subsurface mobility because 1) separation is permanent through physical separation, 2)

reactive iron surfaces are not covered by a secondary material, and 3) chemical load into the soil is reduced [175].

Even distribution of sorbent to metal could allow enhanced reactivity with contaminants sorbed into the matrix and held at nZVI active sites within the material [207]. There was no clear difference between iron embedded through multi-addition or 1-pot regarding distribution. However, multi-addition was much more successful at embedding copper bi-metals within the material. Both methods were equally unsuccessful at embedding nickel bi-metals or copper bi-metals in desired concentrations.

While the goal was to have an even distribution of both iron and bi-metals within the nanosorbent, it is important to note that embedment does not entirely dictate the success of the material to remediate contaminants. The oxidation state of the iron will also play a substantial role, and a more in-depth understanding of other material properties such particle size, surface area and morphology will aid understanding of nZVI-Osorb interactions in application.

3.3.2 Surface Properties

Nanomaterials are valued for their unique properties, particularly enhanced reactivity resulting from high surface area to low mass ratios[264-266]. BET and Scanning Electron Microscopy (SEM) were used to analyse the surface features of the materials produced by all three methods of embedment. BET was used to give values for the total surface area (sq. m) and surface area per gram (sq. m/g) of material (Table 3.4).

Table 3.4 The total surface area per gram (BET) values for a variety of synthesised materials.

Sample	Mass (mg)	BET (sq. m/g)	CC (R^2)
nZVI Control	100.5	0.5	0.74847
Osorb	107.1	466.1	0.99992
1-Pot nZVI	106.4	422.0	0.99998
1-Pot Cu	94.7	392.3	0.99998
MA- nZVI	139.2	449.1	0.99994
MA-Cu-nZVI	100.4	349.7	0.99996
MA-Ni-nZVI	103.6	340.2	0.99996

The nZVI control as a nano-metal with a relatively smooth surface was not expected to have a large surface area. In nZVI-Osorb composites which combined a highly porous material (Osorb) with a relatively non-porous dense material (iron), the total composite surface area by mass was also expected to be less than Osorb alone. The surface area for the nZVI control (Nanofer25) was 0.5 sq. m/g, compared to the high surface area of the nanosorbent control (Osorb), which had the highest recorded surface area at 466.1 sq. m/g. All the synthesised materials had BET values ranging from 340.2 to 449.1 sq. m/g.

No apparent trends distinguished materials embedded via multiple additions or 1-pot synthesis. Materials without bimetal addition had a slightly higher total surface area, but variation between different metal compositions was most likely the result of different iron concentrations embedded in the Osorb in embedment opposed to actual changes to surface morphology resulting from the metal addition. The high surface area and expected surface integrity of the nZVI-Osorb hybrid materials were confirmed by SEM imaging (Fig. 3.9).

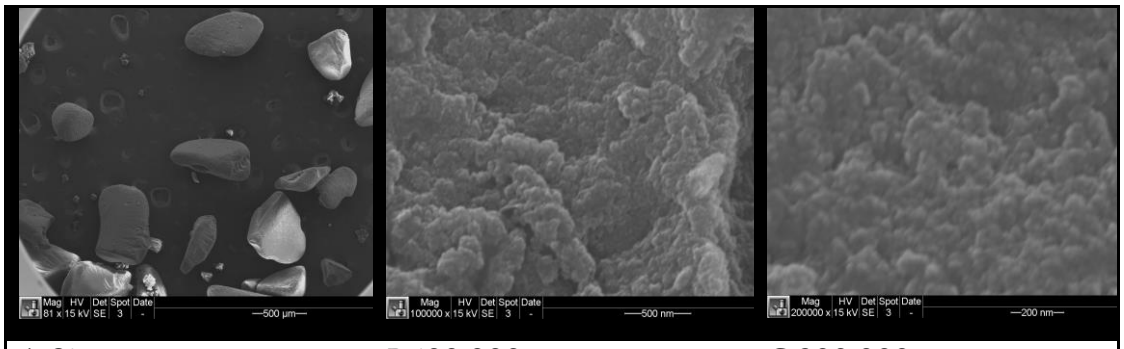

A-81x B-100,000x C-200,000x

Figure 3.9 SEM images of a 1-pot nZVI-Osorb hybrid nanomaterial at increasing levels of magnification exposing a dense highly porous surface composed of 10nm nanoclusters.

The rugged, porous surface of Osorb was retained in nZVI-Osorb composites. This surface morphology was beneficial because high surface area and porosity in sorbents typically allow improved contaminant interaction within a dynamic system which can ultimately lead to better contaminant treatment[267]. Given that adsorptive processes are the first stage of contaminant interaction with nZVI-Osorb, maintenance of high surface

areas remains critical to treatment. Expansion of the sorbent's matrix via swelling from contaminant adsorption is expected to further increase surface area facilitating contaminant absorption and thus result in higher sorptive capacities beyond what could be attributed to solely physioadsorptive mechanisms. Prior work has also indicated that the degree of swelling is relative to the concentration of the sorbate in solution making the material ideal for dilute contaminant streams[134].

Another factor that will influence treatment and design considerations in application is particle size. As discussed in Ch. 1, materials can be deployed through different mechanisms, such as in a packed bed in a fluid system or loosely as a granular filter layer. Particle size considerations will inform design structures for these materials in deployment to ensure materials can be contained and dispersed correctly. This is particularly true in subterranean deployments where particle size will influence fate and transport models. Particle size is also relevant to the discussion of embedment dictating at which size materials can become encapsulated and at which size materials will become excluded.

As discussed, the swelling properties of the silica-based sorbent were utilised to encapsulate metallic nanoparticles which became entrapped inside the silica matrix once the sorbent was dried and the matrix was retensioned. Given this mechanism of embedment, it was expected that metallic particles above a given size would be excluded from the sorbent matrix and would not be embedded in the final composite materials. Similarly, metallic particles which were too small would not be rendered immobile and would be lost during various rinsing cycles in material processing. It was anticipated that only iron particles that were within the particle range of the sorbent could penetrate the matrix and would be retained within the final material. An Occhio Flow Cell was used to test three types of materials from the multi-addition synthesis and two types of materials from the 1-pot synthesis for particle size (Table 3.5).

Table 3.5 Particle size collected from an Occhio flow cell. All values denote diameter in mm. Min and Max values represent the minimum and maximum particles sizes detected. P25, P50, and P75 represent particles falling within the 25th, 50th, and 75th percentile of total measured particles. Mean values represent the average particle size falling within the central particle distribution (P25-P75). The average diameter and standard deviation are representative of the total 4,000-5,000 particles counted in the analysis.

Synthesis	Name	Mean	Min	P25	P50	P75	Max	Dia-meter	ST. DEV.
MA	nZVI-Osorb	0.59	0.047	0.327	0.499	0.681	23.81	2.47	0.516
MA	Cu-nZVI	0.598	0.047	0.310	0.469	0.645	18.58	5.61	0.736
MA	Ni-nZVI	0.66	0.047	0.307	0.479	0.675	13.44	3.21	0.62
1-Pot	Cu-nZVI	0.746	0.047	0.365	0.571	0.786	14.87	3.82	0.824
1-Pot	nZVI-Osorb	0.677	0.047	0.347	0.533	0.731	15.83	4.75	0.749
-	Osorb	0.749	0.047	0.263	0.581	0.675	11.93	6.58	1.13

The average size of the particles falling between the 25th and 75th percentile of all particles was between 0.5 to 0.7 mm in diameter. The largest particles had a maximum diameter significantly higher between 11.9 and 23.8mm. The minimum for all samples gave a reading of 0.047 mm which may indicate that the lower threshold for the instrument may have been reached. Materials made with the 1-pot embedment were only slightly larger than materials made through multi-addition embedment suggesting that varying the method nZVI is embedded into the nano-sorbent matrix did not dramatically affect particle size of the final materials.

The addition of bimetal increased the total composite size with Osorb showing a maximum size of 11.93 mm and all other metal composites showing maximum composites ranging from 13.44 mm to 23.81 mm. The inherent ferromagnetism of nZVI was expected to increase aggregation of some particles in solution despite the substrate restricting iron aggregation within individual particles of the substrate and could account for the larger aggregate sizes observed in the maximum composites.

Embedment processes utilise the swelling mechanism of the sorbent to entrap bimetals throughout its nanoclustered porous matrix as observed in Fig. 1.10, and so it is hypothesised that embedded metals would have particle sizes smaller than individual

Osorb particles. Therefore, total particle size would largely remain unchanged and reflect size characteristics on the nanosorbent, Osorb. This was found to be the case in terms of values reported in the mean and 50th percentile where Osorb particle's sizes were larger than composites and in the 75th percentile where Osorb particle size fell within the distribution of sizes reported for other composites.

All composite materials underwent a washing process and effluent leaching analysis which confirmed that no loosely bound or free iron remained in the samples. Therefore, surface-bound iron and ferromagnetic issues associated with iron could account for variations within particle sizing data and might explain why composite materials in the lower 25th percentile were found to have a slightly larger particle diameter (0.310-0.365 mm) than Osorb (0.263 mm). In general, these results, along with electron imaging and elemental mapping of the composite materials, support the hypothesis that iron particles that were smaller than Osorb had the highest retention in the sorbent matrix after processing.

With an understanding of the hybrid materials surface features in place, the investigation turned toward how embedment and physical properties have affected the oxidation of iron in the composite.

3.3.3 Iron Oxidation

nZVI is highly reactive and will readily react with O_2 to form iron oxides. While such iron oxides do affect water chemistry and can facilitate electron mediated reduction, they are not as advantageous or reactive as un-oxidised nZVI for the breakdown of various water contaminants[186]. Limiting the rate of oxidation of iron or controlling the iron oxide species produced through controlled environmental conditions could dramatically enhance reactivity and prolong the material's period of efficacy after deployment in the field [268].

Two different techniques, X-Ray Photoelectron Spectroscopy (XPS) and Mössbauer Spectroscopy, were utilised to determine the oxidation states of iron in the synthesised

materials to quantify both Fe^0 and iron oxide compositions, as well as, the species of iron oxides produced.

XPS was first utilised. It was expected that through analysing differences in binding energies in the iron $2p^{1/2}$ and $2p^{3/4}$ electron orbital shifting various distinctions could be made between ZVI, iron-halides, and iron oxides. However, the resulting binding energies from XPS analysis overlapped considerably with binding energies of several types of iron oxides and iron-halides making it difficult to draw an accurate conclusion regarding the types of iron present in the sample (Table 3.6)[269].

Table 3.6 (Left) the resulting XPS peaks for various samples and (Right) Expected peak shifts for various iron compounds[269].

Sample	Peak
MA-nZVI	711.56
MA-nZVI-Cu	709.21
1-Pot nZVI	711.62
1-Pot nZVI-CU	711.74

Iron Types	Peaks
Metal Oxides	528-531
Fe_2O_3	530.0
$FeCl_3$	711-711.5
$FeCl_2$	710.5-711
Fe_2O_3	710.9
FeOOH	711.3-711.9

Due to the inconclusive results of the XPS data, a second method utilising Mössbauer Spectroscopy was employed to determine the iron oxidation species. Mössbauer Spectroscopy utilised a radiated cobalt source for element-specific characterisation of iron. The radiated technique allowed for full penetration of the sample and should be representative of iron species at the surface of the material as well as iron embedded within the sorbent matrix. The spectral shifting analysis permitted the distinction of various iron species within the material (Table 3.7).

Table 3.7 The varied species of iron as determined by Mössbauer Spectroscopy.

Sample	% Fe-Oxides	% Fe^0	% Fe-SiO_2
MA-nZVI	95.75	0.25	4
MA-nZVI-Cu	94	2	4
MA-nZVI-Ni	86	7	7
1-Pot nZVI	77	10	13
1-Pot nZVI-Cu	86	7	7

As discussed in Ch. 2, all materials obtained by MA or 1-Pot embedment were stored under ambient aerobic conditions where no advanced oxidation was observable by eye. However, Mössbauer spectroscopy indicated that the majority of iron embedded in the samples from multi-addition and 1-pot iron synthesis had oxidised. Multi-addition samples had nZVI concentrations ranging from 0.25 to 7% with the remaining iron existing as iron oxides or iron silica oxides. Materials manufactured through 1-pot iron embedment had slightly higher concentrations of nZVI at 10 and 7% respectively which could indicate that 1-pot embedment was slightly more effective at preventing oxidation of the embedded iron than multi-addition embedment or merely that iron was less oxidised pre-embedment.

SEM-EDS images of the two synthesis methods highlighted in Fig. 3.6 showed near identical distribution of iron which would suggest that second scenario is more likely. Time to complete the multi-addition synthesis was substantially longer than synthesis by 1-pot addition. This additional time allowed a more extended exposure period of reduced iron nanoparticles to the atmosphere increasing the likelihood of iron oxidation before embedment.

The material that exhibited the highest nZVI content was 1-Pot nZVI, which also exhibited the most significant percentage of Fe-SiO_2 interactions at 13 %. It may be possible that if the iron in the matrix crosslinked with silica in the sorbent, advanced oxidation of the metal could be reduced. However, samples MA-nZVI and MA-nZVI-Cu both had similar percentages of Fe-SiO_2 but differed significantly in their nZVI content. The effect of crosslinking thus may be more strongly due to the type of embedment deployed and its concurrent level of aerobic exposure during the embedment process. Future work is recommended that strives to crosslink iron particles within the silica matrix of the nanosorbent in its sol-gel synthesis procedures under anaerobic conditions could shed further light on this issue and should be evaluated for effects on iron corrosion.

The presence of the bimetals copper and nickel did not appear to increase the rate of oxidation in the material to a significant degree. In multi-addition embedment, samples with bi-metals had a higher Fe^0 content compared to those with a bimetal in a 1-pot synthesis that had a lower Fe^0 content. Because bi-metals constitute such a small

percentage of the overall material (0.02% Cu in 1-Pot, 0.14% in MA), it is unlikely the copper or nickel bimetals had a dramatic effect on the oxidation of the iron.

High rates of oxidation of the material are ultimately unfavourable because they reduce the amount of core reactive iron (Fe^0) thus decreasing the total available electrons which can be transferred to degrade a particular water contaminant[243]. It could not be concluded whether the majority of the oxidation of iron in these compounds occurred before final embedment during the intermediate processing steps or after final processing while the material was in storage. To better determine the rate of oxidation of the iron within the material, a new testing approach was adopted utilising material created and stored in an oxygen-free environment.

3.3.4 The Rate of Oxidation (50 Day Trial)

Materials that could limit the oxidation of nZVI while retaining iron's reactivity to degrade compounds would be exceedingly advantageous. Materials made through the 1-pot, and the multi-addition process had a high percentage of iron oxide formation, but it was unclear whether the bulk of oxidation occurred before embedment, during the storage period after processing, or progressively during both periods. A series of trials was conducted to observe differences between nZVI-Osorb and nZVI control upon first exposure to oxygen to determine the effect of Osorb on iron oxide formation. These measurements were continued over a period of 50 days to determine the rate of oxidation of iron embedded within Osorb (Fig. 3.10).

Figure 3.10 Percent composition of various iron species in Oxygen-Free nZVI-Osorb (Top) and a nZVI control (Bottom) after 1 day and 50 days of air exposure.

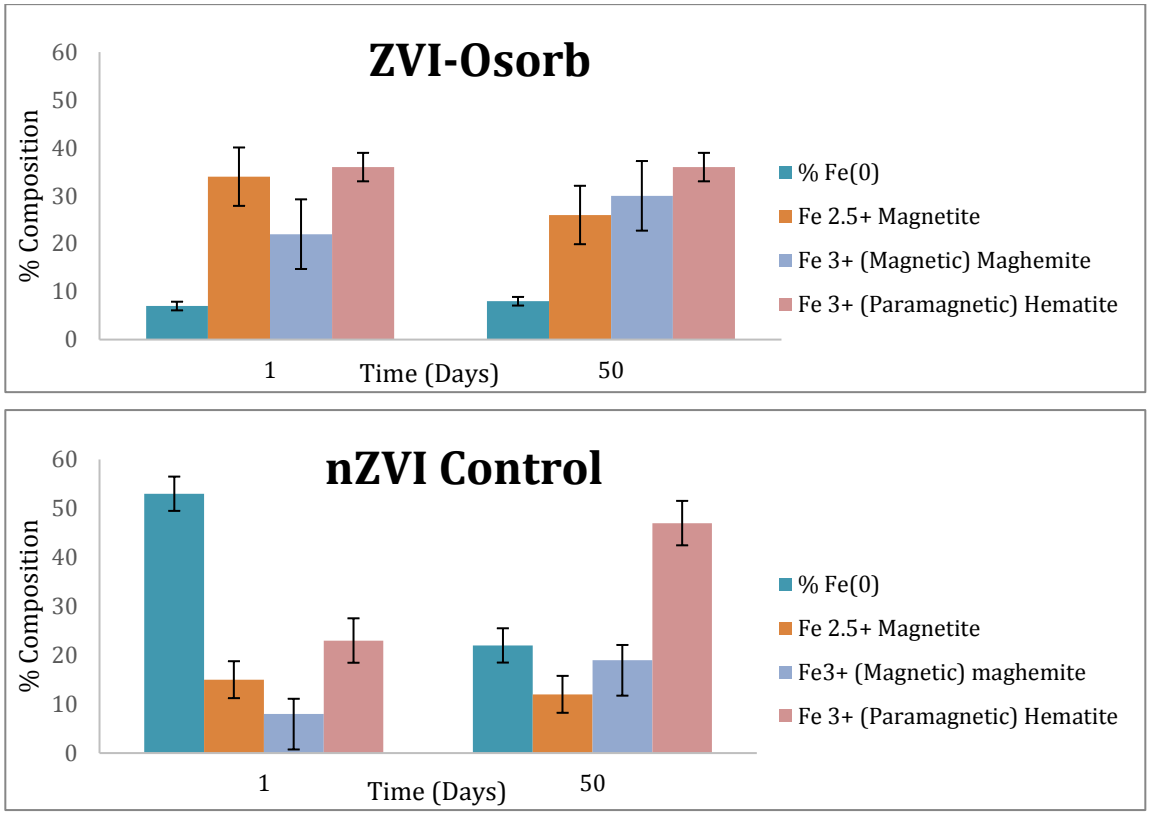

After the minimum of 24hrs (required to run the analysis), nZVI-Osorb contained approximately 7% nZVI compared to the control that contained 53% nZVI. 50 days later the nZVI content of nZVI-Osorb remained relatively unchanged, but the control's nZVI content had decreased to 22%. This result suggested that iron embedded in the sorbent oxidised at a much faster rate than that of the control within the first 24 hrs. of air exposure. Additional results from this trial showing periodic monitoring of iron oxide formation are detailed in Fig. A1.1 and A1.2 in Appendix 1.

As previously illustrated, the nanosorbent was effective at evenly distributing the iron throughout its highly porous matrix, as opposed to nZVI, which readily self-agglomerates limiting surface area. It was possible that by increasing the surface area and distribution of the metal throughout a highly porous sorbent, the volume of O_2 exposure to the surface of the iron was increased, thus leading to an increased formation of iron

oxide which was ultimately undesirable when compared to unoxidized Fe^0 which retains the highest level of reduction potential.

Three types of iron-oxides (Fe^{+3}, magnetic, maghemite), (Fe^{+3}, paramagnetic, hematite), ($Fe^{+2.5}$, magnetic, magnetite) and unoxidized iron Fe^0 were observed in the test samples. These distinctions are important because different types of iron oxide have unique properties such as magnetism and some iron oxide species are more conducive to electron transfer and therefore contaminant degradation than other oxide or hydroxide species (Table 3.8).

Table 3.8 Properties of various iron hydroxide species[152, 247, 252, 260, 268]

Charged Iron Species	**Iron Hydroxide**	**Formula**	**Magnetic**	***e*- transfer from Fe^0 core**
Fe^{2+}	wüstite	FeO	yes	yes
Fe^{2+}	ferrous hydroxide	$Fe(OH)_2$	no	no
Fe^{2+} / Fe^{3+}	magnetite	Fe_2O_4	yes	yes
Fe^{3+}	hematite	α-Fe_2O_3	no	no
Fe^{3+}	maghemite	γ-Fe_2O_3	yes	yes
Fe^{3+}	ferric hydroxide	$Fe(OH)_3$	no	no
Fe^{3+}	goethite	α-FeOOH	no	no
Fe^{3+}	lepidocrocite	γ-FeOOH	no	no

In Fig. 3.8, the nZVI control mostly formed Fe^{+3} oxides (hematite) over the course of the time trial, which is not conducive to electron transfer. Conversely, nZVI-Osorb mainly formed $Fe^{+2.5}$ oxides (magnetite) which still permit electron transfer from core Fe^0 electrons to the surface. When considering the total of nZVI and iron oxides that permit electron transfer, the nZVI-Osorb samples remain relatively consistent over the 50 days starting with 63% active material and ending the trial with 64% active iron material. nZVI control, however, started with a large percentage of active material (78%) yet through hematite formation the total active composition of nZVI control was reduced to 53%.

pH environment in synthesis has been known to influence iron-oxide species formation. Acid conditions tend to favour the formation of Fe^{3+} ions which are more conducive to Fenton's reactions and can accelerate the reduction of a target species. Conversely, in alkaline environment iron oxides tend to form as ferrous hydroxide ($Fe(OH)_2$) which is less favourable to Fenton's reactions [168]. nZVI utilised in the control and nZVI-Osorb in the composite came from the same source and were both synthesised under acidic conditions, so differences in oxide species are most likely not the result of processing conditions but due to effects from the silica sorbent Osorb. Similar types of iron shifting have been observed in other iron spectra when specific inorganic geologic materials surround the element [270, 271].

Another study, which also utilised a type of organically modified silica, methyltriethoxysilane (MTEOS) produced through sol-gel processes, found that the hydrophobicity and methyl groups present in the silica sterically hindered Fe-O-Si bonds driving the formation of Fe^{2+} (Fe_2O_3) oxides[233]. In Mössbauer analysis, Fe-O-Si interactions through either organically modified[233, 272] or naturally occurring silicas in inorganic geological formations produce characteristic spectral shifting[270, 271] similar to the shifts observed for iron oxides detailed in the last column in Table 4.8.

While iron-oxide remain important and some oxide species (magnetite, maghemite) can allow contaminant reduction to proceed, it is however important to note that ZVI is the form of iron which retains the highest reduction potential of any iron species and is the form of iron most likely to lead to the best contaminant degradation results in application. Initial time points detailed in Fig. 3.8 indicated that materials had already undergone partial oxidation. To better assess oxidation rates a shorter time trial utilising oxygen-free nZVI-Osorb was tested.

3.3.5 The Rate of Oxidation (48 hr. Trial)

Given a common nZVI source it was assumed that both materials should have similar percentages of Fe^0 upon first exposure to the atmosphere. An additional trial was undertaken to determine the rate of iron oxidation within the first 24 hrs. of oxygen

exposure because Fig. 3.10 had suggested that significant oxidation of iron had occurred within this time frame when compared to control nZVI (Fig. 3.11).

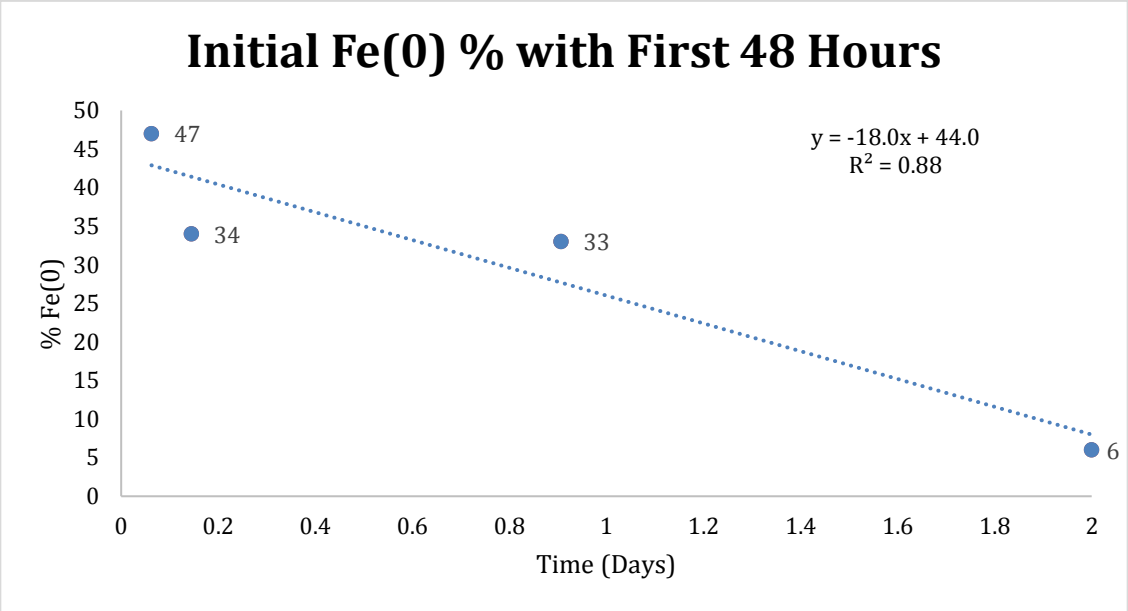

Figure 3.11 The percent composition of nZVI within oxygen-free embedded nZVI-Osorb at 1.5, 4.75, 21.75, and 48 hrs.

Measurement of Fe^0 concentration measured at 1.5 hours found a significantly higher percentage of nZVI (47%). This percentage was closer to values observed with the control after 24hrs (53% nZVI). It was determined that nZVI-Osorb materials lose roughly 18% of their starting iron composition each day until a stabilising concentration of nZVI was observed after 48 hours of atmospheric exposure. This stabilisation of Fe^0 composition could be due to the oxidisation of all atmospherically accessible iron (surface atoms) within the material. Other studies have found that iron-oxides typically form only on the surface of exposed iron, shielding deeper iron particles from oxidation [178, 247]. That is most likely also the case with iron-oxides formed within this study.

In general, it appears that embedding nZVI in the Osorb matrix does not reduce the rate of oxidation of the iron. If anything, it appears to increase the rate of oxidation until rates reach an equilibrium which could be due to the success of the sorbent to

disperse the iron throughout its highly porous matrix. However, such losses of Fe^0 do not necessarily mean that degradation reactions cannot proceed.

The iron-oxide species that were formed in nZVI-Osorb were more favourable to continual electron transfer than iron oxides formed in nZVI controls suggesting that nZVI-Osorb may still outperform control materials in contaminant treatment. Additional investigation into the rates of degradation of a model contaminant would provide additional insight into how these individual particle characteristics affect the overall attributes of the material in treatment.

3.4 Summary

nZVI is a useful nanomaterial known to degrade many common pollutants. The effectiveness of nZVI in field and laboratory applications, however, is often hindered by undesired oxidation and the reduction of surface area from self-agglomeration. A variety of materials were created using three different embedment methods (multi-addition, 1-pot, oxygen-free) with some containing an additional bi-metal (copper or nickel) for enhanced reactivity to address some of these common nZVI issues.

All synthesis procedures resulted in granular particles ranging from 0.5-0.7mm in diameter that were further composed of smaller 10nm nanoclusters arranged in a dense highly porous network. Surface area ranged from 233-435 sq. m/g. Particle size and morphology remained constant throughout all embedment methods suggesting that altering various embedment procedures would not dramatically alter deployment or transport mechanisms. No metallic leaching was detected in effluent waters after final processing, suggesting a stable nanocomposite matrix.

Composite materials were composed of roughly 10 % iron by total mass in 1-pot and multi-addition samples and 29.78 % iron by mass in oxygen-free samples. The 1-pot embedment method allowed for the most substantial control of final iron concentration with a standard deviation of 0.15 % from target compositions. Ni-ZVI and Cu-ZVI bimetal embedments were less successful than iron embedment alone with a minimum of Cu and no Ni detected in final samples. The addition of a surfactant in future synthesis should be

utilised to improve bi-metal embedment. Iron that was embedded was found to be evenly distributed throughout the sorbent suggesting that the composite material restricted iron self-agglomeration.

High surface area and even iron distribution could potentially lead to improved contaminant sorption and degradation by increasing the availability of reactive iron sites. Results suggested that altering various embedment procedures would not dramatically alter deployment or transport mechanisms of the material as particle size and morphology remain constant.

While self-agglomeration was primarily prevented by embedment (via various synthesis methods), it was not successful at limiting the oxidation of the nZVI. Iron was found to oxidise at a faster rate in the created materials than the control materials. Increased oxidation is most likely due to enhanced dispersion facilitating higher surface area exposure of iron particles within the nanocomposite. On average, the nZVI-Osorb materials exhibited an 18% $nZVI^0$ loss per day until reaching stabilised concentration (7 %) after 48 hrs. However, the iron-oxide species produced were primarily conducive to electron transfer and should not prevent contaminant degradation mechanisms from progressing. Corrosion results would suggest that developed material may be most successful in anaerobic and other low-oxygen environments where oxygen is less readily available and reactive core iron (Fe^0) critical to contaminant degradation could be preserved. Materials synthesised by the oxygen-free embedment method and stored in anaerobic environments before immediate use were utilised in all subsequent testing with model contaminants to ensure the highest possible iron reactivity is present in the starting materials.

Chapter 4 : Adsorption and Degradation of 2,4,6 Trichlorophenol by nZVI-Osorb

4.1 Introduction

2,4,6- Trichlorophenol is a toxic water contaminant found in a wide variety of water systems (Ch. 1.1). Current treatment practices for this contaminant are inadequate, and there is a demonstrated need for improved treatment options (Ch. 1.2). nZVI has shown broad applicability in degrading many water pollutants, and nZVI-based nanocomposites, in particular, are promising for the improved treatment of TCP (Ch. 1.3). nZVI-Osorb composites developed in this thesis have the potential to improve TCP treatment further through the incorporation of a novel high capacity sorbent with a broader sorptive range than other widely available sorbents (ref. Table 3.1). Furthermore, the previous chapter demonstrated that the produced nZVI-Osorb nanocomposites were tightly bound with an even iron dispersion that may be promising for the remediation of TCP contaminants through increased stability and improved iron availability in treatment (Ch. 3).

No prior work has evaluated the use of nZVI-Osorb for the sorption or degradation of TCP, and so treatment mechanisms must be derived from first principles and results from relevant studies. The proposed mechanism of treatment of TCP by nZVI-Osorb was modelled after previous work with Osorb[134, 235, 236], similar silica-nZVI composite treatment mechanisms[138, 179, 192, 208, 213], and TCP degradation steps with nZVI[29, 109, 195]. The proposed treatment process involves (1) the sorption of TCP into the nZVI-Osorb matrix by the nanosorbent, Osorb, and (2) the concurrent reductive degradation of TCP by nZVI (Fig. 4.1).

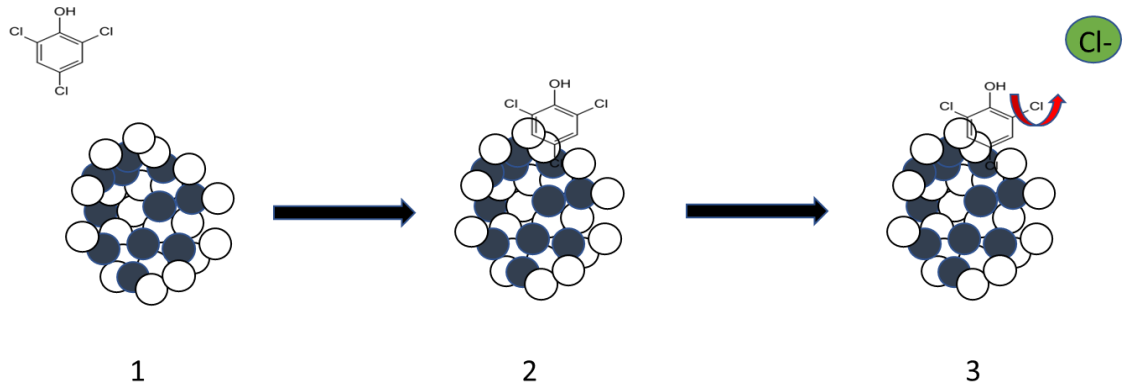

Figure 4.1 A model of the proposed treatment of TCP by nZVI-Osorb. Black dots represent nZVI. White dots represent Osorb. In (1) nZVI-Osorb composites are deployed into a solution containing TCP. (2) TCP becomes absorbed by Osorb in the composite material. (3) nZVI interacts with sorbed TCP and reduces compound by reductive dehalogenation. Degradation pathways proceed from this instance as described in Ch.1.

The nanosorbent Osorb, which makes up the majority (90-70.22% by mass) of the nanocomposite (ref. Table 3.1-3.2, Fig. 3.4) is chemically inert and will remove contaminants of affinity from solution through both adsorptive and absorptive processes detailed in Section 4.1 and observed in step 2 of the treatment mechanism above. Sorptive affinity is highest for small nonpolar organics (ref. Table 1.8) but also has affinity for related chlorinated organics like perchloroethylene which share a similar Log K_{ow} value (Fig. 4.2).

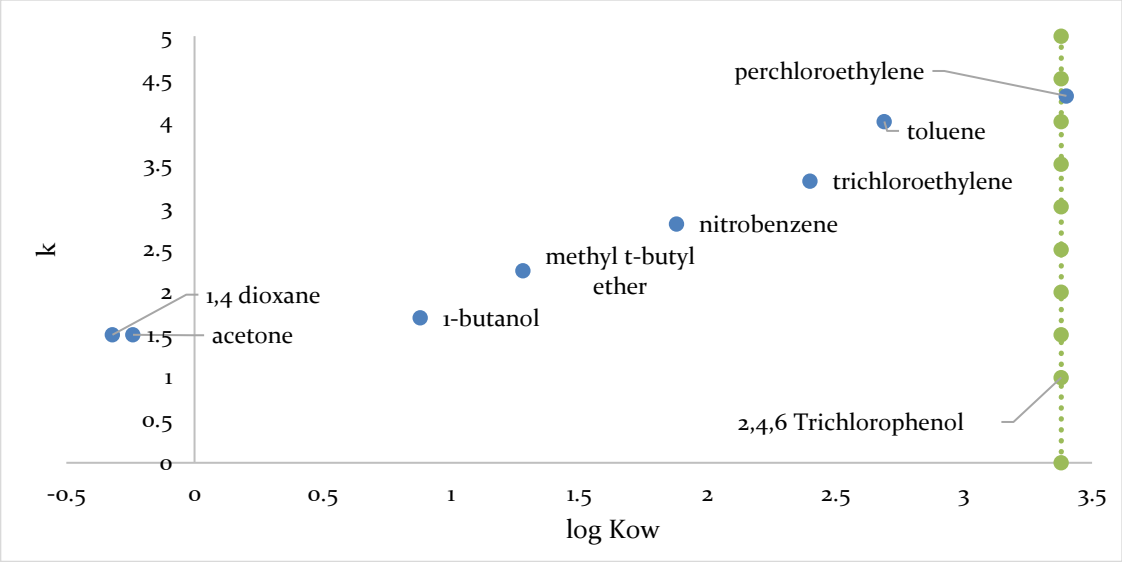

Figure 4.2 A plot of the partition coefficient (log K_{ow}) versus sorption coefficient (log k) for binding of various contaminants (1,4 dioxane, acetone, 1-butanol, methyl t-butyl ether, nitrobenzene, trichlorophenol, toluene, & perchloroethylene) in water by Osorb. Contaminant concentration was 100mg/L with a 0.5% (w/v) addition of Osorb per volume of solution. A linear regression line fitting positive LogK_{ow} contaminants was determined to be log(k)= 0.97 x log(K_{ow}) +0.96, R^2=0.998. The vertical line indicates where the TCP LogK_{ow} value (3.38) falls in relation to tested contaminants[134].

The logK_{ow} value of perchloroethylene of 3.4 is close to TCP's 3.38 and following the log(k) trend observed in Figure 4.2 is believed to be within Osorb's sorptive range with a predicted sorptive coefficient log k of 1.47 and a k value of 4.35 by the linear regression equation **(4.1)** [134].

$$\text{Log (k)} = 0.97 \times \text{Log } (K_{ow}) + 0.96 \qquad \textbf{(4.1)}$$

Breakthrough curves with 145 mg/L perchloroethylene in a packed bed with three different materials (molecular sieves, activated carbon, and Osorb) showed that Osorb has the highest sorptive capacity, absorbing approximately 15,000-bed volumes per relative concentration compared to molecular sieves at approx. 1,000 and activated carbon at 6,000 bed volumes[134]. These results initially suggest that TCP sorption by Osorb may be

competitive with other adsorbents like GAC or molecular sieves and could potentially be utilised on its own as an additive to remove TCP from solution.

Yet, of course, sorptive affinity is unique to both the physical properties of both the sorbent and sorbate [123]. Further studies exploring sorptive features such as contact time and sorptive capacity for TCP removal by nZVI-Osorb are crucial for mechanistic and material understanding. These parameters also facilitated the further development of treatment systems wherein dwell time, bed depth, and sorbent loading are optimised for efficiency and total contaminant removal [133].

While sorption is highly effective at removing contaminants from aqueous streams, further treatment is required to degrade both the sorbate and any residual contamination remaining in solution[170]. In nZVI-Osorb, the high sorptive capacity of the sorbent also serves to concentrate contaminants near iron active sites for improved degradation and also retains degradation by-products for further reduction and decreased by-product release (Fig. 4.1, Step 3).

As discussed in Section 1.3, nZVI is well suited for organic contaminant degradation[138, 179]. However, despite this broad applicability, nZVI and ZVI performance in the degradation of chlorophenols has been variable with some studies finding complete degradation[184], most finding incomplete degradation[179, 217], others finding no degradation at all[195]. The variability in degradation found in these studies is examined at length in Table 4.5 later in this chapter, but largely is the result of the varying molecular properties of the chlorophenols, and differences in the applied materials and their method of deployment.

The base compound, phenol, demonstrates resistance to reductive degradation because π-π stacking stabilises the C6 aromatic ring structure of phenol and thus requires significant reduction energy to cleave. These reduction levels can be met by nZVI, but chlorophenols with an increased number of chlorine substituents (each a strong electron withdrawing group) change the compound's physical properties. These substitutions increase overall electronegativity and as a result, will require higher overall reduction potentials to cleave the chlorides and degrade the base phenol molecule [165]. Typically, degradation occurs more readily in less substituted compounds such as chlorophenol or dichlorophenol than more substituted phenols like TCP or PCP [273]. If degradation does

occur in the higher chlorinated phenols, it is sometimes incomplete, resulting in the formation of less chlorinated by-products like chlorophenol or phenol[274].

Since chlorophenol studies utilising ZVI regularly detected by-product intermediaries (Ch. 1.3), it was expected that some by-products would form during degradation of TCP by nZVI-Osorb. The sorptive affinity of Osorb for different chlorophenol species should be tested to evaluate whether dechlorinated by-products, if formed, would be retained in the sorptive matrix after partial degradation. Retaining these by-products could be beneficial to perpetuating further reduction by embedded iron particles located near the contaminant and reduce overall by-product formation during treatment. Leaching of TCP from the sorptive matrix should also be considered as it will influence overall treatment effectiveness [275].

A second factor that contributed to the variability in TCP treatment by nZVI was the broad nature of nZVI-based materials applied to treatment, each with its own unique experimental set-up and test deployment[29, 109, 178, 179, 195]. As discussed in Ch. 1, nZVI's self-agglomeration and instability in the presence of oxygen reduce the overall reactivity of nZVI and perpetuates incomplete degradation[21, 177, 217, 276]. Modifications to nZVI including a substrate, such as silica, have been found to increase overall treatment over unamended nZVI by addressing these primary material hinderances[168, 179, 184, 186, 217, 241, 277].

One study of note that embedded nZVI into silica beads found the full dechlorination of 100mg/L 2,4,6-trichlorophenol, dichlorophenol, and 4-chlorophenol respectively occurred after 4 hours of recirculation within an nZVI-silica packed bed. Full dechlorination was not observed at contaminant concentrations above 100 mg/L [184]. This study indicates the promise of nZVI embedded into silica to dechlorinate phenols in restricted (e.g. closed-recirculating) aerobic conditions, although further modifications to the original composite that would allow faster treatment rates and complete mineralisation of chlorophenols at higher concentrations in open systems would be preferred [184].

As discussed in 1.5, the work in this thesis utilised a silica sorbent to improve both iron dispersion and stability for higher iron reactivity. The studies revealed a tightly bound network of well-dispersed iron but at the cost of increased oxygen availability and corrosion. Further evaluations are needed to determine whether degradation of TCP in

solution can be improved through combined sorption and degradation mechanisms detailed in Fig. 4.1, as well as, the effect of oxygen availability in solution on treatment.

Full evaluation of relevant sorptive and degradation features of nZVI-Osorb will provide a broader understanding of how the nanocomposite functions in aerobic water treatment scenarios for a model chlorinated contaminant. These experimental features are the foundational step in establishing a detailed understanding of the material's functionality in a contaminated water system, through supplying evidence for a proposed treatment mechanism, contributing to the intellectual grounding for other works involving nZVI and embedded metal composites, and acting as a reference for treatment in more complex contaminated waters. As such, the conclusions from this chapter will be carried forward into experiments examining the effect of specific water conditions on treatment (Ch. 5) and the development of model anaerobic digester systems which explore applied aspects of nZVI-Osorb in anaerobic waste and wastewater systems (Ch. 6).

4.2 Sorption Properties of Trichlorophenol by nZVI-Osorb

4.2.1 Absorptive Capacity and Contacting Time

Adsorption and absorption both require physical contact with the sorbate to permit adherence. Dilute solutions can sometimes require longer retention and contact times than equivalent solutions with high concentrations of contaminants [204]. An understanding of contact time is also crucial in system design and application. In flowing systems, contact time can be increased by lengthening bed depth or slowing flow rates. In pond and pooled systems, required contact time can be reduced through stronger agitation and faster mixing [203].

To determine the optimal contact time for nZVI-Osorb, 25 mg of sorbent were stirred with a fixed concentration of TCP over different time periods (5 mins, 1.5, 24, and 48 hours) (Table 4.1).

Table 4.1 100 mg/L TCP solutions (10 mL, pH 5.11) in water mixed with 25 mg of nZVI-Osorb for 5min, 1.5hrs, 24, 48 hrs. ±0.008hrs. Time points in the series were not continuous and were conducted individually with a universal starting solution.

Time (hrs)	TCP sorbed Q_e (mg/g)	% Reduction
0.08	25.19 ±0.14	62.97 ±3.53
1.5	30.00 ±0.16	74.99 ±4.12
24	35.93 ±0.06	89.83 ±1.62
48	35.24 ±0.05	88.10 ±1.33

It was found that the majority (approx. 62.97%) of sorption occurs rapidly within the first 5 minutes of interaction. A second study utilising continuous sampling was conducted to determine sorptive equilibrium time (Fig. 4.3).

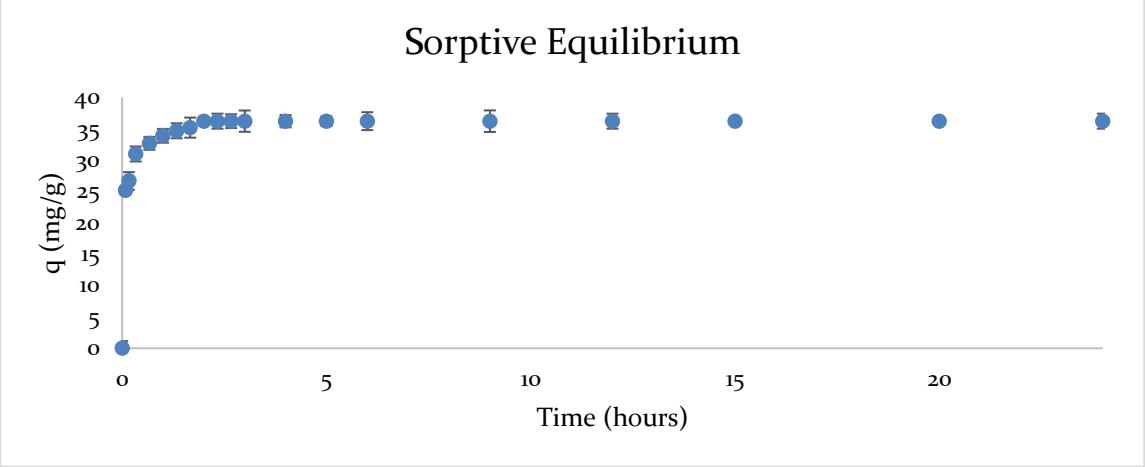

Figure 4.3 100mg/L TCP solution (220mL, pH 5.1) in water was continuously mixed with 550mg nZVI-Osorb (25mg per 10mL) for 24 hrs.

TCP sorption reached equilibrium at proximately 2 hours ±0.83 after which sorptive capacity remained stable. Sorption capacity at equilibrium (Q_e) was calculated by **(4.2)** wherein C_o is initial concentration (mg/L), C_e is the concentration at equilibrium (mg/L), V is the volume of solution (L), and W is the mass of the sorbent (g).

$$Q_e = \frac{(C_o - C_e)\,V}{W} \qquad \textbf{(4.2)}$$

Q_e was determined to be 36.23 ±0.24 mg TCP/g nZVI-Osorb (pH 5.1) with a total reduction of TCP 90.59% ±0.93. 24 hours of contact time was used as a baseline for all the following tests to ensure consistency and that all solutions throughout this trial had reached equilibrium. Contact times for TCP were on par with other sorption equilibrium times for activated carbon within this concentration range (GAC, <20 min, 50-150 mg/L TCP). Contact times above this concentration threshold (200 mg/L) were reported to require 5-6 hours to reach dynamic equilibrium [278].

High sorptive capacities are desired for most sorbents because they can reduce general operational costs associated with replacement and regeneration [122]. In Table 4.1 maximum sorption was determined to be 35.93 ±0.06 mg/L TCP sorbed per 1 g of nZVI-Osorb (100mg/L TCP, 25mg nZVI-Osorb, 10mL). In Fig. 4.3 sorption per mg is slightly higher at 36.23 ±1.10 mg/L TCP sorbed per 1 g of nZVI-Osorb (100mg/L TCP, 125mg nZVI-Osorb, 50mL) but still equivalent when considering the standard deviation. Furthermore, both capacities are consistent with measured maximum capacities with equivalent TCP concentrations discussed elsewhere within this chapter (ref: Fig. 4.7, 35.23 ±0.60 mg/g, Table 4.3 35.89 ±0.44 mg/g, Table 4.4 34.8 ±2.48 mg/g, Table 4.5 35.9 ±1.10 mg/g).

To empirically test kinetic capacity, nZVI-Osorb, Osorb, and granular activated carbon (GAC) were analysed for their capacity to sorb 120 mg/L TCP at four masses (5, 10, 25, 50 mg) (Fig. 4.4).

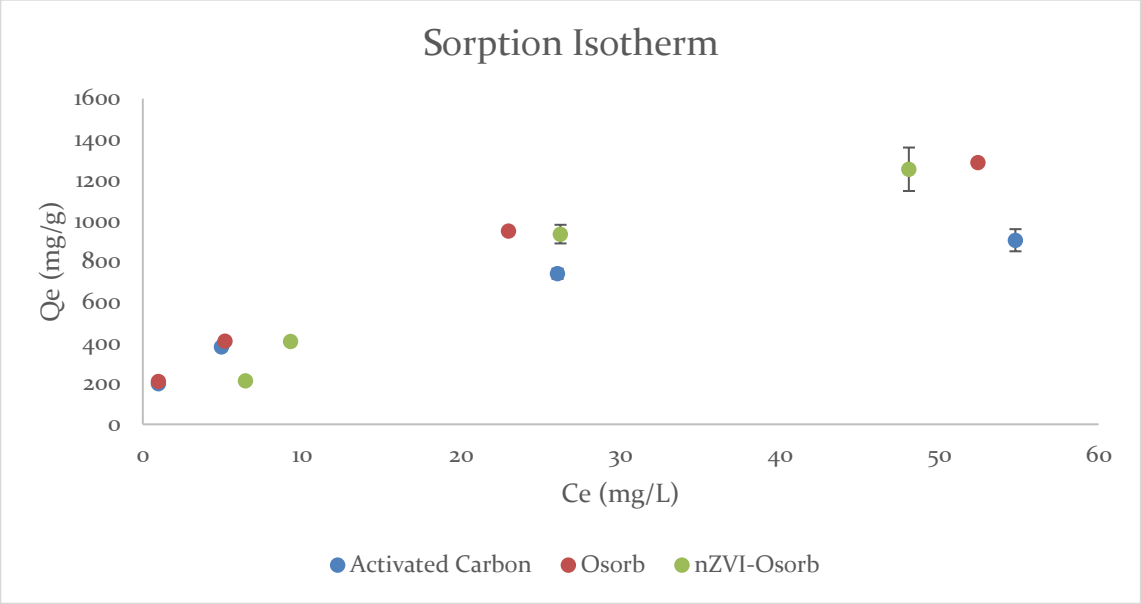

Figure 4.4 Amount of solute sorbed per g sorbent (Q_e) versus the equilibrium concentration of the solute remaining in solution (C_e). TCP concentration was 120±6.63 mg/L. Sorbent masses were 50, 25, 10, 5 mg. All starting pH was consistent at 5.1, and all solutions were shaken for 24 hours.

A sorption isotherm plotting the amount of solute sorbed per g sorbent (Q_e) versus the equilibrium concentration of the solute remaining in solution (C_e) found that nZVI-Osorb and Osorb were better sorbents of TCP for each mass considered (50, 25, 10, 5 mg). The treatment capacity of the three sorbents was closest when contaminant load is low per gram (25 mg, 50 mg, 100 mg/L TCP). At 10 mg, nZVI-Osorb absorbed 19.46 ±2.80 mg/L more than GAC. At 5 mg of TCP, there was an advantage of 17 ±2.86 mg/L. 50mg tests removed all the TCP from solution due to an excess of material in solution. 25mg samples of nZVI-Osorb and Osorb performed slightly better than previous test (~90%) removing 90.73 ±3.49 % and 94.84±1.66 % respectively.

Value of adsorption capacity (Q_e) for activated carbon utilising 50, 25, and 10mg GAC are within the reported maximum monolayer sorptive ranges for GAC (112.35-500.00 mg/g) reported in the literature for 2,4,6-trichlorophenol [278]. Adsorption capacity at equilibrium (Q_e) for 5mg of material was determined to be 1253 ±1 06.7 mg TCP/g sorbent

for nZVI-Osorb, 1286.4 ± 13.5 mg TCP/g sorbent for Osorb, and 904.44 ± 54.5 mg TCP/g sorbent for GAC.

These reported capacities are higher than any reported capacity for TCP with comparative sorbents previously listed in Table 1.4. The maximum nZVI-Osorb capacity was a 35.40 fold improvement over hollow fibres (35.4 mg/g), 7.12 times that of pristine graphene (175.8 mg/g) and 3.70 times that of amino-functionalized silica (338.8 mg/g). The high sorptive capacities observed in this study are attributed to the high surface areas (422.9 sq. m/g) listed previously in Table 3.3.

Fig. 4.4 was plotted against Langmuir and Freundlich isotherm models. The Freundlich isotherm **(4.3)** produced the best fit. In the following equation, k_F and n represent constants, while Q_e denotes the amount of solute (mg) adsorbed per gram of sorbent, and C_e represents the concentration of solute remaining in solution at equilibrium.

$$\ln(Q_e) = \ln k_F + 1/n \ln C_e \qquad \textbf{(4.3)}$$

A plot of ln (Qe) versus ln (C_e) gave a linear correlation (Osorb, R^2 0.9941, nZVI-Osorb R^2 0.9579, GAC R^2 0.9972) supporting the hypothesis of sorption by pseudo-second-order kinetics (Fig. 4.5).

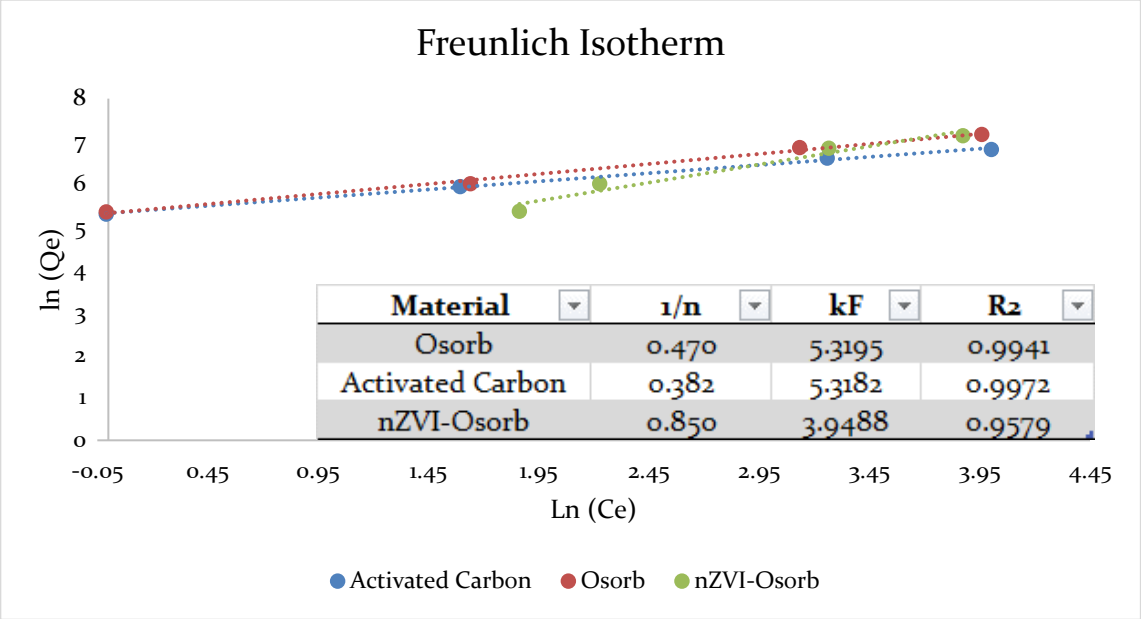

Figure 4.5 A Freundlich isothermal fitted plot of natural log of sorption capacity (ln (Q_e) in mg/g versus the natural log of solute concentration in solution at equilibrium (ln (C_e)) in mg/L.

In Fig. 4.4, the slope is equivalent to 1/n, and the intercept log (k_F) represents the distribution coefficient. Partitioning log (k_F) values (Osorb, 5.32, and nZVI-Osorb, 3.95) are close to the predicted log (k) 4.35 predicted in Fig. 5.2. k_F values of Osorb were slightly higher for Osorb than GAC (0.00.13). Maximum adsorption capacity (Q_m) can not explicitly be predicted by a Freundlich isotherm but provides a useful model for predicting adsorptive capacity (Q_e, mg/g) at a given equilibrium concentration (C_0) **(4.4)**.

$$Q_e = k_F (C_0^{1/n}) \qquad \textbf{(4.4)}$$

To determine the intensity or free energy of adsorption (K_L, L/mg) and maximum adsorption on a monolayer surface (Q_m, mg/g) results were fitted to a Langmuir isotherm **(4.5)** (Fig 4.6)**.**

$$C_e / Q_e = 1 / (Q_m K_L) + C_e/Q_m \qquad \textbf{(4.5)}$$

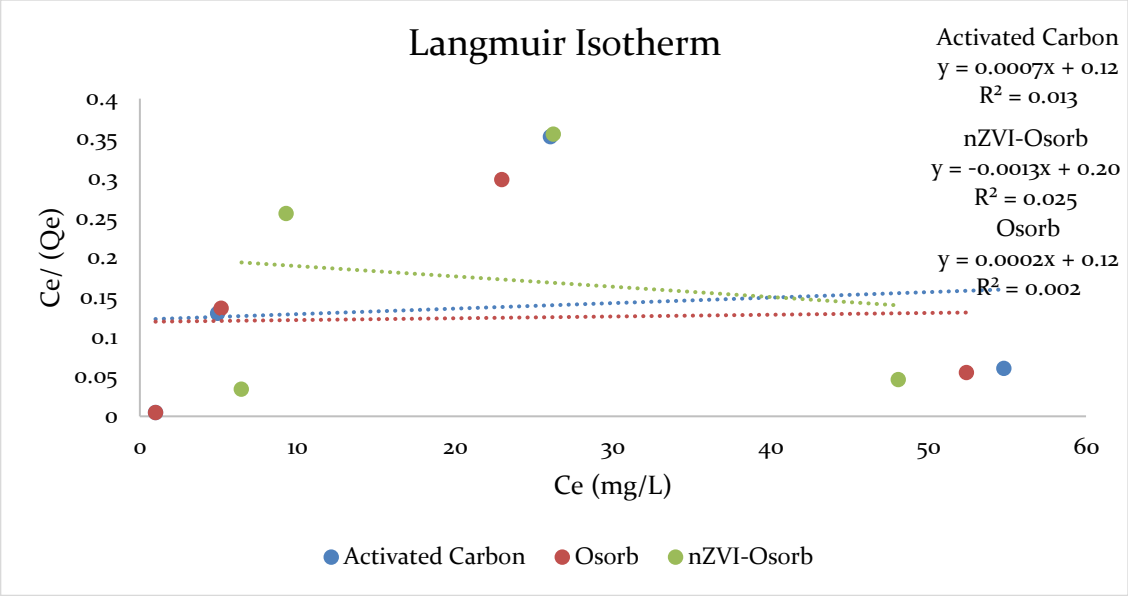

Figure 4.6 Langmuir-isotherm-fitted plot of sorbate concentration at equilibrium (C_e) versus C_e over sorptive capacity at equilibrium. Slope values represent $1/Q_m$, and y-intercepts represent $1/Q_m K_L$.

Langmuir models are suited to homogeneous surface structures with monolayer surface sorption following pseudo first-order kinetics. Correlation values were weak in this model due to heterogeneous surface structures of activated carbon and Osorb that support multi-layer sorption [278]. Correlation values improved significantly (Osorb, R^2 0.922, nZVI-Osorb R^2 0.6762, GAC R^2 0.9542) with the removal of 5 mg sorbent data points (Fig. A1.3 Appendix 1).

Maximum monolayer adsorption (Q_m) and free energy of adsorption (K_L) for Osorb were determined to be 82.64 mg/g and 0.42 L/mg respectively from the adjusted plots assuming first order kinetics. These values are likely below true TCP capacity and affinity for Osorb and are only appropriate indicators when C_e values are below 26 mg/L, and Q_e values are below 200 mg/g.

In general, the results have shown that whereas nZVI-Osorb presented higher sorption capacity at some concentrations, TCP sorption by GAC remained relatively competitive. Activated carbon is particularly advantageous because the sorbent is pervasive within industry and has a lower cost per gram than novel sorbents. However,

there are some significant advantages to utilising Osorb instead of GAC in the treatment of TCP.

(1) Silica-based sorbents have demonstrated a higher sorptive capacity for chlorophenols (Ref: Table 1.4) [127]
(2) Silicon chemistry lends itself to easy chemical modification and creates the potential for the synthesis of selective sorbents and other advanced hybrid materials [124, 279].
(3) A prior study found delayed corrosion of nZVI when embedded into silica while still allowing contaminant degradation [184].
(4) Physical sorption mechanisms of Osorb lend themselves to better embedment and potential dispersion of nZVI (Ref: Ch.3) [134, 235].

These features help provide silica-based sorbents with a competitive edge over carbon-based alternatives and support the case for development and research of iron-silica composites (as explored within this thesis).

Degradation

A second important feature to discuss outwith the sorptive capacity studies is degradation. No degradation by-products were detected in any solutions discussed within this section. Acid digestion processes found full recovery of TCP from nZVI-Osorb nanocomposite in all studies with recoverable yields suggesting that sorption was the primary factor of contaminant removal from solution (Table 4.2).

Table 4.2 Average values of treatment of TCP over the course of the 9-day experiment (pH 5.1) shown in Fig 4.7, and results from the acid digestion of the final recovered nanomaterials. TCP concentration values were determined by GC-FID. No breakdown products of TCP were observed in any sample in the acid digest. These findings were additionally verified by further GC/MS analysis (scan 40 m/z to 500 m/z amu) which found only TCP present in the test solution and acid digestion recovery.

Material	TCP Sorbed (mg/g)	Mean STDEV (mg/g)	% Reduction	TCP Recovery (mg/L)	Mean STDEV (mg/L)	% Recovered
nZVI	0.40	0.90	0.99	-	-	-
nZVI-Osorb	35.23	0.60	88.08	100.0	0.81	Total Recovery
Osorb	37.41	1.12	93.54	100.0	1.07	Total Recovery

TCP degradation rates by nZVI have been reported to be slow as a result of limited reactive sites (2% of total surface sites) and competition from surface passivation [16]. Studies with an excessive reaction/ contacting period (9-days) such as that given in Fig. 4.7 & Table 4.2 found no indication of degradation. Similar results were found with a group utilising nZVI to TCP with an excess of 40 days of contact time [29]. These results would suggest that lack of degradation is observed not because TCP has insufficient time to have contact with the reactive sites of iron's surfaces, but because passivation or corrosion of the surface of iron has prevented sufficient contact and degradation.

To ensure lack of degradation was not due to insufficient reactive iron sites from exiguous quantities of treatment mass, a study utilising 1.3 g (52x standard treatment mass) nZVI-Osorb was utilised to treat a 3.03 mM solution of TCP. This study found 90% reduction in TCP with nZVI and 99.3% removal with nZVI-Osorb, and a consistent lack of by-product formation further suggesting sorptive removal. Lack of TCP degradation is discussed in greater detail in Section 4.3 where methods to improve treatment are discussed.

Another important sorption parameter is partitioning. As expected, complete removal of TCP from solution was not observed in most trials and is attributed to partitioning and solubility affinity issues that play a factor in any physical sorption mechanism[177]. These features are examined in greater detail in the following section.

4.2.2 Sorption and the Effect of Contaminant Partitioning of TCP By-Products (DCP, CP, Phenol)

Sorbents (like activated carbon) utilised to remove organic contaminants from water will typically have a high microporous structure allowing a large negatively charged surface [109]. The material then filters contaminated water and contaminants adsorb to the surface of the material. The affinity initially to adsorb and then retain the contaminant depends on the physical and chemical properties of the contaminant and its corresponding sorbent. These properties include hydrophobicity, electron polarizability, size, and polarity[280]. Osorb in particular favours small, nonpolar, hydrophobic organics for uptake from solution.

Altering the substitution of the aromatic ring in chlorophenols will noticeably alter these molecular properties producing variations in water solubility (K_{sp}), partitioning values ($LogK_{ow}$), and acid dissociation (pK_a) detailed in Table 4.3.

Table 4.3 General properties (K_{sp}, $LogK_{ow}$, pK_a) of phenol and chlorophenol with varying degrees of substitution and recorded pH for 100 mg/L for each CP in DI water.

Contaminant	**pH (aq.) 100 mg/L**	**K_{sp} (g/L)**	**$LogK_{ow}$**	**pK_a**
Phenol	6.76	83	1.46	9.99
o-Chlorophenol	6.45	28	2.39	8.56
2,4 Dichlorophenol	6.26	4.5	3	7.89
2,4,6 Trichlorophenol	5.10	0.9	3.7	6.23
Tetrachlorophenol	n/a	1	4.45	5.14
Pentachlorophenol	n/a	0.018	5.15	4.70

As the aromatic compound becomes more substituted with chlorine atoms, the pK_a decreases through the addition of electron withdrawing groups which also decreases overall water solubility and increases water/octanol partitioning making the resulting

compounds more hydrophobic. Because all chlorophenols are acids, compounds with high substitution also disassociate more readily at lower pH values [127].

Degradation of TCP was expected to produce less substituted by-products which would present different molecular properties, and so sorptive affinity for less substituted by-products (DCP, CP, Phenol) should be tested[15]. A study utilising Osorb (25mg) and Activated Carbon (25mg) to sorb 100 mg/L specific solutions of TCP, DCP, 4-CP, 2-CP, and phenol were undertaken to elucidate sorptive affinity (Figure 4.7).

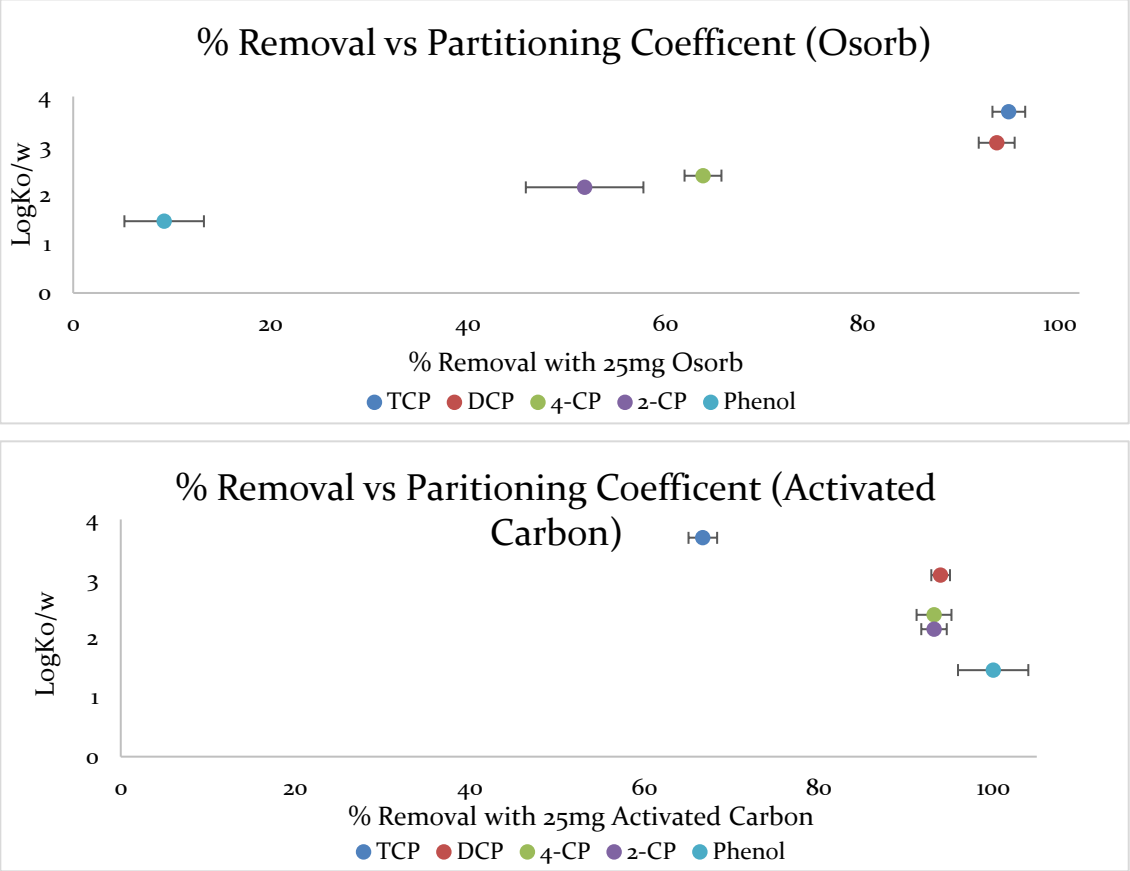

Figure 4.7 25mgs of Osorb (Top) and Activated Carbon (Bottom) were shaken for 24 hrs with a variety of individual chlorinated phenols (TCP, DCP, 4-CP, 2-CP) and phenol. Starting concentration was 100 mg/L for each compound with pH values detailed in Table 4.3.

The results show that Osorb removal efficiency improved with increasing levels of hydrophobicity ($LogK_{o/w}$). Activated carbon demonstrated an opposite trend whereby the more soluble compounds were absorbed with stronger affinity. In the specific case of chlorophenols, Osorb would be more advantageously applied in environments where contamination has higher compositions of more substituted phenols like TCP and PCP. Conversely, in situations where contamination is mostly DCP or less substituted phenols, treatment with activated carbon may suffice. Differences in uptake for specific chlorophenols are most likely due to differences in properties of the individual material and their respective sorption mechanisms.

As previously discussed, Osorb sorbs solutes via passive absorptive process related to swelling. Osorb is best suited to the sorption of sub-micron molecules that are nonpolar, uncharged, and hydrophobic because these compounds will readily disrupt intermolecular forces tensioning the silica matrix to produce swelling. Osorb is inherently highly hydrophobic, and therefore the increasing hydrophobicity of sorbates will naturally partition toward material in aqueous solutions. The swelling mechanism exaggerates natural partitioning capacities providing overall higher capacity when compared to competitive adsorbent processes (like activated carbon) which rely on surface adherence [134].

Because of the aforementioned processes, it was expected that increasing hydrophilicity of the sorbate would result in decreased sorption of the contaminant from water. Therefore conversely, it was expected that nZVI-Osorb and similarly Osorb would provide the best sorption of TCP with decreasing levels of sorptive affinity for its more soluble by-products **(4.4)**.

TCP > DCP > CP > Phenol **(4.4)**

Unlike Osorb, activated carbon facilitates adsorption through a large negatively charged porous surface making it particularly suited for sorption of small non-charged organics. As acids, chlorophenols will dissociate when pH is above pK_a. The pH in every test solution within this trial (typically 5.1) was below the given compound's respective pK_a value and therefore was expected to be uncharged in solution. Differences in sorption of

activated carbon and Osorb are not expected to result from charge exclusion during acid dissociation[22]. pK_a values for TCP and higher substituted chlorophenols are all below 7, and some charge exclusion would be expected for activated carbon in neutral waters with these compounds.

High substitution by strong electronegative groups (such as the chlorines) allows increased electronegative repulsion by the surface of the negatively charged carbon surface. This repulsion could explain why low rates of sorption for more substituted chlorophenols were observed in Fig. 4.7[133].

Osorb's absorptive mechanisms would be favourable over adsorptive carbon or graphene-based mechanisms in water where contaminants possess high overall electronegativity (possible due to strong electron withdrawing groups like halides) but retain an overall neutral charge. Both sorptive mechanisms benefit from increased hydrophobicity and K_{ow} partitioning [123].

Decreased affinity for less substituted chlorophenols by Osorb could be problematic in use if less chlorinated phenols leech from the sorbent as nZVI degrades TCP. If so, this process would expectedly increase by-production formation in treatment. As degradation was not observed in the trials discussed in this chapter and could not explicitly be tested, an additional trial was conducted to assess sorbent affinity for TCP, and the material's propensity to leech sorbate in a non-static system.

4.2.3 Affinity and Leeching of TCP in Kinetic Systems

Contaminant affinity and leaching is an essential factor in sorbent-based or sorbent-mediated treatment because it provides a good indicator of by-product formation and release. Previous studies in Section 4.2 have indicated that TCP is sorbed from solution in excess of >90% with nZVI-Osorb, TCP sorption occurs quickly upon contact, and TCP sorption reaches equilibrium after 2 hrs. Other trials have also indicated that partitioning and solubility values of the sorbate will affect overall sorption rates [165].

Because reductive degradation of TCP by nZVI did not occur in the tests, by-product release could not be assessed directly. Therefore, two different trials were

conducted to test nZVI-Osorb sorptive affinity for bound TCP in a contaminated solution over nine days (Fig. 4.8) and a second study to test TCP leeching from nZVI-Osorb into uncontaminated DI water (Table 4.4).

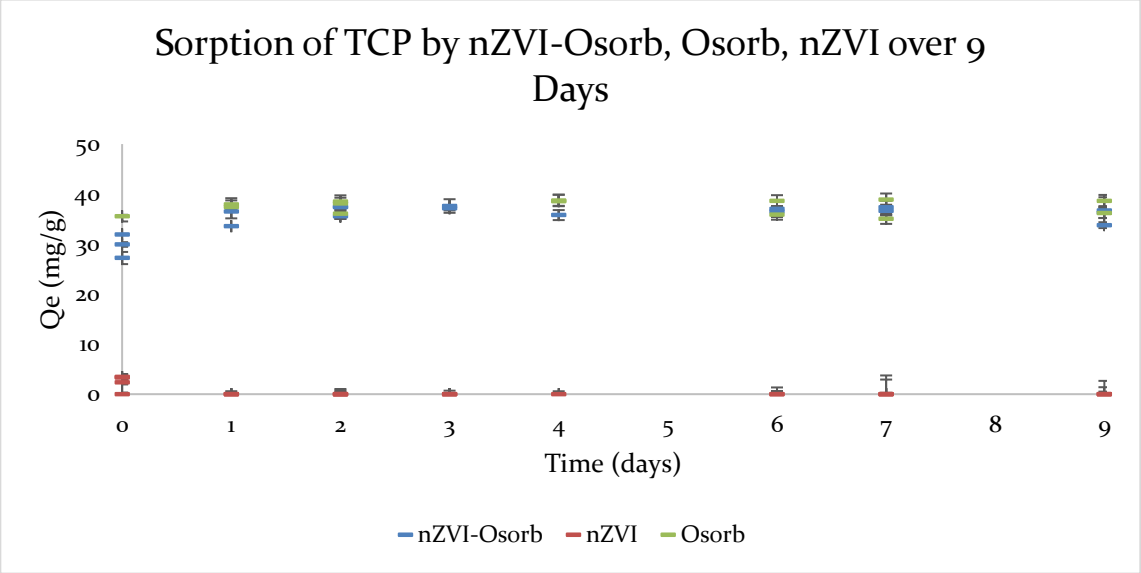

Figure 4.8 Sorptive capacity (mg/g) for 100mg/L TCP (100 mL) solution continuously mixed for 9 days with 250 mg nZVI-Osorb, 250 mg Osorb, and 250 mg nZVI. Samples were collected after 30min (day 0) and the same time on days 1, 2, 3, 4, 6, 7, 9 thereafter (pH 5.11).

Sorption rates of TCP remained relatively constant throughout the 9-day trial suggesting a strong affinity for the sorbed contaminant by Osorb and nZVI-Osorb with a low propensity to leech. It was found that nZVI does initially adsorb TCP, but adsorption is poor (approx. 1%) compared to the other sorbents and any adsorbate leeched after initial sorption most likely due to iron oxide formation [178].

Removal rates by the sorbent nZVI-Osorb (35.23mg/g) are close to the removal rates observed with Osorb (37.41 mg/g) and consistent with sorption rates reported elsewhere within this chapter. Most studies utilising nZVI or ZVI have indicated slow reaction rates for TCP degradation which required several hours to a day of exposure [21, 107]. This study exceeds that reaction time frame by eight days, and as with other studies within

this chapter, no degradation by-products were found. Full recovery of TCP by acid digestion was observed for this trial as previously noted in Table 4.2.

To test the propensity of nZVI to leach TCP sorbate into uncontaminated DI water, a second trial was conducted. In this study, 150 mg/L TCP (100 mL) was sorbed from solution with 150 mg nZVI-Osorb, the treated water was removed, the sorbent underwent four washes with uncontaminated water, and after washing the sorbent was stirred in a DI solution for seven days (Table 4.4, Table 4.5, and Table 4.6).

Table 4.4 150mg of nZVI-Osorb were mixed in a 60mL (equiv. mass/volume to previous trials), 100 mg/L solution of TCP for 24hrs. The solution was left to settle, and the liquid was removed via pipette. An aliquot (7mL) of water was extracted by hexane, and the concentration of TCP in the treated water was determined. The remaining nZVI-Osorb was covered in fresh water and rinsed with 4x 60mL for 30 mins. TCP concentration was determined for each wash. 60mL of water was then added to the remaining nanomaterial and stirred at a moderate speed for seven days. Samples were extracted at days 1, 2, 5, 7, and 9 to determine TCP concentration.

Sample	Final TCP (mg/L)	STDEV (mg/L)	TCP Sorbed (mg/L)	TCP Sorbed per mL
Initial Control	110.24	2.68	-	-
Treated Water	9.65	3.18	100.59	1.68
Rinse 1 (60mL)	3.78	2.97	96.82	0.81
Rinse 2 (60mL)	2.62	0.67	94.20	0.52
Rinse 3 (60mL)	2.00	0.33	92.20	0.38
Rinse 4 (60mL)	1.19	0.14	91.01	0.30
Day 1	3.47	0.39	87.55	0.24
Day 2	1.59	0.33	89.42	0.25
Day 5	0.79	0.81	90.22	0.26
Day 7	-	-	91.01	0.26

Table 4.5 Total TCP (mg/L) measured in sorbent & solution after diff. phases of treatment.

Measured [TCP]	mg/L
TCP sorbed	100.59
TCP in the treated solution	9.65
Total TCP removed in washes (240mL)	9.58
Starting TCP sorbed (post wash)	87.55

Table 4.6 Calculations tracking the % loss and % gain of TCP by nZVI-Osorb during the course of the trial.

% Loss of TCP from Sorbent	% Loss	% Gain
Rinse 1	3.76	
Rinse 2	2.70	
Rinse 3	2.12	
Rinse 4	1.29	
Total Loss from Washes	9.87	
Day 1	3.81	
Day 2		2.06
Day 5		0.88
Day 7		0.87
Net Gain		**3.81**

It was found that 89.93% (100.59 mg/L) of TCP was removed from the solution containing 110.24 mg/L by the nZVI-Osorb sorbent (Table 4.5). Over four rinses (60 mL x4) excess TCP in the treated solution and residual TCP molecules that were lightly bound in the treatment solution were removed (9.87% loss). The loss of TCP ranged from 3.76% with the initial rinse of the sorbent and continued to decrease with each additional rinse to 1.29% loss on the 4th rinse. The total loss of TCP was 9.87% with 240mL or 0.04% loss per mL (Table 4.6). Rinses were carried out in the original treatment vessel in-lieu of extraction and filtration to avoid nZVI-Osorb mass losses in the transfer of material. Following rinsing, 60mL of DI water was added to the residual nZVI-Osorb and desorption of TCP into the DI was monitored over a period of 7 days.

Alteration of the initial solution (100mg/L TCP) to an uncontaminated state (0mg/L TCP) was expected to change contaminant partitioning (K_{ow}) within the solution and result in some dilute leaching of the sorbate [15]. Indeed, some leeching did occur on the first day of monitoring (3.81% or 3.47 mg/L on Day 1) but was fully recovered (reabsorbed) over a period of 7 days (Table 4.6). These results would indicate that some TCP will leech from the sorbent within the first 24 hrs. with shifting water partitioning (K_{ow}) (3.45-0.83%) but that any dilute leachate can be fully recovered after the solution reaches equilibrium and within the 7-day time frame. No further leeching was detected after seven days.

While these two trials provide a good starting point of understanding for affinity and desorption of TCP in stirred open-system solutions, they are not representative of all

deployment modes. Flow forces in the column and packed-bed deployment designs can provide additional challenges through increased hydrodynamic forces, and an additional study should be carried out before applying nZVI-Osorb in these type of systems [200].

Furthermore, by-product formation and by-product release are essential factors in assessing a material's applicability. Studies listed in Fig. 4.8 indicate that nZVI-Osorb has decreased sorptive affinity for less substituted by-products and therefore it is likely that some by-product release will occur in treatment. Degradation of TCP was not observed in any previous trials with nZVI-Osorb so a more in-depth assessment should be made as to why degradation did not occur and what would be the factors that could potentially improve degradation.

4.3 Degradation of TCP by nZVI-Osorb

As discussed in the introduction (Section 4.1) degradation of TCP by nZVI previously reported in the literature has been variable. Degradation of TCP was not observed in any previous trials with nZVI-Osorb composites. Section 4.3 will endeavour to assess why degradation was not observed in previous trials, explore experimental parameters that supported TCP degradation in aerobic conditions in previous literature and propose experimental and material modifications that could enhance overall degradation.

Previous studies in Section 4.2 have reported that lack of degradation is not the result of inadequate iron concentrations (52 times nZVI-Osorb), treatment duration (9-days), or issues associated with analytical detection (verification with GC-FID, GC/MS, & acid digestion). Therefore, it is likely that the lack of degradation is due to surface passivation of iron by corrosion which prevents the 2-electron transfer required for reductive degradation of the chlorophenol[66]. This competitive oxidation reduces the overall acting reductive potential of nZVI in the system.

However, as discussed in Section 1.3, corrosion of nZVI in water produces not only iron oxides, but hydroxyl radicals as well, which can aid in reduction. If this did occur, it is possible that the hydroxyl radicals were too dilute in solution to have a reducing effect [150].

If reduced or inadequate reductive capacity of nZVI is an accurate explanation of the results presented in this thesis it would support other findings in the field that showed greater success in degrading chlorophenols when nZVI was complexed with a secondary bi-metal known to increase reduction potential [188, 281]. In those systems, the higher reducing potential from bimetal complexes, overcome the rate-limiting passivation commonly observed with nZVI applied in aqueous solutions, to degrade target chlorophenol contaminants [186].

4.3.1 TCP Degradation by nZVI Reported in Literature

Other studies found similar results to those in the present thesis with nZVI failing to degrade TCP or other chlorophenol products and reported competitive oxidation of iron [29, 186]. However, four other studies in the literature (which did not utilise a bi-metal system) did report degradation of TCP with nZVI[107, 179, 184, 217]. A closer examination of studies reported a reduction of TCP in mostly aerobic conditions revealed several factors that may account for the difference in results and provide support for further modifications to improve treatment in addition to the addition of a second metal (Table 4.7).

Table 4.7 Comparison of 4 studies that utilised nZVI-based materials to degrade chlorophenols in aerobic aqueous conditions with positive degradation results.

Reference	Material	CPs	[Int.] mg/L	Deployment Conditions	Results for TCP
Dorathi & Kandasamy 2012 [184]	ZVI- SiO_2	TCP, DCP, CP	100	continuous flow column (5 to 25cm) aerobic	100% dechlorination af. 120 mins.
Li, Zhang et al. 2013 [217]	ZVI-CTMA-bentonite	PCP, TCP, DCP, 2-CP	98.73	sealed vials, shaken N_2 deoxygenated solutions aerobic	Good dechlorination with composite (92.8% af. 40 mins.) decent sorption (92.6%, pH 5.5) Partial deg. (1-10%, mix products) w/ ZVI control, moderate sorption (24.6%)
Gao, Zhang et al. 2015[107]	sodium alginate-ZVI w/ sand support	2,4 DCP	Var.	continuous up-flow column (60x8cm) deoxygenated solutions aerobic	Q_e = 0.5112 mg/g DCP sorption, no consistent degradation in column tests 60% deg. in batch test linked to excess H^+ from pH 2
Guan, Wan et al. 2015[179]	nZVI-SiO_2-NH_2	TCP	50	anaerobic granular sludge bioreactor neutral pH	High TCP sorption, 94.6% with composite, 78.3% nZVI control Enhanced natural biodegradation of TCP from 70% to 90% in 120 hrs. through decreased TCP related micro toxicity and boosted methane production

Dorathi and Kandasamy obtained satisfactory dechlorination of TCP, DCP, and CP in a continuous flow column using nZVI impregnated into silica with full dechlorination of 100 mg/L of TCP after 120 mins of column recirculation. They found a significant degree of iron leeching from the silica composite both before (8.5%) and during treatment (76.3%). GC/MS verified intermediate products, but it appeared that the bulk of dechlorination rates were calculated from chloride measurements by IC from column effluent as opposed to direct concentration monitoring by GC which could increase error in dechlorination capacity calculations [184]. The continuous column design of this experiment could explain why degradation results were achieved because flowing systems

will have different contacting dynamics than open stirred and shaken systems. The column design could also have limited the input of oxygen from the atmosphere which would affect corrosion rates.

Li et al. modified nZVI with organobentonite and cetyltrimethylammonium (CTMA), and found satisfactory sorption (92.6 %) and degradation of TCP (92.8%) of 0.5mM TCP with the composite at a pH of 5.5. Sorption (24.6%) and partial degradation (mixed degradation products ranging from 0.01-0.05 mM) were also observed with the nZVI control. In Li et al.'s experiment, deployment conditions were closer to conditions in the present thesis, with solutions mixed in shaken sealed vials. However, Li et al.'s solutions were deoxygenated before use, which could be one of the reasons why degradation occurred with iron controls in Li et al.'s study and not in the present thesis. As with the Dorathi and Kandasamy study, dechlorination rates were monitored by IC. Improvement in treatment with organobentonite was attributed to enhanced adsorption of the contaminant that facilitated mass transfer of chlorophenol from solution to the iron surface [217]. Discrepancies between the results for nZVI controls could also be attributed to starting iron reagents. The Li et al.'s study utilised 100 mesh powdered Fe^0 from a Chinese supplier opposed to the synthesised, wet solution Fe^0 materials procured from a Czech Republic supplier in this work.

In a third study, nZVI was immobilised with sodium alginate on sand within a continuous up-flow column. Solutions were again deoxygenated, and modest sorption of DCP occurred (Q_e = 0.5112 mg/g). Modest degradation of DCP was detected in the first 5 hours of column flow; however initial concentrations of DCP rebounded after this initial period. Studies in batch tests with DCP found 60% degradation of DCP but this was primarily linked to excess H^+ protons from low pH (2.0) which aided reductive mechanisms [107]. The deployment mechanism, lower pH, and differences in composite materials may explain differences in chlorophenol degradation results observed in this trial opposed to results in the present thesis.

One final study utilising anaerobic granular sludge bioreactors found satisfactory sorption of TCP by their amino-functionalized silica-iron composite (nZVI-SiO_2-NH_2) and iron controls (78.3%). Natural biodegradation (discussed in Ch. 1.2) resulted in the degradation of 70% of TCP. The addition of iron-silica composites boosted natural

biodegradation to 90% through decreased micro toxicity via the removal of TCP by sorption from solution. Reactors containing the composite also demonstrated better methane production [179]. Degradation by nZVI in this study is mostly linked to microbial digestion which was absent in all trials conducted in work described in the present chapter. Model anaerobic digesters are prepared and tested for TCP degradation with nZVI-Osorb in Ch. 7 where related phenomena and processes are discussed at length.

These four studies indicate that TCP degradation can be enhanced through the reduction of dissolved and atmospheric oxygen, the increase in available protons from overall pH reduction, and the addition of a substrate to increase mass transport mechanism of TCP to nZVI.

4.3.2 Modifications to Improve TCP Degradation by nZVI-Osorb

The experimental parameters and modifications to improve degradation discussed in the four studies also correlated with modification trends discussed elsewhere in the literature to improve nZVI reductive capacity in treatment. These methods include:

(1) Addition of substrate to increase contaminant and iron contact [16, 217].
(2) Increasing the availability of protons (H+) in solution by increasing the acidity of the solution and decreasing pH [165].
(3) Addition of an oxidant such as hydrogen peroxide into the solution to boost reductive potential [97].
(4) Inclusion of a second reactive metal into the composite[188, 281].
(5) Reduction in dissolved oxygen in test waters to limit aerobic corrosion and/or the adoption of an anaerobic atmosphere [83].

Most of these modifications or features have already been explored in the present work. Firstly, this thesis has focused on the development of a substrate-iron hybrid material that has demonstrated even dispersion of iron particles (Ch.3.3) and high sorptive capacities for TCP (Ch.4.2), which as a result, should optimise contact with the TCP-nZVI active site. Increased dispersion from nZVI-Osorb led to increased atmospheric oxidation

of iron observed in Fig. 3.11. These findings would suggest that while contact mechanisms have been optimised through the addition of the Osorb substrate, this modification alone was not sufficient to counteract subsequent surface passivation of the iron in solution.

No by-product formation or TCP degradation were found to occur in pH trials (pH 3-9) decribed in Section 5.4. This would further suggest degradation was not limited by a lack of available protons in solution but through unavailability of unoxidized nZVI in treatment.

The addition of an oxidant might be suitable in some groundwater and surface water applications. One study found that addition of an oxidant improved TCP degradation by synthetic zeolites [143]. However, addition of an oxidant such as hydrogen peroxide is not appropriate for wastewater and anaerobic digesters where microbes are utilised to digest organics, because a potent oxidising agent could damage biological cells [32]. As these AD applications are the primary focus of this thesis, the use of oxidants are considered to be outside the main scope of research but are recommended for consideration in future studies.

As discussed in Ch. 3 materials containing copper and nickel bi-metals were produced in this research. Characterization of these materials determined that the percent compositions of Cu and Ni bimetals were far below target levels. Further characterisation by Mössbauer determined that these iron composite materials were also significantly oxidised, with only a small minority of Fe^0 remaining. Therefore, it is unlikely that these materials would be sufficient in reducing TCP in their present state. In future work, it could be advantageous to synthesise new nZVI-Osorb composite materials under anaerobic conditions with addition of a Pd bi-metal to increase reaction rates. Cu and Ni bimetal embedment could also be repeated under such anaerobic conditions, with surfactant added to aid dispersion and embedment.

Adoption of anaerobic conditions to reduce iron corrosion is examined in the following chapter (Section 5.3). The trial did not find degradation of TCP under anaerobic conditions with nZVI or nZVI-Osorb. It is likely that with dissolved and atmospheric oxygen removed, corrosion and surface passivation persisted through less energetically favourable interactions with water molecules via the reaction detailed in equation 1.6, 1.9 in Section 1.3. If so, the results would continue to support the earlier hypothesis that TCP

degradation is hindered by corrosion which in turn results in the need for higher reductive capacity to overcome surface passivation and further degrade the contaminant.

5.4 Summary

Parameters related to sorption and degradation mechanisms of TCP by nZVI-Osorb were tested under aerobic conditions, e.g. surface, potable water. nZVI-Osorb materials demonstrated high extraction capacity for TCP from aqueous solutions (Qe = 1286.4 ± 13.5 mg TCP/g Osorb, Qe = 1253 ± 106.7 mg TCP/g nZVI-Osorb, pH 5.1, 120 mg/L TCP). Capacities for TCP were competitive over reported sorption values for standard sorbents in the market. Sorption mechanisms followed pseudo-second-order kinetics supporting multi-layer contaminant uptake. Most sorption occurred within the first 5 minutes of contact time and 2 hours was required to reach complete equilibrium in a 100 mg/L solution.

Affinity for the sorbate was forcible with a low propensity to leech in a treated solution. In the broader class of chlorophenols, sorptive affinity mirrored partitioning values with highly substituted chlorophenols displaying the highest sorption capacities. Such dynamics could present an opportunity for leeching of by-products in degradation. However, degradation of TCP by nZVI-Osorb, or nZVI controls was not observed in trials within this chapter.

Degradation was believed to have been hindered by corrosion of nZVI, resulting in surface passivation. Loss of reactive surface sites from passivation would, therefore, require an increased reductive capacity to compensate for the oxidative loss. The lack of TCP degradation would suggest that nZVI-Osorb may not be suitable for highly aerated surface and potable water treatment systems without additional material modification to enhance overall reductive potential.

Analogous research studies concerning removal of TCP with nZVI materials embedded in a composite sorbent have found that high sorption rate facilitated mass transfer of TCP to nZVI reactive sites improving degradation. Anaerobic environments (such anaerobic waste and wastewater digesters) where corrosion rates are decreased could

be advantageous to nZVI-Osorb's functionality without requiring additional material modifications.

Chapter 5 : Effect of Water Characteristics on TCP Sorption and Degradation Mechanisms by nZVI-Osorb

5.1 Introduction

All naturally occurring water systems contain dilute concentrations of dissolved minerals (e.g. calcium, magnesium, iron) and dissolved gases (e.g. oxygen, carbon dioxide) arising from geological and atmospheric deposits. These dissolved species give rise to distinctive odours and tastes and contribute to the regional characteristic of processed waters throughout the world [282].

Mineral and gas compositions of a water system are further complicated by other environmental factors such as salinity, dissolved oxygen, pH, and the presence of undesired secondary organics. These features ensure that no two water systems are identical both in composition and attributes, which in turn, complicates treatment models for such systems [121].

Previous chapters in this thesis have demonstrated the development of tightly bound well-dispersed nZVI-Osorb nanocomposites (Ch.3) with high sorptive capacity for trichlorophenol (TCP) contaminants in solution (Ch.4). Examination of environmental parameters that can influence sorptive and degradation mechanisms of the composite material for the target sorbate should be undertaken to determine whether TCP degradation can be achieved under particular conditions and to increase understanding of the functionality of the material when applied in diverse water systems.

An analytical study examining the effect of salinity (KCl) on the adsorption of aromatics, such as phenol, toluene, and benzene, onto activated carbon found that increasing salt concentrations (0.05 to 0.8M) adversely affected adsorption of the contaminant (approx. 34-45% loss) through charge neutralising and 'salt out' effects [128]. Increased ion concentrations can also affect partitioning mechanisms of sorbates reducing solubility and driving hydrophobic molecules from solution. Lower solubility in some cases can lead to an increase in total sorption of certain compounds[283]. Increased salinity is also correlated with increased corrosion rates for metals in solution. A higher concentration of

readily available ions supports electrolysis reactions, enhancing electron transport, and driving faster iron-oxide formation[284]. Increased oxide formation in saline environments, therefore, makes improved TCP degradation by nZVI-Osorb improbable. However, Osorb is an uncharged absorbent so it is unlikely similar charge mechanisms occurring with GAC will apply, but a detailed examination of salinity including evaluations of sorbate properties and their effects on corrosion of iron should be examined to bolster understanding of nZVI-Osorb's functionality in marine or ion-rich environments.

As discussed in the literature review (Ch.1) and the previous experimental chapters (3,4) dissolved oxygen interacted with nZVI to form iron-oxides and iron-hydroxides which can in some cases result in loss of active sites and decrease the reductive capacity of iron to sorb and degrade target contaminants [176]. A study examining oxide formations of nZVI in water found that nZVI consumes dissolved oxygen to form a two-layered structure comprising an inner magnetite structure (Fe^{2+}, Fe^{3+}) and an outer lepidocrocite layer (FeO(OH)). The interfacial lepidocrocite layer is thought to impede Fe^0 reactivity in reduction through surface passivation (Ref: Table 4.8). However, the removal of DO was determined only to produce magnetite-based oxides which are not prohibitive to Fe^0 reactivity and can facilitate degradation through enhanced electron transfer from core Fe^0 atoms to the solid-liquid surface[285]. Removal of oxygen should be assessed in terms of its effects on nZVI-Osorb treatment of TCP regarding iron-mediated adsorption and degradation. Such a study would strengthen application evaluations of aerobic versus anaerobic water conditions for material deployment.

As previously discussed, the model contaminant TCP is a weak acid and will readily deprotonate in solutions of $pH > 6.23$. TCP's deprotonation will change the compound's overall electrochemical properties (electronegativity) and resulting in aqueous solubility changes which will influence contaminant-sorbate interactions[98]. One study examining total solubility of TCP as a function of pH found a substantial increase in solubility once TCP was charged in solution (Table 5.1)[22].

Table 5.1 Total solubility (S_T) of 2,4,6-Trichlorophenol for various pH at 25C [22].

pH	S_T (10^3 g/m^3)	StDev (%)
3.18	3.81×10^{-1}	1.34
3.74	4.59×10^{-1}	0.47
5.32	5.03×10^{-1}	2.7
6.69	1.78	0.92
7.04	4.02	0.78
7.15	5.17	0.88
7.37	8.75	0.17
7.55	1.25 x 10	0.30
7.60	1.50 x 10	0.45
8.99	1.71×10^2	0.42
10.23	1.76×10^2	0.63
11.52	1.83×10^2	0.52

Another study found diminished sorptive uptake of TCP by loosestrife activated carbon when TCP was charged in solution (30% loss from initial pH 4 to pH 6 and increasing loss of capacity as pH rises, 150 mg/L TCP, 0.1 g/ 100 mL GAC)[278]. Osorb, unlike activated carbon, is uncharged so the loss in sorptive capacity will most likely be linked to increased solubility of TCP rather than a combination of sorbate properties and charge effects observed with activated carbon. pH, therefore, should be evaluated to determine its influence on the sorptive capacity of Osorb for TCP in solution.

pH changes are also expected to influence degradation mechanisms. A 2008 study observed TCP interactions with Pd-nZVI, and nZVI found that lower pHs (with an excess of H^+ protons) gave favourable hydrodechlorination degradation mechanisms that consumed protons. Interactions with their materials and TCP in low pH more readily produced by-products signifying increased reactivity rates[29]. As degradation did not occur in experiments in chapter 4 where initial unadjusted pH of 5.1 was below the pK_a of TCP, it is unlikely that reduced pH will facilitate additional degradation. However, given the importance of pH in sorptive mechanisms and the lack of degradation in other trials this environmental parameter should be tested for a fuller understanding of functionality.

Lastly, the presence of other compounds in solution will influence mechanistic interactions of sorption and degradation. Competitive exclusion can occur when multiple sorbates all have a different sorptive affinity to a particular sorbent [133]. Active sites can

become inaccessible if blocked by large particulates like humic acid or natural organic matter (NOM) which create surface fouling. Such fouling is a common occurrence with GAC in natural water and will limit both sorption and any tethered degradation mechanism[286]. Secondary compounds can also change solution properties such as pH, which as discussed above, will alter both degradation and sorption properties [29]. Given the significance of pH in treatment mechanisms the present work will focus primarily on effects from secondary compounds of acidic nature over fouling or other competitive properties.

Volatile Fatty Acids (VFAs) offer a good model of secondary compounds in that they commonly occur wherever biological molecular breakdown proceed, particularly in anaerobic digestion processes, where they are a by-product and where nZVI-Osorb materials may be best suited. VFA molecules possess acid properties similar to the contaminant and therefore should affect the overall pH of the solution[287]. A study observing VFA production in a model anaerobic reactor found highest hydrolysis rates at an uncontrolled pH of 4.0 with best VFA production occurring at pH 6.0 [288]. Evaluating sorptive and degradation properties with addition of VFAs as secondary compounds will provide a more robust understanding of how nZVI-Osorb will function in more complex model anaerobic digestion systems and should be evaluated.

Environmental factors, such as salinity, dissolved oxygen, pH, and secondary compounds, influence sorption and degradation mechanisms, and as such, an in-depth study exploring the effect of these parameters on the treatment of TCP by nZVI-Osorb should be pursued. The results would strengthen current understanding of the material's properties and support additional work where these materials are applied in application.

5.2 Effect of Salinity on TCP Sorption by nZVI-Osorb

A salt is an ionic compound that contains equivalent values of cations and anions to carry an overall neutral charge. Sodium chloride (NaCl), the most common salt, will fully dissolve in water[42]. Marine environments possess a variety of saline concentrations (brackish: 0.05-3%, saline 3-5%, brine >5%). It is widely held that salinity can alter sorption

dynamics through direct electrochemical charge effects between sorbate and sorbent as well as by altering the partitioning dynamics of sorbate in solution[41].

Adsorbents, like activated carbon, typically have an overall negatively charged surface which can sometimes lead to 'water clustering' effects in highly saline environments. This water clustering can reduce solute contact which can, in turn, decrease total solute uptake[128]. The concentration and type of salt dissolved into aqueous solution will influence the partitioning of the solute. Typically, increased salinity improves partitioning of hydrophobic solutes from solution via pH and electrochemical repulsion dynamics. This exclusion effect is also observed with individual electrolytes in high salt concentrations and is known as anti-solvent crystallisation or simply the 'salt-out' effect[128].

In anti-solvent crystallization, dissolved oxygen (DO) often readily interacts with dissolved ions through solvation processes and decreases both the availability of ions in solution and the quantity of dissolved oxygen in the system (natural waters, approx. 8-14% DO, oceans approx. 20% less DO; varies by water type, temperature, pressure, etc.). As discussed in the introduction, reduced levels of dissolved oxygen will influence iron corrosion rates. Ergo, increased salinity could decrease iron corrosion by DO through staving off surface passivation and allow better contaminant reduction. However, dissolved ions such as salt are known to boost iron corrosion through improved electron transfer mechanism, so it is likely that no positive effect to degradation will be observed[289].

Most water systems discussed in this thesis (groundwater, surface water, wastewater, etc.) are freshwater sources containing minimal concentrations (<0.05%) of sodium chloride (NaCl)[290]. Evaluation of the effect of salinity on sorptive and degradation models is still beneficial to freshwater sources as these waters will typically contain a variety of dissolved ions, most notable of which include Na^+, K^+, Ca^{2+}, Mg^{2+}, H^+, Cl^-, HCO_3^-, CO_3^{2-}, and SO_4^{-}[128] A in-depth understanding of NaCl's effect on sorption and degradation can improve the robustness of the treatment model in waters where these common ions are present in solution, as well as, in any marine, seawater, or desalination application where salt waters are present[291]. Waters with five different salinities (0, 1, 3, 6, 20%) were therefore examined to determine the effect of salt on nZVI-Osorb's sorption of TCP (Table 5.2).

Table 5.2 100 mg/L TCP solutions containing 5 percentages of salt water (NaCl) (0, 1, 3, 6, 20%) shaken with 25mg of nZVI-Osorb for 24hrs (pH 5.1, 10mL) under aerobic conditions.

Salinity (%)	**% Reduction (mg/L)**	**STDEV (mg/L)**	**Qe (mg/g)**	**STDEV (mg/g)**
0	89.72	1.10	35.89	0.44
1	90.80	6.33	36.32	2.53
3	86.98	12.17	34.79	4.87
6	90.80	2.72	36.32	1.09
20	87.77	2.47	35.11	0.99
Average	*89.22*	*4.96*	*35.69*	*1.98*

As observed in Table 5.2, increasing concentration of salt ions in solution did not influence the sorption of TCP by nZVI-Osorb. No degradation of TCP was observed. The rate of sorption remained stable for all the samples even when salt concentration was increased to 20% (3.3 times that of brine conditions). These results can be explained by considering nZVI-Osorb's physical properties and the solubility and acid properties of the sorbate, TCP.

Firstly, no loss in sorption capacity was detected. This result was most likely due to properties relating to sorbent/sorbate interactions. Osorb is electrochemically inert and as a result, should not experience any surface 'water clustering' effects that have been observed with negatively charged surface adsorbents like GAC. Osorb also does not absorb ions, so competitive solute exclusion was not anticipated[134]. These properties make nZVI-Osorb and other uncharged inorganic sorbents advantageous over carbon-based sorbents in waters containing high concentrations of nutrients and dissolved salts where water clustering is expected and can reduce sorptive capacity.

Overall sorption of TCP was not improved in saline conditions, and that is most likely due to physical properties of the sorbate. The test pH of 5.1 was below the pK_a value for TCP. At that pH, TCP would have an overall neutral charge. Na^+ and Cl^- salt ions fully ionise in water and would not affect the overall pH of the solution. Therefore, increasing salt concentrations in solution would only further ensure a neutral charge in various testing scenarios. Excess Na^+ ions would also negate salt-out effects through electrical charge neutralisation on any stray charged TCP molecules that could be present or would become

present if natural pH was increased[283]. This neutral charge ensured that TCP in solution had similar uptake values as trials in Ch.4. Sorption was not improved in saline environments with TCP because there was no pH change and electrochemical repulsive forces were not in play (e.g. TCP remained uncharged). The role of pH and charge repulsion on TCP sorption are examined in greater detail in 5.4.

An increase in salinity did not produce more favourable degradation results. The nZVI in the composite material carries no charge (Fe^0) until it becomes oxidised and then carries a Fe^{2+} or Fe^{3+} charge, so water clustering was not expected to occur on iron's surface. However, some corrosion was anticipated[285]. Dissolved salt ions, such as Na^+ and Cl^- ions, in this system will more readily interact with water to form NaOH and HCl. These ions increase the electrolytic capacity of water and facilitate enhanced electron transport mechanisms which subsequently lead to enhanced corrosion rates. Long-term trials of steel corrosion in water environments of various salinity would suggest that iron corrosion occurs more readily in saline environments, suggesting ion facilitated corrosion is more favourable than dissolved oxygen facilitated corrosion (Fig. 5.1) [284].

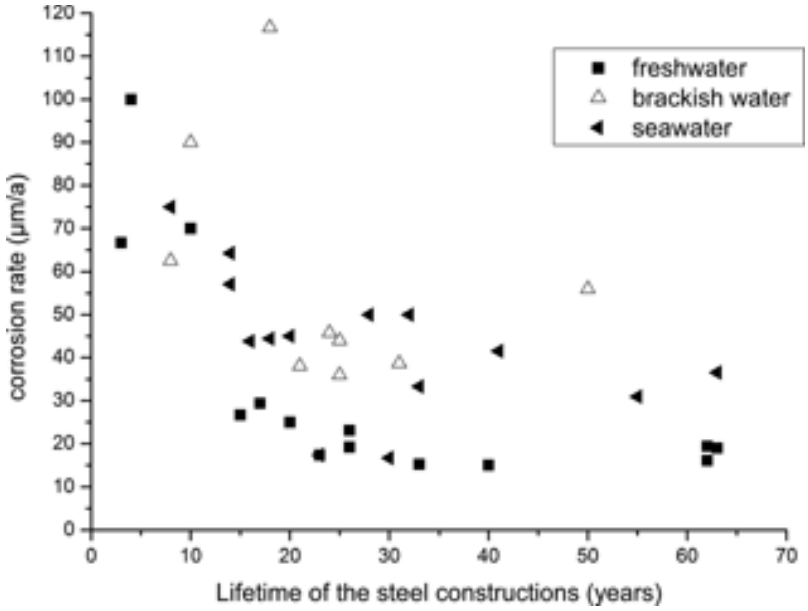

Figure 5.1 Corrosion rates of 41 sheet pile of steel (µm per annum) in three different water environments (freshwater, brackish water, seawater) over time (years)[284].

Cl^- and SO_4^{2-} anions have specifically been found to increase corrosion of nZVI in solution. Anion type can also direct particular iron oxide and iron hydroxide formations. For example, Cl^- and SO_4^{2-} anions resulted in the formation of a mixture of iron oxide products (magnetite (Fe_2O_4), lepidocrocite (FeOOH), and goethite (αFeOOH)). Other common groundwater anions are linked to the formation of different iron hydroxide species (HNO^{3-} produced goethite, NO^{3-} produced mostly magnetite) with nitrate producing the most favourable iron-oxide species[289]. These results would suggest that while high salinity may reduce DO possibly enhancing degradation, the addition of chloride ions may counteract any positive effect through increased corrosion and thus produced no net observable change in degradation properties with nZVI-Osorb. Future works, monitoring rates of corrosion for nZVI-Osorb in saline waters could help quantify the accelerated rates expected from literature evaluation and analysis.

These ion interaction results also have consequences for iron's interactions with metallic contaminants. As discussed in Ch. 1.3, nZVI has been utilised for the immobilisation of heavy metals cations in contaminated groundwater. Sorption and degradation interactions with target metals are influenced by the metals' overall reductive potential (E^0). Typically, metal cations with more negative E^0 are adsorbed (Zn^{2+}, Ba^{2+}), metals with a slightly more positive E^0 are both adsorbed and reduced (Ni^{2+}, Pb^{2+}), and metals with significantly higher E^0 are solely reduced (Ag^+, Cu^{2+}, Hg^{2+})[292]. Anions common in groundwater, like the ones discussed above, can influence sorption/degradation mechanisms of these contaminants. In one study the addition of Cl^- or SO_4^{2-} anions resulted in the advanced desorption of copper and zinc metals as a result of 'anionic pitted corrosion' [289]. These results suggest that careful study of ion species present in applied water systems should be undertaken before implementation because nZVI in nZVI-Osorb will interact differently with various ion species regarding both oxidisation and adsorption.

Given the long-standing issues with oxidation of nZVI, a closer examination of oxygen's role in nZVI adsorptive and degradation mechanisms for TCP could provide a better understanding of the proposed mechanisms of treatment, and elucidate limiting factors hindering degradation.

5.3 The Effect of Atmospheric and Dissolved Oxygen on Treatment

Osorb is a silica-based absorbent, and oxygen or lack thereof, is not expected to affect TCP sorption by the absorbent. However, as extensively discussed in prior chapters, iron, especially zero valent iron, is susceptible to undesired corrosion by oxygen in water in both aerobic **(5.1)** and anaerobic **(5.2)** conditions and therefore oxygen will chiefly effect adsorption and degradation mechanisms of the material.

Aerobic	$2Fe^0 + O_2 + 2H_2O \rightarrow 2Fe^{2+} + 4OH^-$	(E^0 = -0.39)	**(5.1)**
Anaerobic	$Fe^0 + 2H_2O \rightarrow Fe^{2+} + H_2 + 2OH^-$	(E^0 =+1.67)	**(5.2)**

In short, iron corrosion in water is facilitated by the depolarisation of water to produce iron oxides **(5.1, 5.2)**. In depolarisation, water molecules are electrochemically destabilised as oxygen is consumed to form iron oxides and hydrogen protons (H^+) are released. Excess H^+ protons will congregate around the negatively charged surfaces of a metal providing partial oxide shielding (**5.2**). However, dissolved oxygen present in aerobic conditions will readily interact with free hydrogen to form water **(5.1)** removing any shielding effect and thus result in increased corrosion rates. This phenomenon can also be expressed in terms of electrochemical potential where aerobic corrosion with a net negative standard electrode potential of -0.39 will more readily proceed compared to the +1.67 potential required for anaerobic corrosion reactions [150].

In the previous trial in this chapter, no by-products of TCP were detected, suggesting that degradation of the contaminant did not occur and that the primary method of treatment was removal by Osorb absorption. In the air, corrosion rates will be affected by humidity, temperature, atmospheric pressure, air quality, the frequency of rain events and their acidity. Results from the preceding chapter (Ch.3.3) had suggested that aerobic atmospheric corrosion of the nZVI occurs at a rate of 18% loss per day with a minimum concentration of unoxidized nZVI stabilising after 48hrs. Iron hydroxides formed were mostly magnetite-structured (Fe^{2+}, Fe^{3+}) and conducive to electron transfer from an inner Fe^0 core facilitating sorbate degradation [285].

In water, corrosion will be affected by the quantity of dissolved oxygen, the presence of dissolved minerals and ions, temperature, and pH of the water. It was expected that corrosion would occur faster in water than in air, yet given the wide variety of factors that influence corrosion, predictions could not be made of corrosion rates of nZVI in nZVI-Osorb in water. Most studies that were able to degrade TCP with nZVI in water successfully, found degradation products after 2 hours primarily using nitrogen-purged or deoxygenated waters (Ref: Table 4.5). Therefore, 24 hours was considered sufficient contact time to allow for any potential degradation mechanism to proceed with nZVI-Osorb.

As discussed in Ch. 1, 3, and 4 and elsewhere within the present chapter, the removal of dissolved oxygen and the creation of anaerobic conditions should decrease overall iron corrosion rates through increased longevity of the Fe^0 core. This would allow for improved iron-mediated adsorption and degradation of TCP [150]. Removal of dissolved oxygen is also linked to different iron-oxide formations with anaerobic conditions favouring the creation of magnetite-based oxides which are not prohibitive to Fe^0 reactivity and can facilitate degradation through enhanced electron transfer from core Fe^0 atoms to the solid-liquid surface [285]. This is in contrast to two-layered iron oxide structures (inner magnetite structure (Fe^{2+}, Fe^{3+}) and an outer lepidocrocite layer (FeO(OH)) formed from interactions with excess dissolved oxygen in the water as the interfacial lepidocrocite layer is thought to impede Fe^0 reactivity in reduction through surface passivation [176, 285].

A trial was conducted comparing the treatment of two materials (nZVI control, and nZVI-Osorb) in both aerobic and anaerobic conditions to understand the effect of corrosion from dissolved oxygen on iron-mediated adsorption and degradation (Fig. 5.2).

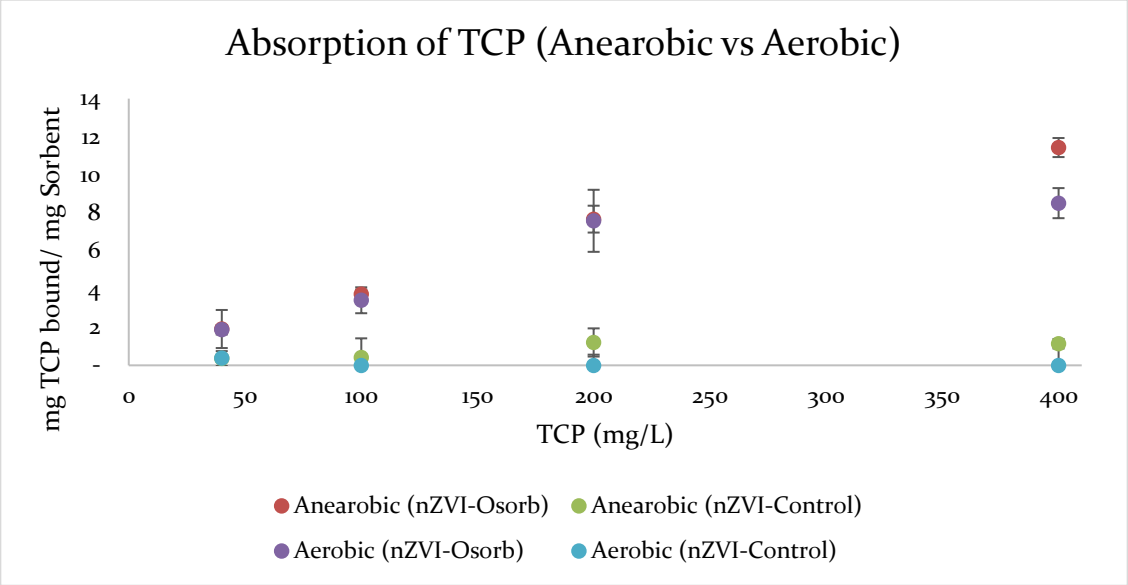

Figure 5.2 Sorption of TCP with nZVI-Osorb and nZVI control tested side-by-side in two different atmospheric oxygen environments (aerobic and anaerobic). Anaerobic starting aq. solutions before TCP addition were deoxygenated via autoclave. Starting pH was 5.10 for both solutions. No degradation products were observed in the analysis.

As with other studies in this work, no breakdown products for TCP were found in test solutions or acid recovery solutions (Appendix 1, Table A1.1) for any compound shown in Fig. 5.2. These results are consistent with previous data and would further suggest that the Fe^0 present in the control and the nZVI-Osorb nanocomposite are not degrading TCP.

Anaerobic conditions minimally improve the sorption of TCP by nZVI-Osorb in contaminant loads below 200 mg/L (40 ppm-1.94%, 100 ppm-7.93%, and 200 ppm-0.89%). At 400 mg/L anaerobic conditions improved treatment by 14.59%. These results are interesting because Osorb in an inert sorbent and the sorption mechanism of Osorb should not be influenced by the presence or lack of oxygen in the system. This difference in TCP sorption is therefore attributed to changes in iron corrosion wherein unoxidized Fe^0 atoms are available for partial TCP adsorption.

This hypothesis was supported by adsorption results of ZVI-control. Adsorption of TCP was improved in most samples under anaerobic conditions 100 ppm (10.41%)- 200 ppm-(6.9%) 400 ppm (4.0%) except the lowest concentration 40 ppm (-1.11%) whose

removal was slightly less than aerobic ZVI-control sorption, but still within the standard deviation range of 1.1. The nZVI-control under aerobic conditions found no sorption of TCP in concentrations above 40 mg/L and was supported by work in the previous chapter (Table 4.2) which found minimal (0.40 mg/L) TCP adsorbed onto nZVI control.

As discussed in Ch. 1.3, nZVI treatment pathways vary depending on the contaminants and can include sorption, complexation, (co)precipitation, and surface-mediated reduction[150]. For TCP, reduction follows partial sorption and concurrent surface-mediated reduction. Similar treatment mechanisms are applied for other chlorinated organics such as trichloroethylene[293]. For other contaminants such as heavy metals, sorptive mechanisms play a stronger role in resulting complexation and co-precipitation removal mechanisms[289]. Large organics such as humic acid typically only observe sorptive mechanisms with nZVI[294]. In all of these cases, sorptive features had to act in competition with oxide formation which can reduce the number of available active sites on Fe^0 surface and therefore decrease target adsorption of a contaminant[177].

As discussed in Section 4.3 the removal of dissolved oxygen typically resulting in trials will cause partial TCP degradation by nZVI (ref. Table 4.5) as opposed to another trial in aerobic conditions that found no degradation[29]. These sorption and dissolved oxygen results along with results from Fig. 5.2 would suggest that anaerobic conditions including the removal of DO lowered rates of surface corrosion and increased the availability of Fe^0 to adsorb TCP. However, decreased corrosion was not sufficient in enabling electron-mediated reduction of TCP in solution.

A prior pilot study with another nZVI-Osorb composite was able to degrade trichloroethylene in groundwater[235] suggesting that nZVI within the composite should remain effective for contaminant degradation in solution regardless of ambient oxygen content. Further studies examining the nZVI-Osorb treatment of less chlorinated phenols with less overall electronegativity should be pursued in future work to further clarify if lack of degradation in the results is solely the product of corrosive hindrance or a combination of iron corrosion and contaminant electrochemical properties which increase resistance to degradation mechanisms.

This trial (Fig. 5.2) would suggest that anaerobic conditions might be the ideal environment for preserving nZVI reactivity and limiting corrosion in treatment

applications if degradation with organics and halogenated organics can eventually be produced. Aerobic conditions may still be suitable for quick experiments or applications where advanced environmental controls on atmosphere or water composition cannot be regulated or modified. An emerging application such as anaerobic digestion (wherein ZVI has shown promise in increasing biogas production and has the potential to buffer/degrade various organic contaminants) could be the ideal application for these materials giving the persistent issues with corrosion in standard aerobic conditions[179].

Given that sorbate properties strongly influence sorption mechanisms and TCP processes, acid properties and in-depth evaluation of pH on degradation and sorption mechanisms is warranted and should also be examined[15, 274].

5.4 Effect of pH on TCP Sorption by nZVI-Osorb

Phenol and chlorophenols are organic monoprotic acids and can donate a proton (H^+) under specific environmental conditions. As acids, changes in pH can strongly affect the chemical behaviour and environmental fate of phenol and chlorophenols in solution. These compounds will exhibit deprotonation of phenol's hydroxyl group (-OH) relative to the pH of the aqueous solution **(5.3)**[15].

$$C_6H_5OH^o{}_{(aq)} \leftrightarrow C_6H_5O^-{}_{(aq)} + H^+{}_{(aq)} \qquad \textbf{(5.3)}$$

25 mg nZVI-Osorb was mixed in four 100 mg/L TCP solutions each adjusted to a different pH to observe the effect of pH on sorption and degradation of TCP (Table 6.3).

Table 5.3 100 mg/L TCP solutions adjusted to 4 distinct starting pH values. The TCP solutions were shaken with 25 mg of nZVI-Osorb for 24 hr under aerobic conditions.

pH	% Reduction	STDEV (mg/g)	Q_e (mg/g)	STDEV (mg/L)
3	91.93	0.78	36.77	1.95
5	87.22	0.97	34.89	2.42
7	30.18	0.63	12.07	1.57
9	3.34	0.82	1.33	2.05

The sorption capacity of nZVI-Osorb for TCP varied widely relative to pH. Sorptive capacity decreased slightly from 36.77 mg/g to 34.89 mg/g with a pH shift of 3 to 5 at a net capacity loss of 1.88 mg/g. However, when the pH was increased further to 7, capacity dropped drastically to 12.07mg/g. Sorption barely occurred once pH reached 9. This loss of capacity at increasing pH is most likely due to the acid-dissociative properties of TCP shown in Eq. 3 resulting in the compound's increased solubility in water (Table 5.1).

In solution, the individual chemistry of a molecule will dictate the point at which a proton becomes donated (dissociated) from the compound. The pH in which the compound's protonated state and deprotonated state are at equilibrium is known as its acid dissociation constant (K_a). Mass action equations for the acid can be expressed mathematically **(5.4)** wherein K_a represents the equilibrium acidity constant, γ is the activity coefficient of the aqueous species, and the concentration of the dissociated species are expressed in molarity [15].

$$K_a = \frac{[C_6H_5O^-]\ \gamma\ C_6H_5O^-\ [H^+]\ \gamma\ H^+}{C_6H_5OH^0} \qquad \textbf{(5.4)}$$

K_a is more commonly expressed and utilised as a logarithmic constant known as pK_a so that the value can more directly be correlated to pH, which is also expressed on a logarithmic scale **(5.5)**.

$$pK_a = -\log_{10}(K_a) \qquad \textbf{(5.5)}$$

pK_a is used as an indicator of acid strength and protonation state in solutions of given pH. The pH in which the compound's protonated state and deprotonated state are at equilibrium is equivalent to the pK_a value of that compound [9]. Typically, the higher the pK_a value, the weaker the acid. In solutions of pH below pK_a, a majority of the compounds in solution will be protonated. Conversely, in solutions with a pH > pK_a, a majority of compounds will be deprotonated. Within the class of chlorophenols, there is a wide range of pK_a values (Table. 5.4).

Table 5.4 Basic properties (structure, molecular weight, pK_a) of phenol and its chlorinated substituents. The compound's recorded pH (100 mg/L) and its relative dissociation state at that pH are also detailed.

Compound	Structure	Molecular Weight (g/mol)	pK_a	pH (100 mg/L in Water)	Protonated
phenol		94.11	9.99	6.76	Yes
o-chlorophenol		128.60	8.56	6.45	Yes
2,4 Dichlorophenol		163.00	7.89	6.26	Yes
2,4,6 Trichlorophenol		197.45	6.23	5.10	Yes
Tetra-chlorophenol		231.88	5.14	n/a	n/a
Penta-chlorophenol		266.34	4.70	n/a	n/a

Phenol has a relatively high pK_a value of 9.99 indicating that phenol is a very weak acid. In acidic conditions, phenol will not readily donate protons and will likely maintain an overall neutral charge. Conversely, pentachlorophenol has a pK_a of 4.70 and will more readily donate its H^+ proton in acidic waters [9].

This broad range in acid dissociation is the result of steric and electrochemical changes from the addition of chlorine atoms onto the aromatic ring. Total acidity (K_a) will increase with increasing Cl^- substitution and will correspond to an overall decrease in solubility (ref. Table 5.4). Acidity is also dependent on the steric positioning of the chlorines on the aromatic ring and Cl^- closer to the hydroxyl –OH group will have increased acidic character [273].

In a 100 mg/L solution, the pH of the overall solution was below the pK_a value for the compound. This suggests that for most experiments in this chapter TCP was protonated and had an overall neutral charge. A more detailed understanding of protonation at given pH can be illustrated by a speciation plot (Fig. 5.3).

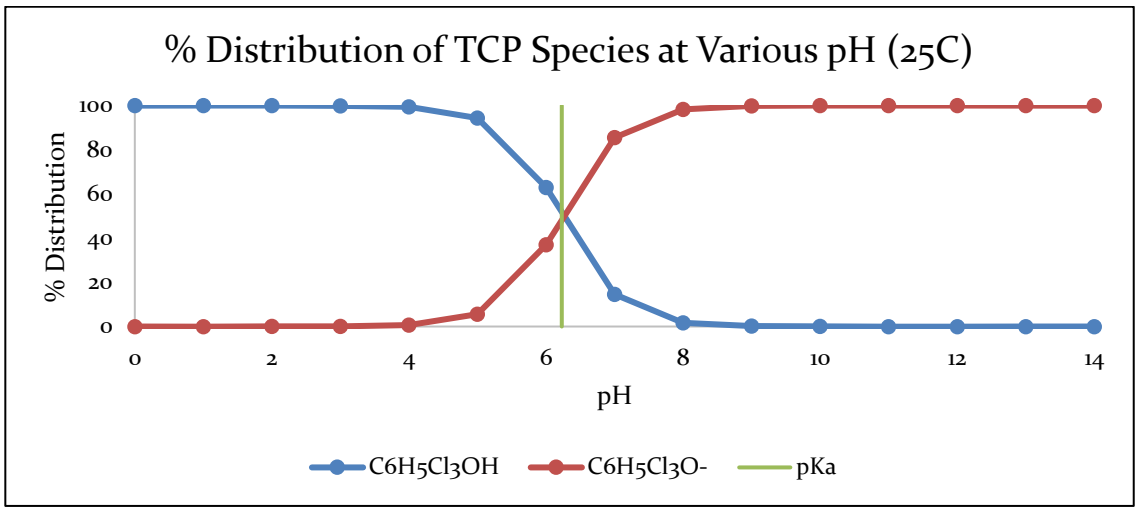

Figure 5.3 A speciation plot for TCP as a function of pH (25C).

The speciation plot of TCP indicates that within a pH range of 4-8, a mixture of protonated and deprotonated species of TCP are expected. At acidic pHs below 4, the majority of TCP molecules are expected to be protonated, carrying an overall neutral charge. At pHs above 8, the majority of TCP will be deprotonated with a negative charge [143].

Table 5.4 and Figure 5.3 help to clarify results listed in Table 5.3. Adsorption of TCP from solution was strongest when TCP was in acidic conditions below the pK_a value (6.23). As the proportion of deprotonated TCP in solution increased, sorption decreased, as evidenced by the slight decrease observed between a pH of 3 and 5. At a pH of 7 when approximately 80% of TCP was deprotonated, there was a significant decrease in sorption from 34.89 mg/g to 12.07 mg/g. When most of TCP was deprotonated at a pH of 9 a reduction of 3.3% was observed. It is clear that sorption of TCP was dramatically affected by the protonation state of the compound.

As discussed in Chapter 3, Osorb is best suited to the absorption of nonpolar uncharged organics following trends observed in Fig, 4.2 [134]. pH studies with TCP support this trend with neutral species absorbed in higher concentrations. Reduced capacity at a neutral pH is particularly problematic because most water treatment systems regulate pH in their systems to be neutral (Table 5.5).

Table 5.5 pH ranges for waters occurring in different systems.

Water Type	pH Range
Surface Water [295]	6.5 - 8.5
Groundwater [296]	6.0 - 8.5
Wastewater Pretreatment [297]	6.5 - 8.5
Wastewater Post-treatment [298]	7.0 - 7.2
Anaerobic Digester (Methane Forming Bacteria) [299]	6.8 - 7.2
Anaerobic Digester (Acid Producing Bacteria) [300]	>5.0

In most of the water environments detailed in Table 5.5, TCP would contain a mixture of protonated and deprotonated TCP which would represent less than ideal sorptive environments. However, pK_a values of less chlorinated phenols are 7.89 and above suggesting that sorption will remain favourable for these compounds and closer to the values reported in Fig. 4.6.

Research reported in the open literature here indicated that slight pH changes are expected to occur naturally within natural and processed waters and that degradation mechanism of nZVI in solution will accompany a pH rise as available protons are consumed by cleaved compounds and molecules[176]. The results confirmed that sorption of TCP was strongly influenced by pH, and so another test was conducted to observe if pH changes occurred during the treatment process of TCP in water and examined whether these changes had any effect on the sorptive capacity of Osorb. 125 mg of nZVI-Osorb was added to a 100 mg/L TCP solution (50mL) with an unadjusted starting pH of 5.1 (Fig. 5.4).

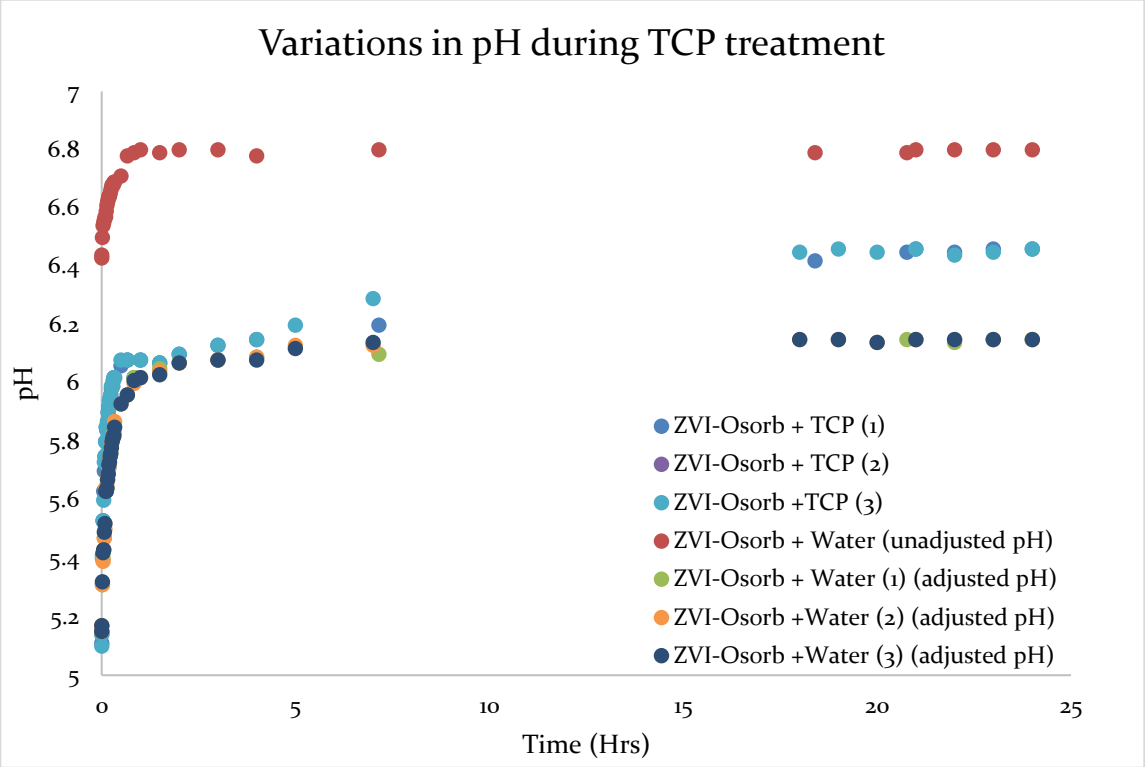

Figure 5.4 Recorded pH values monitored over 24 hours in a continuously stirred solution for a 50 mL solution of DI water containing, (1) 125 mg of nZVI-Osorb *(ZVI-Osorb + Water, unadjusted pH),* (2) 100 mg/L TCP solution containing 125 mg of nZVI-Osorb *(ZVI-Osorb + TCP)* and (3) a solution of DI water containing 125 mg of nZVI-Osorb with the initial pH of the DI solution artificially titrated to a pH of 5.1 *(ZVI-Osorb + Water, adjusted pH)*.

The mass of added nZVI-Osorb is equivalent to other tests when adjusted for volume of the treatment solution. An increase of 1.2 pH in the TCP +nZVI-Osorb sample was observed over 5 hours leading to a final pH of 6.3. The starting unadjusted pH (5.1) is below the pK_a of TCP (6.23) and according to the speciation plot given in Fig. 6.3 the vast majority of TCP will be protonated with a neutral charge, which is advantageous to nZVI-Osorb sorption. The final pH of 6.3 is slightly above the pK_a of TCP and therefore some TCP molecules will likely be deprotonated in solution which will increase solubility and could lead to a loss of sorptive capacity during initial pH adjustment (<2 hrs) and at equilibrium thereafter. However, affinity and leeching trials conducted in Section 4.2 have suggested that any TCP leaching after initial sorption is minimal with no desorption

detected in test waters (Fig. 4.7) and minimal leaching occurring when the sorbent is transferred to uncontaminated water sources (Table 4.4).

As briefly discussed, the detected increase in pH in a solution is the result of H^+ proton consumption in solution. The reduction in free protons would accompany a decrease in the acidic character of the water and would raise the pH. A mechanism of TCP degradation by nZVI suggested in the literature indicated that dehalogenation of the TCP in solution would result in an increase in pH in solution due to consumption of free protons to replace and interact with cleaved chlorine ions from the aqueous solution[82]. This initial result would suggest the possibility of TCP degradation in solution. However, no degradation products of TCP were detected by GC-FID in this or any other trial within this thesis, and so it is unlikely that degradation of TCP is the mechanism responsible for the pH shift (5.1 to 6.3) observed in the test solution.

A control solution of 125 mg of nZVI-Osorb in water also demonstrated a rise in pH from a pH of 6.4 to 6.8. Because there is no TCP in solution in the control trial, the 0.4 pH shift (6.4 to 6.8) solely occurred as the result of oxidation of the iron catalyst (which would also consume free H^+ protons) within the nanocomposite. The change in pH was not as substantial as the change in pH observed with the TCP solution but could be due to differences in starting pH.

An additional trial with nZVI-Osorb in water with a titrated starting pH of 5.1 observed similar pH shifting as the test TCP solutions (5.1 to 6.1). The final pH (6.1) was still slightly lower than the stabilising pH of the TCP solution (6.3) but would suggest that the initial pH shifting found in TCP+ nZVI-Osorb solutions were observed because of proton consumption in iron corrosion rather than proton consumption related to TCP degradation.

The consistent lack of TCP degradation products even when pH is decreased to 3, (Table 5.3), is surprising given that highly acidic pHs often aid nZVI degradation mechanisms through the availability of excess H^+ protons in solution which facilitate electron transport mechanisms[165]. However, pH manipulations must also be considered through the lens of corrosion in aerated water systems. A plot of iron corrosion as a function of pH is detailed in Figure 5.5.

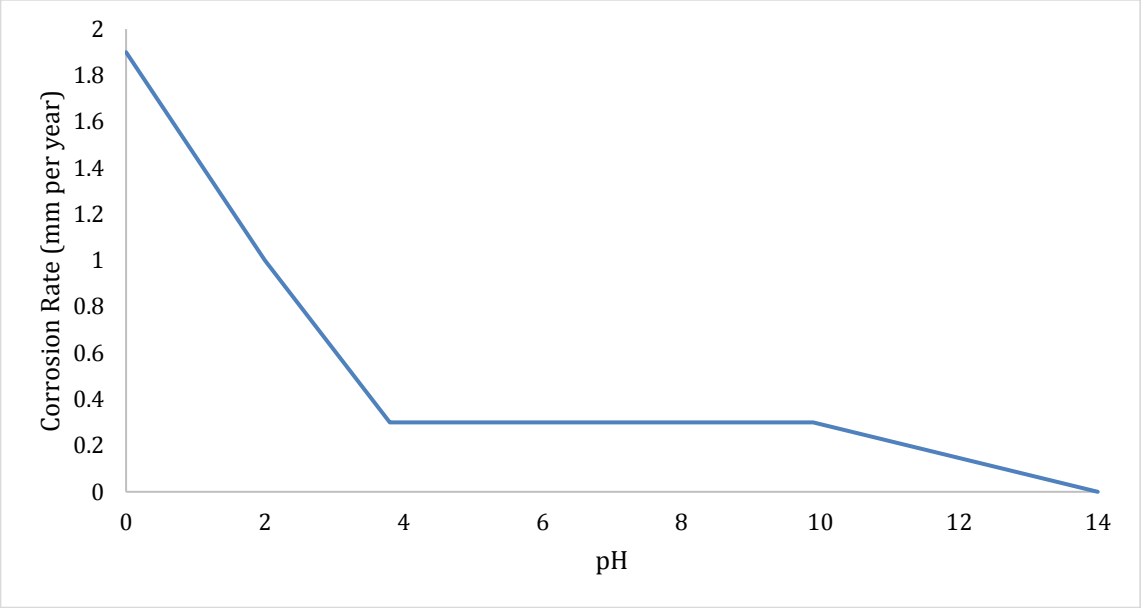

Figure 5.5 Iron corrosion in aerated water determined by the depth of iron oxide formation from the surface per year (mm per year) as a function of pH [248].

Iron corrosion rates are significantly higher below a pH of 4. In aerated systems below this pH value, acidic ions have reached sufficient levels to produce an excess of free H^+ proton in solution. This excess hydrogen can aid corrosion mechanisms through interactions with dissolved oxygen which will readily form additional water molecules and boost overall iron corrosion by mechanisms discussed in the previous section[248]. Furthermore, in these low pH environments, interstitial ferrous oxides (FeO) which typically form a protective oxide film on the nZVI surface, become soluble and dissolve into solution. Without oxide deposition, generated oxides will continually dissolve into solution freeing up deeper iron layers for further corrosion increasing total corrosion rates[176]. These two functions of hydrogen evolution and ferrous oxide stripping could explain why no degradation products were produced even when an excess of protons was available to aid TCP degradation mechanisms in highly acidic waters.

In aerated solutions from pH 4 to 10, hydrogen evolution (as a product of pH) is not expected and therefore corrosion occurs independently of pH as a product of oxygen depolarisation in water. The rate of treatment will follow the rates of oxygen interaction with surface adsorbed hydrogen, which will in turn depolarise the surface of iron and allow

for the continuation of iron's reduction mechanisms to progress with target analytes[301]. All trials within this thesis, except one trial in Table 5.3, were conducted within this pH range, so hydrogen evolution as a product of acid pH is not expected to occur.

In highly alkaline water environments (pH > 10) corrosion is found to decrease as a result of Fe_2O_3 iron oxide formation which is a more protective iron oxide species (Ref. Table 3.8) and will still permit electron transfer from the Fe^0 core. Fe_2O_3 is produced out of further interactions between oxygen and $Fe(OH)_2$ on iron's surface[15]. Highly alkaline environments such as these are not conducive to microbial life, or sorptive mechanisms with nZVI-Osorb for TCP so do not provide a solution for delay corrosion in treatment.

As pH has been found to play a significant role in TCP sorption by Osorb and nZVI corrosion mechanisms are thought to be equally influenced by shifts in potential hydrogen, further investigation should be undertaken with the secondary components in solution that can alter the proton-dependent mechanisms. VFAs, in particular, are a good secondary model as they have acid properties like TCP and are widely found in most biologically active systems[37].

5.5 Effect of Secondary Acids (VFAs) on TCP Treatment

Experimental test solutions utilising a single contaminant allow for a better understanding of interactions and mechanisms at play in treatment. However such solutions rarely model all the complex interactions that occur in realistic water solutions which may contain a variety of dissolved mineral and gases along with secondary contaminant species[133]. An understanding of how secondary contaminants effect nZVI-Osorb is essential as their presence can influence various mechanistic functionalities such as sorption and degradation interactions through competitive exclusion, fouling, and the alteration of water properties such as pH [29, 286].

Experiments in this chapter have revealed that nZVI-Osorb is best suited for TCP treatment in anaerobic acidic water conditions because both pH and dissolved oxygen strongly influence sorption and potential degradation mechanisms. As discussed in Ch. 2, a few newly published studies have identified a positive effect on methane production in

anaerobic digesters with the addition of nZVI in low concentrations [83, 196, 198]. Low oxygen environments found in these reactors, as well as, compatible pollutants inhibiting methanogenesis (e.g. TCP), make anaerobic digesters particularly well-suited to the study of TCP treatment by ZVI-Osorb.

Anaerobic sludges in these reactors are notoriously complex, so a simplified system containing a few essential elements present in these sludges, such as Volatile Fatty Acids (VFAs), provides an exciting study allowing a more fundamental understanding of nZVI-Osorb functionality and treatment properties before examining a complete model system. As with TCP, VFAs are acids and so are expected to influence pH and in turn nZVI-Osorb's sorptive mechanisms in treatment. Examining the effects of these VFAs in anaerobic conditions on sorption mechanisms for TCP would provide closer models closer to actual conditions in anaerobic digesters, and the removal of dissolved and atmospheric oxygen could potentially lead to improved degradation through reduced iron corrosion.

Three model VFAs; acetic acid, propionic acid, and butyric acid, were utilised in these experimental trials as secondary compounds under anaerobic conditions. All three organic acids are commonly produced in digestion processes and have acid properties similar to TCP. Physical and electrochemical properties of the VFAs and TCP are shown in Table 5.6.

Table 5.6 A list of physical properties including structure, dipole moment (measured in Debyes, D), solubility, and pK_a for TCP and three VFAs (acetic, propionic, butyric) at 20C[261].

Compound	Structure	Dipole Moment (D)	Solubility (g/L)	pK_a
TCP	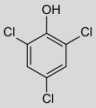	1.380 [302]	0.9	6.23
Acetic Acid		1.739 [303]	miscible	4.76
Propionic Acid	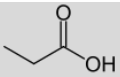	1.751 [304]	miscible	4.88
Butyric Acid	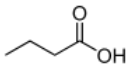	1.649 [302]	miscible	4.82

The dipole moment (D) is an indicator of the total polarity of a compound taking into account the direction and strength of electronegativity within nonsymmetrical compounds[302]. The three VFAs are more polar than TCP, and such electrochemical differences will most likely result in differing sorptive affinity interactions between VFAs and nZVI-Osorb when compared to TCP [303]. Previous experiments with Osorb reported in the literature have also supported weaker sorption of highly polar and ionic sorbate species which are more soluble in water and are less likely to partition out of aqueous solutions [134].

As discussed in Section 6.4, the acid-dissociation of TCP, as a result of pH change and increased contaminant solubility, strongly affected the sorptive mechanisms of nZVI-Osorb. This is also likely to be the case with VFAs which too dissociate in water environments above their pK_a. The pK_a values of these VFAs are lower than TCP ranging from 4.76-4.82 indicating that these acids more readily dissociate in acidic waters than TCP and could lead to impaired sorptive uptake [288, 304].

The acidic character of these VFAs was expected to increase the overall acidity of the total solution by increasing hydrogen (H^+) potential in solution. Baseline pH values were monitored for each acid at several concentrations within a 100mg/L TCP standard solution (Table 5.7).

Table 5.7 Measured pH values for solutions containing 100 mg/L TCP at different concentrations (10, 25, 50, 100) of each organic acid as well as solutions containing an organic acid mix with 100mg/L of each of the three acids.

Acid Concentration (mg/L)	0	10	25	50	100	O.A. Mix (100 mg/L each acid)
Acetic Acid	5.10	4.99	4.60	4.42	4.14	3.30
Propionic Acid	5.10	4.97	4.69	4.49	4.10	3.30
Butyric Acid	5.10	4.93	4.84	4.48	4.17	3.30

The addition of 100 mg/L of a VFA to a solution with an equivalent TCP concentration decreased pH by a full magnitude (5.1 to 4.1). The addition of all three VFAs (100 mg/L) in a 100mg/L TCP solution reduced pH by two magnitudes (5.1 to 3.3). As mentioned, pH will direct acid dissociation of the acids in solution. Because all resulting pH solutions are below 6.23, TCP will remain protonated in all test waters.

In dilute VFA concentrations (10mg/L), the individual acids will be mostly deprotonated and carry an overall charge. At all other VFA concentrations within this study, the majority of the VFA in solution will be protonated and uncharged apart from 25 mg/L butyric acid, which will contain roughly an even mixture of protonated and deprotonated species.

Most tests in this section utilised 100 mg/L concentrations of the VFAs and will, therefore, contain only protonated acid species which are found to be more favourable to sorption by Osorb than charged species[134]. Sorption of VFA by nZVI-Osorb has not previously been tested, so a trial was conducted under anaerobic conditions to observe the sorption of each VFA utilising five masses of nZVI-Osorb (Fig. 5.6).

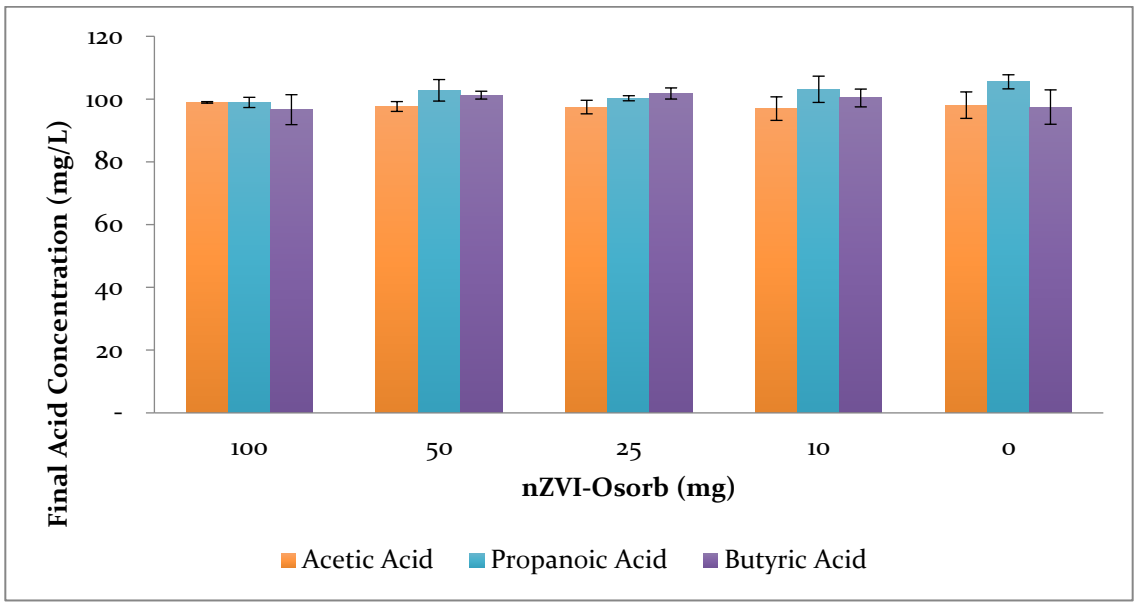

Figure 5.6 100 mg/L of acetic, propionic, or butyric acid in 100 mg/L TCP solutions were mixed with various amounts (100, 50, 25, 10, 0 mg) of nZVI-Osorb for 24 hrs. under anaerobic conditions.

As with other trials in this thesis, no breakdown products were detected in treated samples, suggesting that VFAs and increased acidic properties under anaerobic conditions did not improve nZVI degradation mechanisms to the threshold needed to overcome competitive oxidation and enable the decomposition of TCP.

It was also found that organic acid concentrations remain consistent regardless of the mass of nZVI-Osorb applied, indicating that these organic acids are not sorbed by nZVI-Osorb. Lack of sorptive affinity for VFAs was most likely due to higher polarity and stronger water solubility of these compounds in solution detailed in Table 6.6. Because of these factors, VFAs are unlikely to compete with TCP in solution for sorption but may still alter partitioning and affinity mechanisms through reducing total pH. Table 6.3 indicates that a reduction in pH improved sorption of TCP. 25 mg nZVI-Osorb was utilised to remove a fixed concentration of TCP with variable secondary concentrations of each VFA to determine the effect of VFA presence on TCP sorption (Fig. 5.7).

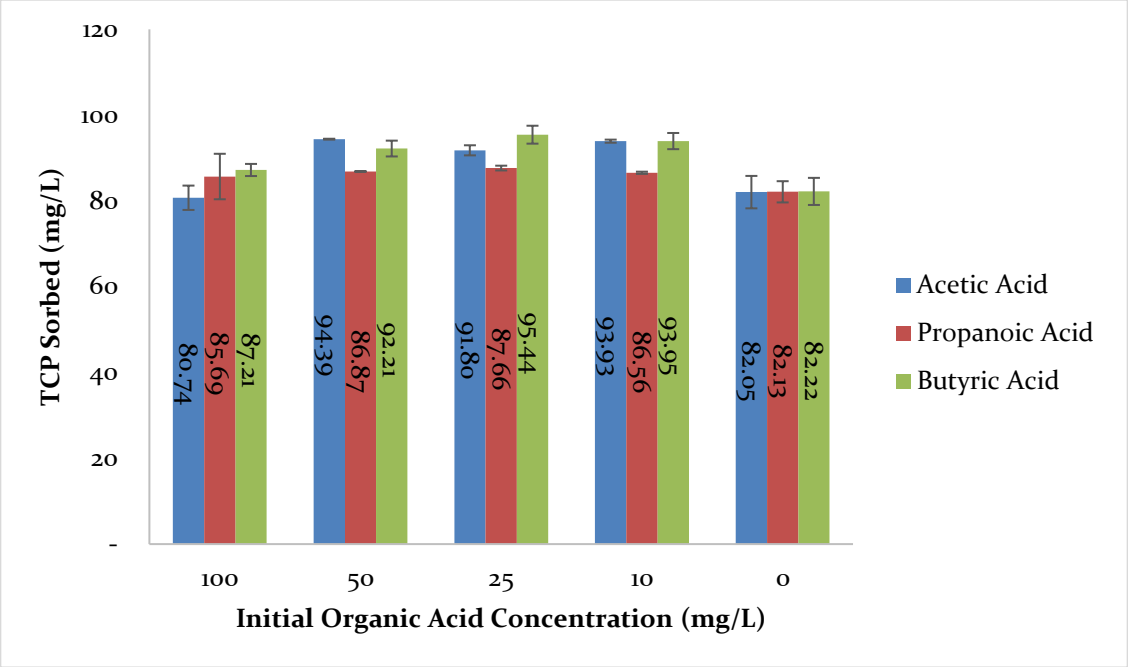

Figure 5.7 TCP sorbed from different initial concentrations (100, 50, 25, 10 and 0 mg/L) of each organic acid (acetic, butyric, or propionic) and 100 mg/L TCP solutions were treated with 25 mg of nZVI-Osorb for 24hrs under anaerobic conditions. Total volume remained constant. Recorded pH values are listed in Table 5.7.

Reduction in pH through addition of VFA was found to improve TCP sorption by nZVI-Osorb. For example, when acetic acid was present in solution (10 mg/L to 50 mg/L) total TCP sorption improved by approximately 11.3% accompanying a pH shift of 5.1 to 4.9-4.42. This TCP sorptive advantage was lost however when acetic acid concentrations were raised to 100 mg/L. As shown in Table 6.6, high concentrations of acetic acid in solution change not only pH characteristics but also electrochemical characteristics of the solution leading to higher overall electronegativity. It is likely that in concentrations at or exceeding 1:1 ratios of TCP to acetic acid, higher overall electronegativity inversely affects hydrophobic interactions and sorption uptake mechanisms. Along similar lines, a study utilising zeolites to adsorb TCP found that cations in solution enhanced TCP sorption through increased attractive electrostatic interactions[15]. Conversely, electrostatic repulsive interaction could decrease sorption in some cases.

However, unlike acetic acid, butyric and propionic acids at 100 mg/L demonstrated improved sorption over control solutions containing no acid. Similar to acetic acid sorption, butyric acid samples were most improved when the acid concentration was between 50-10 mg/L (approx. +11.7%). TCP sorption slightly improved (+4.99%) when butyric acid was at its highest concentration (100 mg/L). Propionic acid samples followed their own trend with slight improvement in TCP sorption at all acid concentrations (approx. 4.6%), the variations were attributed to the individual properties of each acid in solution and the complex intermolecular, and electrostatic interacts at play in a mixed solution.

Overall, as expected, addition of VFA to solution enhanced sorption of TCP from solution. All compounds were neutral and protonated in pH ranges tested in Fig. 5.7 so improved sorption must be attributed to enhanced sorbate partitioning from favourable solubility dynamics produced by reduction in overall pH. When total pH of solutions containing organic acids, TCP, and nZVI-Osorb was artificially adjusted in Fig. 5.8 total sorption followed previously observed patterns.

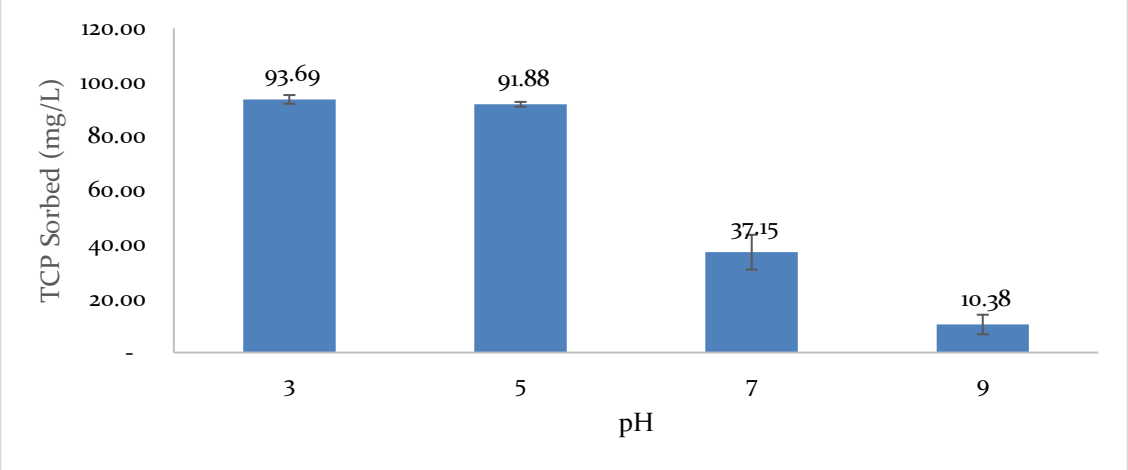

Figure 5.8 100 mg/L TCP with an organic acid mix (100 mg/L acetic, 100 mg/L butyric, and 100 mg/L propionic) adjusted to various starting pHs (3, 5, 7, 9) and then treated with 25 mg of nZVI-Osorb for 24 hrs.

The results would indicate that VFAs present in applied waters most likely will not be absorbed by the sorbate nZVI-Osorb, preventing competitive exclusion. Secondly, the increased acidity produced by their presence should further aid sorptive mechanisms of the material to remove target contaminants like TCP. However, more comprehensive test models containing realistic waters are required to develop a concrete model of multi-contaminant interactions.

5.6 Summary

Similarly to Chapter 4, no degradation of TCP with nZVI-Osorb was observed under any environmental conditions examined in this chapter. These results would suggest that current iron-contaminant interactions lack the required enthalpy to overcome concurrent iron-oxygen interactions which can limit electron transfer and reduce overall reactivity. As nZVI is highly reactive with oxygen and will instantaneously form an iron oxide surface, prevention of complete oxide formation is near impossible to implement in practicality and can only be slowed under tightly controlled anaerobic conditions[284].

However, various types of iron oxide formation are more conducive to electron transfer and therefore contaminant degradation than other iron oxides. For example, iron hydroxide is known actively to hinder electron flow from core Fe^0 atoms whereas FeO iron oxides remain highly reactive. Furthermore, environmental conditions, like the ones discussed in this chapter, can strongly influence iron oxide species formation. Conditions generating various oxides are summarised in Figure 5.9.

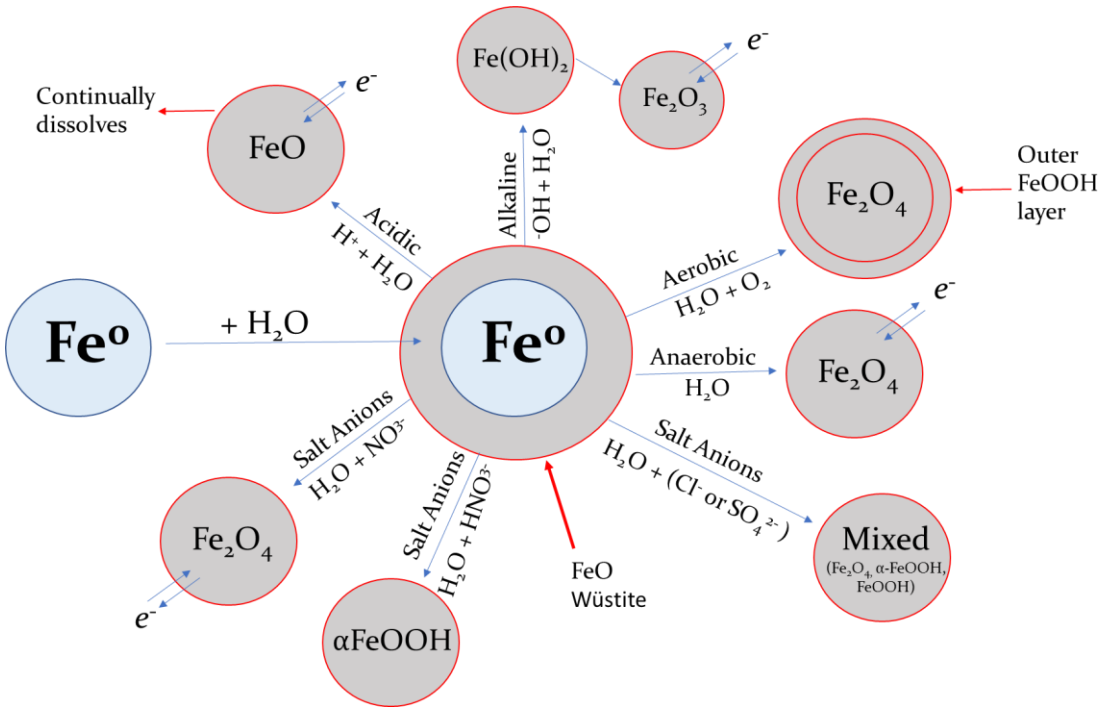

Figure 5.9 A diagram indicating the primary iron oxide (FeO, Fe_2O_4, Fe_2O_3) or iron hydroxide (FeOOH, $Fe(OH)_2$) products formed under various aqueous environmental conditions (acidic, alkaline, aerobic, anaerobic, and various salt anions).

nZVI (Fe^0) immediately forms a protective oxide (FeO) surface layer upon exposure to air or water[174]. Iron oxide will typically allow the transfer of electrons from the Fe^0 core enabling reductive mechanisms with the environments[193]. Iron hydroxide (Fe-OOH) species typically hinder this electron transfer process resulting in surface passivation and the loss of active sites while iron oxide species like FeO, Fe_2O_4, Fe_2O_3 remain conducive to electron transfer[168, 305]. Highly alkaline environments typically result in a two-step oxide formation whereas in highly acid environments the iron oxide layer will dissolve in solution increasing the corrosion rate of nZVI[165, 299, 301]. Environments with high dissolved oxygen will form a two-layer iron oxide structure which also hinders electron transfer[85, 306]. The type of salt anions present in the water will also drive oxide species formation with some producing a mixture of oxide species and others producing primarily iron hydroxides[248, 283].

Overall, water environments that are acid, highly alkaline, or anaerobic permit the formation of iron oxide species that are most conducive to electron transfer and therefore contaminant degradation. These results support previous conclusions that anaerobic digesters may be best suited to test materials[299].

Secondly, environmental factors studied in this chapter such as salinity, oxygen content, pH, and secondary compounds like VFAs were all found to have complex effects on sorption mechanisms of TCP by nZVI-Osorb. Utilizing results from this chapter and details about iron oxide formation given in Fig. 5.9 a schematic diagram was produced summarizing these interactions regarding positive, adverse, or neutral effects on both sorptive (Osorb) and reactive (nZVI) aspects of the composite material (Fig. 5.10).

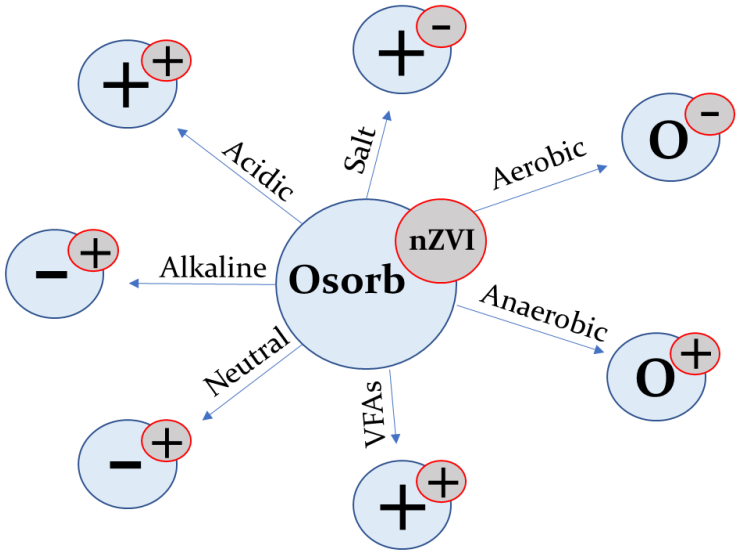

Figure 5.10 A diagram indicating positive (+), negative (-), or no effect (0) on sorption mechanism for Osorb and nZVI under a variety of environmental conditions (salinity, presence of oxygen (aerobic, anaerobic), secondary compounds (VFAs), and pH (acidic, alkaline, neutral)) in water.

High salt concentrations will increase sorptive mechanisms of organics through increased hydrophobicity and partitioning mechanisms yet the high ion concentration will exacerbate corrosion mechanisms, of the iron decreasing its effectiveness in degrading

contaminants[128, 273]. Oxygen content will not influence sorptive mechanisms which are driven by partitioning and other physical processes yet will strongly influence iron's rates of corrosion as well as the types of iron oxides that are formed in that corrosion process[186, 193]. Waters of differing pH will all create electronically active waters which are conducive to nZVI treatment[174]. Alkaline and neutral waters were not conducive to TCP sorption as these waters facilitate the charged species of TCP to predominate which has less affinity for Osorb. VFAs are not absorbed by Osorb but increase the total acidity of the water environment and drive improved sorption. Overall, acidic and anaerobic water environments have the most potent positive effect on TCP treatment by nZVI-Osorb through reducing TCP acid dissociation and oxidative iron corrosion. Applications which meet these criteria, such as anaerobic digesters, might be most suitable for these types of nZVI hybrid materials, but a full-scale model should be investigated first[100, 307].

Chapter 6 : Effect of nZVI-Osorb on Model Anaerobic Digester Dosed with TCP

6.1 Introduction

In the recent centuries, globalisation has led to increasing emissions of methane, nitrous oxide, and carbon dioxide, which are fundamentally reshaping our planet and its atmosphere. Most researchers agree that Global Warming could have catastrophic effects on society if left unmitigated. This need has created the impetus necessary to facilitate development of new sustainable energy practices [308].

One area of development that has made a significant breakthrough in recent years has been anaerobic digesters (AD). This method works concurrently with agricultural waste or municipal wastewaters to drive down greenhouse emissions and detoxify wastewaters while simultaneously generating sustainable energy[309]. This thesis has already discussed at length the significance of reducing water contamination to safeguard animal and environmental welfare in water treatment and water management applications[290], but extending AD's usage into is agricultural wastes has significant secondary benefits for climate change mitigation[86]. Of all greenhouse emissions, 22% may be attributed to farming with 80% of such agricultural emissions resulting directly from livestock production[310]. If the UK is to meet its 2050 targets to reduce greenhouse gas emission by 80%, there must be a fundamental shift in energy production and agricultural practices to reduce wastes. Anaerobic digesters (AD) could play an essential role in meeting those reduction targets [32].

Typically, anaerobic digesters are utilised in wastewater treatment facilities or as stand-alone units in rural areas to degrade organics and produce biogas, notably methane, which can be utilised in combined heat and power generators to produce heat and electricity or directly as the fuel source biomethane[299] (Fig. 6.1).

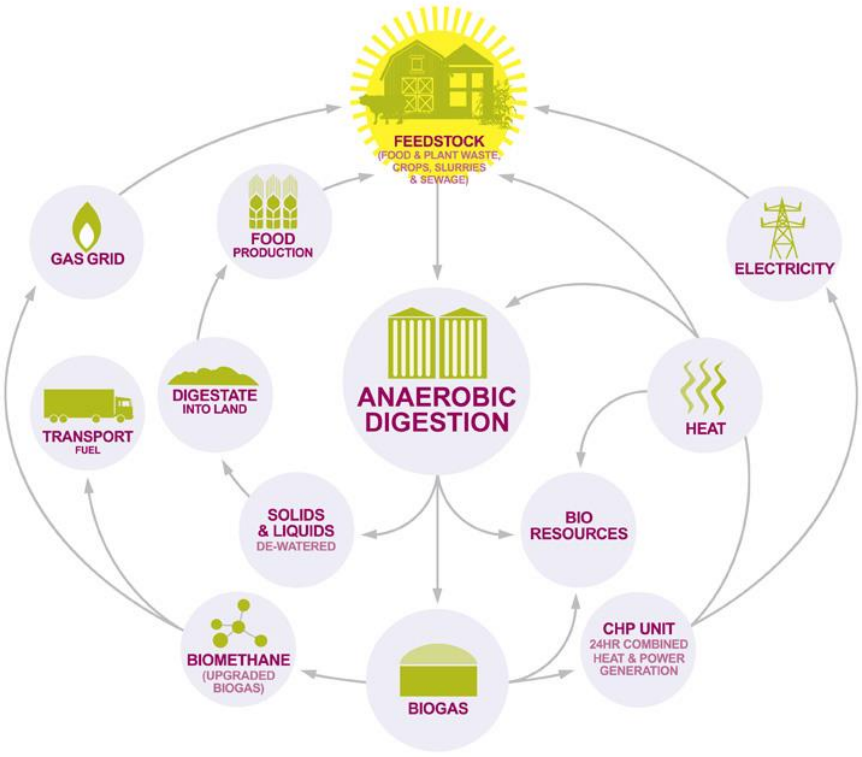

Figure 6.1 The energy and lifecycle use of agricultural based anaerobic digester [311].

Each AD reactor is unique in its biological composition given the diversity of microbial life which is even further exacerbated by the biotic response to nonhomogeneous feedstocks and influent[312]. Despite this microbial diversity, all degradation of biomass into biogas involves four necessary stages of breakdown: hydrolysis, acidogenesis, acetogenesis, and methanogenesis[311]. Recent advancements in AD have focused on safeguarding microbe health, increasing biogas production, ensuring that resulting digestate is safe for use, and decreasing operational costs[313]. Microbial health is particularly concerning in AD processes because microorganisms in these systems, particularly acetogenic and methanogenic bacteria, are highly sensitive to process disturbances, as well as contaminants in wastewaters and agricultural feedstocks which can decrease methane production with varying degrees of severity. Contaminants that can inhibit AD processes can be classed as inorganic toxicants (ammonia, sulphide, heavy metals) and organic toxicants (chlorophenols, halogenated aliphatics, long-chain fatty acids (LCFA))[91].

The most common inorganic contaminants are ammonia and sulphide. Ammonia (an essential molecule) and sulphide inorganics pose an issue at high concentrations. Treatment options for ammonia and sulphide most often include dilution of the wastewater stream or increasing biomass retention in the reactor. Both options remain undesirable due to longer treatment times and increased volumes of wastewater requiring management. Recent work has suggested that a pre-treatment step to remove sulphide from waste streams may be beneficial [93]. Other studies have focused on ammonia treatment have suggested that the addition of zeolites (an inorganic nanosorbents) in concentrations 10-20 g/L with a concurrent decrease in the pH from 8.3 to 6.5 can lower methanogenic inhibition without requiring additional biomass into the reactor [314].

Heavy metals sometimes found in wastewaters and various sludges present the most significant toxicity to anaerobic bacteria. Common detected heavy metals include copper, lead, zinc, mercury, cadmium, chromium, iron, nickel, cobalt, and molybdenum[315]. Unlike organic or inorganic contaminants, metals are not biodegradable, and therefore concentrations can increase over time within the main reactor[316]. In addition to affecting acetogenins[317] and methanogens[318, 319], observed with organic and inorganic contamination, heavy metals can also disrupt acidogens[320-322] and sulfate-reducing bacteria[323]. The severity of toxicity depends on the particular metal and its overall concentration with AD failure occurring when the ion concentration exceeds a particular threshold[324]. The most common methods of treating heavy metals include precipitation, chelation with ligands, and sorption [209].

Unlike the water industry and groundwater remediation where additives must be tightly controlled, additives to AD are applied more liberally to control contamination issues. These additives can be either inorganic or biological and can be utilised for a wide range of features. Macro elements such as P, N, S, and microelements such as Fe, Ni, Mo, Co, W, and Se have been applied as nutrient supplements. Fe^{0} and Fe^{+3} have been utilised to immobilise biomass. Additives are particularly prevalent in regulating ammonia concentrations[13].

Advanced materials have also been deployed to treat organic contaminants within reactors. The most common organic contaminants in AD are long chain fatty acids, chlorophenols, and halogenated aliphatics. High concentration of LCFA can delay methane

production, so treatment has typically included the addition of a competitive sorbent such as bentonite to adsorb or calcium to precipitate out high levels of LCFA and bring concentration under control[325]. While effective, these treatment strategies do not aid the degradation of LCFA and are not fully effective for other contaminants such as chlorophenols and halogenated aliphatics which demonstrate partial resistance to sorption and precipitation strategies in complex reactor systems[13, 306]. As discussed in Ch.1, some biodegradation is expected for these chlorinated organic compounds; however studies of AD systems have found that TCP is particularly recalcitrant and microbial communities were not responsive to the addition of nutrients such as acetate, lactate, pyruvate, vitamin B12 or manganese dioxide to aid contaminant digestion and counteract contaminant toxcity[65, 326].

TCP's resistance to biodegradation and traditional sorption and precipitation methods in AD would suggest that the development of new additive materials that could successfully remove and degrade TCP in a complex environment without harming microbial life would be in high demand. The heavy usage of sorbents to control high inorganic and organic contamination loads suggests that nZVI-Osorb may be particularly well suited in the AD process as Ch.3-5 have demonstrated high sorptive yields of TCP (a particularly recalcitrant pollutant inhibiting methanogenesis) from aqueous solutions with the further potential for broader contaminant uptake[327]. nZVI-Osorb could be particularly beneficial if, in addition to sorption, it could wholly degrade the contaminant without adversely affecting microbial health and biogas production in the process. The anaerobic nature of these systems has the potential to delay rates of iron corrosion while also producing more favourable iron oxides both of which would preserve iron reactivity and potential boost contaminant degradation[83].

Studies has focused on the addition of nanomaterials to AD to remediate contaminated feedstock. In general, added nanomaterials produced mixed results regarding microbial health. Certain nanoparticles such as nano-Ag, Al_2O_3, SiO_2, TiO_2, C_{60}, were found not to have a direct adverse effect on the anaerobic bacterium[328]. Others, such as CeO_2, ZnO, Au, and in some cases even ZVI were found to be toxic or inhibitory[196, 329, 330]. One study utilised the addition of double-walled carbon nanotubes (DWCNT), a seemingly innocuous organic nanomaterial, in a model reactor system, and found that

while the DWCNT did decrease overall trichloroethylene in the system, it inversely affected methane production in proportion to increasing concentration of nanomaterial[91]. Reduced methanogenic activity was linked to a nanotoxic effect from DWCNT mediated cellular damage[331]. These results serve as a reminder that any introduced material to treat contamination must do so without causing microbial harm.

Recent studies have clarified microbial effects of ZVI by suggesting that ZVI is not inhibitory if the total concentration is below a particular threshold (variable but typically below 0.1% of the total slurry composition)[332]. Examinations of nZVI treatment of TCP in AD systems found a mutually beneficial chemical and biological directed dechlorination (to phenol) and then degradation (to methane and carbon dioxide) of the contaminant. nZVI can act independently to dechlorinate TCP while concurrently reducing the total toxicity of the contaminant toward the microorganisms. Hydrogen gas produced in the corrosion of the iron further acts as an electron donor to assist biological mediated dechlorination by *Dehalospirillum multivorans* and *Desulfitobacter sp.*[250] As discussed in Ch. 5, iron-microbial systems were able to degrade sufficiently 30 mg/L DCP in 68 hours[333]. This cometabolic degradation mechanism also resulted in molecular benefits. nZVI in these biological systems was found to increase electron transport system activity (ETS)[21], decrease intracellular and extracellular polysaccharides, and increase microbial diversity[334]. Favourable molecular changes such as these could aid the degradation of other inhibitory contaminants which show greater recalcitrance, like PCP, broadening the potential impact of nZVI dosed AD systems[250].

The reduction in contamination toxicity coupled with molecular process improvements also boosted overall methane production and reduction in CO_2 emissions, particularly when iron particle size was reduced to the nanoscale[83, 198]. One study was able to increase methane production by 28% and reduce released CO_2 by 58% with the addition of 2.5 and 5.0 g/L ZVI[198]. Another study found enhanced methane yields by 25.2 and 40.8% with 0.1% nZVI in addition to degradation of chlorinated personal care products (PPCPs)[83].

This boost in methane production from nZVI addition also results in increased overall pH and lower oxidative reductive potential (ORP)[198]. Evaluation of reactor parameters such as pH and ORP in model experiments could give indications of electron activity and transport which apply to biological mediated redox reactions in metabolic

systems and are affected by the addition of reducing agents like nZVI[333]. Other parameters like biogas and chemical oxygen demand (COD) enable evaluations of microbial activity and should also be evaluated in test systems[37, 105]. Direct monitoring of TCP concentrations has been challenging given the complexity of the total solution and the low concentration of contaminant in the reactor, yet rigorous sample preparation along with low concentration detection systems like LC-MS/MS could provide an answer [83, 196, 198].

These nZVI AD system results are promising and warrant a closer examination of nZVI-Osorb as an AD additive. While nZVI-Osorb in bench-scale experiments within this work so far have not been able to demonstrate the degradation of TCP, the cometabolic degradation mechanisms found in AD systems could provide the additional digestive potential to enable degradation of TCP to proceed despite loss of iron reactivity from corrosion and oxidation (which is expected to occur even under favourable anaerobic conditions). The strong sorptive potential of Osorb for TCP demonstrated in the previous chapters has the potential to further boost cometabolic mechanisms through concentration of the contaminant at iron active sites in complex AD systems. In addition to high sorptive yields, Osorb is also preferential to other competitive sorbents; as work in this thesis has shown, embedded iron can be tightly bound preventing particle loss/leaching and presenting even metal dispersion within the substrate to preserve high metallic reactivity in applied systems. If treatment mechanisms proceed as expected the addition of nZVI-Osorb to AD reactors could improve contaminant degradation, microbial health, and biogas production. Further assessment should be made of nZVI-Osorb's impact in a model AD system.

6.2 Treatment of 2,4,6 Trichlorophenol in a Model Anaerobic Digester

6.2.1 Anaerobic Bioreactor Setup

A series of 9 reactors were prepared in triplicate utilising biomass from a locally sourced commercial anaerobic digester to recreate both the composition and conditions of a functioning anaerobic digester system. The complete setup and composition of each reactor are described in Section 3.9. The bulk of these reactors were composed of biomass,

a feed solution for biological organisms within the reactor, and a buffer solution to stabilise solution pH (Table 6.1).

Table 6.1 Bulk composition of the model anaerobic digester reactors (200mL).

Bioreactor Contents	Volume (mL)
Biomass	125
Feed	12.5
HEPES Buffer	62.5

Individual reactors were doped with 25 mg/L TCP, 3.9 g/L nZVI-Osorb or nZVI control, and dilute concentrations of acetic, propionic, and butyric acids (Table 6.2).

Table 6.2 Contaminant (TCP), nanomaterial (1-pot nZVI-Osorb, nZVI), and VFA concentrations for the model anaerobic digester reactors (200 mL).

Component	Concentration
nZVI-Osorb or nZVI Control	3.9 g/L
2,4,6-Trichlorphenol	25 mg/L
Acetic Acid	240 mg/L
Propionic Acid	120 mg/L
Butyric Acid	120 mg/L

Solutions were prepared under anaerobic conditions in an anaerobic chamber and sealed in air-tight containers for transfer to an incubated rotary shaker in a secondary location between anaerobic sampling periods. Reactors containing biomass were dark greenish brown (Fig. 6.2).

Figure 6.2 A series of bioreactor produced. The biomass appears a murky brown colour. Samples that contain iron were closer to black in colour.

Nine reactor types (A through I) of equal volume were produced to provide a robust understanding of interactions. Both nZVI-Osorb and nZVI Control were utilised in experiments to establish an effect. Test reactors B and C contained all three reactor components (biomass, TCP, and nanomaterial). Biomass control (I), biomass and TCP control (A), and biomass and nanomaterial (D, E) were utilised to establish a biological baseline for the anaerobic bioreactor system. Control reactors F and G established a baseline for TCP interactions with the nanomaterials without biological presence. Control TCP (H) was utilised to ensure TCP compound stability in solution throughout the trial. The baseline components of VFA, buffer, and feed solutions were present in all reactors (Table 6.3).

Table 6.3 Components of each type of bioreactors prepared.

Sample	Biomass	TCP	nZVI Control	ZVI-Osorb
A	X	X		
B	X	X	X	
C	X	X		X
D	X		X	
E	X			X
F		X	X	
G		X		X
H		X		
I	X			

The duration of the experiment was 14 days after which a majority of biomass was expected to die off from lack of additional feed and nutrient solutions. Sampling periods were scheduled on days 0, 5, and 14. A second trial excluding additional controls H and I was also prepared and is described in Appendix 1 (pH Fig. A1.4, COD Fig. A1.5, Head Pressure Fig. A1.6). A collaborative study utilising identical control bioreactor setup focusing on biogas production was utilised throughout this chapter to cross-reference results and increase the robustness of the obtained data[198].

6.2.2 Quantitative Water Quality Parameters

Five quantitative water quality parameters (pH, ORP, COD, head pressure, TCP concentration) were evaluated to determine the effect of nZVI-Osorb and nZVI on TCP doped model anaerobic reactors. Previous chapters of this thesis have established that nZVI-Osorb can remove TCP from solution through sorptive mechanisms and pH strongly affects this process through altering contaminant and solubility properties. No degradation of TCP was observed by nZVI reductive mechanisms, yet anaerobic conditions are thought to boost favourable iron-oxide formation and increase iron's longevity in use (ref: Fig. 3.13, 3.14).

Effect of pH on model systems

Anaerobic bacteria are sensitive to pH changes within operating reactors and require a stable environment to maintain optimal methanogenic production[299]. Most anaerobic digestion reactors operate at a pH range of 6.8 to 7.2[335]. In one study, low pH environments (5.5) in a model anaerobic digester increased overall chemical oxygen demand through higher production levels of soluble phosphorus and volatile fatty acids. The test reactor reduced total methane production by 50% through shifting biological processes to favour acidogenic behaviour and reduce organic particulate digestion[299]. Given the importance of pH in a healthy anaerobic digester processes, initial biological reactors were buffered to near neutral pH (7.2), and pH was monitored over the course of the 14-day trial with measurements taken at days 1, 5, 10, and 14 (Fig. 6.3).

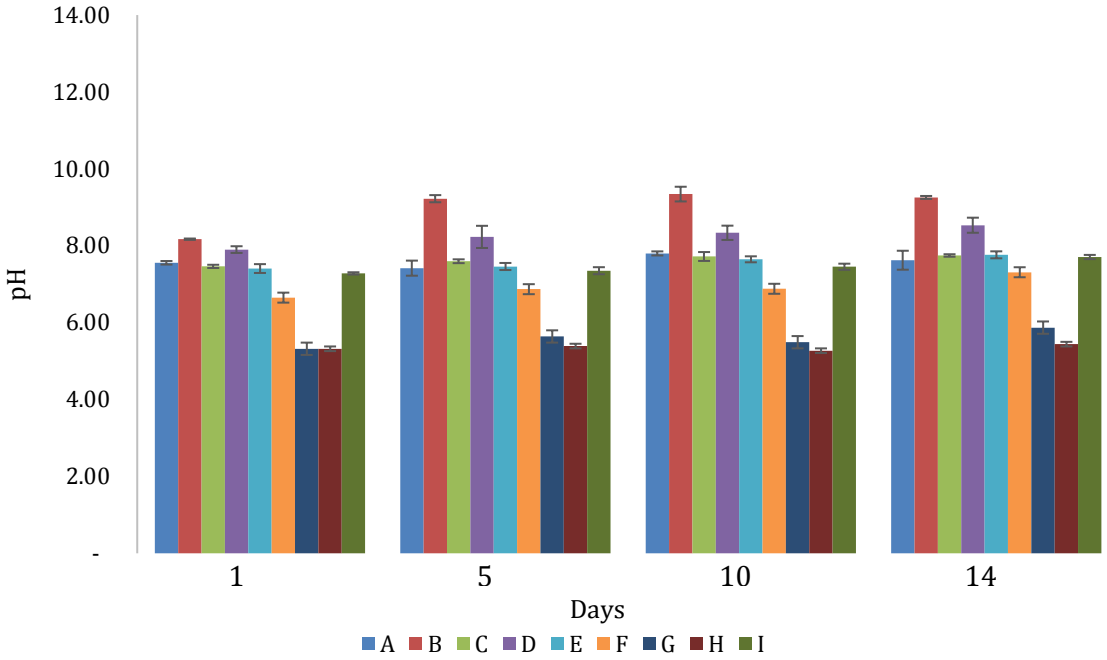

Figure 6.3 pH in the reactor as measured on days 1, 5, 10, and 14.

Four reactors, B, F, G, and C, experienced a rise in pH over the course of the trial with the remaining reactors maintaining a stable pH over the course of the trial. Reactors B and F both contained nZVI-control material and TCP, and had a pH increases of 1.086 and 0.66 respectively. Reactor G contained nZVI-Osorb and TCP, and went from a starting pH of 5.32 to 5.87, a net change of 0.55. A smaller rise (0.284) in pH was observed in reactor C (pH 7.463 to pH 7.746) which contained biomass, TCP, and nZVI-Osorb. The rise in pH with nZVI-based materials has also been observed with test materials in other studies in the literature[198].

A rise in pH was also observed in trials indicated in Fig. 5.4 and was attributed to nZVI's consumption of free protons within the water through either interaction with TCP and/or oxidative mechanisms with water producing iron-oxides. Slightly smaller pH shifts in nZVI-Osorb over nZVI control samples could be due to higher concentrations of iron per unit mass of material or possibly from lower percentages of Fe^0 as observed in Fig. 3.12.

The starting value of pH observed in reactor B (8.17) is higher than the optimal range for anaerobic digesters in operation yet could be buffered to a more suitable range

in application. Small increases in pH from nZVI interactions could be beneficial in application as they can counter small reductions in pH that occur naturally from acetogen activity[83, 198]. Furthermore, the additional monitoring biological reactivity (oxidation-reduction potential) in the system can aid understanding of system efficiency and determine which types of adjustments should be made to pH to optimise methanogenic activity[336].

Oxidation-Reduction Potential

Anaerobic digestion relies strongly on the biological reduction of complex organics to produce digested products like methane. Monitoring the electron transfer or oxidation-reduction potential (ORP) in these breakdown mechanisms gives a reliable indicator of the overall level of molecular reactivity and efficiency in these systems. Anaerobic bacteria are sensitive to electrolyte imbalances in anaerobic reactors which can upset overall methanogenesis processes if imbalances become too high[336].

The presence of oxygen typically increases overall ORP while reducing agents like nZVI typically reduce ORP values. ORP values are usually between -175 to -400mV for methane production in anaerobic digestion systems. Adjusting oxidants (oxygen) and reductants (nZVI) in a system in accordance with ORP can restore anaerobic digestion activity to optimal ranges to produce high methane yields[32]. For example, elevated levels of hydrogen sulphide (H_2S) inhibit methanogenic activity by promoting sulphate-reducing bacteria which are competitive with methanogens for organic feedstocks[337]. In one study, micro-oxygen injections decreased H_2S concentrations over six days from 6000 mg/L to 30 mg/L with a corresponding change in ORP from -485mV to -320 to -270mV. All other parameters (pH, volatile solids (VS), and chemical oxygen demand (COD)) remained stable[336]. ORP was monitored for anaerobic digesters within this trial over the 14-day test period to determine if any changes in anaerobic activity occurred as a result of iron addition (Fig. 6.4).

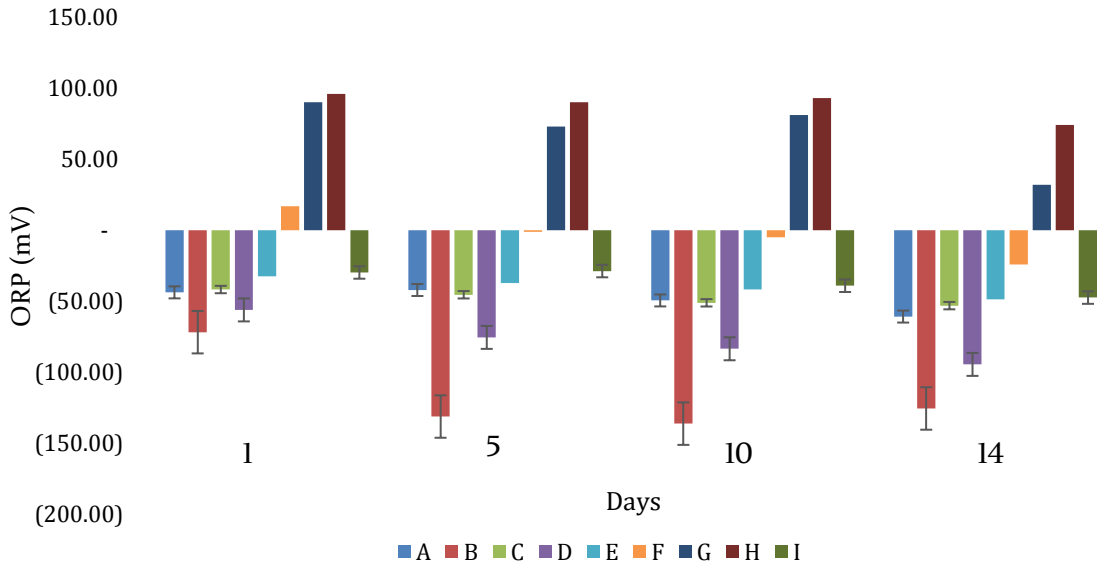

Figure 6.4 ORP values for bioreactor solution measured on days 1, 5, 10, and 14.

As expected, all reactors containing biomass (A-E, I) had a negative ORP value ranging from -50mV to -150mV in potential suggesting reducing behaviour. Reactor F containing TCP and nZVI control started with a positive ORP but became negative over the course of the experiment. This behaviour would suggest that nZVI is gaining electrons and becomes reduced either through interactions with TCP or oxygen in the system. Similarly controls G and H also lose potential over the course of the experiment further suggesting reducing behaviour.

It was expected that nZVI would decrease overall ORP of the anaerobic digester through increased reducing potential and indeed reducing behaviour was most influential in reactor B which contained biomass, TCP, and nZVI control and showed a 2.66 fold increase (-47.3 to -125.3) in ORP over biomass controls (I). Reducing behaviour was not as strong with nZVI-Osorb (1.12x, -47.3 to -53.0) as with nZVI control. These results would suggest that a majority of the iron in nZVI-Osorb may have been oxidised prior to treatment. Examinations of 1-pot nZVI-Osorb in Chapter 3 (Table 3.7) via Mössbauer analysis did find a majority of the material had become iron-oxide yet species analysis (Table 3.8) suggested that these iron-oxides would still be conducive to reducing

behaviour[306]. Future trials in anaerobic digesters should make use of oxygen-free nZVI-Osorb to ensure maximum reduction capacity in the system.

The addition of nZVI into the anaerobic digestion system increased overall reduction capacity boosting overall system reactivity. This reduction in ORP is not beyond levels where reduction capacity could become problematic (< -400mV) and could be a useful tool in adjusting system reactivity to ensure optimal methane production.

Unlike ORP results reported in literature utilising an identical reactor design[198], ORP values for nZVI containing reactors (B, C) did not converge or increase over time suggesting that neither iron reactivity was retained over the 14-day trial or that any loss in reactivity occurred prior the first day of sampling. Results described in chapter 4 concerning observed iron oxide formation under atmospheric aerobic conditions (Table 3.7, Fig. 3.12) found that, once all surface iron particles had formed oxide structures, the remaining core Fe^0 concentrations remained stable (>50 days) which could account for the stabilisation of ORP values in test reactors containing iron. While it was expected that anaerobic conditions would also reduce iron oxide formation rates, the addition of a multitude of organics and particulates into solution complicated interactions and could have reduced iron effectiveness in the degradation processes. Further examination of secondary parameters such as chemical oxidative demand and biogas production could help clarify iron's effects in interactions with these anaerobic digestion reactors.

Chemical Oxygen Demand

Like ORP, chemical oxygen demand (COD) is a useful measurement in anaerobic digesters. COD monitors the total oxidizable organics available for microbes to digest in a system and is also used as a factor in assessing water quality in wastewater systems. As microbes degrade and metabolise organics in the feed solutions total COD is expected to decrease[198]. Low COD values are valued in wastewater treatment where dilute domestic wastewaters can range from 300-500 mg/L, and water purification is the goal. However, in systems where biogas recovery is the primary objective, high COD values (1,000 to 25,000 mg/L) are desirable both to give microorganisms sufficient feedstock and to enable sufficient methane recovery from water in some up-flow system designs[38]. The desired

range of COD input to the system will vary depending on the design of the anaerobic reactor along with concurrent factors such as the biodegradability of the effluent, nitrogen to carbon ratio, and system flow[37].

To monitor the degradation of organics by microbial communities in the reactors and verify phenomena observed with pH and ORP, a third measurement, COD, was recorded in the reactor trial (Fig. 6.5).

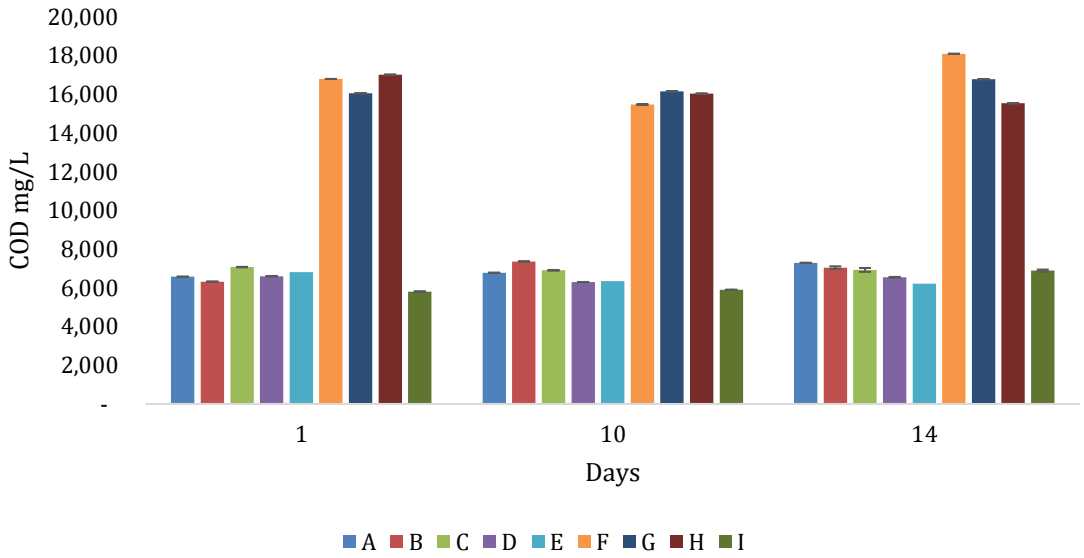

Figure 6.5 COD values (mg/L) of the bioreactor solutions recorded at day 1, 10, and 14.

COD values were highest in solutions that did not contain biomass (F-H) with COD values ranging from 15,480 to 17,020 mg/L. Reactors containing biomass reduced this organic level by approximately 10,000 mg/L by day 1. Further significant reductions in COD were not found in the following days of testing. Reactor E, containing biomass and nZVI-Osorb had the most substantial reduction in COD (6,820 to 6,220 mg/L) followed by reactor C containing biomass, TCP, nZVI-Osorb (7,073 to 6,927 mg/L) and D containing biomass and nZVI-control (6,820 to 6,547 mg/L) which showed a gradual reduction in COD over time.

The COD of the biomass control increased over the course of the experiment (5,807 mg/L to 6,893 mg/L) suggesting that the microbial communities may have failed near the

end of the experiment (day 14) without the addition of further feedstocks. Some variability in COD measurements were expected due to sorption of organics onto nZVI and other solid particulates within the reactors[37, 38].

Addition of nZVI-Osorb or nZVI-control did not appear to significantly enhance COD reduction in solution after the initial reduction observed in Day 1 trials. This contradicted results in the literature which found continual reductions in COD with the addition of nZVI[98, 198, 293]. COD measurements obtained in a preliminary trial (Appendix 1, Fig. A1.5) did show a more significant reduction in COD values from Day 0 to Day 5 of testing particularly with biomass doped with nZVI-Osorb, and further testing would be required to help clarify stated interactions.

pH and ORP data supported the activity of nZVI (increasing pH, decreasing day 1 ORP values) in the test solution yet it is possible that the iron present had become significantly diminished from the iron-oxide formation or through sequestration by particulates[37]. These limitations could have reduced nZVI reactivity by preventing the bolstering of organic degradation both independently and cooperatively with microorganisms in the reactors. This conclusion is supported by trials in Ch.3 which showed high levels of iron-oxide formation in 1-pot and multi-addition composites and in Ch. 4 and Ch. 5 which failed to observe TCP degradation with nZVI-Osorb or iron controls under a variety of conditions including anaerobic environments, secondary organics (VFA), and variable pH conditions with oxygen-free nZVI-Osorb. Further evaluation of biogas production could help illuminate the biological effect of nZVI-Osorb within these reactors on methanogenic activity.

Biogas Production

Biogas production is the primary concern of anaerobic digesters, and high methane yields ensure that the total systems are operating efficiently. Recent studies have found that the addition of nZVI into anaerobic digester systems in pre-treatment procedures donate electrons that decrease ORP and increase methane yields in biogas production[250, 255, 256, 309, 312, 313, 332, 334, 338-347]. Another study utilising the same bioreactor setup as the present thesis found that the addition of 2.5 g/L nZVI produced 182 mL of methane, a 28.3%

increase in methane production, over control reactors which did not contain iron. Carbon dioxide was also significantly reduced (57%) in the bioreactors from redox interactions with nNZVI producing iron carbonate and hydrogen gas (**6.1**)[198].

$$Fe^{o} + CO_2 + H_2O \longrightarrow FeCO_3 + H_2 \qquad \textbf{(6.1)}$$

Improvements in methane production and carbon dioxide reduction were not observed when bulk iron (ZVI) was utilised in reactors, supporting the need for nano-sized particles for higher reactivity in anaerobic digester systems[198]. In this study, biogas composition was not directly monitored as the focus was on TCP degradation and contaminant interaction; however, reactor head pressure was monitored for every reactor and indicated total biogas produced (Fig 6.6).

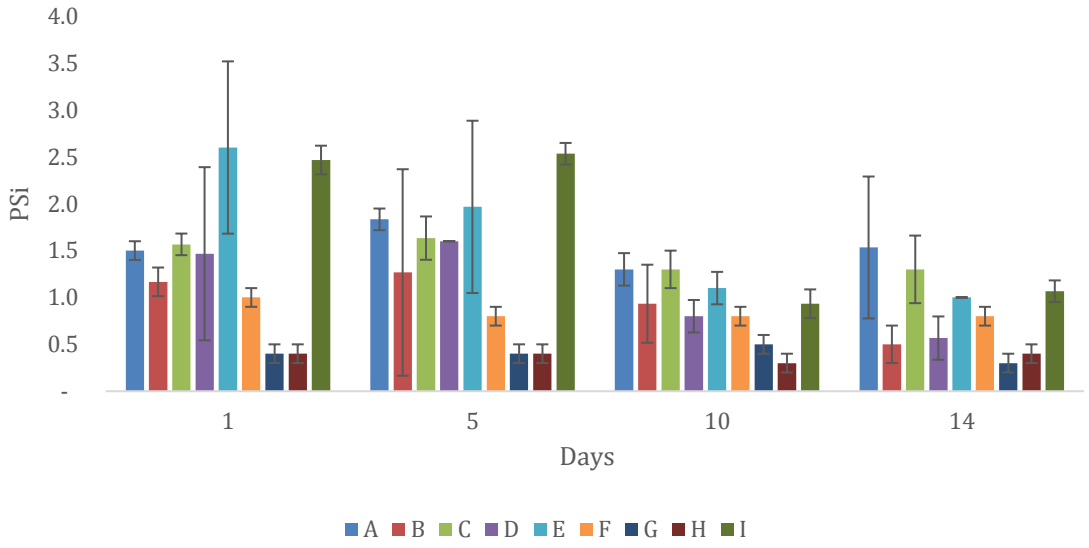

Figure 6.6 Recorded head pressure within each of bioreactors at day 1, 5, 10, and 14.

Results indicated significant variability in head pressure (0.4 to 2.7 psi) of the individual reactors, which was most likely due to variations in microbial activity. Such variability makes it difficult to reach definitive conclusions; however, the overall pressure showed a general downward trend. This result ran contrary to results from a preliminary trial detailed in Fig. A1.6 of Appendix 1 which found an overall increase from day 0 to day

5 in head pressure. The downward trend expressed here would support conclusions from the COD tests that biomass health may be failing near the end of the trial due to lack of additional feedstocks. Further studies examining TCP concentration in the reactors could help elicit reactor interactions with added iron concentrations.

The Concentration of TCP in Test Reactors

TCP has been found to inhibit methanogenic processes through acidification and biological destabilisation in anaerobic digesters[326]. As discussed in Ch. 1, nZVI can degrade chlorophenol compounds[82, 251, 348] and has been shown to booster methane production[343, 344]. Most published studies treat TCP and nZVI interactions in AD systems as independent variables, given the complexity of the system and difficulty of organic analysis. However, one study utilising amino functionalized nZVI-SiO_2 nanomaterials in an anaerobic sludge digester uniquely focused on both factors and found a 94.6% reduction of TCP under neutral conditions, with a concurrent increase in methane production. The composite nanomaterial in these reactors was found to promote anaerobic biodechlorination of TCP through reduced system toxicity and enhanced electron transport system activity[179].

To observe if nZVI and nZVI-Osorb boosted TCP degradation, TCP and potential breakdown products were monitored in the model anaerobic biodigester systems at day 0, 5, and 14 (TCP, Table 6.4, DCP, Table 6.5 and CP, Table 6.6).

Table 6.4 Concentration of TCP (µg/mL) from aliquots at days 0, 5, and 14.

Sample	Day 0	±	Day 5	±	Day 14	±
A	2.32	0.47	2.16	0.40	1.51	0.06
B	1.85	0.21	2.91	0.18	2.07	0.16
C	1.6	0.49	1.00	0.34	1.59	0.03
D	0.02	0.02	0.03	0.05	0.00	n/a
E	0.00	n/a	0.03	0.03	0.00	n/a
F	1.31	0.02	2.07	0.03	2.03	0.13
G	0.72	0.05	1.35	0.06	0.78	0.15
H	1.88	0.08	1.58	0.08	0.41	0.05
I	0.01	0.004	0.01	0.02	0.00	n/a

Table 6.5 DCP (μg/mL) concentrations at days 0, 5, and 14.

Sample	Day 0	±	Day 5	±	Day 14	±
A	0.002	0.004	0.037	0.01	0.221	0.02
B	0.004	0.003	0.010	0.002	0.013	0.002
C	0.004	0.007	0.005	0.004	0.030	0.009
D	N.D.		N.D.		N.D.	
E	N.D.		N.D.		N.D.	
F	N.D.		N.D.		0.007	n/a
G	N.D.		N.D.		N.D.	
H	N.D.		N.D.		N.D.	
I	N.D.		N.D.		N.D.	

Table 6.6 CP concentrations μg/mL at days 0, 5, and 14.

Sample	Day 0	±	Day 5	±	Day 14	±
A	N.D.		0.001	0.001	0.030	0.030
B	0.011	0.013	0.001	0.001	N.D.	
C	N.D.		N.D.		0.043	0.025
D	N.D.		0.001	0.002	N.D.	
E	N.D.		N.D.		N.D.	
F	N.D.		N.D.		N.D.	
G	N.D.		N.D.		N.D.	
H	0.017	n/a	N.D.		N.D.	
I	N.D.		0.001	0.001	N.D.	

Results from LC/MS/MS analysis found deficient concentrations of TCP in test waters (Table 6.4) with a majority of the 25mg/L of TCP not recovered in analysis despite extensive acid extraction and sample processing. This result would suggest that TCP concentrations in reactors underwent extensive biodegradation upon contact or more likely that the vast majority of TCP in reactors was immobilised by solids in the biomass and various organics in the feed solution in the test reactors and therefore was not recoverable from liquid aliquots removed for mass spectroscopy. Other studies in the literature have indicated TCP in surface water will partition to soils and can accumulate in fatty tissues of organisms, supporting the conclusions of low TCP recovery from solid partitioning and immobilisation [46, 68]. One study of the fate of contaminants in anaerobic digesters found high variability in biodegradability and transport mechanisms with reactor characteristics such as temperature, sludge properties, an adaptation of biomass, and the

bioavailability of the compounds all influencing transport and fate dynamics[329]. It is recommended that future analysis work involving TCP in complex organic systems should process an aliquot of solids and sludge to increase contaminant recovery. The overall low TCP concentrations in control reactors that did not contain biomass would further suggest that additional modifications to sample preparation, extraction, and analysis may additionally be required if full recovery cannot be achieved through sludge processing and analysis alone.

Despite the low TCP recovery, there are still some exciting features to the data set that indicated for the first time the presence of breakdown products DCP and CP in test solutions (Table 6.5 and Table 6.6). These breakdown products are most likely the results of biodegradation as DCP concentrations in reactors A-C increase over the course of the trial (Table 6.5) and DCP was not detected in control reactors that did not contain TCP and biomass. Some biodegradation of TCP was expected as numerous field and experimental trials have found biologically driven degradation (Sec. 1.2) and these organisms were not present in solutions tested in earlier chapters of this thesis where TCP degradation was not observed.

nZVI or nZVI-Osorb's direct effect on TCP degradation in these bioreactors could not be elucidated given the low recovery of TCP and variability of recorded concentration. A controlled anaerobic trial containing 25 mg/L TCP, VFA (240 mg/L acetic acid, 120 mg/L propionic acid, butyric acid), and 3.9 g/L nZVI or nZVI-Osorb at a neutral pH (7.1) was conducted to clarify nZVI and nZVI-Osorb's interactions in solution independent of biomass activity (Fig. 6.7).

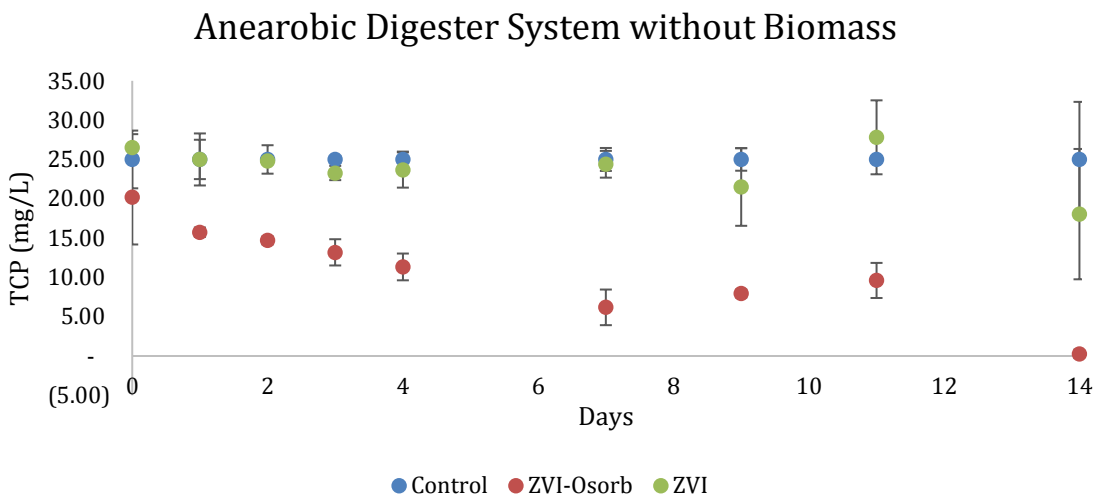

Figure 6.7 TCP concentrations of 7 mL samples extracted from the mini-reactors at days 0, 1, 2, 3, 4, 7, 9, 11, and 14. The starting TCP concentration in the reactors was 25 mg/L.

In this trial, TCP concentration is reduced over time by nZVI-Osorb through sorptive mechanisms promoted by the nanosorbent Osorb, and no breakdown products were detected in solution similar to previous trials with the materials discussed in this thesis. TCP concentrations with nZVI samples were slightly below control values indicating that some sorption onto iron or iron oxides may have occurred. In a broader context, these results suggest that nZVI-Osorb should still reduce TCP concentrations through sorption in neutral anaerobic waters containing high concentrations of VFA. Provided that biomass does not prevent contact of nZVI-Osorb and TCP it is expected that similar reduction in TCP concentration should occur. The potential reduction in TCP concentration in solution could reduce overall toxicity in the system which coupled with nZVI effects on pH and ORP could potentially improve methanogenic activity and produce results similar to those observed with amino-functionalized nZVI-SiO_2 in the literature[179].

6.3 Summary

Anaerobic bioreactors are complex environments enabling both biological and chemical interactions to produce valuable biogas. Previous research reported in the literature has supported the benefits of adding nZVI to anaerobic digestion systems to aid methane production[312, 346, 347] but few studies have observed the effect on inhibitory contaminants, like TCP, from addition of nZVI[85, 179]. Through examination of water quality measurements and contaminant monitoring a better model of nZVI-Osorb's interactions in anaerobic digesters systems could be elucidated.

nZVI is an electron donor and its addition to a complex slurry was expected to have a direct effect on pH and ORP values. Addition of nZVI-Osorb and nZVI raised the pH of the overall reactor (0.248-1.0) and decreased ORP through proton consumption as expected. Small increases in pH could be beneficial in system operations if they counteract small reductions in pH from organic degradation in methanogenesis processes. However, significant fluctuations in pH are undesirable, and iron addition could be reduced if such fluctuations become apparent in the system[299]. Similarly, iron concentrations could be adjusted to tailor ORP reduction to optimal methanogenic levels.

COD levels remained stable throughout the trial suggesting that microbial health may have failed over the course of the experiment without the introduction of additional feedstocks. It should be noted that other studies have supported nZVI reducing overall COD levels over time leading to improved microbial health from reduced environmental toxicity[105, 198] this study found no such effects on COD most likely due to issues in the quantity of feedstock applied to the initial reactors.

As discussed, a number of studies support improved biogas production and microbial health as a result of nZVI addition; however, results directly monitoring biogas production and TCP concentrations in the reactors were inconclusive. Some breakdown products of TCP were observed in test samples over the course of the trial as a result of biodegradation, yet additional studies monitoring gas composition and concentration as well as sludge and solid processing for TCP quantification would be required for a clearer understanding of these effects on anaerobic digester systems.

Oxidation of the iron appears to play an active role in dictating quantitative effects on pH, ORP, and COD values as nZVI control samples often produced stronger variations from the control than nZVI-Osorb samples. New anaerobic processing methods for nZVI-Osorb should be adopted for subsequent trials with anaerobic digesters to preserve Fe^0 content and overall reactivity in electron transfer. Additional modifications could also include the addition of secondary metals to bolster total reactivity, provided the bimetal is not toxic to microbial life.

Overall, nZVI and nZVI-Osorb demonstrated promise as an anaerobic digester additive, boosting electron activity to increase pH and decrease ORP. Inconclusive data from TCP concentrations in reactors made it impossible to judge whether Osorb boosted reactor activity and methanogenesis through sorptive sequestration mechanisms in the reactor. nZVI control reactors appeared to have higher electron activity than nZVI-Osorb in reactors most likely due to oxidation of nZVI in the composite material. Additional modification and studies would be required to improve nZVI-Osorb's degradation of target contaminants, like TCP, and synthesis methods should be tailored to reduce unfavourable oxidation and increase total reactivity before nZVI-Osorb can be considered advantageous over unamended nZVI nanomaterials for these AD systems. However, despite these shortfalls, AD remains the application with the highest potential benefit for nZVI-Osorb deployment, and additional work should be pursued.

Chapter 7 : Conclusions

2,4,6-trichlorophenol (TCP) is a toxic water contaminant that has been found in a wide variety of waste and water systems and has shown resistance to standard water and waste treatment procedures. The development of new treatment materials that can amend or enhance existing treatment structures should be developed for improved contaminant removal. One material, in particular, zero-valent iron (nZVI) has signalled high success in the removal and degradation of a wide assortment of inorganic and organic water contaminants including chlorophenols. Broader use of nZVI outside groundwater remediation where contamination is localised in low oxygen environments has remained limited due to corrosion, particle distribution, and confinement issues in deployment.

This thesis, therefore, examined the development, functionality, and potential application of new organically modified nZVI based materials (nZVI-Osorb) with the primary objectives of:

- ***Development*:** the synthesis of nZVI nanocomposite materials with an understanding of the material's intrinsic physical properties and optimal embedment method through advanced characterisation techniques and oxidation studies.
- ***Functionality*:** the evaluation of the nanocomposite's capacity to absorb and degrade a model contaminant, TCP, providing a further understanding of how environmental water quality parameters will affect these sorption and degradation processes.
- ***Application*:** the utilisation of knowledge gained in the present work to determine the most suitable application for the developed materials and hence implementation of their usage in a model system.

Development of nanomaterials in Chapter 3 resulted in nZVI-Osorb composite materials prepared by three different embedment procedures (1-pot, multiple additions, oxygen-free). While 1-pot embedment provided the most substantial control over final iron

composition, the oxygen-free method allowed the most reliable preservation of initial $nZVI^0$ concentrations through restricted oxidation. All embedment methods resulted in tightly bound nZVI-Osorb composites featuring high surface areas (340.2-449.1 sq. m/g) with net iron composition ranging from 10% to 29.78% by mass, and no observed particle loss after processing. Electron imaging microscopy verified even dispersion of iron throughout the substrate as desired. Composite materials containing secondary metal catalysts, nickel and copper, were also prepared for higher reactivity yields in application but their usage was discontinued because embedment of these secondary metals was found to be weak (0.02% Cu, 0.00% Ni) with high yields of iron oxidation (>86%). Oxygen-free nZVI-Osorb composites were utilised instead of bimetal complexes in all following experimentation.

Mössbauer analysis revealed that nZVI-Osorb composite materials did not exhibit a delayed rate of atmospheric corrosion over nZVI controls evincing an 18% $nZVI^0$ loss per day until a stabilised concentration (7%) was reached after 48 hrs. This higher rate of corrosion was linked to increased dispersion of nZVI particles within the composite material which enabled higher surface exposure and subsequent oxidation to occur. Interestingly, modification of nZVI particles also directed the formation of more favourable iron oxide species, maghemite and magnetite, which remain conducive to electron transfer mechanisms from unoxidized Fe^0 core atoms. After 50 days of atmospheric exposure, the majority of nZVI in nZVI-Osorb oxidised to maghemite (30%) and magnetite (26%) unlike the control nZVI which produced 19% and 12% respectively. Unreactive hematite accounted for 47% of the control and just 36% of the composite. Shifts in oxide formation were attributed to solution acidity in nZVI particle formation from iron salts and silica-based interactions from the nanosorbent Osorb.

Parameters related to sorption and degradation mechanisms of TCP by nZVI-Osorb were tested under aerobic conditions to elucidate the functionality of the material. nZVI-Osorb materials demonstrated high extraction capacity for TCP from aqueous solutions (Qe = 1286.4 ±13.5 mg TCP/g Osorb, Qe = 1253 ±106.7 mg TCP/g nZVI-Osorb, pH 5.1, 120 mg/L TCP) which followed pseudo 2^{nd} order kinetics. High sorptive capacity was attributed directly to the sorptive features of the nanosorbent Osorb within the composites. In the broader class of chlorophenols, nZVI-Osorb's sorptive affinity mirrored partitioning values

of the various chlorophenols. As expected, highly substituted chlorophenols such as TCP were absorbed at higher capacities then less substituted chlorophenols like 2-chlorophenol. Degradation of TCP by nZVI-Osorb or nZVI controls was not observed in experimentation due to corrosive hindrance and inadequate reductive capacity to overcome reactivity loss due to corrosion. Lack of degradation of TCP in aerobic environments suggested that the produced materials did not appear to shield nZVI from corrosion and may not be suitable for recalcitrant contaminants that show resistance to nZVI degradation in highly aerated surface and potable water treatment systems where a high rate of iron corrosion is expected.

Environmental conditions pertinent to sorption and degradation mechanisms were evaluated to broaden understanding and robustness of functionality in low-oxygen applications, such as wastewater and anaerobic digesters, where nZVI-Osorb treatment is anticipated to be advantageous to TCP treatment and methane production. pH was found to influence sorption dramatically. Acidic solutions below 5 exhibited sorption > 90%. This capacity was reduced to < 30% when pH was raised above TCP pK_a value (6.23) to 7 and above. Further trials found a positive effect on TCP sorption (+7.55%) linked to net pH reduction (5.1 to 3.3) with the addition of secondary acids (volatile fatty acids: acetic, propionic, butyric, 3x 100 mg/L) which were not absorbed by nZVI-Osorb but are commonly found in anaerobic digester systems. Diminished capacity for TCP at neutral pH because of acid-related deprotonation could be problematic for TCP treatment in systems like AD that primarily operate close to pH 7. However, sorptive capacity should not diminish for related contaminants that lack acidic properties such as alkyl halides and an increase in net material input could counteract any capacity reductions.

Contaminated marine environments, desalination processes, and off-shore-produced water treatment applications were deemed inappropriate for iron-based remediation given an accelerated rate of ion assisted metal corrosion. Sorptive mechanisms, conversely, are still beneficial in these applications and studies with nZVI-Osorb found that salinity did not affect the sorptive uptake of TCP from a wide range of saline solutions.

Given the previous results, anaerobic and low-oxygen applications, e.g. groundwater, wastewater, and anaerobic digester systems were deemed the most

appropriate applications for usage. The removal of dissolved and atmospheric oxygen increased total sorption (40 mg/L-1.94%, 100 mg/L-7.93%, 200 mg/L-0.89%, 400 mg/L-14.59%) through reduced iron corrosion and the production of favourable iron oxides, but was not sufficient to overcome corrosion and facilitate contaminant degradation. The addition of secondary metals to boost total reductive potentials could address this issue, but unfortunately the bimetallic materials produced in the research presented in this thesis demonstrated critically poor embedment and could not be utilised.

Alternatively, biodegradation mechanisms for TCP have broadly been established, and new research has supported the improved cometabolic degradation of recalcitrant contaminants like TCP and PCP in nZVI-dosed anaerobic digesters. Such nZVI based AD amendments have also been linked to a slew of positive systemic outcomes such as reduced contaminant toxicity, increased electron transport system activity, a decrease in intracellular and extracellular polysaccharides, and increased microbial diversity all resulting in an overall reduction in carbon dioxide and a significant increase in methane output. Model anaerobic digester systems (3.9 g/L nZVI-Osorb, 25mg/L TCP, 240 mg/L acetic, 120mg/L propionic, 120mg/L butyric acid) containing bioreactor sludge (62.5%) were observed through standard water quality diagnostics (pH, ORP, COD, head pressure) for 14 days and results suggested that nZVI-Osorb did not inhibit cellular processes. Increased electron activity from iron corrosion and hydrogen gas production, increased overall pH and decreased total ORP in these AD systems. TCP degradation by-products (DCP, CP) were detected in dilute concentrations (<0.01 mg/L) with poor recovery by LC-MS/MS linked to contaminant partitioning from solution in the reactors. These results strongly suggest that nZVI-Osorb is well suited as an additive for AD systems and further work should be pursued.

This study contributes to knowledge of the properties, functionality, and treatment mechanisms of metal-sorbent composites with a model chlorinated aromatic water contaminant in aerobic and anaerobic environments. The work identifies favourable environmental and process conditions to apply these materials in larger scale applications, particularly, anaerobic digestion. Lack of contaminant degradation support that need for bimetal addition in Osorb composites to treat aromatic contaminants to overcome

significant oxidative surface passivation and provides support for the continued refinement and improvement of nZVI based remediation systems to overcome treatment challenges.

Chapter 8 : Further Research

Early characterisation indicated the formation of tightly bound nZVI-Osorb composite materials with evenly dispersed iron nanoparticles. The synthesis of bimetal complexes such as Ni-nZVI-Osorb and Cu-nZVI-Osorb were mostly unsuccessful, with little to no secondary metal embedded in the final materials. Future work could focus on additional modifications to the embedment procedures to improve placement of these bimetals. Drying time and minimal oxygen exposure remain critical to reduced iron corrosion and reactivity, and so modifications could include the addition of a surfactant such as sodium dodecyl sulfate (SDS) to help reduce metal loss to agglomeration, precipitation, or adherence to reaction vessels [177, 349].

nZVI-Osorb was not able to demonstrate degradation of TCP in this study. The use of Pd as a bimetal in addition to Cu and Ni could also be utilised as a bimetal if experimental costs are not prohibitive to provide even higher reductive potential increasing the likelihood of degradation[159, 289]. Critically, the use of these bimetals should also be evaluated in terms of final applications as Cu[318, 350], Ni[351], and Pd[195, 352] which have all been linked to biotoxic effects on microorganisms and may not be suitable for anaerobic digestion processes[353]. However, one study utilising Cu, Pd, Pt, Ni, Co, Ag, and Fe nanoparticles in a porous silica (SiO_2) structure found improved methanogenesis from acetate with Ni, Co, and Fe particles. The effect of Ni was the most robust in increasing methane production by 72.5% over controls[354]. Another recent study has also supported the use of Pd-nZVI composites for the degradation of chlorinated hydrocarbons in AD systems suggesting bimetal may be a viable solution for TCP degradation in use[355]. Apart from secondary metal inclusion organic modifications with amino groups (such as NH_4-nZVI-SiO_2) have also demonstrated success at improving TCP treatment in AD systems[179], and as a heavy metal (Cr (IV)) sorbent (NH_4-Fe_3O_4)[356], and could be attempted in future synthesis and study.

Evaluations in Ch. 3 found that while Osorb increased nZVI dispersion, improving particle availability and subsequent reactivity, it ultimately accelerated corrosion through the increased overall surface area and exposure to the atmosphere. Undesired corrosion of nZVI remained a central issue in the further development of nZVI in water treatment and

remediation applications. As discussed in Ch. 1, the application of surface coatings on nZVI surfaces has decreased corrosion rates however these coatings often decreased particle accessibility and reactivity[207]. Careful processing, like the oxygen-free embedment technique utilised in this work, and further usage in anaerobic or low oxygen environments are still believed to be the best solution to minimising undesired iron corrosion without compromising reactivity. It is recommended that further work focus on analysing the rate of corrosion of nZVI nanoparticles in nZVI-Osorb in aqueous environments for a better understanding of corrosion rates relative to dissolved oxygen in solution and would give an understanding of the materials' longevity in water treatment applications.

Further studies in Ch. 4 found that TCP can be absorbed in high capacities from solution. Packed-bed systems should be examined in future work to ensure that composite materials are stable and do not leach nanomaterials and that contaminant affinity is not lost under flow forces. As mentioned, modifications to nZVI-Osorb (bimetal addition, amino-functionalized) could potentially increase degradation of TCP in solution; however additional testing of nZVI-Osorb with other contaminants such as alkyl halides which show less resistance to degradation[160, 164] and related compounds like brominated aromatics (bromobenzene)[357, 358] should be evaluated and could provide clarity on nZVI-Osorb's degradation capacity in environments with various levels of expected corrosion. Previous studies have indicated that Osorb can be regenerated for continual reuse and that sorbed organics can be recovered via thermal or solvent rinsing processes [134, 135, 228]. Future work should consider regenerative and sorbate recovery consideration within applied applications and existing treatment infrastructure.

The broad scope of Ch. 5 found that environmental conditions affected both sorption and potentially degradation mechanisms in treatment. Further studies evaluating iron oxide formation and how oxide-type effects degradation pathways with these new materials should be undertaken to provide deeper understanding of how shifting environments will effect degradation and final treatment of contaminants in solution[285, 309].

Lastly, the final experimental chapter (Ch. 6) gave a brief examination of TCP treatment in a model anaerobic digestion system and suggested that the application may be well-suited for nZVI-Osorb materials. However, significant additional work would be

required to increase understanding of system interactions and effect before model applications should be piloted in the field. This future work should include the quantification and characterisation of biogas output from AD systems including rate, composition, and concentration. Additional AD monitoring parameters such as organic load rate (OLR)[359, 360], total volatile solids[361, 362], temperature[363, 364], VFA concentration and speciation[37, 288], ammonia concentration[365, 366], total alkalinity[367] should also be evaluated for a more detailed understanding of AD system health and biogas production efficiency[268, 309].

Improvements to analytical techniques utilised in the measurement of TCP post application should be improved to increase recovery yields and data confidence. Such improvements could include solid extraction/desorption with accelerated solvent extraction (ASE) techniques and further refinements to the LC-MSMS methodology[368]. These results along with concurrent evaluation of TCP's fate and transport in A.D. systems should address TCP monitoring issues in experiments and future applications[46, 60, 326].

Experiments in this thesis utilised a single sludge stream from one reactor for all experimentation. It is expected that sludge characteristics will vary greatly depending on the reactor and its unique composition of feedstock and microbial lifeforms[13, 32]. Broadening the test programme to include experiments with diverse sludge microbes from both wastewater and agricultural reactors would increase the robustness of the study and broaden its usage in AD application[86]. Furthermore, increasing trial duration and applying additional feedstock could improve models of effect and interaction in AD systems[13]. Lastly, a closer biochemical and biological examination of nZVI-Osorb's effect on microbial life should be carried out to ensure that such addition supports other results in the field that have researched the effects of nZVI based interactions[87, 369]. These AD studies could then be utilised in the design and implementation of pilot scale anaerobic digestion systems with composite materials distributed throughout the feed and performance evaluated in terms of biogas production.

Reducing water contamination and improving waste management systems remain critical missions in safeguarding natural resources and biotic life. The diversity of such systems poses real challenges to innovative technologies and their implementation, but the effort is not without reward. New nZVI based materials have great potential in water

and waste applications and a multitude of studies, including the ones discussed in this thesis, help drive innovation forward despite the complexity and challenges that remain.

Glossary

1-Pot	1-Pot Embedment
A	Anoxic
AD	Anaerobic Digestion
ASE	Accelerated Solvent Extraction
BET	Brunauer-Emmett-Teller
BTEX	Benzene, Toluene, Ethylbenzene and Xylene
CHP	Combined Heat and Power
CM	Continuous Microfiltration
COD	Chemical Oxidative Demand
CP	Chlorophenol
CTMA	Cetyltrimethylammonium
DBP	Disinfection By-Products
DCP	Dichlorophenol
DI	Deionized Water
DNAPL	Dense Non-Aqueous Phase Liquid
DO	Dissolved Oxygen
ECD	Electron Capture Detector
EDS	Energy Dispersive X-Ray Spectrometer
ESEM	Environmental Scanning Electron Microscope
ETS	Electron Transport System Activity
FID	Flame Ionization Detector
GAC	Granular Activated Carbon
GC	Gas Chromatography
HA	Haloacetaldehydes
HAAs	Haloacetic acids
HANs	Haloactonitriles
HPLC	High-Pressure Liquid Chromatography
IC	Ion Chromatography

LC/MS	Liquid Chromatography Mass Spectroscopy
LCFA	Long-Chain Fatty Acids
MA	Multiple Addition Embedment
MBR	Membrane Bioreactor
MRL	Minimal Risk Level
MSDS	Materials Safety Data Sheets
NOM	Natural Organic Matter
nZVI	nano Zero-Valent Iron
O	Oxic
O2-Free	Oxygen Free Embedment
OLR	Organic Load Rate
ORP	Oxidative Reductive Potential
PAC	Powdered Activated Carbon
PAHs	Polyaromatic Hydrocarbons
PBRs	Permeable Reactive Barriers
PCBs	Polychlorinated Biphenyls
PCP	Pentachlorophenol
PES	Polyethersulfone
pH	Potential of Hydrogen
PPCPs	Personal Care Products
PVA	Polyvinyl Alcohols
REDOX	Oxidation-Reduction Reactions
SDS	Sodium Dodecyl Sulphate
SEM	Scanning Electron Microscopy
SmiF	Shared Materials Instrumentation Facility
TCA	2,4,6-Trichloroanisole
TCNM	Trichloronitromethane
TCP	2,4,6 Trichlorophenol
TEM	Transmission Electron Microscopy
THMs	Trihalomethanes
THMs	Trihalomethanes

UASB	Up-Flow Anaerobic Sludge Blanket
UF	Ultrafiltration
UV	Ultra-Violet
VFA	Volatile Fatty Acid
VOCs	Volatile Organic Compounds
VS	Volatile Solids
WQC	Water Quality Criteria
XPS	X-Ray Photoelectron Spectrometer
ZVI	Zero-Valent Iron

List of Symbols

C_e	Concentration at Equilibrium (mg/L)
C_o	Initial Concentration (mg/L)
E_{red}^o	Standard Reductive Potential (mV)
K_a	Equilibrium Acidity Constant
k_F	Distribution Coefficient
K_L	Free Energy of Adsorption
K_{ow}	Octanol-Water Partitioning Coefficient
K_{sp}	Water Solubility (mg/L)
pK_a	Acid Dissociation
Q_e	Sorption Capacity at Equilibrium (mg/g)
Q_m	Maximum Adsorption Capacity (mg/g)
S_T	Total Solubility (mg/L)
V	Volume (L)
W	Mass (g)
γ	Activity Coefficient

List of Figures

Figure 1.1 Ministers representing 170 countries gathered to attend the 2016 signing of the Paris Agreement at UN headquarters in New York City[5]..... 2
Figure 1.2 The chemical structure of 2,4,6 trichlorophenol. 5
Figure 1.3 Lake Tai in Jiangsu province near Shanghai in China has been a useful case study in studying the effects of TCP contaminated surface waters. Surface waters have been found to contain 152.2 ng/L 2,4,6-TCA, a metabolite of TCP and familiar taste and odour compound[5]. 11
Figure 1.4 (Left) Arabidopsis thaliana known commonly as Mouse-Ear Cress and (Right) the mushroom species Clitocybe maxima[5]. 14
Figure 1.5 A simplified diagram of the standard water treatment process [79]. 16
Figure 1.6 Left: A simplified model of wastewater treatment utilising a UASB system for biogas production[79]. Right: A simplified model of a UASB reactor[5]. 17
Figure 1.7 A photo of anaerobic digesters within the Newtown Creek Wastewater Treatment Plant in Brooklyn, New York [90].....18
Figure 1.8 Osorb nanomaterial utilised in the synthesis of the novel nanomaterials generated in the present. The materials are composed of semi-opaque granular particles. 48
Figure 1.9 A series of photographs showing the swelling of Osorb at 0, 5, and 10 seconds from the dropwise addition of acetone onto the matrix in real time[136]. 49
Figure 1.10 A sorption model demonstrating the uptake of an organic compound from an aqueous solution by Osorb. (1) Organics in the water adsorb onto the surface of Osorb. (2) Initial sorption triggers the release of the tensioned silica matrix resulting in swelling, i.e. the expansion of the of the sorbent matrix, thus exposing new surface area and permitting the absorption of organics from solution. (3) Pores become filled with sorbate facilitating further transport of organics deeper into the silica matrix. (4) Additional swelling increases both void volume and available surface area allowing further sorptive processes to proceed[136].....50
Figure 2.1 The ChromQuest Trace 2000 utilised for experimentation. 72
Figure 2.2 The 883 Basic IC Plus Metrohm Ion Chromatography (IC) and 863-compact autosampler utilised for VFA analysis.....74
Figure 2.3 A photograph showing the preparation of bioreactor samples in the anaerobic chamber. ...82
Figure 3.1 Iron improperly embedded into Osorb with black indicating zero valent iron and the burnt orange indicating the formation of iron oxide. 88
Figure 3.2 An image of the three types of material produced utilising muti-addition synthesis. (1) 3.1 g nZVI-Osorb, (2) 3.2 g Ni-nZVI-Osorb, (3) 3.0 g Cu-nZVI-Osorb. The dark colour indicated that embedment was successful and prior issues with iron oxidation did not occur at comparable severity. 89
Figure 3.3 The resulting nanomaterials from 1-pot synthesis (1) 75.85g nZVI-Osorb (2) 47.86 g nZVI-Ni-Osorb, (3) 39.76 nZVI-Cu-Osorb, (4) 31.355g Osorb. The dark colour indicated that embedment was successful and prior issues with iron oxidation observed in Figure 3.1 did not occur.....91
Figure 3.4 19.21g of nZVI-Osorb produced in an oxygen-free environment. 92
Figure 3.5 TEM images of a 1-pot nZVI-Osorb at increasing levels of magnification. 93
Figure 3.6 Side-by-side comparison of iron distribution between materials synthesised by two different synthesis techniques (Multiple Addition vs 1-Pot) in nZVI-Osorb materials.....94
Figure 3.7 An image of nZVI-Osorb synthesised by Multiple Addition by SEM-EDS. Various rough patches on the surface of the material appear brighter from charging effects highlighting the roughness of the surface of the material. 95
Figure 3.8 Indication of copper bimetal (A) and copper/iron distribution (B, C) from multi-addition synthesis. 97

Figure 3.9 SEM images of a 1-pot nZVI-Osorb hybrid nanomaterial at increasing levels of magnification exposing a dense highly porous surface composed of 10nm nanoclusters. 99
Figure 3.10 Percent composition of various iron species in Oxygen-Free nZVI-Osorb (Top) and a nZVI control (Bottom) after 1 day and 50 days of air exposure. 106
Figure 3.11 The percent composition of nZVI within oxygen-free embedded nZVI-Osorb at 1.5, 4.75, 21.75, and 48 hrs. 109
Figure 4.1 A model of the proposed treatment of TCP by nZVI-Osorb. Black dots represent nZVI. White dots represent Osorb. In (1) nZVI-Osorb composites are deployed into a solution containing TCP. (2) TCP becomes absorbed by Osorb in the composite material. (3) nZVI interacts with sorbed TCP and reduces compound by reductive dehalogenation. Degradation pathways proceed from this instance as described in Ch.1. 114
Figure 4.2 A plot of the partition coefficient (log K_{ow}) versus sorption coefficient (log k) for binding of various contaminants (1,4 dioxane, acetone, 1-butanol, methyl t-butyl ether, nitrobenzene, trichlorophenol, toluene, & perchloroethylene) in water by Osorb. Contaminant concentration was 100mg/L with a 0.5% (w/v) addition of Osorb per volume of solution. A linear regression line fitting positive LogK_{ow} contaminants was determined to be log(k)= 0.97 x log(K_{ow}) +0.96, R^2=0.998. The vertical line indicates where the TCP LogK_{ow} value (3.38) falls in relation to tested contaminants[136]. 115
Figure 4.3 100mg/L TCP solution (220mL, pH 5.1) in water was continuously mixed with 550mg nZVI-Osorb (25mg per 10mL) for 24 hrs. 119
Figure 5.1 Corrosion rates of 41 sheet pile of steel (μm per annum) in three different water environments (freshwater, brackish water, seawater) over time (years)[284] 149
Figure 5.2 Sorption of TCP with nZVI-Osorb and nZVI control tested side-by-side in two different atmospheric oxygen environments (aerobic and anaerobic). Anaerobic starting aq. solutions before TCP addition were deoxygenated via autoclave. Starting pH was 5.10 for both solutions. No degradation products were observed in the analysis. 153
Figure 5.3 A speciation plot for TCP as a function of pH (25C). 158
Figure 5.4 Recorded pH values monitored over 24 hours in a continuously stirred solution for a 50 mL solution of DI water containing, (1) 125 mg of nZVI-Osorb *(ZVI-Osorb + Water, unadjusted pH),* (2) 100 mg/L TCP solution containing 125 mg of nZVI-Osorb *(ZVI-Osorb + TCP)* and (3) a solution of DI water containing 125 mg of nZVI-Osorb with the initial pH of the DI solution artificially titrated to a pH of 5.1 *(ZVI-Osorb + Water, adjusted pH)*. 160
Figure 5.5 Iron corrosion in aerated water determined by the depth of iron oxide formation from the surface per year (mm per year) as a function of pH [249]. 162
Figure 5.6 100 mg/L of acetic, propionic, or butyric acid in 100 mg/L TCP solutions were mixed with various amounts (100, 50, 25, 10, 0 mg) of nZVI-Osorb for 24 hrs. under anaerobic conditions. 167
Figure 5.7 TCP sorbed from different initial concentrations (100, 50, 25, 10 and 0 mg/L) of each organic acid (acetic, butyric, or propionic) and 100 mg/L TCP solutions were treated with 25 mg of nZVI-Osorb for 24hrs under anaerobic conditions. Total volume remained constant. Recorded pH values are listed in Table 5.7. 168
Figure 5.8 100 mg/L TCP with an organic acid mix (100 mg/L acetic, 100 mg/L butyric, and 100 mg/L propionic) adjusted to various starting pHs (3, 5, 7, 9) and then treated with 25 mg of nZVI-Osorb for 24 hrs. 169
Figure 5.9 A diagram indicating the primary iron oxide (FeO, Fe_2O_4, Fe_2O_3) or iron hydroxide (FeOOH, $Fe(OH)_2$) products formed under various aqueous environmental conditions (acidic, alkaline, aerobic, anaerobic, and various salt anions). 171
Figure 5.10 A diagram indicating positive (+), negative (-), or no effect (0) on sorption mechanism for Osorb and nZVI under a variety of environmental conditions (salinity, presence of oxygen

(aerobic, anaerobic), secondary compounds (VFAs), and pH (acidic, alkaline, neutral)) in water. 172
Figure 6.1 The energy and lifecycle use of agricultural based anaerobic digester [311]. 175
Figure 6.2 A series of bioreactor produced. The biomass appears a murky brown colour. Samples that contain iron were closer to black in colour. 181
Figure 6.3 pH in the reactor as measured on days 1, 5, 10, and 14. 183
Figure 6.4 ORP values for bioreactor solution measured on days 1, 5, 10, and 14. 185
Figure 6.5 COD values (mg/L) of the bioreactor solutions recorded at day 1, 10, and 14. 187
Figure 6.6 Recorded head pressure within each of bioreactors at day 1, 5, 10, and 14. 189
Figure 6.7 TCP concentrations of 7 mL samples extracted from the mini-reactors at days 0, 1, 2, 3, 4, 7, 9, 11, and 14. The starting TCP concentration in the reactors was 25 mg/L. 193

List of Tables

Table 1.1 General properties for phenol and various chlorophenols of interest[19]. 4
Table 1.2 Detectable TCP concentration ranges found bioaccumulated in aquatic biota, excreted in human urine, and neat in various environmental systems[31]. 7
Table 1.3 A wastewater treatment study observing the effect of various processes to treated chlorophenols[33]. 23
Table 1.4 Sorption capacities (mg/g) for a variety of sorbents for various chlorophenols [129]. 29
Table 1.5 A overview of available nanomaterials and their potential applications in water treatment [2, 143]. 32
Table 1.6 A list of the types of contaminants that can be removed or treated by ZVI [152]. 34
Table 1.7 A list of pK_a and standard reductive potential (pH=12) for various chlorophenol [167]. The standard reductive potential is a value that demonstrates the compounds propensity to be reduced under standard conditions. 37
Table 1.8 Masses of various contaminants sorbed by three different sorbents (Osorb, Activated Carbon, and Molecular Sieves) in a stationary dry bed mass (μg/mg). The elution constant C is measured at bed exit when the concentration entering the bed was at 10% and 90% wherein C_0: C/C_0=0.1 and C/C_0= 0.9 [136]. 51
Table 2.1 General properties of the utilised volatile fatty acids[19]. 68
Table 2.2 The determined limit of detection for various chlorophenols and phenol on GC-FID and GCMS. 69
Table 2.3 Concentrations of primary components in the anaerobic bioreactors. 80
Table 2.4 Total composition of each reactor & the concentration of components of interest. 81
Table 3.1 The three resulting materials produced by multi-addition synthesis. 88
Table 3.2 Three resulting materials produced by 1-pot synthesis. 90
Table 3.3 A representation of the elemental composition of the various nanomaterials resulting from Scanning Electron Microscopy enabled with Energy Dispersive X-Ray Spectroscopy (EDS). In this spectroscopy, a high-energy incident beam excites outer electrons causing numerous X-rays of various energies to be emitted. These X-rays are matched to the unique peaks of the electromagnetic emission spectrum allowing for elemental determination. Analyzing the breadth of the total emitted X-rays the software determined the percent composition of each element detected in every sample within its detection window[263]. 96
Table 3.4 The total surface area per gram (BET) values for a variety of synthesised materials. 98
Table 3.5 Particle size collected from an Occhio flow cell. All values denote diameter in mm. Min and Max values represent the minimum and maximum particles sizes detected. P25, P50, and P75 represent particles falling within the 25th, 50th, and 75th percentile of total measured particles. Mean values represent the average particle size falling within the central particle distribution (P25-P75). The average diameter and standard deviation are representative of the total 4,000-5,000 particles counted in the analysis. 101
Table 3.6 (Left) the resulting XPS peaks for various samples and (Right) Expected peak shifts for various iron compounds[269]. 103
Table 3.7 The varied species of iron as determined by Mössbauer Spectroscopy. 103
Table 3.8 Properties of various iron hydroxide species[154, 248, 253, 261, 268] 107
Table 4.1 100 mg/L TCP solutions (10 mL, pH 5.11) in water mixed with 25 mg of nZVI-Osorb for 5min, 1.5hrs, 24, 48 hrs. ±0.008hrs. Time points in the series were not continuous and were conducted individually with a universal starting solution. 119
Table 4.2 Average values of treatment of TCP over the course of the 9-day experiment (pH 5.1) shown in Fig 4.7, and results from the acid digestion of the final recovered nanomaterials. TCP concentration values were determined by GC-FID. No breakdown products of TCP

were observed in any sample in the acid digest. These findings were additionally verified by further GC/MS analysis (scan 40 m/z to 500 m/z amu) which found only TCP present in the test solution and acid digestion recovery. 126
Table 4.3 General properties (K_{sp}, $LogK_{ow}$, pK_a) of phenol and chlorophenol with varying degrees of substitution and recorded pH for 100 mg/L for each CP in DI water. 127
Table 4.4 150mg of nZVI-Osorb were mixed in a 60mL (equiv. mass/volume to previous trials), 100 mg/L solution of TCP for 24hrs. The solution was left to settle, and the liquid was removed via pipette. An aliquot (7mL) of water was extracted by hexane, and the concentration of TCP in the treated water was determined. The remaining nZVI-Osorb was covered in fresh water and rinsed with 4x 60mL for 30 mins. TCP concentration was determined for each wash. 60mL of water was then added to the remaining nanomaterial and stirred at a moderate speed for seven days. Samples were extracted at days 1, 2, 5, 7, and 9 to determine TCP concentration. 132
Table 4.5 Total TCP (mg/L) measured in sorbent & solution after diff. phases of treatment. 132
Table 4.6 Calculations tracking the % loss and % gain of TCP by nZVI-Osorb during the course of the trial. 133
Table 4.7 Comparison of 4 studies that utilised nZVI-based materials to degrade chlorophenols in aerobic aqueous conditions with positive degradation results. 136
Table 5.1 Total solubility (S_T) of 2,4,6-Trichlorophenol for various pH at 25C [25]. 145
Table 5.2 100 mg/L TCP solutions containing 5 percentages of salt water (NaCl) (0, 1, 3, 6, 20%) shaken with 25mg of nZVI-Osorb for 24hrs (pH 5.1, 10mL) under aerobic conditions. ... 148
Table 5.3 100 mg/L TCP solutions adjusted to 4 distinct starting pH values. The TCP solutions were shaken with 25 mg of nZVI-Osorb for 24 hr under aerobic conditions. 155
Table 5.4 Basic properties (structure, molecular weight, pK_a) of phenol and its chlorinated substituents. The compound's recorded pH (100 mg/L) and its relative dissociation state at that pH are also detailed. 157
Table 5.5 pH ranges for waters occurring in different systems. 159
Table 5.6 A list of physical properties including structure, dipole moment (measured in Debyes, D), solubility, and pK_a for TCP and three VFAs (acetic, propionic, butyric) at 20C[19]. 165
Table 5.7 Measured pH values for solutions containing 100 mg/L TCP at different concentrations (10, 25, 50, 100) of each organic acid as well as solutions containing an organic acid mix with 100mg/L of each of the three acids. 166
Table 6.1 Bulk composition of the model anaerobic digester reactors (200mL). 180
Table 6.2 Contaminant (TCP), nanomaterial (1-pot nZVI-Osorb, nZVI), and VFA concentrations for the model anaerobic digester reactors (200 mL). 180
Table 6.3 Components of each type of bioreactors prepared. 181
Table 6.4 Concentration of TCP (µg/mL) from aliquots at days 0, 5, and 14. 190
Table 6.5 DCP (µg/mL) concentrations at days 0, 5, and 14. 191
Table 6.6 CP concentrations µg/mL at days 0, 5, and 14. 191

Thesis Related Publications

1. Underwood, LA, Khasanov, A, Vidmar, M, Semiao, A, and Wiesner, M. Synthesis and Characterisation of nano Zero Valent Iron-Organically Mofidied Silica Nanocomposites for Advanced Iron Dispersion. Enviro. Science & Tech. *In preparation.* 2018.

2. Carpenter AW, Laughton SN, and Wiesner MR. Enhanced Biogas Production from Nanoscale Zero Valent Iron-Amended Anaerobic Bioreactors. *Environmental Engineering Science*. 2015; 32: 647-55.

3. Underwood L. Synthesis and Use of a Novel Nanomaterial for the Removal of Phenol in Water Systems. *Institute for Infrastructure & Environment*. Edinburgh: University of Edinburgh, 2013, p. 100.

4. Edmiston PL, Osborne C, Reinbold KP, Pickett DC and Underwood LA. Pilot scale testing composite swellable organosilica nanoscale zero-valent iron-Iron-Osorb®-for in situ remediations of trichloroethylene. *Remediation Journal*. 2011; 22: 105-23.

5. Edmiston PL and Underwood LA. Absorption of dissolved organic species from water using organically modified silica that swells. *Separation and Purification Technology*. 2009; 66: 532-40.

Presentations

1. Underwood, L. Novel Modified Iron Nanoparticles for Remediation of 2,4,6-Trichlorophenol. SET For Britain Poser Presentation. London, U.K. March 7th, 2016.

2. Underwood, L. Novel Iron Nanocomposites for Treatment of TCP and Use in Anaerobic Biodigesters. School of Engineering 2nd Year Poster Exposition. Edinburgh, U.K. April 22nd, 2015.

Appendix 1

For clarity and brevity, some supplemental results were not included in the main body of the text and are therefore presented here. These results support claims made in the thesis in experimental chapters 3-6, and are all referenced accordingly.

Periodic Iron Oxide Formation (50 Day Trial)

Results shown in Fig. 3.12 indicated iron oxide species formation over a 50-day trial in nZVI and nZVI-Osorb. Figures A1.1 and A1.2 give a more detailed overview of those results showing oxide species monitored periodically throughout the trial.

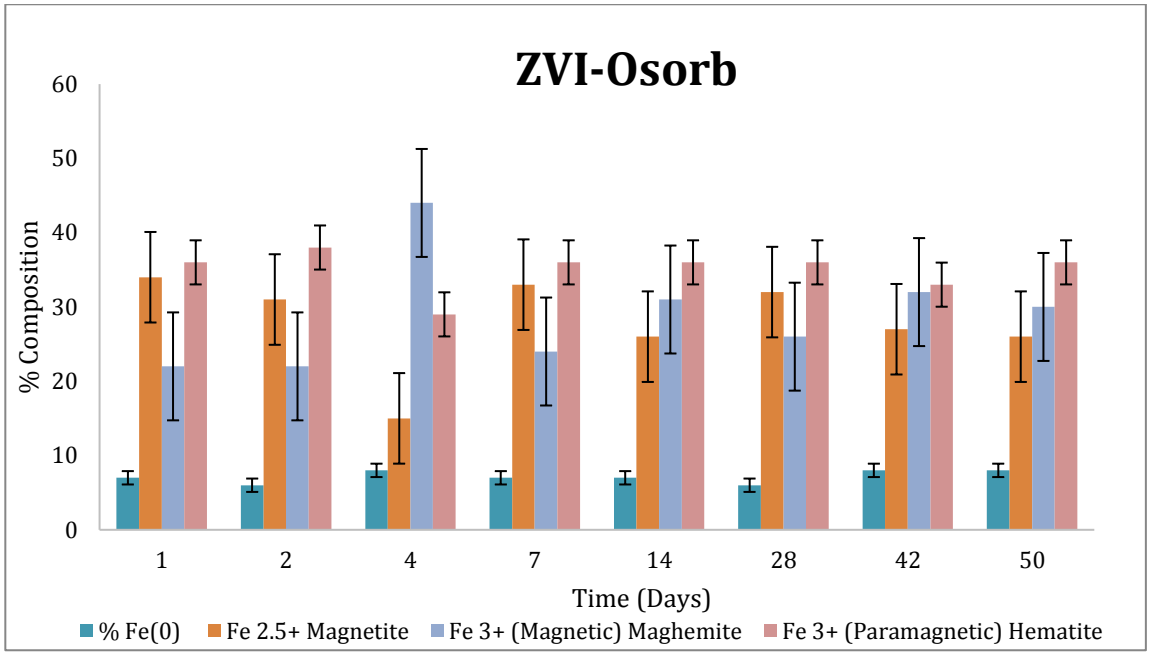

Figure A1.1 Percent composition of various iron species within the nZVI-Osorb over 50 days as determined by Mössbauer Spectroscopy.

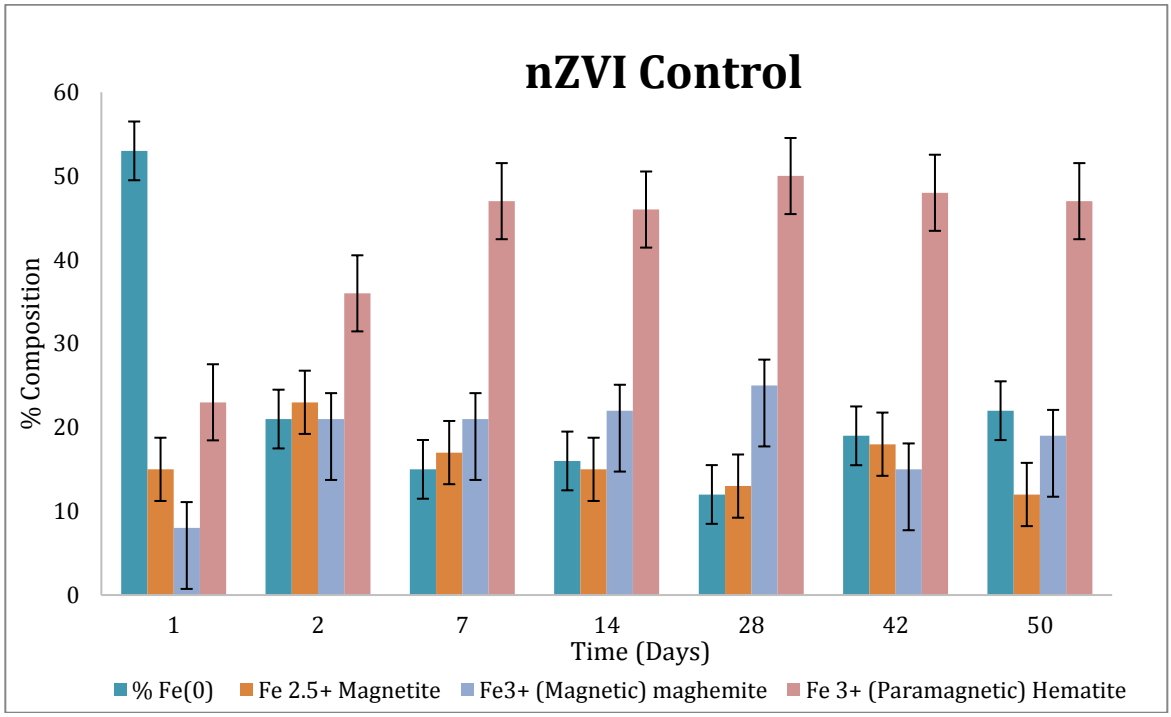

Figure A1.2 Percent composition of various iron species within the nZVI control over 50 days as determined by Mössbauer Spectroscopy.

Results suggest that oxide formation stabilises after day 10 of exposure in both nZVI-Osorb and nZVI control samples. No significant fluctuation occurred in iron-oxide species type suggesting that this species determination occurred within the first 48 hours of atmospheric exposure. Again these results support findings in Fig. 4.12 that nZVI control samples produce more paramagnetic Fe^{+3} iron oxides than nZVI-Osorb composites.

Langmuir Isotherm Modified for Better Fit

Adsorption isotherms of TCP utilising nZVI-Osorb showed a poor fit to Langmuir-fitted plots (Ref. Fig. 4.6) suggesting that sorption mechanisms do not follow monolayer deposition. The removal of the 5mg nZVI-Osorb sample set greatly improved correlation results (Fig. A1.3).

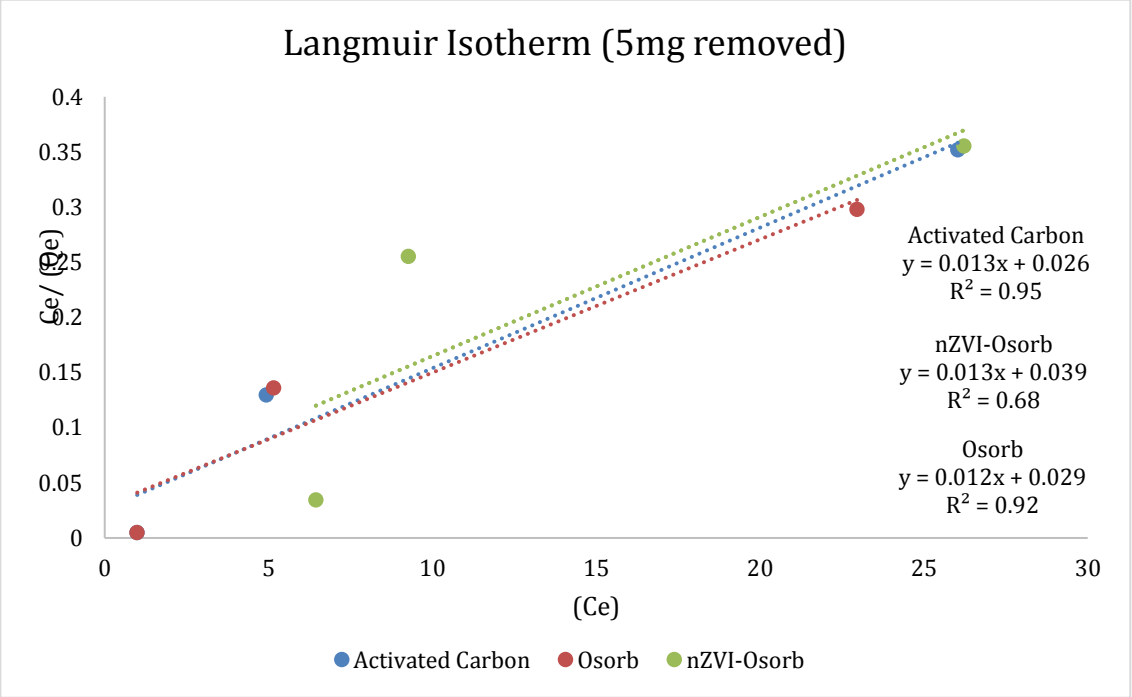

Figure A1.3 TCP sorption for three sorbents, activated carbon, Osorb, and nZVI-Osorb detailed in Fig. 4.4 in Ch. 4, but with the 5 mg data points removed for better correlation.

However nZVI-Osorb correlation plots (R^2 0.67) remain unusable for maximum sorption calculations. Although activated carbon and Osorb had correlations above 0.9 with only three data points considered, and the removal of the lower mg results, the final maximum sorption calculations would be suspect. As such, these values are not reported herein in lieu of more accurate calculations using Freundlich isotherms (Ref. Fig. 4.5) and sorption isotherms (Ref. Fig 4.4) described in Chapter 4.

Acid Recovery for Aerobic vs Anaerobic Sorption Trials

Results detailed in Fig. 6.2 in Chapter 6 showed the sorptive uptake of nZVI-Osorb and nZVI controls in environments of varying oxygen content (anaerobic vs aerobic). These results and acid recovery analysis of the sorbate are listed in Table A1.1 below.

Table A1.1 5 masses (50, 25, 10, 5, 0 mg) of nZVI-Osorb and nZVI control were tested side-by-side in two different oxygen environments (aerobic and anaerobic). The concentration of TCP was 100mg/L. All samples were run in triplicate and analysed for TCP concentration and breakdown products via GC-FID. TCP sorbed to the materials was recovered via acid digestion and analysed via GC-FID.

Anaerobic

nZVI-Osorb

Mg (nZVI-Osorb)	AVG TCP Sorbed (mg/L)	STD EV (mg/L)	% Reduction	Acid Recovery %	% Error Acid Recovery
50	95.3	2.0	95.31	Full	9.68
25	93.3	0.2	93.31	Full	13.58
10	76.7	0.7	76.75	97	6.37
5	57.2	5.5	57.16	Full	2.12
0	0.6	1.2	0.58	n/a	n/a

NZVI-CONTROL

Mg (nZVI)	AVG TCP Sorbed (mg/L)	STD EV (mg/L)	% Reduction	Acid Recovery %	% Error Acid Recovery
50	17.8	1.1	17.76	Full	1.74
25	10.4	2.1	10.41	90	2.12
10	12.0	6.9	12.00	Full	1.80
5	5.7	4.0	5.66	Full	4.09
0	-	0.6	-	n/a	n/a

Aerobic

nZVI-Osorb

Mg (nZVI-Osorb)	AVG TCP Sorbed (mg/L)	STD EV (mg/L)	% Reduction	Acid Recovery %	% Error Acid Recovery
50	93.4	2.6	93.37	Full	9.02
25	85.4	5.3	85.38	Full	5.39
10	75.9	1.6	75.86	Full	5.46
5	42.6	4.9	42.57	Full	5.96
0	-	9.8	n/a	n/a	n/a

NZVI-CONTROL

Mg (nZVI)	AVG TCP Sorbed (mg/L)	STD EV (mg/L)	% Reduction	Acid Recovery %	% Error Acid Recovery
50	18.9	0.1	18.87	Full	3.79
25	-	4.6	-	n/a	n/a
10	-	11.5	-	n/a	n/a
5	-	2.5	-	n/a	n/a
0	-	5.6	-	n/a	n/a

Results show near full recovery for all samples that had absorbed TCP except two which showed 97% and 90% recovery. Sorption of TCP remained high as reported previously in Fig. 5.2.

Preliminary Model Anaerobic Digestion Trial Excluding Controls H and I

A preliminary anaerobic digestion trial was conducted utilising the same preparation and setup as detailed in Ch. 6 utilising 1-pot nZVI-Osorb. However, this trial made use of older acquired sludge and excluded controls H (TCP only) and I (biomass only) in testing. Furthermore, ORP results were not recorded for this trial. These presented results serve to support claims and results recorded in Ch. 6, yet it is assumed that all results will not be identical given variations in sludge and human and experimental error in measurements and processing.

The potential of hydrogen (pH) in this preliminary trial was measured at days 5 and 7 (Fig. A1.4).

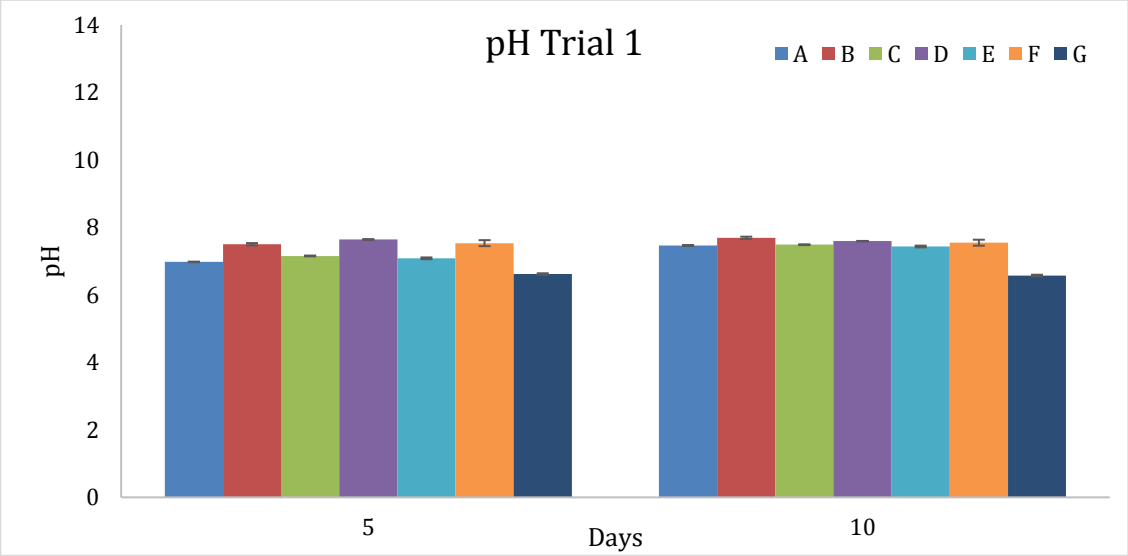

Figure A1. 4 Changes in pH from the first bioreactor trial from 5 to 10 days.

Results show that pH rises in all samples with biomass except D which contained no TCP. Control groups G and F remained stable on these two sampling days. Samples with nZVI-Osorb had a lower pH at day five than samples with control nZVI yet both types were the same pH five days later. These results follow previous reporting of pH in Fig. 6.3 but with significantly less variability. COD values were also monitored at days 0, 5, and 10 in this preliminary trial (Fig. A1.5).

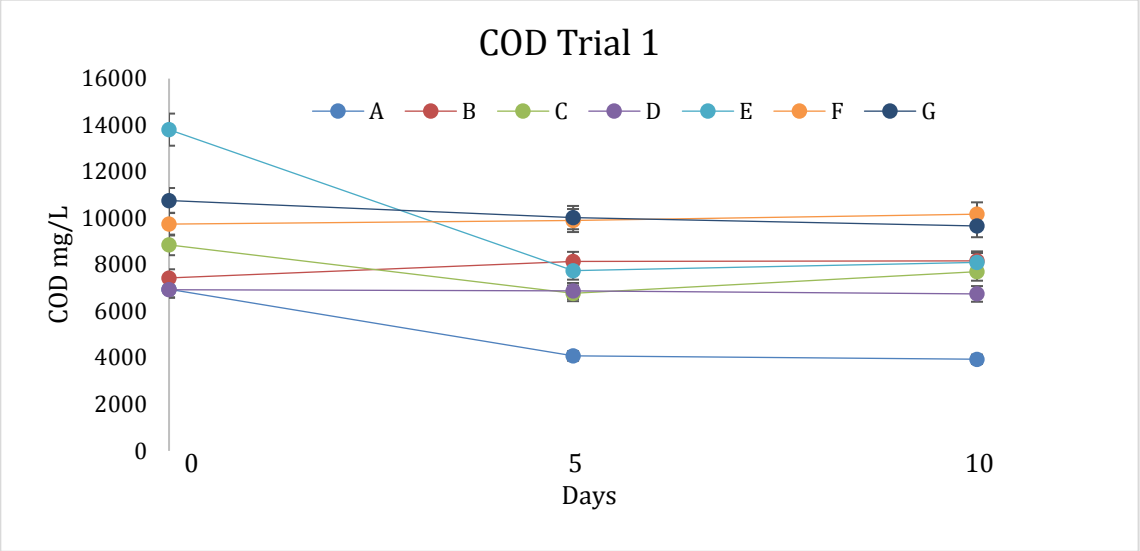

Figure A1.5 A plot of COD values from trial 1 of the bioreactor experiment with measurements taken at Day 0, 5, and 10.

Results from COD support results in Fig. 6.5 that found a levelling off in COD reduction between days 1 and 14. However, the results considered here show a slight reduction in COD in reactors A, C, and G from day 0 suggesting that reactor reactivity is highest initially and then slows to a stable rate after day 1. The most dramatic reduction in COD was in reactor E which contained biomass and nZVI-Osorb suggesting that the nanocomposite did not inversely affect microbial health. Reactor D remained stable and reactors F and B showed a slight increase in COD. While results in chapter 6 appeared mostly stable, these results would suggest that while reactivity may not be at its highest threshold nZVI and nZVI-Osorb do not appear to affect the overall chemical-oxidative demand in the system adversely.

Lastly, the head pressure of the reaction vessels was measured at days 0, 5, 10, and 16 (Fig. A1.6).

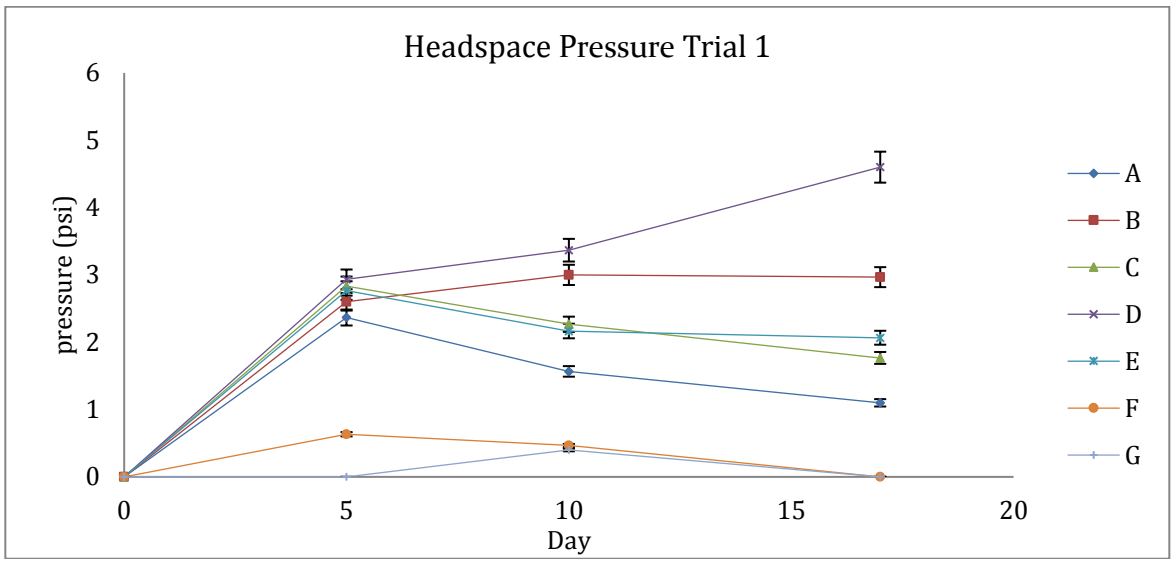

Figure A1.6 Head pressure over time in trial 1 of the bioreactor study.

Results were slightly less erratic than measurements in Ch.7 and show a significant rise in head pressure from day 0 to day 5 of the study. Head pressure was highest in reactor D which had both biomass and nZVI. Additional head pressure could be the result of iron corrosion and the production of hydrogen gas and/or improved respiration of microorganisms. Controls F and G displayed some head pressure buildup similar to Ch. 6 results most likely due to water incubation.

This preliminary trial does help to contextualise results detailed in Ch. 6, however, a great deal of additional work detailed in Ch. 8 would be required to complete a more thorough assessment of interactions.

References

1. The 2015 Revision of the UN's World Population Projections. *Population & Development Review* 2015; 41: 557-561. Article. DOI: 10.1111/j.1728-4457.2015.00082.x.
2. Santhosh C, Velmurugan V, Jacob G, et al. Role of nanomaterials in water treatment applications: A review. *Chemical Engineering Journal* 2016; 306: 1116-1137. DOI: https://doi.org/10.1016/j.cej.2016.08.053.
3. John R C. United States Abstains on General Assembly Resolution Proclaiming Human Right to Water and Sanitation. *The American Journal of International Law* 2010; 104: 672-673. DOI: 10.5305/amerjintelaw.104.4.0672.
4. Salawitch RJ, Canty TP, Hope AP, et al. *Paris Climate Agreement: Beacon of Hope*. Springer Climate, 2017.
5. Wiki Commons. https://commons.wikimedia.org/wiki/: Wikimedia Commons, 2017, p. Photo.
6. Sohn H, Celik G, Gunduz S, et al. Hydrodechlorination of trichloroethylene over Pd supported on swellable organically-modified silica (SOMS). *Applied Catalysis B: Environmental* 2017; 203: 641-653. DOI: http://dx.doi.org/10.1016/j.apcatb.2016.10.032.
7. Sanitation WUJMPfWSa. *Global Water Supply and Sanitation Assessment*. 2000.
8. Clapham D. Water and public health. In: Thompson KC and Gray J (eds) *Water Contamination Emergencies Can We Cope?* : The Royal Society of Chemistry, 2004, pp.65-72.
9. Stuart M, Talbot, Crane. *2011 Emerging Contaminants in Groundwater.* 2011. British Geological Survey.
10. Sustich RC, Shannon M and Pianfetti B. Introduction: Water Purification in the Twenty-First Century—Challenges and Opportunities. *Nanotechnology Applications for Clean Water (Second Edition)*. Oxford: William Andrew Publishing, 2014, pp.xxxvii-xlvi.
11. Smethurst CBMKG. *Basic Water Treatment*. 3rd ed. London: Royal Society of Chemistry, 2002.
12. Adeleye AS, Conway JR, Garner K, et al. Engineered nanomaterials for water treatment and remediation: Costs, benefits, and applicability. *Chemical Engineering Journal* 2016; 286: 640-662. DOI: https://doi.org/10.1016/j.cej.2015.10.105.
13. Li R, Zhang L and Wang P. Rational design of nanomaterials for water treatment. *Nanoscale* 2015; 7: 17167-17194. 10.1039/C5NR04870B. DOI: 10.1039/C5NR04870B.
14. Lu H, Wang J, Stoller M, et al. An Overview of Nanomaterials for Water and Wastewater Treatment. *Advances in Materials Science and Engineering* 2016; 2016: 10. DOI: 10.1155/2016/4964828.
15. Romero-Güiza MS, Vila J, Mata-Alvarez J, et al. The role of additives on anaerobic digestion: A review. *Renewable and Sustainable Energy Reviews* 2016; 58: 1486-1499. DOI: http://dx.doi.org/10.1016/j.rser.2015.12.094.
16. Pera-Titus M, García-Molina V, Baños MA, et al. Degradation of chlorophenols by means of advanced oxidation processes: a general review. *Applied Catalysis B: Environmental* 2004; 47: 219-256. DOI: http://dx.doi.org/10.1016/j.apcatb.2003.09.010.
17. Yang H, Hu Y and Cheng H. Sorption of chlorophenols on microporous minerals: mechanism and influence of metal cations, solution pH, and humic acid. *Environmental Science and Pollution Research* 2016; 23: 19266-19280. DOI: 10.1007/s11356-016-7128-9.
18. Buddhika G, Naresh S and Peter S. Review Papers : Degradation of Chlorinated Phenols by Zero Valent Iron and Bimetals of Iron: A Review. *Environmental Engineering Research* 2011; 16: 187.
19. Aldrich S. Material Safety and Data Sheets (MSDS), https://www.sigmaaldrich.com/safety-center.html (2017, 2017).
20. Plotkin JS. What's New In Phenol Production? *Industrial Chemistry and Engineering*, https://www.acs.org/content/acs/en/pressroom/cutting-edge-chemistry/what-s-new-in-phenol-production-.html (2016, accessed May 4th 2017).
21. Bommer M, Kunze C, Fesseler J, et al. Structural basis for organohalide respiration. *Science* 2014; 346: 455-458. DOI: 10.1126/science.1258118.
22. *Chlorophenols in Drinking-water: Background document for development of WHO Guidelines for Drinking-Water Quality*. 2003 2003. Geneva: World Health Organization.
23. Huff J. Long-term toxicology and carcinogenicity of 2,4,6-trichlorophenol. *Chemosphere* 2012; 89: 521-525. DOI: http://dx.doi.org/10.1016/j.chemosphere.2012.05.015.
24. Wang W, Wang S, Zhang J, et al. Degradation kinetics of pentachlorophenol and changes in anaerobic microbial community with different dosing modes of co-substrate and zero-valent iron. *International Biodeterioration & Biodegradation* 2016; 113: 126-133. DOI: http://dx.doi.org/10.1016/j.ibiod.2015.12.006.

25. Huang G-L, Xiao H, Chi J, et al. Effects of pH on the Aqueous Solubility of Selected Chlorinated Phenols. *Journal of Chemical & Engineering Data* 2000; 45: 411-414. DOI: 10.1021/je990262k.
26. Agus E, Lim MH, Zhang L, et al. Odorous Compounds in Municipal Wastewater Effluent and Potable Water Reuse Systems. *Environmental Science & Technology* 2011; 45: 9347-9355. DOI: 10.1021/es202594z.
27. khan MZ, Mondal PK, Sabir S, et al. Degradation pathway, toxicity and kinetics of 2,4,6-trichlorophenol with different co-substrate by aerobic granules in SBR. *Bioresource Technology* 2011; 102: 7016-7021. DOI: http://dx.doi.org/10.1016/j.biortech.2011.04.057.
28. Lu Q and Sorial GA. Adsorption of phenolics on activated carbon––impact of pore size and molecular oxygen. *Chemosphere* 2004; 55: 671-679. DOI: http://dx.doi.org/10.1016/j.chemosphere.2003.11.044.
29. Igbinosa EO, Odjadjare EE, Chigor VN, et al. Toxicological Profile of Chlorophenols and Their Derivatives in the Environment: The Public Health Perspective. *The Scientific World Journal* 2013; 2013: 460215. DOI: 10.1155/2013/460215.
30. Wang X, Mao Y, Tang S, et al. Disinfection byproducts in drinking water and regulatory compliance: A critical review. *Frontiers of Environmental Science & Engineering* 2015; 9: 3-15. DOI: 10.1007/s11783-014-0734-1.
31. U.S. Department of Health and Human Services PHS, National Toxicology Program. Report on Carcinogens. 2016.
32. Choi J-H, Choi SJ and Kim Y-H. Hydrodechlorination of 2,4,6-trichlorophenol for a permeable reactive barrier using zero-valent iron and catalyzed iron. *Korean Journal of Chemical Engineering* 2008; 25: 493-500. journal article. DOI: 10.1007/s11814-008-0083-5.
33. Wenjue Z, Donghong W and Xiaowei X. Phenol removal efficiencies of sewage treatment processes and ecological risks associated with phenols in effluents. *Journal of Hazardous Materials* 2012; 217-218: 286-292. Article. DOI: 10.1016/j.jhazmat.2012.03.026.
34. Ramamoorthy S. *Chlorinated Organic Compounds in the Environment: Regulatory and Monitoring Assessment*. CRC Press, 1997.
35. Mir MA, Hussain A and Verma C. Design considerations and operational performance of anaerobic digester: A review. *Cogent Engineering* 2016; 3. DOI: 10.1080/23311916.2016.1181696.
36. Gaitan IJ, Medina SC, González JC, et al. Evaluation of toxicity and degradation of a chlorophenol mixture by the laccase produced by Trametes pubescens. *Bioresource Technology* 2011; 102: 3632-3635. DOI: http://dx.doi.org/10.1016/j.biortech.2010.11.040.
37. Villeneuve PJ and Steenland K. RE: "MORTALITY RATES AMONG TRICHLOROPHENOL WORKERS WITH EXPOSURE TO 2,3,7,8-TETRACHLORODIBENZO-p-DIOXIN". *American Journal of Epidemiology* 2010; 171: 129-130. DOI: 10.1093/aje/kwp380.
38. Lampi P, Tuomisto J, Hakulinen T, et al. Follow-up study of cancer incidence after chlorophenol exposure in a community in southern Finland. *Scandinavian Journal of Work, Environment & Health* 2008; 34: 230-233.
39. Chaisse J. *The Regulation of the Global Water Services Market*. Cambridge: Cambridge University Press, 2017.
40. Méndez-Acosta HO, Campos-Rodríguez A, González-Álvarez V, et al. A hybrid cascade control scheme for the VFA and COD regulation in two-stage anaerobic digestion processes. *Bioresource Technology* 2016; 218: 1195-1202. DOI: https://doi.org/10.1016/j.biortech.2016.07.076.
41. Méndez-Acosta HO, García-Sandoval JP, González-Álvarez V, et al. Regulation of the organic pollution level in anaerobic digesters by using off-line COD measurements. *Bioresource Technology* 2011; 102: 7666-7672. DOI: https://doi.org/10.1016/j.biortech.2011.05.053.
42. Nichkova M, Galve R and Marco MP. Biological Monitoring of 2,4,5-Trichlorophenol (I): Preparation of Antibodies and Development of an Immunoassay Using Theoretical Models. *Chemical Research in Toxicology* 2002; 15: 1360-1370. DOI: 10.1021/tx025555h.
43. Razavi-Shirazi F and Veenstra JN. Development of a biological permeable barrier to remove 2,4,6-trichlorophenol from groundwater using immobilized cells. *Water Environment Research* 2000; 72: 460-468. DOI: 10.2175/106143000X138003.
44. Zhang Q, Sun F-y, Dong W-y, et al. Micro-polluted surface water treatment and trace-organics removal pathway in a PAC-MBR system. *Process Biochemistry* 2015; 50: 1422-1428. DOI: http://dx.doi.org/10.1016/j.procbio.2015.05.021.
45. Bu Q, Luo Q, Wang D, et al. Screening for over 1000 organic micropollutants in surface water and sediments in the Liaohe River watershed. *Chemosphere* 2015; 138: 519-525. DOI: http://doi.org/10.1016/j.chemosphere.2015.07.013.

46. Chen Y, Yu S, Tang S, et al. Site-specific water quality criteria for aquatic ecosystems: A case study of pentachlorophenol for Tai Lake, China. *Science of The Total Environment* 2016; 541: 65-73. DOI: http://dx.doi.org/10.1016/j.scitotenv.2015.09.006.
47. Wegman RCC and Hofstee AWM. Chlorophenols in surface waters of the Netherlands (1976–1977). *Water Research* 1979; 13: 651-657. DOI: http://dx.doi.org/10.1016/0043-1354(79)90015-0.
48. Koistinen J, Kukkonen JVK, Sormunen A, et al. Bioaccumulation, bioavailability and environmental fate of chlorophenol impurities, polychlorinated hydroxydiphenylethers and their methoxy analogues. *Chemosphere* 2007; 68: 1382-1391. DOI: http://doi.org/10.1016/j.chemosphere.2007.01.027.
49. Quémerais B, Lemieux C and Lum KR. Distribution and fate of chlorophenols in the St. Lawrence River basin, Canada. *Chemosphere* 1994; 28: 1943-1960. DOI: http://dx.doi.org/10.1016/0045-6535(94)90145-7.
50. Frankki S, Persson Y, xd, et al. Mobility of Chloroaromatic Compounds in Soil: Case Studies of Swedish Chlorophenol-Contaminated Sawmill Sites. *Ambio* 2007; 36: 452-457.
51. Matthiessen P and Law RJ. Contaminants and their effects on estuarine and coastal organisms in the United Kingdom in the late twentieth century. *Environmental Pollution* 2002; 120: 739-757. DOI: http://dx.doi.org/10.1016/S0269-7491(02)00175-6.
52. Zhang K, Luo Z, Zhang T, et al. Study on formation of 2,4,6-trichloroanisole by microbial O-methylation of 2,4,6-trichlorophenol in lake water. *Environmental Pollution* 2016; 219: 228-234. DOI: http://dx.doi.org/10.1016/j.envpol.2016.10.042.
53. Jin X, Gao J, Zha J, et al. A tiered ecological risk assessment of three chlorophenols in Chinese surface waters. *Environmental Science and Pollution Research* 2012; 19: 1544-1554.
54. Gao J, Liu L, Liu X, et al. Levels and spatial distribution of chlorophenols – 2,4-Dichlorophenol, 2,4,6-trichlorophenol, and pentachlorophenol in surface water of China. *Chemosphere* 2008; 71: 1181-1187. DOI: http://doi.org/10.1016/j.chemosphere.2007.10.018.
55. Bello D, Trasar-Cepeda C, Leirós MC, et al. Modification of enzymatic activity in soils of contrasting pH contaminated with 2,4-dichlorophenol and 2,4,5-trichlorophenol. *Soil Biology and Biochemistry* 2013; 56: 80-86. DOI: http://dx.doi.org/10.1016/j.soilbio.2012.02.011.
56. Kern S, Singer H, Hollender J, et al. Assessing Exposure to Transformation Products of Soil-Applied Organic Contaminants in Surface Water: Comparison of Model Predictions and Field Data. *Environmental Science & Technology* 2011; 45: 2833-2841. DOI: 10.1021/es102537b.
57. Biswas AK. *Water Security, Climate Change and Sustainable Development*. 1st edition 2016.. ed.: Singapore : Springer Singapore, 2016.
58. Kaluarachchi JJ. *Groundwater Contamination by Organic Pollutants*. 1 ed.: American Society of Civil Engineers, 2001, p.249.
59. Chris P and Michael A. *A Dictionary of Environment and Conservation*. 3rd ed.: Oxford University Press, 2013.
60. Kuwayama Y, Young R and Brozović N. Chapter 3.1.5 - Groundwater Scarcity: Management Approaches and Recent Innovations A2 - Ziolkowska, Jadwiga R. In: Peterson JM (ed) *Competition for Water Resources*. Elsevier, 2017, pp.332-350.
61. Persson Y, Tysklind M, Öberg L, et al. *Chlorinated organic pollutants in soil and groundwater at chlorophenol-contaminated sawmill sites*. Umeå University, Umeå, 2007.
62. Snyder CJP, Asghar M, Scharer JM, et al. Biodegradation kinetics of 2,4,6-Trichlorophenol by an acclimated mixed microbial culture under aerobic conditions. *Biodegradation* 2006; 17: 535-544. journal article. DOI: 10.1007/s10532-005-9024-8.
63. Aranda C, Godoy F, Gonzalez B, et al. Effects of glucose and phenylalanine upon 2,4,6-trichlorophenol degradation by Pseudomonas paucimobilis S37 cells in a no-growth state. *Microbios* 1999; 100: 73-82. 1999/12/03.
64. Martinez M, Baeza J, Freer J, et al. Chlorophenol tolerant and degradative bacteria isolated from a river receiving pulp mill discharges. *Toxicological & Environmental Chemistry* 2000; 77: 159-170. DOI: 10.1080/02772240009358947.
65. Mohn WW and Kennedy KJ. Limited degradation of chlorophenols by anaerobic sludge granules. *Applied and Environmental Microbiology* 1992; 58: 2131.
66. Fahmy M, Heinzle E and Kut OM. Treatment of bleaching effluents in aerobic/anaerobic fluidized biofilm systems. *International Water Association* 1991; 24: 179-187.
67. Chang BV, Chiang CW and Yuan SY. Microbial dechlorination of 2,4,6 - trichlorophenol in anaerobic sewage sludge. *Journal of Environmental Science and Health, Part B* 1999; 34: 491-507. DOI: 10.1080/03601239909373210.

68. Langwaldt JH and Puhakka JA. Competition for oxygen by iron and 2,4,6-trichlorophenol oxidizing bacteria in boreal groundwater. *Water Research* 2003; 37: 1378-1384. DOI: http://dx.doi.org/10.1016/S0043-1354(02)00480-3.
69. Su Z-H, Xu Z-S, Peng R-H, et al. Phytoremediation of Trichlorophenol by Phase II Metabolism in Transgenic Arabidopsis Overexpressing a Populus Glucosyltransferase. *Environmental Science & Technology* 2012; 46: 4016-4024. DOI: 10.1021/es203753b.
70. Liu H, Guo S, Jiao K, et al. Bioremediation of soils co-contaminated with heavy metals and 2,4,5-trichlorophenol by fruiting body of Clitocybe maxima. *Journal of Hazardous Materials* 2015; 294: 121-127. DOI: http://dx.doi.org/10.1016/j.jhazmat.2015.04.004.
71. Bosso L and Cristinzio G. A comprehensive overview of bacteria and fungi used for pentachlorophenol biodegradation. *Reviews in Environmental Science and Bio/Technology* 2014; 13: 387-427. DOI: 10.1007/s11157-014-9342-6.
72. Xie Y, Dong H, Zeng G, et al. The interactions between nanoscale zero-valent iron and microbes in the subsurface environment: A review. *Journal of Hazardous Materials* 2017; 321: 390-407. DOI: http://dx.doi.org/10.1016/j.jhazmat.2016.09.028.
73. Andreoni V, Baggi G, Colombo M, et al. Degradation of 2,4,6-trichlorophenol by a specialized organism and by indigenous soil microflora: bioaugmentation and self-remediability for soil restoration. *Letters in Applied Microbiology* 1998; 27: 86-92. DOI: 10.1046/j.1472-765X.1998.00393.x.
74. Petri M, Jiang J-Q and Maier M. Screening analysis of volatile organic contaminants in commercial inorganic coagulants used for drinking water treatment. *Journal of Environmental Management* 2009; 91: 142-148. DOI: https://doi.org/10.1016/j.jenvman.2009.07.015.
75. Jiang J-Q, Zhou Z and Sharma VK. Occurrence, transportation, monitoring and treatment of emerging micro-pollutants in waste water — A review from global views. *Microchemical Journal* 2013; 110: 292-300. DOI: https://doi.org/10.1016/j.microc.2013.04.014.
76. Jiang J and Lloyd B. Progress in the development and use of ferrate(VI) salt as an oxidant and coagulant for water and wastewater treatment. *Water Res* 2002; 36: 1397.
77. Jiang J-Q. Advances in the development and application of ferrate(VI) for water and wastewater treatment. *Journal of Chemical Technology & Biotechnology* 2014; 89: 165-177. DOI: 10.1002/jctb.4214.
78. Jiang JQ, Stanford C and Alsheyab M. The online generation and application of ferrate(VI) for sewage treatment: A pilot scale trial. *Sep Purif Technol* 2009; 68: 227.
79. Activated Sludge Process and Wastewater Treatment Process Diagrams Cherry Creek Schools, 2017.
80. Rajasulochana P and Preethy V. Comparison on efficiency of various techniques in treatment of waste and sewage water – A comprehensive review. *Resource-Efficient Technologies* 2016; 2: 175-184. DOI: https://doi.org/10.1016/j.reffit.2016.09.004.
81. Kuśmierek K, Sankowska M and Świątkowski A. Kinetic and equilibrium studies of simultaneous adsorption of monochlorophenols and chlorophenoxy herbicides on activated carbon. *Desalination and Water Treatment* 2014; 52: 178-183. DOI: 10.1080/19443994.2013.780984.
82. Fu J, Lee W-N, Coleman C, et al. Pilot investigation of two-stage biofiltration for removal of natural organic matter in drinking water treatment. *Chemosphere* 2017; 166: 311-322. DOI: http://doi.org/10.1016/j.chemosphere.2016.09.101.
83. Gardin H, Lebeault J and Pauss A. Degradation of 2,4,6-trichlorophenol (2,4,6-TCP) by co-immobilization of anaerobic and aerobic microbial communities in an upflow reactor under air-limited conditions. *Applied Microbiology and Biotechnology* 2001; 56: 524-530. DOI: 10.1007/s002530000577.
84. Milia S, Porcu R, Rossetti S, et al. Performance and Characteristics of Aerobic Granular Sludge Degrading 2,4,6-Trichlorophenol at Different Volumetric Organic Loading Rates. *CLEAN – Soil, Air, Water* 2016; 44: 615-623. DOI: 10.1002/clen.201500127.
85. Suanon F, Sun Q, Li M, et al. Application of nanoscale zero valent iron and iron powder during sludge anaerobic digestion: Impact on methane yield and pharmaceutical and personal care products degradation. *Journal of Hazardous Materials* 2017; 321: 47-53. DOI: http://dx.doi.org/10.1016/j.jhazmat.2016.08.076.
86. Limam I, Limam RD, Mezni M, et al. Penta- and 2,4,6-tri-chlorophenol biodegradation during municipal solid waste anaerobic digestion. *Ecotoxicology and Environmental Safety* 2016; 130: 270-278. DOI: http://dx.doi.org/10.1016/j.ecoenv.2016.04.030.
87. Wang W and Wu Y. Combination of zero-valent iron and anaerobic microorganisms immobilized in luffa sponge for degrading 1,1,1-trichloroethane and the relevant microbial community analysis. *Applied Microbiology and Biotechnology* 2017; 101: 783-796. journal article. DOI: 10.1007/s00253-016-7933-6.

88. Zhou J, Zhang R, Liu F, et al. Biogas production and microbial community shift through neutral pH control during the anaerobic digestion of pig manure. *Bioresource Technology* 2016; 217: 44-49. DOI: http://dx.doi.org/10.1016/j.biortech.2016.02.077.
89. Hu Y, Hao X, Zhao D, et al. Enhancing the CH4 yield of anaerobic digestion via endogenous CO2 fixation by exogenous H2. *Chemosphere* 2015; 140: 34-39. DOI: http://dx.doi.org/10.1016/j.chemosphere.2014.10.022.
90. Jeff Goldberg EA. Newtown Creek Wastewater Treatment Plant. Ennead Architects, 2017.
91. Yang M and Zheng S. Pollutant removal-oriented yeast biomass production from high-organic-strength industrial wastewater: A review. *Biomass and Bioenergy* 2014; 64: 356-362. DOI: http://dx.doi.org/10.1016/j.biombioe.2014.03.020.
92. Zhang Q, Sun F-y, Dong W-y, et al. Treatment of micro-polluted water resource loaded with 2,4,6-trichlorophenol by a membrane bioreactor (MBR). *Desalination and Water Treatment* 2016; 57: 11019-11028. DOI: 10.1080/19443994.2015.1044911.
93. Chen JL, Ortiz R, Steele TWJ, et al. Toxicants inhibiting anaerobic digestion: A review. *Biotechnology Advances* 2014; 32: 1523-1534. DOI: http://dx.doi.org/10.1016/j.biotechadv.2014.10.005.
94. Ganzoury MA and Allam NK. Impact of nanotechnology on biogas production: A mini-review. *Renewable and Sustainable Energy Reviews* 2015; 50: 1392-1404. DOI: http://dx.doi.org/10.1016/j.rser.2015.05.073.
95. Chen Y, Cheng JJ and Creamer KS. Inhibition of anaerobic digestion process: A review. *Bioresource Technology* 2008; 99: 4044-4064. DOI: http://dx.doi.org/10.1016/j.biortech.2007.01.057.
96. Eker S and Kargi F. Biological treatment of 2,4,6-trichlorophenol (TCP) containing wastewater in a hybrid bioreactor system with effluent recycle. *Journal of Environmental Management* 2009; 90: 692-698. DOI: http://dx.doi.org/10.1016/j.jenvman.2008.01.001.
97. Borden RC, Crimi M, Siegrist RL, et al. *In situ chemical oxidation for groundwater remediation*. New York: New York : Springer, 2011.
98. Jin Z. Phenol Removal from Water with Potassium Permanganate Modified Granular Activated Carbon. *Journal of Environmental Protection* 2013; 4: 411-417. Article. DOI: 10.4236/jep.2013.45049.
99. Quality OoL. In-Situ Chemical Oxidation. In: Management IDoE, (ed.). *IDEM Technical Guidance*. Indianapolis, IN: Indiana, 2016, p. 1-14.
100. Xing L, Liu H, Giesy JP, et al. pH-dependent aquatic criteria for 2,4-dichlorophenol, 2,4,6-trichlorophenol and pentachlorophenol. *Science of The Total Environment* 2012; 441: 125-131. DOI: http://dx.doi.org/10.1016/j.scitotenv.2012.09.060.
101. Mondal PK, Ahmad R and Usmani SQ. Anaerobic biodegradation of triphenylmethane dyes in a hybrid UASFB reactor for wastewater remediation. *Biodegradation* 2010; 21: 1041-1047. DOI: 10.1007/s10532-010-9364-x.
102. Ibrahim RK, Hayyan M, AlSaadi MA, et al. Environmental application of nanotechnology: air, soil, and water. *Environmental Science and Pollution Research* 2016; 23: 13754-13788. DOI: 10.1007/s11356-016-6457-z.
103. Shaban YA, El Sayed MA, El Maradny AA, et al. Photocatalytic degradation of phenol in natural seawater using visible light active carbon modified (CM)-n-TiO2 nanoparticles under UV light and natural sunlight illuminations. *Chemosphere* 2013; 91: 307-313. DOI: http://dx.doi.org/10.1016/j.chemosphere.2012.11.035.
104. Ghanbari F, Moradi M and Gohari F. Degradation of 2,4,6-trichlorophenol in aqueous solutions using peroxymonosulfate/activated carbon/UV process via sulfate and hydroxyl radicals. *Journal of Water Process Engineering* 2016; 9: 22-28. DOI: https://doi.org/10.1016/j.jwpe.2015.11.011.
105. Li G, Park S, Kang D-W, et al. 2,4,5-Trichlorophenol Degradation Using a Novel TiO2-Coated Biofilm Carrier: Roles of Adsorption, Photocatalysis, and Biodegradation. *Environmental Science & Technology* 2011; 45: 8359-8367. DOI: 10.1021/es2016523.
106. Hongquan J, Qingyuan W, Shuying Z, et al. Enhanced photoactivity of Sm, N, P-tridoped anatase-TiO2 nano-photocatalyst for 4-chlorophenol degradation under sunlight irradiation. *Journal of Hazardous Materials* 2013; 261: 44-54. Article. DOI: 10.1016/j.jhazmat.2013.07.016.
107. González LF, Sarria V and Sánchez OF. Degradation of chlorophenols by sequential biological-advanced oxidative process using Trametes pubescens and TiO2/UV. *Bioresource Technology* 2010; 101: 3493-3499. DOI: https://doi.org/10.1016/j.biortech.2009.12.130.
108. Diallo MS. Chapter 15 - Water Treatment by Dendrimer-Enhanced Filtration: Principles and Applications A2 - Street, Anita. In: Sustich R, Duncan J and Savage N (eds) *Nanotechnology Applications for Clean Water (Second Edition)*. Oxford: William Andrew Publishing, 2014, pp.227-239.

109. Gao W, Zhang Y, Zhang X, et al. Permeable reactive barrier of coarse sand-supported zero valent iron for the removal of 2,4-dichlorophenol in groundwater. *Environmental Science and Pollution Research* 2015; 22: 16889-16896. DOI: 10.1007/s11356-015-4912-x.
110. Tan IAW, Ahmad AL and Hameed BH. Adsorption isotherms, kinetics, thermodynamics and desorption studies of 2,4,6-trichlorophenol on oil palm empty fruit bunch-based activated carbon. *Journal of Hazardous Materials* 2009; 164: 473-482. DOI: https://doi.org/10.1016/j.jhazmat.2008.08.025.
111. Ruiz C, Mena E, Cañizares P, et al. Removal of 2,4,6-Trichlorophenol from Spiked Clay Soils by Electrokinetic Soil Flushing Assisted with Granular Activated Carbon Permeable Reactive Barrier. *Industrial & Engineering Chemistry Research* 2014; 53: 840-846. DOI: 10.1021/ie4028022.
112. Cheng S, Oatley DL, Williams PM, et al. Positively charged nanofiltration membranes: Review of current fabrication methods and introduction of a novel approach. *Advances in Colloid and Interface Science* 2011; 164: 12-20. DOI: 10.1016/j.cis.2010.12.010.
113. Adham SS, Snoeyink VL, Clark MM, et al. Predicting and Verifying Organics Removal by PAC in an Ultrafiltration System. *Journal (American Water Works Association)* 1991; 83: 81-91.
114. Komesvarakul N, Scamehorn JF and Gecol H. Purification of Phenolic-Laden Wastewater from the Pulp and Paper Industry by Using Colloid-Enhanced Ultrafiltration. *Separation Science and Technology* 2003; 38: 2465-2501. DOI: 10.1081/SS-120022283.
115. Palit S. 17 - Application of nanotechnology, nanofiltration, and drinking and wastewater treatment—a vision for the future A2 - Grumezescu, Alexandru Mihai. *Water Purification*. Academic Press, 2017, pp.587-620.
116. Anadão P. 15 - Nanocomposite filtration membranes for drinking water purification A2 - Grumezescu, Alexandru Mihai. *Water Purification*. Academic Press, 2017, pp.517-549.
117. Bunani S, Yörükoğlu E, Sert G, et al. Application of nanofiltration for reuse of municipal wastewater and quality analysis of product water. *Desalination* 2013; 315: 33-36. Article. DOI: 10.1016/j.desal.2012.11.015.
118. Pal P. Chapter 2 - Chemical Treatment Technology. *Industrial Water Treatment Process Technology*. Butterworth-Heinemann, 2017, pp.21-63.
119. Marley MCD, E.X; Hopkins, H.H.; Bruel, C.J. Use Air Sparging and Vapor Extraction to Remediate Subsurface Organics, http://www.globalspec.com/reference/9391/349867/use-air-sparging-and-vapor-extraction-to-remediate-subsurface-organics (2017, accessed June 13th 2017 2017).
120. Abdallah MAM. The potential of different bio adsorbents for removing phenol from its aqueous solution. *Environmental Monitoring And Assessment* 2013; 185: 6495-6503. DOI: 10.1007/s10661-012-3041-y.
121. Sun D, Guo S, Ma N, et al. Sewage sludge pretreatment by microwave irradiation combined with activated carbon fibre at alkaline pH for anaerobic digestion. *Water Science and Technology* 2016; 73: 2882-2887. DOI: 10.2166/wst.2016.149.
122. Lin Y, Choi D, Wang J, et al. Chapter 17 - Nanomaterials-Enhanced Electrically Switched Ion Exchange Process for Water Treatment A2 - Street, Anita. In: Sustich R, Duncan J and Savage N (eds) *Nanotechnology Applications for Clean Water (Second Edition)*. Oxford: William Andrew Publishing, 2014, pp.271-280.
123. Baer DR, Tratnyek PG, Qiang Y, et al. *Environmental Applications of Nanomaterials: Synthesis, Sorbents, and Sensors*. 2007.
124. Corwin CJ and Summers RS. Scaling Trace Organic Contaminant Adsorption Capacity by Granular Activated Carbon. *ENVIRONMENTAL SCIENCE & TECHNOLOGY* 2010; 14: 6.
125. Lin S-H and Juang R-S. Adsorption of phenol and its derivatives from water using synthetic resins and low-cost natural adsorbents: A review. *Journal of Environmental Management* 2009; 90: 1336-1349. DOI: http://dx.doi.org/10.1016/j.jenvman.2008.09.003.
126. Herrero-Hernández E, Rodríguez-Gonzalo E, Rodríguez-Cruz MS, et al. Efficiency of a molecularly imprinted polymer for selective removal of phenols and phenoxyacids from contaminated waters. *International Journal of Environmental Science and Technology* 2015; 12: 3079-3088. DOI: 10.1007/s13762-014-0721-x.
127. Jiang J-Q and Ashekuzzaman SM. Development of novel inorganic adsorbent for water treatment. *Current Opinion in Chemical Engineering* 2012; 1: 191-199. DOI: https://doi.org/10.1016/j.coche.2012.03.008.
128. Lin SH and Lin RC. Adsorption and Mass Transfer Characteristics of Pentane and Cyclopentane by Various Adsorbents. *Environmental Technology* 1999; 20: 11-19. DOI: 10.1080/09593332008616787.
129. Fan H-T, Zhao C-Y, Liu S, et al. Adsorption Characteristics of Chlorophenols from Aqueous Solution onto Graphene. *Journal of Chemical & Engineering Data* 2017; 62: 1099-1105. DOI: 10.1021/acs.jced.6b00918.

130. Arafat HA, Franz M and Pinto NG. Effect of Salt on the Mechanism of Adsorption of Aromatics on Activated Carbon. *Langmuir* 1999; 15: 5997-6003. DOI: 10.1021/la9813331.
131. ten Hulscher TEM and Cornelissen G. Effect of temperature on sorption equilibrium and sorption kinetics of organic micropollutants - a review. *Chemosphere* 1996; 32: 609-626. DOI: https://doi.org/10.1016/0045-6535(95)00345-2.
132. Greenlee LF, Lawler DF, Freeman BD, et al. Reverse osmosis desalination: Water sources, technology, and today's challenges. *Water Research* 2009; 43: 2317-2348. DOI: http://dx.doi.org/10.1016/j.watres.2009.03.010.
133. Bandosz T. *Activated Carbon Surfaces in Environmental Remediation*. New York: Elsevier Ltd., 2006.
134. Lee H, Yoo H-Y, Choi J, et al. Oxidizing Capacity of Periodate Activated with Iron-Based Bimetallic Nanoparticles. *Environmental Science & Technology* 2014; 48: 8086-8093. DOI: 10.1021/es5002902.
135. Liu X-b, Xie X-x, Yan H, et al. A review of the adsorption of organic pollutants on mesoporous carbons and carbon/silica hybrids. *Carbon* 2013; 64: 557. DOI: http://dx.doi.org/10.1016/j.carbon.2013.07.070.
136. Edmiston PL and Underwood LA. Absorption of dissolved organic species from water using organically modified silica that swells. *Separation and Purification Technology* 2009; 66: 532-540. DOI: 10.1016/j.seppur.2009.02.001.
137. Edmiston PL, West LJ, Chin A, et al. Adsorption of Gas Phase Organic Compounds by Swellable Organically Modified Silica. *Industrial & Engineering Chemistry Research* 2016; 55: 12068-12079. DOI: 10.1021/acs.iecr.6b02403.
138. Li Y, Li X, Dong C, et al. Selective recognition and removal of chlorophenols from aqueous solution using molecularly imprinted polymer prepared by reversible addition-fragmentation chain transfer polymerization. *Biosensors and Bioelectronics* 2009; 25: 306-312. DOI: http://dx.doi.org/10.1016/j.bios.2009.07.001.
139. Tang L, Tang J, Zeng G, et al. Rapid reductive degradation of aqueous p-nitrophenol using nanoscale zero-valent iron particles immobilized on mesoporous silica with enhanced antioxidation effect. *Applied Surface Science* 2015; 333: 220-228. DOI: http://dx.doi.org/10.1016/j.apsusc.2015.02.025.
140. Kour G, Gupta M, Vishwanathan B, et al. Iron nanotube-silica composite (ZVI-S-PCAT modified silica composite) preparation, characterization and application as a recyclable catalytic system for 5-membered ring organic transformations. *Dalton Transactions* 2015; 44: 14975-14990. 10.1039/C5DT02028J. DOI: 10.1039/C5DT02028J.
141. Fosso-Kankeu E and Mishra AK. 9 - Photocatalytic degradation and adsorption techniques involving nanomaterials for biotoxins removal from drinking water A2 - Grumezescu, Alexandru Mihai. *Water Purification*. Academic Press, 2017, pp.323-354.
142. Bharati R, Sundaramurthy S and Thakur C. 14 - Nanomaterials and food-processing wastewater A2 - Grumezescu, Alexandru Mihai. *Water Purification*. Academic Press, 2017, pp.479-516.
143. Theron J, Walker JA and Cloete TE. Nanotechnology and water treatment: applications and emerging opportunities. *Critical Reviews In Microbiology* 2008; 34: 43-69.
144. Zango ZU, Garba ZN, Abu Bakar NHH, et al. Adsorption studies of Cu2 +–Hal nanocomposites for the removal of 2,4,6-trichlorophenol. *Applied Clay Science* 2016; 132–133: 68-78. DOI: http://dx.doi.org/10.1016/j.clay.2016.05.016.
145. Zhang Y, Prigent B and Geißen S-U. Adsorption and regenerative oxidation of trichlorophenol with synthetic zeolite: Ozone dosage and its influence on adsorption performance. *Chemosphere* 2016; 154: 132-137. DOI: http://dx.doi.org/10.1016/j.chemosphere.2016.03.079.
146. Shen H-Y, Chen Z-X, Li Z-H, et al. Controlled synthesis of 2,4,6-trichlorophenol-imprinted amino-functionalized nano-Fe3O4-polymer magnetic composite for highly selective adsorption. *Colloids and Surfaces A: Physicochemical and Engineering Aspects* 2015; 481: 439-450. DOI: http://dx.doi.org/10.1016/j.colsurfa.2015.06.007.
147. Yang J, Chen H, Gao J, et al. Synthesis of Fe3O4/g-C3N4 nanocomposites and their application in the photodegradation of 2,4,6-trichlorophenol under visible light. *Materials Letters* 2016; 164: 183-189. DOI: http://dx.doi.org/10.1016/j.matlet.2015.10.130.
148. Abbas HA, Jamil TS and Hammad FF. Synthesis, characterization and photocatalytic activity of nano sized undoped and Ga doped SrTi0.7Fe0.3O3 for 2,4,6-trichlorophenol photodegradation. *Journal of Environmental Chemical Engineering* 2016; 4: 2384-2393. DOI: http://dx.doi.org/10.1016/j.jece.2016.04.019.
149. Hou Y, Li X, Zhao Q, et al. Electrochemically Assisted Photocatalytic Degradation of 4-Chlorophenol by ZnFe2O4–Modified TiO2 Nanotube Array Electrode under Visible Light Irradiation. *Environmental Science & Technology* 2010; 44: 5098-5103. DOI: 10.1021/es100004u.

150. Kim HN, Walker SL and Bradford SA. Macromolecule mediated transport and retention of Escherichia coli O157:H7 in saturated porous media. *Water Research* 2010; 44: 1082-1093. DOI: 10.1016/j.watres.2009.09.027.
151. Kim J-H, Tratnyek PG and Chang Y-S. Rapid Dechlorination of Polychlorinated Dibenzo-p-dioxins by Bimetallic and Nanosized Zerovalent Iron. *Environmental Science & Technology* 2008; 42: 4106-4112. DOI: 10.1021/es702560k.
152. Crane RA and Scott TB. Nanoscale zero-valent iron: Future prospects for an emerging water treatment technology. *Journal of Hazardous Materials* 2012; 211–212: 112-125. DOI: http://doi.org/10.1016/j.jhazmat.2011.11.073.
153. Savage N, Diallo M, Duncan J, et al. *Nanotechnology Applications for Clean Water*. William Andrew Publishing, 2009.
154. Yan WL, Herzing AA, Kiely CJ, et al. Nanoscale zero-valent iron (nZVI): Aspects of the core-shell structure and reactions with inorganic species in water. *Journal of Contaminant Hydrology* 2010; 118: 96-104.
155. Demarchis L, Minella M, Nisticò R, et al. Photo–Fenton reaction in the presence of morphologically controlled hematite as iron source. *Journal of Photochemistry and Photobiology A: Chemistry* 2015; 307-308: 99-107. DOI: https://doi.org/10.1016/j.jphotochem.2015.04.009.
156. He H, Zhong Y, Liang X, et al. Natural Magnetite: an efficient catalyst for the degradation of organic contaminant. 2015; 5: 10139. Article. DOI: 10.1038/srep10139 https://www.nature.com/articles/srep10139#supplementary-information.
157. Fu F, Dionysiou DD and Liu H. The use of zero-valent iron for groundwater remediation and wastewater treatment: A review. *Journal of Hazardous Materials* 2014; 267: 194-205. DOI: http://dx.doi.org/10.1016/j.jhazmat.2013.12.062.
158. Cross KM, Lu Y, Zheng T, et al. Chapter 27 - Water Decontamination Using Iron and Iron Oxide Nanoparticles A2 - Street, Anita. In: Sustich R, Duncan J and Savage N (eds) *Nanotechnology Applications for Clean Water (Second Edition)*. Oxford: William Andrew Publishing, 2014, pp.423-439.
159. Ouellette RJ and Rawn JD. 8 - Alcohols and Phenols. *Principles of Organic Chemistry*. Boston: Elsevier, 2015, pp.209-238.
160. Yadav VK. *Steric and Stereoelectronic Effects in Organic Chemistry*. Singapore : Springer Singapore, 2016.
161. Jia H and Wang C. Dechlorination of chlorinated phenols by subnanoscale Pd0/Fe0 intercalated in smectite: pathway, reactivity, and selectivity. *Journal of Hazardous Materials* 2015; 300: 779-787. DOI: http://dx.doi.org/10.1016/j.jhazmat.2015.08.017.
162. Costentin C, Robert M and Savéant J-M. Fragmentation of Aryl Halide π Anion Radicals. Bending of the Cleaving Bond and Activation vs Driving Force Relationships. *Journal of the American Chemical Society* 2004; 126: 16051-16057. DOI: 10.1021/ja045989u.
163. Shimizu A, Tokumura M, Nakajima K, et al. Phenol removal using zero-valent iron powder in the presence of dissolved oxygen: Roles of decomposition by the Fenton reaction and adsorption/precipitation. *Journal of Hazardous Materials* 2012; 201–202: 60-67. DOI: http://doi.org/10.1016/j.jhazmat.2011.11.009.
164. Vogt C, Kleinsteuber S and Richnow HH. Anaerobic benzene degradation by bacteria. *Microbial biotechnology* 2011; 4: 710-724. DOI: 10.1111/j.1751-7915.2011.00260.x.
165. Howell JO, Goncalves JM, Amatore C, et al. Electron transfer from aromatic hydrocarbons and their .pi.-complexes with metals. Comparison of the standard oxidation potentials and vertical ionization potentials. *Journal of the American Chemical Society* 1984; 106: 3968-3976. DOI: 10.1021/ja00326a014.
166. Sheppard TD. Metal-catalysed halogen exchange reactions of aryl halides. *Organic & Biomolecular Chemistry* 2009; 7: 1043-1052. 10.1039/B818155A. DOI: 10.1039/B818155A.
167. Li C and Hoffman MZ. One-Electron Redox Potentials of Phenols in Aqueous Solution. *The Journal of Physical Chemistry B* 1999; 103: 6653-6656. DOI: 10.1021/jp983819w.
168. Chen L-H, Huang C-C and Lien H-L. Bimetallic iron–aluminum particles for dechlorination of carbon tetrachloride. *Chemosphere* 2008; 73: 692-697. DOI: 10.1016/j.chemosphere.2008.07.005.
169. Jung YS, Lim WT, Park JY, et al. Effect of pH on Fenton and Fenton ‐ like oxidation. *Environmental Technology* 2009; 30: 183-190. DOI: 10.1080/09593330802468848.
170. Ortiz de la Plata GB, Alfano OM and Cassano AE. 2-Chlorophenol degradation via photo Fenton reaction employing zero valent iron nanoparticles. *Journal of Photochemistry and Photobiology A: Chemistry* 2012; 233: 53-59. DOI: http://dx.doi.org/10.1016/j.jphotochem.2012.02.023.
171. Hlophe M and Hillie T. Chapter 40 - Challenges to Implementing Nanotechnology Solutions to Water Issues in Africa A2 - Street, Anita. In: Sustich R, Duncan J and Savage N (eds) *Nanotechnology Applications for Clean Water (Second Edition)*. Oxford: William Andrew Publishing, 2014, pp.611-621.

172. Lin CJ, Liou YH and Lo S-L. Supported Pd/Sn bimetallic nanoparticles for reductive dechlorination of aqueous trichloroethylene. *Chemosphere* 2009; 74: 314-319. DOI: 10.1016/j.chemosphere.2008.08.046.
173. Li X-q, Elliott DW and Zhang W-x. Zero-valent iron nanoparticles for abatement of environmental pollutants: materials and engineering aspects. *Critical reviews in solid state and materials sciences* 2006; 31: 111-122.
174. Segura Y, Martínez F, Melero JA, et al. Enhancement of the advanced Fenton process (Fe0/H2O2) by ultrasound for the mineralization of phenol. *Applied Catalysis B: Environmental* 2012; 113–114: 100-106. DOI: http://doi.org/10.1016/j.apcatb.2011.11.024.
175. Kim YH and Carraway ER. Dechlorination of chlorinated phenols by zero valent zinc. *Environmental Technology* 2003; 24: 1455-1463. DOI: 10.1080/09593330309385690.
176. Li L, Hu J, Shi X, et al. Nanoscale zero-valent metals: a review of synthesis, characterization, and applications to environmental remediation. *Environmental Science and Pollution Research* 2016; 23: 17880-17900. journal article. DOI: 10.1007/s11356-016-6626-0.
177. Lefevre E, Bossa N, Wiesner MR, et al. A review of the environmental implications of in situ remediation by nanoscale zero valent iron (nZVI): Behavior, transport and impacts on microbial communities. *Science of The Total Environment* 2016. DOI: http://dx.doi.org/10.1016/j.scitotenv.2016.02.003.
178. Ezzatahmadi N, Ayoko GA, Millar GJ, et al. Clay-supported nanoscale zero-valent iron composite materials for the remediation of contaminated aqueous solutions: A review. *Chemical Engineering Journal* 2017; 312: 336-350. DOI: http://dx.doi.org/10.1016/j.cej.2016.11.154.
179. Liu H, Ruan X, Zhao D, et al. Enhanced Adsorption of 2,4-Dichlorophenol by Nanoscale Zero-Valent Iron Loaded on Bentonite and Modified with a Cationic Surfactant. *Industrial & Engineering Chemistry Research* 2017; 56: 191-197. DOI: 10.1021/acs.iecr.6b03864.
180. Zhu L, Gao K, Jin J, et al. Analysis of ZVI corrosion products and their functions in the combined ZVI and anaerobic sludge system. *Environmental Science and Pollution Research* 2014; 21: 12747-12756. journal article. DOI: 10.1007/s11356-014-3215-y.
181. Guan Z, Wan J, Ma Y, et al. Application of Novel Amino-Functionalized NZVI@SiO2 Nanoparticles to Enhance Anaerobic Granular Sludge Removal of 2,4,6-Trichlorophenol. *Bioinorganic Chemistry & Applications* 2015; 2015: 1-12. Article. DOI: 10.1155/2015/548961.
182. Krishna MVB, Chandrasekaran K, Karunasagar D, et al. A combined treatment approach using Fenton's reagent and zero valent iron for the removal of arsenic from drinking water. *Journal of Hazardous Materials* 2001; 84: 229-240. DOI: http://doi.org/10.1016/S0304-3894(01)00205-9.
183. Yan XL, Lin LY, Liao XY, et al. Arsenic stabilization by zero-valent iron, bauxite residue, and zeolite at a contaminated site planting Panax notoginseng. *Chemosphere* 2013; 93: 661-667. DOI: http://doi.org/10.1016/j.chemosphere.2013.05.083.
184. Liang Y, Min X, Chai L, et al. Stabilization of arsenic sludge with mechanochemically modified zero valent iron. *Chemosphere* 2017; 168: 1142-1151. DOI: http://doi.org/10.1016/j.chemosphere.2016.10.087.
185. K. Goyal A, S. Johal E and Rath G. Nanotechnology for Water Treatment. *Current Nanoscience* 2011; 7: 640-654. DOI: 10.2174/157341311796196772.
186. Dorathi PJ and Kandasamy P. Dechlorination of chlorophenols by zero valent iron impregnated silica. *Journal of Environmental Sciences* 2012; 24: 765-773. DOI: http://dx.doi.org/10.1016/S1001-0742(11)60817-6.
187. Morales J, Hutcheson R and Cheng IF. Dechlorination of chlorinated phenols by catalyzed and uncatalyzed Fe(0) and Mg(0) particles. *Journal of Hazardous Materials* 2002; 90: 97-108. DOI: 10.1016/s0304-3894(01)00336-3.
188. Tso C-p and Shih Y-h. The reactivity of well-dispersed zerovalent iron nanoparticles toward pentachlorophenol in water. *Water Research* 2015; 72: 372-380. DOI: http://dx.doi.org/10.1016/j.watres.2014.12.038.
189. Gunawardana B, Singhal N and Swedlund P. Dechlorination of pentachlorophenol by zero valent iron and bimetals: effect of surface characteristics and bimetal preparation procedure. In: *Proceedings of the Annual International Conference on Soils, Sediments, Water and Energy* 2012, p.8.
190. Cheng R, Zhou W, Wang J-L, et al. Dechlorination of pentachlorophenol using nanoscale Fe/Ni particles: Role of nano-Ni and its size effect. *Journal of Hazardous Materials* 2010; 180: 79-85. DOI: http://doi.org/10.1016/j.jhazmat.2010.03.068.
191. Kim Y-H and Carraway ER. Dechlorination of Pentachlorophenol by Zero Valent Iron and Modified Zero Valent Irons. *Environmental Science & Technology* 2000; 34: 2014-2017. DOI: 10.1021/es991129f.
192. Mohammadi AS, Sardar M and Almasian M. Fenton's oxidation of para-chlorophenol with zero-valent iron. *Desalination and Water Treatment* 2015; 53: 2924-2930. DOI: 10.1080/19443994.2013.870063.

193. Shi Z, Fan D, Johnson RL, et al. Methods for characterizing the fate and effects of nano zerovalent iron during groundwater remediation. *Journal of Contaminant Hydrology* 2015; 181: 17-35. DOI: http://dx.doi.org/10.1016/j.jconhyd.2015.03.004.
194. Li H, Wan J, Ma Y, et al. Influence of particle size of zero-valent iron and dissolved silica on the reactivity of activated persulfate for degradation of acid orange 7. *Chemical Engineering Journal* 2014; 237: 487-496. DOI: http://dx.doi.org/10.1016/j.cej.2013.10.035.
195. Suanon F, Sun Q, Mama D, et al. Effect of nanoscale zero-valent iron and magnetite (Fe3O4) on the fate of metals during anaerobic digestion of sludge. *Water Research* 2016; 88: 897-903. DOI: http://dx.doi.org/10.1016/j.watres.2015.11.014.
196. Pliego G, Zazo JA, Garcia-Muñoz P, et al. Trends in the Intensification of the Fenton Process for Wastewater Treatment: An Overview. *Critical Reviews in Environmental Science and Technology* 2015; 45: 2611-2692. DOI: 10.1080/10643389.2015.1025646.
197. Chang J, Woo H, Ko M-S, et al. Targeted removal of trichlorophenol in water by oleic acid-coated nanoscale palladium/zero-valent iron alginate beads1. *Journal of Hazardous Materials* 2015; 293: 30-36. DOI: http://dx.doi.org/10.1016/j.jhazmat.2015.03.021.
198. Yang Y, Guo J and Hu Z. Impact of nano zero valent iron (NZVI) on methanogenic activity and population dynamics in anaerobic digestion. *Water Research* 2013; 47: 6790-6800. DOI: http://dx.doi.org/10.1016/j.watres.2013.09.012.
199. Liang Y-g, Li X-j, Zhang J, et al. Effect of microscale ZVI/magnetite on methane production and bioavailability of heavy metals during anaerobic digestion of diluted pig manure. *Environmental Science and Pollution Research* 2017; 24: 12328-12337. journal article. DOI: 10.1007/s11356-017-8832-9.
200. Carpenter AW, Laughton SN and Wiesner MR. Enhanced Biogas Production from Nanoscale Zero Valent Iron-Amended Anaerobic Bioreactors. *Environmental Engineering Science* 2015; 32: 647-655. Article. DOI: 10.1089/ees.2014.0560.
201. Damianovic MHRZ, Saia FT, Moraes EM, et al. Gas chromatographic methods for monitoring of wastewater chlorophenol degradation in anaerobic reactors. *Journal Of Environmental Science And Health Part B, Pesticides, Food Contaminants, And Agricultural Wastes* 2007; 42: 45-52.
202. Antizar-Ladislao B and Galil NI. Biodegradation of 2,4,6-trichlorophenol and associated hydraulic conductivity reduction in sand-bed columns. *Chemosphere* 2006; 64: 339-349. DOI: http://dx.doi.org/10.1016/j.chemosphere.2005.12.047.
203. Pourrezaei P, Alpatova A, Khosravi K, et al. Removal of organic compounds and trace metals from oil sands process-affected water using zero valent iron enhanced by petroleum coke. *Journal of Environmental Management* 2014; 139: 50-58. DOI: http://doi.org/10.1016/j.jenvman.2014.03.001.
204. Kim H-S, Ahn J-Y, Kim C, et al. Effect of anions and humic acid on the performance of nanoscale zero-valent iron particles coated with polyacrylic acid. *Chemosphere* 2014; 113: 93-100. DOI: http://doi.org/10.1016/j.chemosphere.2014.04.047.
205. Johnson RL, Nurmi JT, O'Brien Johnson GS, et al. Field-Scale Transport and Transformation of Carboxymethylcellulose-Stabilized Nano Zero-Valent Iron. *Environmental Science & Technology* 2013; 47: 1573-1580. DOI: 10.1021/es304564q.
206. Terzi K, Sikinioti-Lock A, Gkelios A, et al. Mobility of zero valent iron nanoparticles and liposomes in porous media. *Colloids and Surfaces A: Physicochemical and Engineering Aspects* 2016; 506: 711-722. DOI: http://doi.org/10.1016/j.colsurfa.2016.07.054.
207. Mosaferi M, Nemati S, Khataee A, et al. Removal of Arsenic (III, V) from aqueous solution by nanoscale zero-valent iron stabilized with starch and carboxymethyl cellulose. *Journal of Environmental Health Science and Engineering* 2014; 12: 74-74. DOI: 10.1186/2052-336X-12-74.
208. Chen J, Xiu Z, Lowry GV, et al. Effect of natural organic matter on toxicity and reactivity of nano-scale zero-valent iron. *Water Research* 2011; 45: 1995-2001. DOI: http://doi.org/10.1016/j.watres.2010.11.036.
209. Cai-jie W and Xiao-yan L. Surface coating with Ca(OH)2 for improvement of the transport of nanoscale zero-valent iron (nZVI) in porous media. *Water Science & Technology* 2013; 68: 2287-2293. Article. DOI: 10.2166/wst.2013.494.
210. Fatisson J, Ghoshal S and Tufenkji N. Deposition of Carboxymethylcellulose-Coated Zero-Valent Iron Nanoparticles onto Silica: Roles of Solution Chemistry and Organic Molecules. *Langmuir* 2010; 26: 12832-12840. DOI: 10.1021/la1006633.
211. Raychoudhury T and Scheytt T. Potential of zerovalent iron nanoparticles for remediation of environmental organic contaminants in water: a review. *Water Science & Technology* 2013; 68: 1425-1439. Article. DOI: 10.2166/wst.2013.358.

212. Li Y, Jin Z, Li T, et al. Removal of hexavalent chromium in soil and groundwater by supported nano zero-valent iron on silica fume. *Water Science and Technology* 2011; 63: 2781-2787. DOI: 10.2166/wst.2011.454.
213. Zhang R, Li J, Liu C, et al. Reduction of nitrobenzene using nanoscale zero-valent iron confined in channels of ordered mesoporous silica. *Colloids and Surfaces A: Physicochemical and Engineering Aspects* 2013; 425: 108-114. DOI: http://dx.doi.org/10.1016/j.colsurfa.2013.02.040.
214. Qiu X, Fang Z, Liang B, et al. Degradation of decabromodiphenyl ether by nano zero-valent iron immobilized in mesoporous silica microspheres. *Journal of Hazardous Materials* 2011; 193: 70-81. DOI: http://dx.doi.org/10.1016/j.jhazmat.2011.07.024.
215. Petala E, Dimos K, Douvalis A, et al. Nanoscale zero-valent iron supported on mesoporous silica: Characterization and reactivity for Cr(VI) removal from aqueous solution. *Journal of Hazardous Materials* 2013; 261: 295-306. DOI: http://dx.doi.org/10.1016/j.jhazmat.2013.07.046.
216. Luo J, Song G, Liu J, et al. Mechanism of enhanced nitrate reduction via micro-electrolysis at the powdered zero-valent iron/activated carbon interface. *Journal of Colloid and Interface Science* 2014; 435: 21-25. DOI: http://doi.org/10.1016/j.jcis.2014.08.043.
217. Fu F, Ma J, Xie L, et al. Chromium removal using resin supported nanoscale zero-valent iron. *Journal of Environmental Management* 2013; 128: 822-827. DOI: http://doi.org/10.1016/j.jenvman.2013.06.044.
218. Su F, Zhou H, Zhang Y, et al. Three-dimensional honeycomb-like structured zero-valent iron/chitosan composite foams for effective removal of inorganic arsenic in water. *Journal of Colloid and Interface Science* 2016; 478: 421-429. DOI: http://doi.org/10.1016/j.jcis.2016.06.035.
219. Li Y, Zhang Y, Li J, et al. Enhanced reduction of chlorophenols by nanoscale zerovalent iron supported on organobentonite. *Chemosphere* 2013; 92: 368-374. DOI: http://dx.doi.org/10.1016/j.chemosphere.2013.01.030.
220. Yu K, Sheng GD and McCall W. Cosolvent Effects on Dechlorination of Soil-Sorbed Polychlorinated Biphenyls Using Bentonite Clay-Templated Nanoscale Zero Valent Iron. *Environmental Science & Technology* 2016; 50: 12949-12956. DOI: 10.1021/acs.est.6b02933.
221. Gu C, Jia H, Li H, et al. Synthesis of Highly Reactive Subnano-Sized Zero-Valent Iron Using Smectite Clay Templates. *Environmental Science & Technology* 2010; 44: 4258-4263. DOI: 10.1021/es903801r.
222. Li X, Zhao Y, Xi B, et al. Removal of nitrobenzene by immobilized nanoscale zero-valent iron: Effect of clay support and efficiency optimization. *Applied Surface Science* 2016; 370: 260-269. DOI: http://doi.org/10.1016/j.apsusc.2016.01.141.
223. Jiang Z, Lv L, Zhang W, et al. Nitrate reduction using nanosized zero-valent iron supported by polystyrene resins: Role of surface functional groups. *Water Research* 2011; 45: 2191-2198. DOI: http://doi.org/10.1016/j.watres.2011.01.005.
224. Choi H, Al-Abed SR, Agarwal S, et al. Synthesis of Reactive Nano-Fe/Pd Bimetallic System-Impregnated Activated Carbon for the Simultaneous Adsorption and Dechlorination of PCBs. *Chemistry of Materials* 2008; 20: 3649-3655. DOI: 10.1021/cm8003613.
225. Botes M and Eugene Cloete T. The potential of nanofibers and nanobiocides in water purification. *Critical Reviews in Microbiology* 2010; 36: 68-81.
226. Arkas M, Allabashi R, Tsiourvas D, et al. Organic/Inorganic Hybrid Filters Based on Dendritic and Cyclodextrin "Nanosponges" for the Removal of Organic Pollutants from Water. *Environmental Science & Technology* 2006; 40: 2771-2777. DOI: 10.1021/es052290v.
227. Sawicki R and Mercier L. Evaluation of Mesoporous Cyclodextrin-Silica Nanocomposites for the Removal of Pesticides from Aqueous Media. *Environmental Science & Technology* 2006; 40: 1978-1983. DOI: 10.1021/es051441r.
228. Pradeep T and Anshup. Noble metal nanoparticles for water purification: A critical review. *Thin Solid Films* 2009; 517: 6441-6478. DOI: 10.1016/j.tsf.2009.03.195.
229. Qiu X, Fang Z, Liang B, et al. Degradation of decabromodiphenyl ether by nano zero-valent iron immobilized in mesoporous silica microspheres. *Journal of Hazardous Materials* 2011; 193: 70-81. DOI: http://dx.doi.org/10.1016/j.jhazmat.2011.07.024.
230. ABSMaterials. ABSMaterials: Applying 21st century material science to problems of the 20th century chemistry, http://www.absmaterials.com/ (2014, accessed July 14 2014 2014).
231. Berenguer R, Marco-Lozar JP, Quijada C, et al. Effect of electrochemical treatments on the surface chemistry of activated carbon. *Carbon* 2009; 47: 1018-1027. DOI: http://dx.doi.org/10.1016/j.carbon.2008.12.022.
232. Alvarez G, Foglia M, Copello G, et al. Effect of various parameters on viability and growth of bacteria immobilized in sol–gel-derived silica matrices. *Applied Microbiology & Biotechnology* 2009; 82: 639-646. Article. DOI: 10.1007/s00253-008-1783-9.

233. Hegde N, Hirashima H and Venkateswara Rao A. Two step sol-gel processing of TEOS based hydrophobic silica aerogels using trimethylethoxysilane as a co-precursor. *Journal of Porous Materials* 2007; 14: 165-171. DOI: 10.1007/s10934-006-9021-2.
234. Jitianu A, Crisan M, Meghea A, et al. Influence of the silica based matrix on the formation of iron oxide nanoparticles in the Fe2O3-SiO2 system, obtained by sol-gel method. *Journal of Materials Chemistry* 2002; 12: 1401-1407. 10.1039/B110652J. DOI: 10.1039/B110652J.
235. Heaney PJ, Prewitt CT and Gibbs GV. *Silica : physical behavior, geochemistry and materials applications / editors: P.J. Heaney, C.T. Prewitt, G.V. Gibbs*. Washigton, D.C. : Mineralogical Society of America, [1994], ©1994., 1994.
236. Edmiston PL, Osborne C, Reinbold KP, et al. Pilot scale testing composite swellable organosilica nanoscale zero-valent iron-Iron-Osorb®-for in situ remediation of trichloroethylene. *Remediation Journal* 2011; 22: 105-123. Article. DOI: 10.1002/rem.21302.
237. Underwood L. *Synthesis and Use of a Novel Nanomaterial for the Removal of Phenol in Water Systems*. University of Edinburgh, Edinburgh, 2013.
238. Schrick B, Blough JL, Jones AD, et al. Hydrodechlorination of Trichloroethylene to Hydrocarbons Using Bimetallic Nickel–Iron Nanoparticles. *Chemistry of Materials* 2002; 14: 5140-5147. DOI: 10.1021/cm020737i.
239. Cao J, Xu R, Tang H, et al. Synthesis of monodispersed CMC-stabilized Fe–Cu bimetal nanoparticles for in situ reductive dechlorination of 1, 2, 4-trichlorobenzene. *Science of The Total Environment* 2011; 409: 2336-2341. DOI: 10.1016/j.scitotenv.2011.02.045.
240. Fang Y-L, Miller JT, Guo N, et al. Structural analysis of palladium-decorated gold nanoparticles as colloidal bimetallic catalysts. *Catalysis Today* 2011; 160: 96-102. DOI: 10.1016/j.cattod.2010.08.010.
241. Zheng C, Zhao J, Bao P, et al. Dispersive liquid–liquid microextraction based on solidification of floating organic droplet followed by high-performance liquid chromatography with ultraviolet detection and liquid chromatography–tandem mass spectrometry for the determination of triclosan and 2,4-dichlorophenol in water samples. *Journal of Chromatography A* 2011; 1218: 3830-3836. DOI: 10.1016/j.chroma.2011.04.050.
242. Wu P, Liu C, Huang Z, et al. Enhanced dechlorination performance of 2,4-dichlorophenol by vermiculite supported iron nanoparticles doped with palladium. *RSC Advances* 2014; 4: 25580-25587. 10.1039/C4RA02618G. DOI: 10.1039/C4RA02618G.
243. Wang X, Li F and Yang J. Polyvinyl pyrrolidone-modified Pd/Fe nanoparticles for enhanced dechlorination of 2,4-dichlorophenal. *Desalination and Water Treatment* 2014; 52: 7925-7936. DOI: 10.1080/19443994.2013.833870.
244. Fan J, Wang H and Ma L. Oxalate-assisted oxidative degradation of 4-chlorophenol in a bimetallic, zero-valent iron–aluminum/air/water system. *Environmental Science and Pollution Research* 2016; 23: 16686-16698. DOI: 10.1007/s11356-016-6628-y.
245. Wang C-B and Zhang W-x. Synthesizing Nanoscale Iron Particles for Rapid and Complete Dechlorination of TCE and PCBs. *Environmental Science & Technology* 1997; 31: 2154-2156. DOI: 10.1021/es970039c.
246. Lien H-L and Zhang W-x. Transformation of Chlorinated Methanes by Nanoscale Iron Particles. *Journal of Environmental Engineering* 1999; 125: 1042-1047. DOI: doi:10.1061/(ASCE)0733-9372(1999)125:11(1042).
247. Choe S, Lee S-H, Chang Y-Y, et al. Rapid reductive destruction of hazardous organic compounds by nanoscale Fe0. *Chemosphere* 2001; 42: 367-372. DOI: https://doi.org/10.1016/S0045-6535(00)00147-8.
248. Reardon EJ, Fagan R, Vogan JL, et al. Anaerobic Corrosion Reaction Kinetics of Nanosized Iron. *Environmental Science & Technology* 2008; 42: 2420-2425. DOI: 10.1021/es0712120.
249. Odesie. Iron Corrosion in Aerated Water as a Function of pH, https://www.myodesie.com/wiki/index/returnEntry/id/3049 (2017, accessed December 12 2017).
250. Greenlee LF and Hooker SA. Development of stabilized zero valent iron nanoparticles. *Desalination & Water Treatment* 2012; 37/38: 114-121. Article. DOI: 10/5004/dwt.2012.2526.
251. Xu Y, Wang C, Hou J, et al. Application of zero valent iron coupling with biological process for wastewater treatment: a review. *Reviews in Environmental Science and Bio/Technology* 2017; 16: 667-693. journal article. DOI: 10.1007/s11157-017-9445-y.
252. Olu-Owolabi BI, Alabi AH, Diagboya PN, et al. Adsorptive removal of 2,4,6-trichlorophenol in aqueous solution using calcined kaolinite-biomass composites. *Journal of Environmental Management* 2017; 192: 94-99. DOI: https://doi.org/10.1016/j.jenvman.2017.01.055.
253. He F, Zhao D and Roberts C. Chapter 31 - Stabilization of Zero-Valent Iron Nanoparticles for Enhanced In Situ Destruction of Chlorinated Solvents in Soils and Groundwater A2 - Street, Anita. In: Sustich R,

Duncan J and Savage N (eds) *Nanotechnology Applications for Clean Water (Second Edition)*. Oxford: William Andrew Publishing, 2014, pp.491-501.
254. Han Y, Li W, Zhang M, et al. Catalytic dechlorination of monochlorobenzene with a new type of nanoscale Ni(B)/Fe(B) bimetallic catalytic reductant. *Chemosphere* 2008; 72: 53-58. DOI: 10.1016/j.chemosphere.2008.02.002.
255. Ficai D, Ficai A and Andronescu E. 1 - Recent advances in using magnetic materials for environmental applications A2 - Grumezescu, Alexandru Mihai. *Water Purification*. Academic Press, 2017, pp.1-32.
256. Su C. Environmental implications and applications of engineered nanoscale magnetite and its hybrid nanocomposites: A review of recent literature. *Journal of Hazardous Materials* 2017; 322: 48-84. DOI: https://doi.org/10.1016/j.jhazmat.2016.06.060.
257. Li Y, Zhang J, Zhang Y, et al. Scaling-up of a zero valent iron packed anaerobic reactor for textile dye wastewater treatment: a potential technology for on-site upgrading and rebuilding of traditional anaerobic wastewater treatment plant. *Water Science and Technology* 2017; 76: 823-831. DOI: 10.2166/wst.2017.270.
258. Feng J and Lim T-T. Pathways and kinetics of carbon tetrachloride and chloroform reductions by nano-scale Fe and Fe/Ni particles: comparison with commercial micro-scale Fe and Zn. *Chemosphere* 2005; 59: 1267-1277. DOI: 10.1016/j.chemosphere.2004.11.038.
259. Determination of the specific surface area of solids by gas adsorption. BET method.
260. Do DD, Do HD and Nicholson D. A computer appraisal of BET theory, BET surface area and the calculation of surface excess for gas adsorption on a graphite surface. *Chemical Engineering Science* 2010; 65: 3331-3340. DOI: http://dx.doi.org/10.1016/j.ces.2010.02.023.
261. Stevens JG, Khasanov AM and Mabe DR. Mössbauer and X-Ray Diffraction Investigations of a Series of B-Doped Ferrihydrites. *Hyperfine Interactions* 2005; 161: 83-92. journal article. DOI: 10.1007/s10751-005-9170-8.
262. Du D, Asiri AM, Wang J, et al. Chapter 3 - Electrochemical Biosensors Based on Nanomaterials for Detection of Pesticides and Explosives A2 - Street, Anita. In: Sustich R, Duncan J and Savage N (eds) *Nanotechnology Applications for Clean Water (Second Edition)*. Oxford: William Andrew Publishing, 2014, pp.47-62.
263. Eisenbeis G. Scanning Electron Microscopy and X-Ray Microanalysis: Joseph Goldstein, Dale E. Newbury, David C. Joy, Charles E. Lyman, Patrick Echlin, Eric Lifshin, Linda C. Sawyer, J.R. Michael (Eds.), Kluwer Academic/Plenum Publishers, New York/Boston/Dordrecht/London/Moscow, 2003, pp. 689 (Hardbound. Price: €76.50/US $75.00/GB £48.00). *Micron* 2003; 34: 453. DOI: http://dx.doi.org/10.1016/j.micron.2003.08.001.
264. Dékány I. Chapter 3.9 Adsorption and immersional wetting on hydrophilic and hydrophobic silicates. In: Dąbrowski A and Tertykh VA (eds) *Studies in Surface Science and Catalysis*. Elsevier, 1996, pp.879-897.
265. Papirer E and Balard H. Chapter 2.6 Chemical and morphological characteristics of inorganic sorbents with respect to gas adsorption. In: Dąbrowski A and Tertykh VA (eds) *Studies in Surface Science and Catalysis*. Elsevier, 1996, pp.479-502.
266. Dąbrowski A, Leboda R, Goworek J, et al. Chapter 3.1 Characterization of inorganic sorbents by means of adsorption at the liquid—solid interface. In: Dąbrowski A and Tertykh VA (eds) *Studies in Surface Science and Catalysis*. Elsevier, 1996, pp.649-672.
267. Tertykh VA and Yanishpolskii VV. Chapter 3.3 Equilibria of adsorption from solutions on the silica surface. In: Dąbrowski A and Tertykh VA (eds) *Studies in Surface Science and Catalysis*. Elsevier, 1996, pp.705-727.
268. Shi Z, Nurmi JT and Tratnyek PG. Effects of Nano Zero-Valent Iron on Oxidation−Reduction Potential. *Environmental Science & Technology* 2011; 45: 1586-1592. DOI: 10.1021/es103185t.
269. Commerce UDo. National Institute of Standards in Technology. In: Govenment U, (ed.). 2017.
270. Spijkerman JJ. *Mossbauer spectroscopy standard for the chemical shift of iron compounds*. Washington: U.S. Dept. of Commerce, National Bureau of Standards: for sale by the Supt. of Docs., U.S. Govt. Print. Off., 1967, p.47 p.
271. Greenblatt S and King FT. Mössbauer Spectra of Some Magnetic Iron Hydroxides Precipitated by Porous Silica. *Journal of Applied Physics* 1969; 40: 4498-4500. DOI: doi:http://dx.doi.org/10.1063/1.1657221.
272. Sunil D, Dong J and Gafney HD. Influence of Amorphous Silica Matrices on the Formation, Structure, and Chemistry of Iron and Iron Oxide Nanoparticles. *Journal of the American Chemical Society* 2009; 131: 14768-14777. DOI: 10.1021/ja9031874.

273. Wightman PG and Fein JB. Experimental study of 2,4,6-Trichlorophenol and pentachlorophenol solubilities in aqueous solutions: derivation of a speciation-based Chlorophenol solubility model. *Applied Geochemistry* 1999; 14: 319-331. DOI: https://doi.org/10.1016/S0883-2927(98)00054-7.
274. Yan H, Du Q, Yang H, et al. Efficient removal of chlorophenols from water with a magnetic reduced graphene oxide composite. *Science China Chemistry* 2016; 59: 350-359. DOI: 10.1007/s11426-015-5482-y.
275. Liu Y, Chen J, Chen M, et al. Adsorption characteristics and mechanism of sewage sludge-derived adsorbent for removing sulfonated methyl phenol resin in wastewater. *RSC Advances* 2015; 5: 76160-76169. 10.1039/C5RA17125C. DOI: 10.1039/C5RA17125C.
276. Garbou AM, Clausen CA and Yestrebsky CL. Comparative study for the removal and destruction of pentachlorophenol using activated magnesium treatment systems. *Chemosphere* 2017; 166: 267-274. DOI: http://dx.doi.org/10.1016/j.chemosphere.2016.09.139.
277. Chang C, Lian F and Zhu L. Simultaneous adsorption and degradation of γ-HCH by nZVI/Cu bimetallic nanoparticles with activated carbon support. *Environmental Pollution* 2011; 159: 2507-2514. DOI: 10.1016/j.envpol.2011.06.021.
278. Fan J, Zhang J, Zhang C, et al. Adsorption of 2,4,6-trichlorophenol from aqueous solution onto activated carbon derived from loosestrife. *Desalination* 2011; 267: 139-146. DOI: http://dx.doi.org/10.1016/j.desal.2010.09.016.
279. Murray A and Ormeci B. Application of molecularly imprinted and non-imprinted polymers for removal of emerging contaminants in water and wastewater treatment: a review. *Environmental Science And Pollution Research International* 2012; 19: 3820-3830. DOI: 10.1007/s11356-012-1119-2.
280. Chen W, Duan L and Zhu D. Adsorption of Polar and Nonpolar Organic Chemicals to Carbon Nanotubes. *Environmental Science & Technology* 2007; 41: 8295-8300. DOI: 10.1021/es071230h.
281. Wang X, Ning P, Liu H, et al. Dechlorination of chloroacetic acids by Pd/Fe nanoparticles: Effect of drying method on metallic activity and the parameter optimization. *Applied Catalysis B: Environmental* 2010; 94: 55-63. DOI: http://doi.org/10.1016/j.apcatb.2009.10.020.
282. Scotland AG. *Drinking Water Quality in Scotland 2010*. 2011. Drinking Water Quality Regulator.
283. Xie W, Zheng Z, Tang M, et al. Solubilities and Activity Coefficients of Chlorobenzenes and Chlorophenols in Aqueous Salt Solutions. *Journal of Chemical & Engineering Data* 1994; 39: 568-571. DOI: 10.1021/je00015a038.
284. Ruppert J, Frimmel F, Baier R, et al. Comparison of corrosion rates obtained from laboratory and field data. *Materials and Corrosion* 2016; 67: 660-666. DOI: 10.1002/maco.201608935.
285. Huang YH and Zhang TC. Effects of dissolved oxygen on formation of corrosion products and concomitant oxygen and nitrate reduction in zero-valent iron systems with or without aqueous Fe2+. *Water Research* 2005; 39: 1751-1760. DOI: https://doi.org/10.1016/j.watres.2005.03.002.
286. Aslam M, McCarty PL, Bae J, et al. The effect of fluidized media characteristics on membrane fouling and energy consumption in anaerobic fluidized membrane bioreactors. *Separation and Purification Technology* 2014; 132: 10-15. Article. DOI: 10.1016/j.seppur.2014.04.049.
287. Yu B, Huang X, Zhang D, et al. Response of sludge fermentation liquid and microbial community to nano zero-valent iron exposure in a mesophilic anaerobic digestion system. *RSC Advances* 2016; 6: 24236-24244. 10.1039/C6RA02591A. DOI: 10.1039/C6RA02591A.
288. Wang K, Yin J, Shen D, et al. Anaerobic digestion of food waste for volatile fatty acids (VFAs) production with different types of inoculum: Effect of pH. *Bioresource Technology* 2014; 161: 395-401. DOI: http://dx.doi.org/10.1016/j.biortech.2014.03.088.
289. Pullin H, Crane RA, Morgan DJ, et al. The effect of common groundwater anions on the aqueous corrosion of zero-valent iron nanoparticles and associated removal of aqueous copper and zinc. *Journal of Environmental Chemical Engineering* 2017; 5: 1166-1173. DOI: https://doi.org/10.1016/j.jece.2017.01.038.
290. Karar E. *Freshwater Governance for the 21st Century*. Cham : Springer International Publishing : Imprint: Springer, 2017.
291. Ziolkowska JR and Reyes R. Chapter 3.1.3 - Prospects for Desalination in the United States—Experiences From California, Florida, and Texas. *Competition for Water Resources*. Elsevier, 2017, pp.298-316.
292. Li X-q and Zhang W-x. Sequestration of Metal Cations with Zerovalent Iron NanoparticlesA Study with High Resolution X-ray Photoelectron Spectroscopy (HR-XPS). *The Journal of Physical Chemistry C* 2007; 111: 6939-6946. DOI: 10.1021/jp0702189.

293. Zhang M, He F, Zhao D, et al. Degradation of soil-sorbed trichloroethylene by stabilized zero valent iron nanoparticles: Effects of sorption, surfactants, and natural organic matter. *Water Research* 2011; 45: 2401-2414. DOI: https://doi.org/10.1016/j.watres.2011.01.028.
294. Giasuddin ABM, Kanel SR and Choi H. Adsorption of Humic Acid onto Nanoscale Zerovalent Iron and Its Effect on Arsenic Removal. *Environmental Science & Technology* 2007; 41: 2022-2027. DOI: 10.1021/es0616534.
295. Sjöstedt CS, Gustafsson JP and Köhler SJ. Chemical Equilibrium Modeling of Organic Acids, pH, Aluminum, and Iron in Swedish Surface Waters. *Environmental Science and Technology* 2010; 44: 8587-8593. DOI: 10.1021/es102415r.
296. Wilkin RT and DiGiulio DC. Geochemical Impacts to Groundwater from Geologic Carbon Sequestration: Controls on pH and Inorganic Carbon Concentrations from Reaction Path and Kinetic Modeling. *Environmental Science & Technology* 2010; 44: 4821-4827. DOI: 10.1021/es100559j.
297. Segura Y, Puyol D, Ballesteros L, et al. Wastewater sludges pretreated by different oxidation systems at mild conditions to promote the biogas formation in anaerobic processes. *Environmental Science and Pollution Research* 2016; 23: 24393-24401. DOI: 10.1007/s11356-016-7535-y.
298. Raffin M, Germain E and Judd S. Wastewater polishing using membrane technology: a review of existing installations. *Environmental Technology* 2013; 34: 617-627. Article. DOI: 10.1080/09593330.2012.710385.
299. Latif MA, Mehta CM and Batstone DJ. Influence of low pH on continuous anaerobic digestion of waste activated sludge. *Water Research* 2017; 113: 42-49. DOI: http://dx.doi.org/10.1016/j.watres.2017.02.002.
300. Fanaie VR, Karrabi M, Amin MM, et al. Biosorption of 4-chlorophenol by dried anaerobic digested sludge: artificial neural network modeling, equilibrium isotherm, and kinetic study. *International Journal of Environmental Science and Technology* 2017; 14: 37-48. DOI: 10.1007/s13762-016-1139-4.
301. Wang T, Wang S, Luo Q, et al. Hydrogen Adsorption Structures and Energetics on Iron Surfaces at High Coverage. *The Journal of Physical Chemistry C* 2014; 118: 4181-4188. DOI: 10.1021/jp410635z.
302. Yaws CL and Narasimhan PK. Chapter 19 - Dipole moment—Organic compounds. *Thermophysical Properties of Chemicals and Hydrocarbons*. Norwich, NY: William Andrew Publishing, 2009, pp.672-682.
303. Dorosh O and Kisiel Z. Electric dipole moments of acetone and of acetic acid measured in supersonic expansion. *Acta Phys Pol A* 2007; 112: S95-S104.
304. Stiefvater OL. Microwave spectrum of propionic acid. I. Spectrum, dipole moment, barrier to internal rotation, and low‐frequency vibrations of c i s ‐propionic acid. *The Journal of Chemical Physics* 1975; 62: 233-243. DOI: 10.1063/1.430268.
305. Fu F, Cheng Z and Lu J. Synthesis and use of bimetals and bimetal oxides in contaminants removal from water: a review. *RSC Advances* 2015; 5: 85395-85409. 10.1039/C5RA13067K. DOI: 10.1039/C5RA13067K.
306. Abdelsalam E, Samer M, Attia YA, et al. Influence of zero valent iron nanoparticles and magnetic iron oxide nanoparticles on biogas and methane production from anaerobic digestion of manure. *Energy* 2017; 120: 842-853. DOI: http://dx.doi.org/10.1016/j.energy.2016.11.137.
307. Zhang Y, Feng Y and Quan X. Zero-valent iron enhanced methanogenic activity in anaerobic digestion of waste activated sludge after heat and alkali pretreatment. *Waste Management* 2015; 38: 297-302. DOI: http://dx.doi.org/10.1016/j.wasman.2015.01.036.
308. Behnassi M, Ramachandran G, Shelat K, et al. *Vulnerability of agriculture, water and fisheries to climate change toward sustainable adaptation strategies*. Dordrecht : Springer, 2014.
309. Zhao Z, Li Y, Yu Q, et al. Ferroferric oxide triggered possible direct interspecies electron transfer between Syntrophomonas and Methanosaeta to enhance waste activated sludge anaerobic digestion. *Bioresource Technology* 2018; 250: 79-85. DOI: https://doi.org/10.1016/j.biortech.2017.11.003.
310. McMichael AJ, Powles JW, Butler CD, et al. Food, livestock production, energy, climate change, and health. *The Lancet*; 370: 1253-1263. DOI: http://dx.doi.org/10.1016/S0140-6736(07)61256-2.
311. The AD Cycle & Inside the Digester, http://adbioresources.org/about-ad/what-is-ad/ (2017, accessed March 22nd 2017 2017).
312. Hao X, Wei J, van Loosdrecht MCM, et al. Analysing the mechanisms of sludge digestion enhanced by iron. *Water Research* 2017; 117: 58-67. DOI: https://doi.org/10.1016/j.watres.2017.03.048.
313. Nelles M and Pivato A. Special Section: Biological Waste to Energy. *Waste Management* 2018; 71: 603-604. DOI: https://doi.org/10.1016/j.wasman.2017.11.046.
314. Ho L and Ho G. Mitigating ammonia inhibition of thermophilic anaerobic treatment of digested piggery wastewater: Use of pH reduction, zeolite, biomass and humic acid. *Water Research* 2012; 46: 4339-4350. DOI: http://dx.doi.org/10.1016/j.watres.2012.05.016.

315. Altaş L. Inhibitory effect of heavy metals on methane-producing anaerobic granular sludge. *Journal of Hazardous Materials* 2009; 162: 1551-1556. DOI: http://dx.doi.org/10.1016/j.jhazmat.2008.06.048.
316. Nayono SE, Winter J and Gallert C. Anaerobic digestion of pressed off leachate from the organic fraction of municipal solid waste. *Waste Management* 2010; 30: 1828-1833. DOI: http://dx.doi.org/10.1016/j.wasman.2009.09.019.
317. Li C and Fang HHP. Inhibition of heavy metals on fermentative hydrogen production by granular sludge. *Chemosphere* 2007; 67: 668-673. DOI: http://dx.doi.org/10.1016/j.chemosphere.2006.11.005.
318. Karri S, Sierra-Alvarez R and Field JA. Toxicity of copper to acetoclastic and hydrogenotrophic activities of methanogens and sulfate reducers in anaerobic sludge. *Chemosphere* 2006; 62: 121-127. DOI: http://dx.doi.org/10.1016/j.chemosphere.2005.04.016.
319. Mori K, Hatsu M, Kimura R, et al. Effect of heavy metals on the growth of a methanogen in pure culture and coculture with a sulfate-reducing bacterium. *Journal of Bioscience and Bioengineering* 2000; 90: 260-265. DOI: http://dx.doi.org/10.1016/S1389-1723(00)80079-1.
320. Yu HQ and Fang HHP. Inhibition on Acidogenesis of Dairy Wastewater by Zinc and Copper. *Environmental Technology* 2001; 22: 1459-1465. DOI: 10.1080/09593332208618183.
321. Yu HQ and Fang HHP. Inhibition by chromium and cadmium of anaerobic acidogenesis. *Water Science and Technology* 2001; 43: 267-274.
322. Zayed G and Winter J. Inhibition of methane production from whey by heavy metals – protective effect of sulfide. *Applied Microbiology and Biotechnology* 2000; 53: 726-731. journal article. DOI: 10.1007/s002530000336.
323. Utgikar VP, Tabak HH, Haines JR, et al. Quantification of toxic and inhibitory impact of copper and zinc on mixed cultures of sulfate-reducing bacteria. *Biotechnology and Bioengineering* 2003; 82: 306-312. DOI: 10.1002/bit.10575.
324. Leighton IR and Forster CF. The Effect of Heavy Metal Ions on the Performance of a Two-Phase Thermophilic Anaerobic Digester. *Process Safety and Environmental Protection* 1997; 75: 27-32. DOI: http://dx.doi.org/10.1205/095758297528742.
325. Palatsi J, Laureni M, Andrés MV, et al. Strategies for recovering inhibition caused by long chain fatty acids on anaerobic thermophilic biogas reactors. *Bioresource Technology* 2009; 100: 4588-4596. DOI: http://dx.doi.org/10.1016/j.biortech.2009.04.046.
326. Díaz-Báez MC and Valderrama-Rincon JD. Rapid restoration of methanogenesis in an acidified UASB reactor treating 2,4,6-trichlorophenol (TCP). *Journal of Hazardous Materials* 2017; 324: 599-604. DOI: https://doi.org/10.1016/j.jhazmat.2016.11.031.
327. Puyol D, Sanz JL, Rodriguez JJ, et al. Inhibition of methanogenesis by chlorophenols: a kinetic approach. *New Biotechnology* 2012; 30: 51-61. DOI: http://dx.doi.org/10.1016/j.nbt.2012.07.011.
328. Nyberg L, Turco RF and Nies L. Assessing the Impact of Nanomaterials on Anaerobic Microbial Communities. *Environmental Science & Technology* 2008; 42: 1938-1943. DOI: 10.1021/es072018g.
329. Stasinakis AS. Review on the fate of emerging contaminants during sludge anaerobic digestion. *Bioresource Technology* 2012; 121: 432-440. DOI: http://dx.doi.org/10.1016/j.biortech.2012.06.074.
330. Yang Y, Zhang C and Hu Z. Impact of metallic and metal oxide nanoparticles on wastewater treatment and anaerobic digestion. *Environmental Science: Processes & Impacts* 2013; 15: 39-48. 10.1039/C2EM30655G. DOI: 10.1039/C2EM30655G.
331. Yadav T, Mungray AA and Mungray AK. Effect of multiwalled carbon nanotubes on UASB microbial consortium. *Environmental Science and Pollution Research* 2016; 23: 4063-4072. journal article. DOI: 10.1007/s11356-015-4385-y.
332. Zhang Z-Z, Xu J-J, Shi Z-J, et al. Unraveling the impact of nanoscale zero-valent iron on the nitrogen removal performance and microbial community of anammox sludge. *Bioresource Technology* 2017; 243: 883-892. DOI: https://doi.org/10.1016/j.biortech.2017.07.049.
333. T C, Y. Z DAI, C C, et al. Zero-Valent Iron Supported Microbial Reductive Dechlorination of 2,4-Dichlorophenol. *Asian Journal of Chemistry* 2012; 24: 2579-2584. Article.
334. Wang T, Zhang D, Dai L, et al. Effects of Metal Nanoparticles on Methane Production from Waste-Activated Sludge and Microorganism Community Shift in Anaerobic Granular Sludge. *Scientific Reports* 2016; 6: 25857. Article. DOI: 10.1038/srep25857 https://www.nature.com/articles/srep25857#supplementary-information.
335. Cioabla AE, Ionel I, Dumitrel G-A, et al. Comparative study on factors affecting anaerobic digestion of agricultural vegetal residues. *Biotechnology for Biofuels* 2012; 5: 39-39. DOI: 10.1186/1754-6834-5-39.
336. Nghiem LD, Manassa P, Dawson M, et al. Oxidation reduction potential as a parameter to regulate micro-oxygen injection into anaerobic digester for reducing hydrogen sulphide concentration in biogas. *Bioresource Technology* 2014; 173: 443-447. DOI: https://doi.org/10.1016/j.biortech.2014.09.052.

337. Hilton MG and Archer DB. Anaerobic digestion of a sulfate-rich molasses wastewater: Inhibition of hydrogen sulfide production. *Biotechnology and Bioengineering* 1988; 31: 885-888. DOI: 10.1002/bit.260310817.
338. Wang Q, Sun J, Song K, et al. Combined zero valent iron and hydrogen peroxide conditioning significantly enhances the dewaterability of anaerobic digestate. *Journal of Environmental Sciences* 2017. DOI: https://doi.org/10.1016/j.jes.2017.04.004.
339. Li X, Zhang W, Xue S, et al. Enrichment of d-lactic acid from organic wastes catalyzed by zero-valent iron: an approach for sustainable lactate isomerization. *Green Chemistry* 2017; 19: 928-936. 10.1039/C6GC02402E. DOI: 10.1039/C6GC02402E.
340. Dykstra CM and Pavlostathis SG. Zero-Valent Iron Enhances Biocathodic Carbon Dioxide Reduction to Methane. *Environmental Science & Technology* 2017; 51: 12956-12964. DOI: 10.1021/acs.est.7b02777.
341. Kong X, Yu S, Xu S, et al. Effect of Fe0 addition on volatile fatty acids evolution on anaerobic digestion at high organic loading rates. *Waste Management* 2018; 71: 719-727. DOI: https://doi.org/10.1016/j.wasman.2017.03.019.
342. Wang T, Qin Y, Cao Y, et al. Simultaneous addition of zero-valent iron and activated carbon on enhanced mesophilic anaerobic digestion of waste-activated sludge. *Environmental Science and Pollution Research* 2017; 24: 22371-22381. journal article. DOI: 10.1007/s11356-017-9859-7.
343. Puyol D, Flores-Alsina X, Segura Y, et al. Exploring the effects of ZVI addition on resource recovery in the anaerobic digestion process. *Chemical Engineering Journal* 2018; 335: 703-711. DOI: https://doi.org/10.1016/j.cej.2017.11.029.
344. Antwi P, Li J, Boadi PO, et al. Dosing effect of zero valent iron (ZVI) on biomethanation and microbial community distribution as revealed by 16S rRNA high-throughput sequencing. *International Biodeterioration & Biodegradation* 2017; 123: 191-199. DOI: https://doi.org/10.1016/j.ibiod.2017.06.022.
345. Xu X, Gao X, Jin J, et al. A novel bioelectrode and anaerobic sludge coupled system for p-ClNB degradation by magnetite nanoparticles addition. *Environmental Science and Pollution Research* 2017; 24: 16220-16227. DOI: 10.1007/s11356-017-9047-9.
346. Jia H, Yang G, Ngo H-H, et al. Enhancing simultaneous response and amplification of biosensor in microbial fuel cell-based upflow anaerobic sludge bed reactor supplemented with zero-valent iron. *Chemical Engineering Journal* 2017; 327: 1117-1127. DOI: https://doi.org/10.1016/j.cej.2017.06.181.
347. Pan F, Zhong X, Xia D, et al. Nanoscale zero-valent iron/persulfate enhanced upflow anaerobic sludge blanket reactor for dye removal: Insight into microbial metabolism and microbial community. *Scientific Reports* 2017; 7: 44626. Article. DOI: 10.1038/srep44626 https://www.nature.com/articles/srep44626#supplementary-information.
348. Günay T and Çimen Y. Degradation of 2,4,6-trichlorophenol with peroxymonosulfate catalyzed by soluble and supported iron porphyrins. *Environmental Pollution* 2017; 231: 1013-1020. DOI: https://doi.org/10.1016/j.envpol.2017.08.059.
349. Lopez RFV, Seto JE, Blankschtein D, et al. Enhancing the transdermal delivery of rigid nanoparticles using the simultaneous application of ultrasound and sodium lauryl sulfate. *Biomaterials* 2011; 32: 933-941. DOI: https://doi.org/10.1016/j.biomaterials.2010.09.060.
350. Manusadžianas L, Caillet C, Fachetti L, et al. Toxicity of copper oxide nanoparticle suspensions to aquatic biota. *Environmental Toxicology & Chemistry* 2012; 31: 108-114. Article. DOI: 10.1002/etc.715.
351. Muñoz A and Costa M. Elucidating the mechanisms of nickel compound uptake: A review of particulate and nano-nickel endocytosis and toxicity. *Toxicology & Applied Pharmacology* 2012; 260: 1-16. Article. DOI: 10.1016/j.taap.2011.12.014.
352. Hosseini MJ, Jafarian I, Farahani S, et al. New mechanistic approach of inorganic palladium toxicity: impairment in mitochondrial electron transfer. *Metallomics* 2016; 8: 252-259. 10.1039/C5MT00249D. DOI: 10.1039/C5MT00249D.
353. Mountfort DO and Kaspar HF. Palladium-Mediated Hydrogenation of Unsaturated Hydrocarbons with Hydrogen Gas Released during Anaerobic Cellulose Degradation. *Applied and Environmental Microbiology* 1986; 52: 744-750.
354. Al - Ahmad AE, Hiligsmann S, Lambert S, et al. Effect of encapsulated nanoparticles on thermophillic anaerobic digestion. In: Cwbi, (ed.). 2014.
355. Windt WD, Aelterman P and Verstraete W. Bioreductive deposition of palladium (0) nanoparticles on Shewanella oneidensis with catalytic activity towards reductive dechlorination of polychlorinated biphenyls. *Environmental Microbiology* 2005; 7: 314-325. DOI: 10.1111/j.1462-2920.2005.00696.x.

356. Zhao D, Gao X, Wu C, et al. Facile preparation of amino functionalized graphene oxide decorated with Fe3O4 nanoparticles for the adsorption of Cr(VI). *Applied Surface Science* 2016; 384: 1-9. DOI: https://doi.org/10.1016/j.apsusc.2016.05.022.
357. Liu W. Reductive dehalogenation of polyhalogenated solvents and flame retardents using zero valent iron based bimetallic particles. In: Huang W, Gerstl Z, Rodenburg L, et al., (eds.). Edinburgh: ProQuest Dissertations Publishing, 2012.
358. Gu J, Shi W, Tang L, et al. Method for degrading bromobenzene in water body by utilizing irradiation. 2010.
359. Huang Z, Levlin E and Plaza E. Enhanced biogas production by increasing organic load rate in mesophilic anaerobic digestion with sludge recirculation. 2012.
360. Gou C, Yang Z, Huang J, et al. Effects of temperature and organic loading rate on the performance and microbial community of anaerobic co-digestion of waste activated sludge and food waste. *Chemosphere* 2014; 105: 146-151. DOI: https://doi.org/10.1016/j.chemosphere.2014.01.018.
361. Flavia L, Giuseppe dA, Giovanni E, et al. Effect of total solids content on methane and volatile fatty acid production in anaerobic digestion of food waste. *Waste Management & Research* 2014; 32: 947-953. DOI: 10.1177/0734242X14550740.
362. Wang T, Chen J, Shen H, et al. Effects of total solids content on waste activated sludge thermophilic anaerobic digestion and its sludge dewaterability. *Bioresource Technology* 2016; 217: 265-270. DOI: https://doi.org/10.1016/j.biortech.2016.01.130.
363. Bialek K, Cysneiros D and O'Flaherty V. Hydrolysis, acidification and methanogenesis during low-temperature anaerobic digestion of dilute dairy wastewater in an inverted fluidised bioreactor. *Applied Microbiology and Biotechnology* 2014; 98: 8737-8750. DOI: 10.1007/s00253-014-5864-7.
364. Meng Y, Jost C, Mumme J, et al. An analysis of single and two stage, mesophilic and thermophilic high rate systems for anaerobic digestion of corn stalk. *Chemical Engineering Journal* 2016; 288. Article. DOI: 10.1016/j.cej.2015.11.072.
365. Desloover J, Abate Woldeyohannis A, Verstraete W, et al. Electrochemical Resource Recovery from Digestate to Prevent Ammonia Toxicity during Anaerobic Digestion. *Environmental Science & Technology* 2012; 46: 12209-12216. DOI: 10.1021/es3028154.
366. Zhang Y and Angelidaki I. Counteracting ammonia inhibition during anaerobic digestion by recovery using submersible microbial desalination cell. *Biotechnology and Bioengineering* 2015; 112: 1478-1482. DOI: 10.1002/bit.25549.
367. Li H, Li C, Liu W, et al. Optimized alkaline pretreatment of sludge before anaerobic digestion. *Bioresource Technology* 2012; 123: 189-194. DOI: https://doi.org/10.1016/j.biortech.2012.08.017.
368. Pang L, Yang P, Ge L, et al. Accelerated solvent extraction combined with solid phase extraction for the determination of organophosphate esters from sewage sludge compost by UHPLC–MS/MS. *Analytical and Bioanalytical Chemistry* 2017; 409: 1435-1440. DOI: 10.1007/s00216-016-0078-8.
369. Demirel B. The impacts of engineered nanomaterials (ENMs) on anaerobic digestion processes. *Process Biochemistry* 2016; 51: 308-313. DOI: http://dx.doi.org/10.1016/j.procbio.2015.12.007.